TEXTE
06/2023

P-Ident2 – Persistence Assessment in Surface Waters - addressing uncertainties in OECD 309 and OECD 308 studies

Final report

German Environment Agency

Umwelt Bundesamt

TEXTE 06/2023

Ressortforschungsplan of the Federal Ministry for the Enviroment, Nature Conservation, Nuclear Safety and Consumer Protection

Project No. (FKZ) 3717 65 409 0

Report No. (UBA-FB) FB000676/ENG

P-Ident2 – Persistence Assessment in Surface Waters - addressing uncertainties in OECD 309 and OECD 308 studies

Final report

by

Carolin Seller, Elizabeth Kitching, Kathrin Fenner
Eawag, Department of Environmental Chemistry,
Überlandstrasse 133, 8600 Dübendorf, Switzerland

Laura Varga, Mark Honti
Budapest University of Technology and Economics,
Department of Sanitary and Environmental Engineering and
MTA-BME Water Research Group, Eötvös Loránd Research Network,
Müegyetem rakpart 3, 1111 Budapest, Hungary

On behalf of the German Environment Agency

Imprint

Publisher
Umweltbundesamt
Wörlitzer Platz 1
06844 Dessau-Roßlau
Tel: +49 340-2103-0
Fax: +49 340-2103-2285
buergerservice@uba.de
Internet: www.umweltbundesamt.de

/umweltbundesamt.de
/umweltbundesamt

Report performed by:
Eawag – Swiss Federal Institute for Aquatic Science and Technology
Überlandstrasse 133
8600 Dübendorf
Switzerland

Report completed in:
October 2021

Edited by:
IV2.2 Pharmaceuticals, IV1.3 Plant protection products
Silvia Berkner, Janina Wöltjen

Publication as pdf:
http://www.umweltbundesamt.de/publikationen

ISSN 1862-4804

Dessau-Roßlau, February 2023

Abstract: P-Ident2 – Persistence Assessment in Surface Waters - addressing uncertainties in OECD 309 and OECD 308 studies

The project P-Ident 2 aims (i) for a better understanding of the transformation behavior/persistence of chemicals in surface waters, and (ii) to address uncertainties in (regulatory) persistence assessment. Therefore, existing laboratory test methods (OECD 308 and 309) and evaluation methods were modified and further evaluated. Alongside, the transformation behavior/persistence of chemicals in a real surface water body (Rhine) was quantified based on field measurements and modeling. The outcomes of the laboratory biotransformation tests, as well as the results compiled by the model framework describing compound transformation in the Rhine river catchment allow for a comparison of a chemical's transformation behavior in laboratory studies and a real surface water.

Kurzbeschreibung: Persistente Stoffe in Oberflächengewässern – Unsicherheiten bei der Persistenzbewertung adressieren

Im Projekt P-Ident 2 geht es darum, das Transformationsverhalten/die Persistenz von Chemikalien in Oberflächengewässern besser zu verstehen und Unsicherheiten zu adressieren. Ziele des Projektes sind es existierende Labortestmethoden (OECD 308 und 309) und Auswertemethoden weiterzuentwickeln. Des Weiteren soll das Transformationsverhalten/die Persistenz von Chemikalien in einem realen Oberflächengewässer (Rhein) mittels Modellierung von Feldmessdaten quantifiziert werden. Die Ergebnisse aus den Labortests, aus vorliegenden Daten aus Zulassungsverfahren sowie aus der Modellierung für den Rhein erlauben einen Vergleich des Transformationsverhaltens zwischen Labor und einem realen Oberflächengewässer.

Table of Content

List of Tables

List of Figures

List of Abbreviations

API	Active Pharmaceutical Ingredient
BAfU	Bundesamt für Umwelt
CMP	Cressbrook Mill Pond
CMP1	Suspension test containing 1 g solids L^{-1} sampled from Cressbrook Mill Pond (Derbyshire, UK). Sediment was kept in suspensions via orbital shaker.
CMP10	Suspension test containing 10 g solids L^{-1} sampled from Cressbrook Mill Pond (Derbyshire, UK). Sediment was kept in suspensions via orbital shaker.
CMP1-Stirrer	Suspension test containing 1 g solids L^{-1} sampled from Cressbrook Mill Pond (Derbyshire, UK). Sediment was kept in suspensions via magnetic stirrer.
CMP10-Stirrer	Suspension test containing 10 g solids L^{-1} sampled from Cressbrook Mill Pond (Derbyshire, UK). Sediment was kept in suspensions via magnetic stirrer.
CO_2	Carbon dioxide
CV	Coefficient of variation
$DegT_{50}$	Degradation half-life
DT_{50}	Dissipation half-life
EtOH	Ethanol
f_{cons}	Mean daily consumption over the entire population based on the marketed amount
f_{oc}	Organic carbon content
F_{pce}	Per capita effluent
ICPR	International Commission for the Protection of the Rhine
IMS	IQVIA (formerly IMS Health, www.iqvia.com)
k'_{bio}	Second-order and biomass-normalized biotransformation rate constant
K_d	Sediment-water partitioning coefficient
k_{esc}	Escape rate of API
k_{exc}	Extracted fraction of non-metabolized API from the body
k_{hydro}	Abiotic hydrolysis rate constant
K_{oc}	Organic carbon-water partitioning coefficient
k_{photo}	Phototransformation rate constant
k_{rem}	Removal efficiency in the wastewater treatment plant
LANUV	Landesamt für Natur, Umwelt und Verbraucherschutz Nordrhein-Westfalen
LOD	Limit of detection
LOQ	Limit of quantification
Mod308CMP	Modified OECD 308-type experiments conducted with water and sediment sampled from Cressbrook Mill Pond (Derbyshire, UK)

Mod308R	Modified OECD 308-type experiments conducted with water and sediment sampled from the Rhine (Mumpf, Switzerland)
NER	Non-extractable residues
OECD	Organisation for Economic Cooperation and Development
PIdent-I project	Suitability of laboratory simulation tests for identification of persistence in surface waters' project
Q	Discharge
R^2	Coefficient of determination
R1-Fall	Suspension test containing 1 g solids L^{-1} sampled from the Rhine (Mumpf, Switzerland). Samples were taken in Fall 2018.
R1-Spring	Suspension test containing 1 g solids L^{-1} sampled from the Rhine (Mumpf, Switzerland). Samples were taken in Spring 2019.
R10-Fall	Suspension test containing 10 g solids L^{-1} sampled from the Rhine (Mumpf, Switzerland). Samples were taken in Fall 2018.
REACH	Registration, Evaluation, Authorization and Restriction of Chemicals
RSD	Relative standard deviation
S	Settled sediment stock in the active sediment layer
SMPC	Sondermessprogramm Chemie (Measurement campaign of chemicals)
SMPC P1	SMPC sampling between 19.03.2017 and 06.04.2017 in the Rhine
SMPC P3	SMPC sampling between 10.07.2017 and 27.07.2017 in the Rhine
SSC	Suspended sediment concentration
Std308	Standard OECD 308 studies
TOC	Total organic carbon
UBA	Umweltbundesamt
WP	Work Package
WWTP	Wastewater Treatment Plant
Z_a	Height of the active sediment layer
Z_w	Height of the water column
τ_W	Hydraulic retention time

Summary

Synthetic substances such as plant protection products, human and veterinary pharmaceuticals, biocides, and industrial chemicals inevitably pollute surface water bodies throughout their lifecycle due to accidental spills, use in the open environment, and incomplete removal during wastewater treatment. Since most of these substances intentionally exhibit biological activity, they bear the potential to harm non-target organisms in the environment, including humans. Chemicals that are persistent, i.e., recalcitrant toward biotic and abiotic degradation, are of special concern as they can distribute widely, reach high concentrations, and result in unintended environmental exposure that is difficult to control and reverse. Persistent chemicals can accumulate both temporally and spatially in specific environmental compartments such as water bodies. In the Rhine catchment, for instance, certain chemicals released in treated wastewater have been shown to exhibit both increased loads and even concentrations along the Rhine (Ruff et al. 2015). It is therefore crucial to easily and robustly assess persistence of chemicals in laboratory experiments to prevent the release of persistent chemicals into the environment, and, consequently, persistence assessment of organic chemicals is an integral part of many international regulatory frameworks.

To characterize persistence in surface waters, two OECD test guidelines are relevant for chemicals that are not readily biodegradable: The OECD 308 guideline (*"Aerobic and Anaerobic Transformation in Aquatic Sediment Systems"*), which targets transformation at the water-sediment interface, and the OECD 309 guideline (*"Aerobic mineralization in surface water – Simulation biodegradation test"*), which assesses transformation in the pelagic water body (with or without some suspended sediment). However, since the introduction of both guidelines, concerns regarding the performance and environmental relevance of those so-called simulation studies have been raised. OECD 308 biotransformation experiments are to be carried out in the dark under stagnant conditions with a 2-3 cm thick sediment layer covered by a shallow water column to yield a water-sediment ratio of 3:1 to 4:1 (v/v). Major points of criticism refer to (i) the recommended water-sediment ratio, which does not reflect conditions in many natural surface water bodies and shifts compound mass distribution excessively toward the sediment phase, thus measuring sorption rather than transformation, and (ii) not sufficiently standardized conditions allowing for variability in test setup that can impact the outcome (e.g., vessel geometry, thickness of sediment layer, aeration or stagnant conditions). OECD 309 studies are carried out in natural water without or with some suspended sediment. This test system is also being criticized for its vaguely standardized test conditions (e.g., pelagic/ suspension test, light/ dark), which can be expected to lead to highly variable outcomes. It has previously been suggested that some of the aforementioned shortcomings of OECD 308 studies could be addressed by increasing the water-sediment ratio and by ensuring full aeration and some agitation of the test system (Shrestha et al. 2016). While the former was expected to shift the compound mass from being sorbed to sediment more towards the aqueous phase and hence increase the fraction of compound mass being available for degradation, the latter modification, in combination with a thinner sediment layer, was expected to reduce anaerobic zones in the sediment and hence increase reproducibility and interpretability of the observed transformation signal. Similarly, it has been suggested that increasing the amount of suspended sediment in OECD 309 studies might increase the observable transformation signal in those and thus lead to more robust outcomes (Shrestha et al. 2016).

While changing the design of experimental test systems might improve their interpretability and repeatability, it will not answer the question of how and to what extent outcomes of such laboratory studies relate to observations of degradation in actual field situations. Indeed, it is not well understood to what extent laboratory simulation studies represent substance behavior in the field. As has been discussed in the report for the previous UBA project "Suitability of laboratory simulation tests for the identification of persistence in surface waters" (Fenner et al. 2017), this is to a large extent due to a lack of data, both on the sides of publicly available laboratory simulation study data for water-relevant substances such as pharmaceuticals, but also on the sides of

quantified half-lives in natural surface waters. Also, it is important to note that dissipation half-lives derived from biotransformation studies in water-sediment systems lump together transformation and phase transfer processes, and are dependent on the geometry of the experimental system, the sediment-water ratio and the physicochemical properties of the employed water and sediment (Honti et al. 2015). As a consequence, dissipation half-lives might not be proper descriptors of biotransformation behavior in the field where all of these conditions might vary considerably.

With these challenges in mind, the authors of this study previously introduced a data evaluation framework that derives a second-order biotransformation rate constant (k'_{bio}) from biotransformation study outcomes, which is less dependent on some of these system-specific differences (Honti et al. 2016). k'_{bio} is corrected for the substance's bioavailability, assuming that only dissolved compound mass is available for biotransformation, and thus allows disentangling biotransformation from phase transfer and partitioning. Further, k'_{bio} is normalized to the amount of organic carbon in the sediment and water compartment, taking, first, the organic carbon as a proxy that is assumed to be proportional to degrader biomass, and, second, assuming a compound's potential for biotransformation to depend on its contact with degrader biomass. It has been suggested that such a bioavailability-corrected and biomass-normalized second-order rate constant should be a more robust indicator of a substance's biotransformation potential than experiment-specific half-lives. Thus, k'_{bio} could allow unifying observations from different water-sediment systems, including OECD 308/309 tests, or even allow extrapolating from laboratory systems to natural water bodies such as rivers.

Yet, to actually derive a compound's k'_{bio} value from either laboratory-derived concentration-time series or concentration patterns measured in a river system, inverse modeling is required. This not only requires a model framework that appropriately describes all processes in the system (e.g., a river catchment or a laboratory vessel), but also good quantitative estimates for the other parameters relevant in the system (i.e., (meta)data on system dimensions, chemical properties etc.). For instance, to derive $k'_{bio,field}$ values for a given chemical from its concentration patterns in a river, its emission rates into the river system, as well as its other relevant environmental fate properties, i.e., organic carbon-water partitioning coefficient (K_{oc}) and susceptibility towards abiotic transformation (i.e., hydrolysis and phototransformation), need to be known as accurately as possible. Otherwise, uncertainty in emission, sorption, and transformation will prevent an accurate determination of $k'_{bio,field}$ in field systems. Similar identifiability issues apply to laboratory studies as well, where information on system geometry, sorption and abiotic transformation properties are needed to accurately determine $k'_{bio,lab}$.

Another method that is increasingly being highlighted and discussed as potentially helpful in comparing degradation behaviour across systems, is the so-called benchmarking approach (McLachlan, Zou, and Gouin 2017). The hypothesis behind benchmarking is that the relative degradation behaviour between chemicals is more conserved than absolute measures of persistence, which are influenced by a number of system-specific factors such as biomass concentration and activity, temperature, solid phase concentrations and many more. Assuming that assumption to be true, benchmarking could support persistence assessment in at least two ways. First, when attempting to evaluate degradation in the field, cumbersome mass balance considerations may be circumvented by evaluating a compounds concentration relative to an appropriate stable benchmark. Second, it might be assumed that chemicals would exhibit equal relative persistence or at least equal rank order of persistence in laboratory study setting and in the field. Hence, benchmarking could potentially help to translate outcomes of laboratory studies into behaviour in the field.

Against this scientific background, the goal of our study was to more thoroughly assess how outcomes from laboratory biotransformation studies compare to biotransformation derived by modeling from field measurements, and to use these insights to derived recommendations on how to conduct and evaluate OECD 308 and 309-type studies to yield outcomes that are as relevant to

predict the behavior in the aquatic environment as possible. To reach that objective, the specific aims of the project were as follows:

1. To improve the test design for laboratory studies on transformation in surface water and water-sediment systems to reduce variability in study outcomes and to improve their interpretability regarding biotransformation;
2. To provide guidance and a tool to evaluate laboratory study results from OECD 308-type studies regarding biotransformation, including additional (meta)data requirements needed for the improved evaluation;
3. To compare different persistence indicators derived from laboratory studies (i.e., different half-lives, k'_{bio}) to persistence indicators derived by measurements and modeling for a river catchment.

To fulfill the specific aims of the project, we, first, studied biotransformation in laboratory experiments for a broad set of >40 test compounds (plant protection products, pharmaceuticals, biocides and other chemicals) at environmentally relevant concentration levels in both standard and modified OECD 308- and 309-type systems and calculated half-lives and k'_{bio} values from that data (see Chapter 2). To derive k'_{bio} values with as little uncertainty as possible, we conducted complementary sorption, hydrolysis and phototransformation experiments, which provided prior estimates for Bayesian parameter inference when calibrating the k'_{bio}-models (Chapter 3). We then refined an existing model for the Rhine catchment, particularly with an explicit derivation of per-capita emissions of wastewater-relevant compounds (pharmaceuticals, one biocide and other chemicals) from measured wastewater treatment plant (WWTP) effluent data, and used it, together with substance fluxes measured in samples from a comprehensive Rhine monitoring campaign carried out in 2017, to derive half-lives and k'_{bio} values for the Rhine catchment for 28 compounds frequently detected in WWTP effluents and surface water bodies (Chapter 4). Finally, we systematically compared half-lives and biotransformation rate constants observed in laboratory test systems and in the field for those same 28 compounds to evaluate which biotransformation indicator that can be derived from laboratory biotransformation studies would most suitably predict biotransformation in the natural aquatic environment (Chapter 5). Additionally, the authors further developed the OECD Analyser, a software tool that can be used to derive k'_{bio} values and compartment-specific half-lives based on OECD 308 and OECD 309-type data.

Evaluation of Aquatic Biotransformation Half-Lives from OECD 309- and 308-type Test Systems

Experimental and analytical methods. Biotransformation experiments were carried out for 43 test compounds of known environmental relevance, i.e., often measured in wastewater treatment plant effluents or surface water bodies, including 24 pharmaceuticals, 15 pesticides, 3 artificial sweeteners, and 1 industrial chemical. For 19 of those, data from standard OECD 308 studies were additionally available to compare against. Experiments were carried out with water and sediment sampled from two sources, i.e., the wastewater effluent-impacted river Rhine (Mumpf, Switzerland) and the pristine Cressbrook Mill Pond (CMP, Derbyshire, UK), which differed strongly in texture and organic carbon content. Sampling of Rhine sediment was conducted twice, in spring and fall.

OECD 309 experiments were run as sediment-amended suspension experiments (600 mL water) and were mostly in accordance with OECD 309 guidelines, with the exceptions noted as follows: (i) Sediment was added to 1 and 10 g solids L^{-1} (wet weight), with the latter solids concentration being 10 times higher than the maximum recommended sediment concentration in the OECD 309 guideline (altogether, this resulted in five OECD 309-type experiments, i.e., R1/10-Fall, R1-Spring, CMP1/10); (ii) Compounds were spiked as mixtures of unlabelled compounds, to final

concentrations of 1 µg L^{-1} each, which is at the lower end of recommendations in the OECD 309 guideline. It is further worth noting that the sandy Rhine sediment was kept in suspension via orbital shaking rather than by a magnetic stirrer to avoid grinding of coarse-textured sediment. For comparison, both setups, horizontal shaker and magnetic stirrer, were employed to keep fine CMP sediment in suspension. Chemical dissipation from the water phase was followed up to 63 days using LC-MS/MS. Since, at each sampling time point, we sacrificed at least one test vessel for downstream microbial analysis, experiments run contained up to 18 replicates initially, yet the resulting length of individual replicates' time series obviously differ. These large numbers of replicates provided an exceptional basis for assessing inter-replicate variability (see below). To be consistent with data evaluation recommendations in regulatory frameworks, half-lives were calculated from total compounds residues by fitting a first-order degradation model considering lag phases. We defined the total system degradation half-life ($DegT_{50,TS,309}$) as the time interval needed to reach 50% primary degradation, once compound dissipation has started. In contrast, the total system half-life ($DT_{50,TS}$) was defined as the sum of $DegT_{50,TS,309}$ and the length of the lag phase (t_{lag}).

Modified OECD 308-type experiments were run in 1 L amber glass bottles (i.e., Ø = 10 cm) with a water-sediment ratio of 10:1 (v/v), which translates to 780 mL water covering a 1 cm thick sediment layer containing 30 g and 100 g of dry sediment in case of the CMP and Rhine sediment, respectively. The water column was aerated with wet air pumped through a syringe ending 1.5 cm above the sediment surface to avoid disturbing its upper layer. As in the OECD 309 experiments, compounds were spiked as mixtures of unlabelled compounds, to final concentrations of 1 µg L^{-1} each, which is lower (by a factor of 100-500) than concentration levels commonly applied in standard OECD 308 studies. To determine compound concentrations in the sediment, compounds were extracted using pressurized liquid extraction (PLE) with a mixture of nanopure water, methanol, and acetone (50:25:25 v/v/v). For each sediment, 18 replicates were set up and two replicates were sacrificed at nine sampling time points throughout >54 days. As for the OECD 309 data, half-lives were calculated using a first-order degradation model considering lag phases. We calculated dissipation half-lives in water ($DT_{50,w}$) based on the compounds residues in the water column, and dissipation half-lives from the total system ($DT_{50,TS}$). For the latter, total compound residues (C_{TS}) in the experimental vessels were calculated as the sum of the parent compound residues in the water phase and parent compound mass in the sediment. In any case, since both study design and data evaluation differed in relevant aspects from standard OECD 308 studies, they will be referred to as modified OECD 308-type studies in the following.

All OECD 308- and 309-type studies were complemented with abiotic and sorption control experiments using autoclaved liquid and solid samples to distinguish biotransformation from other possible loss processes.

Results for OECD 309-type studies. In terms of results for the OECD 309-type studies, sterile controls indicated that for both hydrochlorothiazide and irbesartan, compound dissipation was mostly attributable to abiotic transformation. Results from stirring of CMP1/10 experiments further confirmed previous results that keeping sediment in suspension via magnetic stirring led to grinding of particles and continuously increased sorption of chemicals, which made differentiation between transformation and sorption difficult. Consequently, we suggest that keeping sediments in suspension in OECD 309-type studies should be done via orbital shaking rather than stirring, and we will only discuss results from the former type of approach in the following.

Generally, compound dissipation via biotransformation was faster in suspensions with increased sediment content. Least compound losses were observed in CMP1 and R1-Fall - only six substances showed up to 50% removal by the end of those experiments - while dissipation of most

substances could be observed in R1-Spring, R10-Fall and CMP10. The differing grade of biotransformation between R1-Fall and R1-Spring further suggest that microbial test communities' composition or activity as influenced by seasonal variations also influences the extent of biotransformation. Besides interstudy variations, we observed drastic differences between replicates of the same study for most compounds ("intrastudy variation"), with the exception of a few compounds, i.e., atenolol, bezafibrate, and fenoxycarb, that showed little interreplicate variation, likely because of their biotransformation being catalyzed by enzymes widespread amongst microorganisms. Another important feature of the results from OECD 309-type experiments, was the observation of lag phases in most concentration-time series. There was again a trend with sediment content which generally indicated shorter lag phases in tests carried out with 10 g solids L^{-1}, especially in CMP10. Again, we also observed intrastudy variation of lag phases, which were most significant in R1-Spring.

Taken together, our results indicate that interpretation of OECD 309 outcomes is challenged by two factors. First, intrastudy variations, i.e., experimental replicates drifting apart over the time course of an experiment. Second, guidance is lacking on how to deal with lag phases when assessing a substance's persistence, i.e., whether $DegT_{50,309}$ or $DT_{50,309}$ are to be used. Since lag phases are a sign of microbial adaptation and reduced lag phases could be speculated for compounds continuously or repeatedly released to the aquatic environment, it has been argued that $DegT_{50,309}$ should be used as persistence metric. However, our experiments do not directly support this hypothesis as we determined shortest and least variable lag phases in suspensions employing a microbial community sourced from a pristine environment (CMP10). *Therefore, and in light of the current lack of understanding of observed variability in lag phases, the use of $DT_{50,309}$ values to assess persistence would seem the more cautious and environmentally protective approach.*

Results for OECD 308-type studies. In the modified OECD 308-type studies, we were able to observe the behavior of 42 compounds in at least one of the two modified OECD 308-type studies. 38 of those clearly dissipated from the test systems with biotransformation most likely being the dominant removal pathway for 36 compounds, whereas abiotic transformation again seemed the dominant removal pathway for the two compounds hydrochlorothiazide and irbesartan. There were two very notable differences in results of the modified OECD 308-type studies compared to those from OECD 309-type studies. First, variation between experimental replicates appeared to be negligible in modified OECD 308-type studies, despite the fact that each concentration-time point was from sacrificial sampling and hence from independent systems run in parallel. Second, we observed hardly any lag phases, with only one compound showing a lag phase > 10 d. It was also very interesting to note that $DT_{50,TS,mod308}$ values derived from modified OECD 308-type experiments did not differ significantly between the Rhine- and the CMP study for the majority of test compounds. The exception were three artificial sweeteners (acesulfame, cyclamate and saccharin) that showed increased biotransformation in the system incubated with Rhine sediment, which had previously been exposed to rather high concentrations of these compounds. Concentration-time series from experiments with both Rhine and CMP sediments identified the same 11 compounds as most rapidly degrading, i.e., fenoxycarb, atenolol, sulfamethoxazole, bezafibrate, trimethoprim, trinexapac-ethyl, valsartan, levetiracetam, iprovalicarb, and fenhexamid ($DT_{50,TS,mod308}$ ≤10 days) and the same five compounds as slowly transforming, i.e., aliskiren, atazanavir, citalopram, carbamazepine, and lamotrigine. The latter overlap to large parts with those compounds showing strongest sorption – accumulation of >70% of initially spiked compound mass in the sediment layer by the end of biotransformation experiments was observed for aliskiren, atazanavir, citalopram, azoxystrobin, and sitagliptin, as well as for lamotrigine in case of CMP sediment.

For 19 compounds, a comparison between results from standard OECD 308 studies and the here conducted modified OECD 308-type studies was possible. The most notable difference was that

$DT_{50,TS,std308}$ values derived from standard OECD 308 studies were usually higher (independent of the fact whether NER in the standard OECD 308 studies was considered as parent or not). We interpret these differences between standard and modified studies as being mostly due to the higher sediment content and reduced homogeneity in the sediment layer in standard studies, i.e., sediment-water ratio of 1:3 or 1:4 (v/v), as compared to the modified studies using a sediment-water ratio of 1:10 (v/v). Indeed, more than half of the compounds for which regulatory data was available had >70% of their initial compound mass sorbed (partially irreversible) to the sediment at time points comparable to the end of the modified OECD 308 studies. However, an influence of the stronger extraction methods used in this project (ASE) compared to the standard tests (mostly just shaking with (different) solvents) cannot be ruled out.

In line with the goals of this project, we complemented the standard dissipation and total system half-lives ($DT_{50,w,mod308}$ and $DT_{50,TS,mod308}$) with derivation of $k'_{bio,lab}$, which was then also used to calculate compartment-specific transformation half-lives, i.e., $DegT_{50,w,mod308}$ and $DegT_{50,sed,mod308}$. $k'_{bio,lab}$ was only derived from the modified OECD 308-type experiments since the large interreplicate variability and the long lag phases observed in the OECD 309-type studies made derivation of $k'_{bio,lab}$ from the latter data questionable. For the derivation of $k'_{bio,lab}$ from modified OECD 308-type data, we adapted the model framework of Honti et al. (2016), which describes transformation and sorption processes in a two-compartment system. Specifically, due to the rather thin sediment layer and constant aeration of the water column throughout the modified OECD 308-type experiments, we assumed the sediment layer to be fully aerobic. We used a Bayesian parameter estimation framework to calibrate the model for individual Rhine and CMP experiments separately, and jointly across both experiments. The joint fit was performed to verify whether the model can fit experimental data from both biotransformation studies with one set of substance-specific parameters. Importantly, for all substances other than pesticides, priors for the organic-carbon water partition coefficient (K_{oc}) needed to estimate bioavailability in the test systems, were derived from our own sorption experiments (see Chapter 3).

As already observed for $DT_{50,TS,mod308}$ values, mean $k'_{bio,lab}$ values derived from data of Rhine experiments were higher than those derived from data of CMP experiments. Nevertheless, it was possible to derive $k'_{bio,lab}$ values that were valid across both experiments for 38 compounds. In line with previous results for a limited set of compounds, comparing the individual fits to the joint fit revealed that the joint model solution was statistically preferable and that $k'_{bio,lab,joint}$ values derived from the joint fit were considerably less uncertain than values from individual fits.

Comparison of half-lives across test systems and types of half-lives. Based on all available results, we compared the different dissipation and degradation half-lives calculated based on OECD 309-type studies as well as standard and modified OECD 308-type studies. The major findings are as follows:

1. The comparison of dissipation half-lives with degradation half-lives confirms that dissipation half-lives in water ($DT_{50,w}$) were in most cases significantly shorter than degradation half-lives in water ($DegT_{50,w}$). Persistence assessment based on $DT_{50,w}$ would hence be less conservative, but does not seem justified given the fact that $DT_{50,w}$ lumps together phase transfer and transformation processes. Rather, persistence assessment in water should be based on $DegT_{50,w}$, which describes compound removal from the water phase via transformation exclusively.
2. Generally, biotransformation in standard and modified OECD 308-type studies appeared more stable than in suspension tests, as indicated by short lag phases and low intra-study variabilities. When comparing compound dissipation from standard and modified OECD 308-type studies, biotransformation appeared to be enhanced in modified systems. Our results indicate that this is mostly likely due to (i) the fact that compounds are more bioavailable in the modified system due to the increased water-sediment ratio, and (ii) larger parts of the

sediment being oxygenated in the modified relative to the standard OECD 308-type studies, resulting in enhanced homogeneity in the sediment layer of modified OECD 308-type studies. Overall, looking across results for OECD 309-type studies, and comparing the outcomes of the modified OECD 308-type studies to the standard OECD 308 studies, we conclude that the modified OECD 308-type studies exhibit increased interpretability compared to the existing OECD 309 and OECD 308-type studies and seem to be best suited to deliver information on aerobic biotransformation. However, standardizing experimental conditions such as to achieve a clear signal for aerobic biotransformation needs to consider that the variability in real environments (e.g., the presence of anaerobic redox conditions in deeper sediment layers or under stagnant or eutrophicated conditions) is not covered by the experimental design.

Rhine Catchment Study to Evaluate Biotransformation in the Field

Analytical methods and modeling approach. To evaluate biotransformation in the field, the river Rhine catchment was used as case study. To this end, we were able to use samples taken as part of the SMPC campaign (*Sondermessprogramm Chemie*) of ICPR (International Commission for the Protection of the Rhine). Concretely, we used samples from two water parcels that had been followed down the Rhine during two seasons of 2017 (P1: March to April, P3: July) and sampled at 14 locations in the Rhine, as well as samples from 6 large tributaries for those same seasons. In those samples, we quantified 36 substances for which a continuous and constant emission into the Rhine from WWTPs could reasonably be assumed, and for which we expected detectable presence in the Rhine catchment based on previous measurements or consumption relative to known measurable substances. Of those, 28 overlapped with substances for which biotransformation data in laboratory simulation studies had also been generated in this project. Quantification was done by HPLC-MS/MS using a Triple Quad Mass spectrometer, which yielded limits of quantification below 1 ng L^{-1} for 14 compounds, and below 10 ng L^{-1} for the majority of analytes (35 compounds). Highest LOQs were detected at 50 ng L^{-1} for oxypurinol and benzotriazole. Measured concentrations were converted into compound fluxes by multiplication with discharge information collected during the respective sampling campaigns.

For the estimation of biotransformation rate constants in the Rhine catchment, we used a previously developed model that allows estimating an average, bioavailability and biomass-normalized biotransformation rate constant ($k'_{bio,field}$) through calibration against measured compound fluxes. Since previous runs of the model had shown strong interactions between $k'_{bio,field}$ and two other parameters that are simultaneously calibrated, i.e., k_{esc} characterizing emissions and K_{oc} describing sorption behavior, particular attention was paid in this project to refine the prior estimates for these two parameters. For K_{oc} this was achieved by running dedicated sorption experiments for the study compounds and a number of relevant sediments. The “escape factor”, k_{esc}, is a dimensionless factor that describes the proportion of the marketed APIs that reach the stream network, and was calculated as the ratio of per-capita marketed amounts and WWTP effluent fluxes, and hence allows for consideration of country- and year-specific consumption data in the calculation of compound fluxes into the Rhine. To estimate k_{esc}, annual consumption data of pharmaceuticals for Germany (for the period of 2010-2018) and Switzerland (for 2014-2016) available from IQVIA were used. For some compounds, we were also able to investigate year-to-year and seasonal trends thanks to quarterly sales data. To calculate WWTP effluent fluxes, measured WWTP effluent concentrations were obtained from three Swiss and two German (Baden-Württemberg, Nordrhein-Westfalen) monitoring campaigns and multiplied with available discharge information. Quality of those data varied as Swiss data was mostly from composite sampling, while German data was mostly from grab samples. Also, while most of campaigns cover

rather short time periods of a few weeks to a few months, one campaign extended over a time period of > 10 years.

The Rhine model used was based on river reaches where partitioning and transformation in an equilibrium state is described as functions of the physical properties of the reach and the sorption/biotransformation properties of the API. The APIs' behavior in the entire catchment is then simulated by connecting multiple stream reaches following the topology of the stream network. This model was used in a calibration procedure, whereby the model tries to fit its simulated flux to the observations derived from the SMPC campaigns by adjusting the parameters k_{esc}, K_{oc}, and $k'_{bio,field}$. The calibration procedure took place in a Bayesian framework and yielded (i) the fitted flux profile for the Rhine, and (ii) posterior marginal distributions for all three calibrated parameters, including $k'_{bio,field}$.

Since the explicit modeling approach obviously requires a complicated model that builds on various, difficult-to-prove assumptions on the physical properties of reaches and suffers to some extent from weak parameter identifiability, we also tried the alternative concept of using benchmarking to derive rate constants. In benchmarking, the behavior of a given compound of interest is assessed relative to a benchmark compound, assumed to be non-transforming and undergoing the same fate processes (e.g., sorption) and exhibiting similar emission patterns. To apply benchmarking to our data, we conceptually extended an already existing benchmarking approach for lakes (Zou et a. 2014) to make it applicable to river systems.

Estimated field biotransformation rate constants. Consumption data indicated country-specific differences for some compounds (e.g., metoprolol, mefenamic acid), as well as seasonal trends for clarithromycin (antibiotic, increased consumption in first quarter of the year), fexofenadine (used to treat allergy symptoms, increased consumption in the second quarter of the year) and phenazone (potentially due to use as veterinary medicine too). Escape rates were similar between Switzerland and Germany for most compounds, as expected from wastewater treatment technologies being rather similar too. Unfortunately, escape rate estimates still showed a rather large variability between the individual samples in the five involved studies, which ultimately propagated into uncertainty in estimate field biotransformation rate constants. This variability could only be considered as randomness, as we found no significant deterministic relations between escape rates and potentially influencing factors that were covered by data, e.g., WWTP size and season. Potential sources of uncertainty for escape rate estimations included the lack of quarterly consumption data, interpolations or extrapolations for years lacking consumption data, lack of effluent discharge data specific to the observation period, uncertainty in connected inhabitants per WWTP and input sources other than via WWTP (e.g., via stormwater overflow or from production and formulation facilities).

In calibration, the model generally achieved good fits to the fluxes derived from the SMPC samples. Also, the posterior marginal distributions of $k'_{bio,field}$ showed that this second-order degradation parameter can be estimated from field data, with the interquartile range usually covering less than one order of magnitude. However, the extreme quantiles (outside the interquartile range) often spanned over 3-4 orders of magnitude. On the whole, while distributions of $k'_{bio,field}$ overlapped to some extent between compounds, they still showed significant differences among subgroups of compounds. Hence, it could be expected that comparison with experimental values generated in laboratory experiments may detect at least qualitative similarities between persistence in the laboratory and in the Rhine catchment. It was further interesting to note that, for many compounds, $k'_{bio,field}$ in P3 (July 2017) was higher than in P1 (March - April 2017). For phototransformation, the effect of increased irradiation in P3 was directly accounted for in the model, and the difference in $k'_{bio,field}$ between P3 and P1 should thus mostly be due to increased biotransformation. These effects could be direct in the form of higher bioactivity due to higher

temperature, or indirect in the form of specific microbial community changes that occur during summer, yet we lacked additional information to test these assumptions.

We also converted $k'_{bio,field}$ values into half-lives by assuming mean characteristic properties of a river stretch, representing the „average Rhine" from the Aare mouth to Lobith. Total system half-lives calculated in this way ranged from half an hour to thousands of days, while water half-lives covered the range from 10 hours to more than 10 000 days. Considering the water travel time in the Rhine (less than 9 days, 4-5 days on average across all water parcels of the Rhine catchment), these numbers suggest that most compounds show very limited to no degradation in the main channel of the river Rhine. Rather, the model suggested that biotransformation will mostly happen in small to medium streams because they (i) receive most of the emissions (since most WWTP are along small and medium streams), (ii) have less water per unit sediment surface, which, in-line with the k'_{bio}-hypothesis, should reduce total system half-lives, and (iii) their sediment is likely to be staying settled longer due to the weaker resuspension capacity of shallower flow.

Benchmarking based on field data. The benchmarking model yielded acceptable fits to the observed relative concentration ratios for most compounds. Nevertheless, the distance-specific rate constants from the benchmarking procedure were found to be as uncertain as $k'_{bio,field}$. However, the two methods have no assumptions in common, so they may be free of each other's systematic errors. A conversion of the distance-specific rate constants into half-lives ($DL_{50,benchmark}$) using the mean flow rate showed that the benchmarking procedure can be used to determine half-lives in the Rhine between about half a day and sixty days. Calculating half-lives from distance-specific rate constants affects compounds differently depending on their sorption properties. Highly sorptive compounds are likely to be transported more slowly because of their stronger affinity for entering the riverbed, so their half-lives may be underestimated. The usefulness of benchmarking is therefore limited by the need for a benchmark compound that strongly resembles the target compounds in terms of physico-chemical properties and is not transformed. Yet, based on the independently determined half-lives from benchmarking, $DT_{50,TS,mod308}$ appears to be a conservative estimate of dissipation in the field, although there is little correlation between $DL_{50,benchmark}$ and $DT_{50,TS,mod308}$ values.

Comparison of Biotransformation in Laboratory Systems and the River Rhine Catchment

Data from biotransformation simulation studies, in particular from modified OECD 308-type studies, and from the field study in the river Rhine catchment allowed deriving different persistence indicators, i.e., different half-lives and k'_{bio} values, that each describe in a specific way a compound's recalcitrance toward transformation. These data were therefore used to investigate the question which of those indicators are best suited to relate outcomes of laboratory studies to compound behavior in a real, large-scale system like the river Rhine catchment. To this end, we directly compared half-lives and k'_{bio} values derived from modified OECD 308-type experiments to values derived from the field study in the river Rhine catchment, both in terms of absolute and relative values. In the following, we only discuss the comparison based on field rate constants derived from P3 data because, during the P3 campaign (July 2017), the water temperatures in the Rhine were comparable to temperatures during biotransformation simulation studies, and because P3 data allowed to more clearly observe a biotransformation signal for the majority of compounds.

We first compared dissipation half-lives $DT_{50,w.mod308}$ observed during modified OECD 308-type studies in inoculum sampled from the Rhine to degradation half-lives $DegT_{50,w,field}$ derived from the P3 campaign. These two parameters indeed showed a statistically significant, moderate correlation ($R^2 = 0.5$, Pearson's $r = 0.71$) and were scattered around the 1:1-line. However, we noticed that several compounds had shorter $DT_{50,w,mod308}$ than $DegT_{50,w,field}$, and that this was

particularly the case for compounds with higher K_{oc} values. *This confirms insights from comparison of dissipation and degradation half-lives from laboratory studies. Using $DT_{50,w,mod308}$ as a persistence indicator may result in an underestimation of a compound's environmental persistence, which is increasing with increasing K_{oc} values.*

Next, we compared degradation half-lives $DegT_{50,w,mod308}$ calculated for the modified OECD 308-type studies in inoculum sampled from the Rhine to degradation half-lives $DegT_{50,w,field}$ derived from the P3 campaign. In this case, both degradation half-lives – in laboratory and field – were calculated based on the compounds' respective k'_{bio} values. The two parameters showed a statistically significant correlation with a rather high explained variance (R^2= 0.79, Pearson's r = 0.89). Accordingly, when directly comparing $k'_{bio,lab}$ values from modified OECD 308-type studies in Rhine inoculum ($k'_{bio,lab,R}$) to $k'_{bio,field}$ values derived from P3 data, we also found a statistically significant correlation, yet with slightly lower explained variance (R^2=0.5, Pearson's r = 0.71). However, in absolute terms, degradation in the field was found to be higher than degradation in the laboratory system with Rhine inoculum for all compounds, both when comparing half-lives (i.e., $DegT_{50,w,mod308}$ vs $DegT_{50,w,field}$) and when comparing transformation rate constants (i.e., $k'_{bio,lab,}$ vs $k'_{bio,field}$). These results agree with previous results by the same authors for a much smaller set of compounds (Honti et al. 2016). This absolute difference of often more than one order of magnitude between field and laboratory systems may result from actual differences in activity of the microbial biomass between the laboratory and field system, yet may also result from using TOC as a very crude approximation for biomass. *Nevertheless, the good quality of the correlations suggests that k'_{bio} values or degradation half-lives derived thereof may indeed support the translation of laboratory to field values. The correlation may be further increased with a more precise measure of degrader biomass in aquatic systems.*

Since total system half-lives ($DT_{50,TS}$) are more easily derived from laboratory OECD 308-type studies than compartment-specific degradation indicators completely excluding effects of phase transfer that require more complicated inverse modeling, we finally also compared total system half-lives $DT_{50,TS,mod308}$ calculated for the modified OECD 308-type studies in inoculum sampled from the Rhine to total system degradation $DegT_{50,TS,field}$ derived from the P3 campaign. This resulted in a statistically significant moderate correlation (R^2=0.41, Pearson's r= 0.64). In line with the findings for the degradation indicators above, we also found that $DT_{50,TS,mod308}$ values are generally higher than $DegT_{50,TS,field}$ values, by about one order of magnitude on average.

Overall, there is no generally valid answer to the question how well persistence indicators derived from laboratory studies can predict observed degradation behavior in the field. We can think about this in terms of rough categories, relative and absolute behavior. In terms of categories, compounds consistently classified as hardly degraded in the laboratory simulation studies were also found to be persistent in the field. Similarly, compounds consistently degraded to large extents in the laboratory simulation studies also showed clearly observable degradation in the field during the P3 campaign. In terms of relative behavior, total system half-lives derived from modified OECD 308 test systems as well as k'_{bio} values yield moderate, statistically significant correlations between laboratory and field data. *Interestingly, correlations were stronger in case persistence indicators were derived based on the k'_{bio}-concept indicating that k'_{bio} and half-lives derived thereof indeed enable a more accurate read-across, at least in relative terms, than total system degradation half-lives.* The absolute comparison between persistence indicators derived from laboratory experiments and the field study suggested that biotransformation is generally slower in modified OECD 308-type experiments than in the Rhine river catchment. However, this absolute difference could also result from the fact that a microbial degrader activity does not scale with TOC. *We therefore recommend to explore further methods for improved characterization of specific degrader biomass in order to re-evaluate the k'_{bio}-concept, as it has the theoretical potential to further improve the estimation of persistence in the field from laboratory-based simulation studies.*

Zusammenfassung

Synthetische Stoffe wie Pflanzenschutzmittel, Human- und Tierarzneimittel, Biozide und Industriechemikalien können während ihres gesamten Lebenszyklus Oberflächengewässer verschmutzen, da sie in der freien Natur verwendet werden oder bei der Abwasserbehandlung unvollständig entfernt werden. Da die meisten dieser Stoffe eine biologische Aktivität aufweisen, haben sie das Potenzial, Nichtzielorganismen in der Umwelt, sowie auch Menschen, zu schädigen. Persistente Chemikalien, d. h. solche, die biotisch und abiotisch schwer abbaubar sind, sind besonders besorgniserregend, da sie sich weit verbreiten, hohe Konzentrationen erreichen können und zu einer unbeabsichtigten Umweltexposition führen können, die nur schwer zu kontrollieren und rückgängig zu machen ist. Persistente Chemikalien können sich sowohl zeitlich als auch räumlich in bestimmten Umweltkompartimenten wie Gewässern anreichern. Im Rheineinzugsgebiet beispielsweise zeigen bestimmte Chemikalien, die mit gereinigtem Abwasser freigesetzt werden, sowohl erhöhte Frachten als auch Konzentrationen entlang des Rheins (Ruff et al. 2015). Daher ist es von entscheidender Bedeutung, die Persistenz von Chemikalien in Laborexperimenten einfach und zuverlässig zu prüfen, um die Freisetzung persistenter Chemikalien in die Umwelt zu verhindern. Die Bewertung der Persistenz von organischen Chemikalien ist daher fester Bestandteil vieler internationaler Rechtsvorschriften.

Zur Charakterisierung der Persistenz in Oberflächengewässern sind zwei OECD-Prüfrichtlinien relevant: Die OECD-Richtlinie 308 (*"Aerobic and Anaerobic Transformation in Aquatic Sediment Systems"*), die auf die Biotransformation an der Wasser- Sediment-Grenzfläche abzielt, und die OECD-Richtlinie 309 (*"Aerobic mineralization in surface water - Simulation biodegradation test"*), die die Biotransformation im pelagischen Wasserkörper (mit oder ohne Schwebesediment) bewertet. Seit der Einführung der beiden Prüfrichtlinien wurden jedoch Bedenken hinsichtlich der Aussagekraft und Umweltrelevanz dieser so genannten Simulationsstudien geäussert. Die Biotransformationsversuche nach OECD 308 sollen im Dunkeln unter stagnierenden Bedingungen mit einer 2-3 cm dicken Sedimentschicht, die von einer flachen Wassersäule bedeckt ist, durchgeführt werden, um ein Wasser-Sediment-Verhältnis von 3:1 bis 4:1 (v/v) zu erreichen. Die Hauptkritikpunkte beziehen sich auf (i) das empfohlene Wasser-Sediment-Verhältnis, das die Bedingungen in vielen natürlichen Oberflächengewässern nicht widerspiegelt und die Massenverteilung der Verbindungen übermäßig in Richtung der Sedimentphase verschiebt, so dass eher die Sorption als die Umwandlung gemessen wird, und (ii) nicht ausreichend standardisierte Bedingungen, die verschiedene Versuchsaufbaus ermöglichen, die sich wiederum auf das Ergebnis auswirken können (z. B. Gefäßgeometrie, Dicke der Sedimentschicht, Belüftung oder stagnierende Bedingungen). Die OECD-309-Studien werden in natürlichem Wasser ohne oder unter Zugabe von Schwebstoffen durchgeführt. Dieses Testsystem wird ebenfalls wegen seiner unzureichend standardisierten Testbedingungen (z. B. pelagischer Test/Suspensionstest, hell/dunkel), welche zu sehr unterschiedlichen Ergebnissen führen dürften, kritisiert. Es wurde bereits vorgeschlagen, dass einige der oben genannten Mängel der OECD-308-Studien durch eine Erhöhung des Wasser-Sediment- Verhältnisses und durch eine vollständige Belüftung und ein gewisses Rühren des Testsystems behoben werden könnten (Shrestha et al. 2016). Während man davon ausging, dass ersteres die Verbindungen stärker in die wässrige Phase verlagert und somit den Anteil der für den Abbau verfügbaren Masse der Verbindung erhöht, sollte die letztgenannte Änderung in Kombination mit einer dünneren Sedimentschicht die anaeroben Zonen im Sediment verringern und somit die Reproduzierbarkeit und Interpretierbarkeit des beobachteten Biotransformationssignals erhöhen. In ähnlicher Weise wurde vorgeschlagen, dass eine Erhöhung des Anteils an Schwebstoffen in OECD-309-Studien das beobachtbare Biotransformationssignals in diesen Studien erhöhen und somit zu robusteren Ergebnissen führen könnte (Shrestha et al. 2016).

Eine Änderung des Designs experimenteller Testsysteme könnte zwar deren Interpretierbarkeit und Reproduzierbarkeit verbessern, beantwortet aber nicht die Frage, wie und in welchem Ausmaß die Ergebnisse solcher Laborstudien mit den Beobachtungen des Abbaus in tatsächlichen Feldsituationen zusammenhängen. In der Tat ist nicht klar, inwieweit Laborsimulationsstudien das Verhalten von Stoffen im Feld wiedergeben. Wie im Bericht über das vorangegangene UBA-Projekt "Eignung von Laborsimulationstests zur Ermittlung der Persistenz in Oberflächengewässern" erörtert (Fenner et al. 2017), ist dies zu einem großen Teil auf einen Mangel an Daten zurückzuführen, und zwar sowohl im Bezug auf öffentlich zugängliche Laborsimulationsstudien für wasserrelevante Stoffe wie Arzneimittel als auch im Bezug auf quantifizierte Halbwertszeiten in natürlichen Oberflächengewässern. Außerdem ist zu beachten, dass die aus Biotransformationsstudien in Wasser-Sediment-Systemen typischerweise abgeleiteten Dissipationshalbwertszeiten Transformations- und Phasentransferprozesse zusammenfassen und von der Geometrie des Versuchssystems, dem Sediment-Wasser-Verhältnis und den physikalisch-chemischen Eigenschaften des verwendeten Wassers und Sediments abhängen (Honti et al. 2015). Folglich sind Dissipationshalbwertszeiten möglicherweise keine geeigneten Deskriptoren des Biotransformationsverhaltens im Feld, wo all diese Bedingungen stark unterschiedlich ausfallen können.

Vor dem Hintergrund dieser Herausforderungen haben die Autoren dieser Studie ein neues Konzept für die Datenauswertung eingeführt, welches aus den Ergebnissen der Biotransformationsstudien eine Biotransformationsratenkonstante zweiter Ordnung (k'_{bio}) ableitet, die weniger von systemspezifischen Unterschieden abhängig ist (Honti et al. 2016). k'_{bio} ist für die Bioverfügbarkeit der Substanz korrigiert, wobei davon ausgegangen wird, dass nur der gelöste Anteil einer Verbindung für die Biotransformation zur Verfügung steht, und ermöglicht somit die Entkopplung der Biotransformation vom Phasentransfer und der Verteilung. Darüber hinaus ist k'_{bio} auf die Menge an organischem Kohlenstoff im Sediment und im Wasserkompartiment normiert. Hierbei wird angenommen, ersten, dass der organische Kohlenstoff als Proxy für die abbauende Biomasse verwendet werden kann, und, zweitens, dass das Biotransformationspotenzial einer Verbindung von ihrem Kontakt mit der abbauenden Biomasse abhängt. Es wurde vorgeschlagen, dass eine solche Bioverfügbarkeits-korrigierte und Biomassen-normalisierte Geschwindigkeitskonstante zweiter Ordnung ein zuverlässigerer Indikator für das Biotransformationspotenzial einer Substanz sein sollte als experimentelle Halbwertszeiten. So könnte k'_{bio} die Vereinheitlichung von Beobachtungen aus verschiedenen Wasser-Sediment- Systemen, einschließlich OECD 308/309-Tests, oder sogar die Extrapolation von Laborsystemen auf natürliche Gewässer wie Flüsse ermöglichen.

Um jedoch den k'_{bio}-Wert einer Verbindung entweder aus im Labor ermittelten Konzentrations-Zeitreihen oder aus in einem Flusssystem gemessenen Konzentrationsmustern abzuleiten, ist eine inverse Modellierung erforderlich. Dies erfordert nicht nur ein Modell, das alle relevanten Prozesse im jeweiligen System (z. B. einem Flusseinzugsgebiet oder einem Laborgefäß) angemessen beschreibt, sondern auch gute quantitative Schätzungen für die anderen, im System relevanten Parameter. Um beispielsweise $k'_{bio,field}$-Werte für eine bestimmte Chemikalie aus ihren Konzentrationsmustern in einem Fluss abzuleiten, müssen ihre Emissionsraten sowie ihre anderen relevanten Umwelteigenschaften, d. h. der Verteilungskoeffizient zwischen organischem Kohlenstoff und Wasser (Koc) und ihre Anfälligkeit für abiotische Umwandlung (d. h. Hydrolyse und Phototransformation), so genau wie möglich bekannt sein. Andernfalls verhindern Unsicherheiten bei Emission, Sorption und Transformation eine genaue Bestimmung von $k'_{bio,field}$. Ähnliche Probleme der Identifizierbarkeit gelten auch für Laborstudien, für deren Auswertung Informationen über die Systemgeometrie, das Sorptionsverhalten der Substanz und potentielle abiotische Umwandlungsprozesse erforderlich sind, um $k'_{bio,lab}$ genau zu bestimmen.

Eine weitere Methode, die zunehmend als potenziell hilfreich für den Vergleich des Abbauverhaltens verschiedener Systeme hervorgehoben und diskutiert wird, ist der sogenannte

Benchmarking-Ansatz (McLachlan, Zou und Gouin 2017). Die Hypothese hinter dem Benchmarking ist, dass das relative Abbauverhalten zwischen Chemikalien konservierter ist als absolute Maße der Persistenz, die von einer Reihe systemspezifischer Faktoren wie Biomasse–konzentration und -aktivität, Temperatur, Festphasenkonzentrationen und vielen anderen beeinflusst werden. Unter der Annahme, dass diese Annahme zutrifft, könnte das Benchmarking die Persistenzbewertung auf mindestens zwei Arten unterstützen. Erstens könnten bei dem Versuch, den Abbau im Feld zu bewerten, umständliche Massenbilanzüberlegungen umgangen werden, indem die Konzentration einer Verbindung im Verhältnis zu einer geeigneten stabilen Benchmarkverbindung bewertet wird. Zweitens könnte man davon ausgehen, dass Chemikalien in Laborstudien und im Feld die gleiche relative Persistenz oder zumindest die gleiche Rangfolge der Persistenz aufweisen würden. Daher könnte das Benchmarking potenziell dabei unterstützen, die Ergebnisse von Laborstudien ins Feld zu übertragen.

Vor diesem wissenschaftlichen Hintergrund bestand das Ziel unserer Studie darin, zu untersuchen, wie die Ergebnisse von Biotransformationsstudien im Labor mit der im Feld beobachteten Biotransformation zu vergleichen sind. Aus diesen Erkenntnissen sollten dann Empfehlungen für die Durchführung und Bewertung von Studien des Typs OECD 308 und 309 abgeleitet werden, mit dem Ziel, diese so durchzuführen, dass die gewonnen Informationen möglichst relevant für die Beschreibung des Substanzverhalten in der aquatischen Umwelt sind. Dafür wurden folgende spezifische Projektziele verfolgt:

1. Verbesserung des Testdesigns für Laborstudien zur Biotransformation in Oberflächengewässern und Wasser-Sediment-Systemen, um die Variabilität der Studienergebnisse zu verringern und ihre Interpretierbarkeit hinsichtlich der Biotransformation zu verbessern;
2. Bereitstellung eines Leitfadens und eines Instruments zur Evaluierung kinetischer Information aus Laborstudien in Bezug auf die Biotransformation, einschließlich zusätzlicher (Meta-)Datenanforderungen, die für eine verbesserte Bewertung erforderlich sind;
3. Vergleich verschiedener Persistenzindikatoren, die aus Laborstudien abgeleitet wurden (d. h. unterschiedliche Halbwertszeiten, k'_{bio}), mit Persistenzindikatoren, die durch Messungen und Modellierung für ein Flusseinzugsgebiet abgeleitet wurden.

Um die spezifischen Projektziele zu erreichen, untersuchten wir zunächst die Biotransformation in Laborexperimenten für eine breite Palette von >40 Testverbindungen (Pflanzenschutzmittel, Pharmazeutika, Biozide und andere Chemikalien) bei umweltrelevanten Konzentrationen sowohl in Standard- als auch in modifizierten Systemen vom Typ OECD 308 und 309 und berechneten Halbwertszeiten und k'_{bio}-Werte aus diesen Daten (Kapitel 2). Um k'_{bio}-Werte mit möglichst geringer Unsicherheit abzuleiten, führten wir ergänzende Sorptions-, Hydrolyse- und Phototransformations–experimente durch. Die Ergebnisse dieser Studien verwendeten wir für die Vorabschätzung von Modellparametern für die Kalibrierung der k'bio-Modelle (Kapitel 3). Anschließend verfeinerten wir ein bestehendes Modell für das Rheineinzugsgebiet, insbesondere mit einer expliziten Ableitung der Pro-Kopf-Emissionen von abwasserrelevanten Verbindungen (Arzneimittel, ein Biozid und andere Chemikalien) aus gemessenen Kläranlagenabflussdaten, und nutzten es zusammen mit Stoffflüssen, die in Proben aus einer umfassenden Rhein-Monitoring-Kampagne im Jahr 2017 gemessen wurden, zur Ableitung von Halbwertszeiten und k'bio-Werten für das Rheineinzugsgebiet für 28 Verbindungen, die häufig in Kläranlagenabflüssen und Oberflächengewässern nachgewiesen wurden (Kapitel 4). Schließlich führen wir einen systematischen Vergleich durch von Halbwertszeiten und Biotransformationsratenkonstanten, die in Labortestsystemen und im Freiland für dieselben 28 Verbindungen beobachtet wurden. Dies um zu bewerten, welcher der Biotransformationsdeskriptoren, die aus Biotransformationsstudien im Labor abgeleitet werden können, die Biotransformation in der natürlichen aquatischen Umwelt am besten vorhersagen würde (Kapitel 5). Darüber hinaus entwickelten die Autoren den OECD

Analyser weiter, ein Software-Tool, das zur Ableitung von k'bio-Werten und kompartiment-spezifischen Halbwertszeiten auf der Grundlage von Daten vom Typ OECD 308 und OECD 309 verwendet werden kann.

Bewertung der Halbwertszeiten für die aquatische Biotransformation anhand von OECD 309- und 308-Testsystemen

Experimentelle und analytische Methoden. Biotransformationsexperimente wurden für 43 Test-verbindungen durchgeführt, die bekanntermaßen umweltrelevant sind, d. h. häufig in Abwässern von Kläranlagen oder Oberflächengewässern gemessen werden, darunter 24 Arzneimittel, 15 Pestizide, 3 künstliche Süßstoffe und 1 Industriechemikalie. Für 19 dieser Stoffe standen zusätzlich Daten aus OECD-308-Standardstudien zum Vergleich zur Verfügung. Die Experimente wurden mit Wasser- und Sedimentproben durchgeführt, die aus zwei Quellen stammten, nämlich aus dem durch Abwässer belasteten Rhein (Mumpf, Schweiz) und dem unberührten Cressbrook Mill Pond (CMP, Derbyshire, Großbritannien). Die Sedimente unterschieden sich in Bezug auf Textur und organischen Kohlenstoffgehalt stark. Die Probenahme von Rheinsedimenten wurde zweimal durchgeführt, im Frühjahr und im Herbst.

Die OECD 309-Experimente wurden als Sediment-angereicherte Suspensionsexperimente (600 ml Wasser) durchgeführt und entsprachen größtenteils den OECD 309-Leitlinien, mit den im Folgenden aufgeführten Ausnahmen: (i) Dem Sediment wurden 1 und 10 g Feststoffe L-1 (Nassgewicht) zugesetzt, wobei die letztgenannte Feststoffkonzentration zehnmal höher war als die in der OECD 309-Richtlinie empfohlene maximale Sedimentkonzentration (insgesamt führte dies zu fünf Experimenten des OECD 309-Typs, d.h. R1/10-Fall, R1-Spring, CMP1/10); (ii) Die Verbindungen wurden als Mischungen von unmarkierten Verbindungen in Endkonzentrationen von jeweils 1 µg L-1 zugesetzt, was am unteren Ende der Empfehlungen der OECD 309-Richtlinie liegt. Ferner ist anzumerken, dass das sandige Rheinsediment durch orbitales Schütteln und nicht durch einen Magnetrührer in Suspension gehalten wurde, um ein Zermahlen des grobkörnigen Sediments zu vermeiden. Zum Vergleich wurden beide Versuchsaufbauten, Horizontalschüttler und Magnetrührer, verwendet, um feines CMP-Sediment in der Schwebe zu halten. Die chemische Freisetzung aus der Wasserphase wurde bis zu 63 Tage lang mittels LC-MS/MS verfolgt. Da wir zu jedem Probenahmezeitpunkt den Inhalt mindestens eines Testgefäßes für die anschließende mikrobielle Analyse verwendet haben, umfassten die durchgeführten Experimente bis zu 18 Wiederholungen, wobei die Länge der Zeitreihen der einzelnen Wiederholungen natürlich unterschiedlich war. Diese große Anzahl von Wiederholungen bot eine hervorragende Gelegenheit für die Bewertung der Variabilität zwischen Wiederholungen (siehe unten). Um mit den Empfehlungen zur Datenauswertung in den Rechtsvorschriften übereinzustimmen, wurden die Halbwertszeiten anhand der Gesamtrückstände der Verbindungen berechnet, indem ein Abbaumodell erster Ordnung unter Berücksichtigung von «lag phases» angepasst wurde. Wir definierten die Halbwertszeit für den Abbau des Gesamtsystems ($DegT_{50,TS,309}$) als das Zeitintervall, das benötigt wird, um 50 % des primären Abbaus zu erreichen, sobald der Abbau der Verbindung begonnen hat. Im Gegensatz dazu wurde die Halbwertszeit des Gesamtabbaus ($DT50_{,TS}$) als die Summe von $DegT_{50,TS,309}$ und der Länge der «lag phases» definiert.

Die modifizierten Experimente vom Typ OECD 308 wurden in 1-L-Braunglasflaschen (Ø = 10 cm) mit einem Wasser-Sediment-Verhältnis von 10:1 (v/v) durchgeführt, was bedeutet, dass 780 ml Wasser eine 1 cm dicke Sedimentschicht bedeckten, welche wiederum 30 g bzw. 100 g Trocken-sediment im Falle des CMP- bzw. Rheinsediments enthält. Die Wassersäule wurde mit feuchter Luft belüftet, die durch eine Spritze gepumpt wurde und 1,5 cm über der Sedimentoberfläche endete, um die Sedimentschicht nicht zu stören. Wie bei den OECD-309-Experimenten wurden die Verbindungen als Mischungen unmarkierter Verbindungen in Endkonzentrationen von jeweils 1 µg L-1 zugegeben, was um den Faktor 100-500 unter den Konzentrationswerten liegt, die

üblicherweise in OECD-308- Standardstudien verwendet werden. Um die Konzentrationen der Verbindungen im Sediment zu bestimmen, wurden die Verbindungen durch Flüssigextraktion unter Druck (PLE) mit einem Gemisch aus Nanopur-Wasser, Methanol und Aceton (50:25:25 v/v/v) extrahiert. Für jedes Sediment wurden 18 Wiederholungen erstellt und zwei Wiederholungen wurden an neun Probenahmezeitpunkten über einen Zeitraum von mehr als 54 Tagen beprobt. Wie bei den OECD- 309-Daten wurden die Halbwertszeiten anhand eines Abbaumodells erster Ordnung unter Berücksichtigung von «lag phases» berechnet. Wir berechneten die Dissipationshalbwertszeiten in Wasser ($DT_{50,w}$) auf der Grundlage der Rückstände der Verbindungen in der Wassersäule sowie die Abbauhalbwertszeiten des Gesamtsystems ($DT_{50,TS}$). Für letzteres wurden die Gesamtverbindungsrückstände in den Versuchsgefäßen als Summe der Rückstände der Ausgangsverbindung in der Wasserphase und im Sediment berechnet. Da sich sowohl das Studiendesign als auch die Datenauswertung in relevanten Aspekten von den Standard-OECD-308-Studien unterscheiden, werden sie im Folgenden als modifizierte Studien vom Typ OECD 308 bezeichnet.

Alle Studien vom Typ OECD 308 und 309 wurden durch abiotische und Sorptionskontrollversuche mit autoklavierten flüssigen und festen Proben ergänzt, um die Biotransformation von anderen möglichen Verlustprozessen zu unterscheiden.

Ergebnisse der Studien des Typs OECD 309. Was die Ergebnisse der OECD 309-Studien betrifft, so zeigten die sterilen Kontrollen, dass sowohl für Hydrochlorothiazid als auch für Irbesartan der beobachtete Substanzverlust hauptsächlich auf eine abiotische Transformation zurückzuführen war.

Die Ergebnisse der CMP1/10-Rührexperimente bestätigten frühere Ergebnisse, wonach die Verwendung von magnetischen Rührern, um das Sediment in Suspension zu halten, zu einer Zerkleinerung der Partikel und zu einer kontinuierlich erhöhten Sorption von Chemikalien führte, was die Unterscheidung zwischen Transformation und Sorption erschwerte. Folglich schlagen wir vor, dass das Halten von Sedimenten in Suspension in Studien des OECD 309-Typs eher durch orbitales Schütteln als durch Rühren erfolgen sollte.

Im Allgemeinen war der Abbau von Substanzen durch Biotransformation in Suspensionen mit erhöhtem Sedimentgehalt schneller. Die geringsten Substanzverluste wurden in CMP1 und R1-Fall beobachtet - nur sechs Substanzen wurden bis zum Ende dieser Experimente um bis zu 50 % abgebaut - während in R1-Spring, R10-Fall und CMP10 die meisten Substanzen einen beobachtbaren Abbau zeigten. Beobachtete Unterschiede in der Biotransformation zwischen R1-Fall und R1-Spring deuteten zudem darauf hin, dass die Zusammensetzung oder Aktivität der mikrobiellen Testgemeinschaften, die durch saisonale Schwankungen beeinflusst wird, auch das Ausmaß der Biotransformation beeinflussten. Neben den unterschiedlichen Ergebnissen zwischen den Studien beobachteten wir für die meisten Verbindungen drastische Unterschiede zwischen Wiederholungen derselben Studie ("Intra-Studien-Variabilität"). Ausnahmen stellen die Verbindungen Atenolol, Bezafibrat und Fenoxycarb dar, die nur geringe Variationen zwischen den Wiederholungen aufwiesen, was wahrscheinlich darauf zurückzuführen ist, dass ihre Biotransformation von Enzymen katalysiert wird, die unter Mikroorganismen weit verbreitet sind. Ein weiteres wichtiges Merkmal der Ergebnisse von Experimenten des Typs OECD 309 war die Beobachtung von «lag phases» in den meisten Konzentrations-Zeitreihen. Auch hier gab es einen Trend mit dem Sedimentgehalt, der im Allgemeinen auf kürzere «lag phases» bei Versuchen mit 10 g Feststoffen L-1 hinwies, insbesondere bei CMP10. Auch bei den «lag phases» beobachteten wir eine Variabilität zwischen Wiederholungen innerhalb einer Studie, welche bei R1-Spring am deutlichsten war.

Insgesamt zeigen unsere Ergebnisse, dass die Interpretation der OECD-309-Ergebnisse durch zwei Faktoren erschwert wird. Erstens werfen stark unterschiedliche Beobachtungen zwischen Wiederholungen innerhalb einer Studie die Frage auf, wie diese Variabilitäten berücksichtigt werden

können, wenn abgeleitete Halbwertszeiten mit Persistenz-Kriterien verglichen werden, die in gesetzlichen Rahmenwerken festgelegt sind. Zweitens ist in den derzeitigen Richtlinien nicht festgelegt, wie bei der Beurteilung der Persistenz eines Stoffes mit «lag phases» umzugehen ist, d.h. ob $DegT_{50,309}$ *oder* $DT_{50,309}$ *zu verwenden ist.* Da «lag phases» ein Zeichen für mikrobielle Anpassung sind und reduzierte «lag phases» für Verbindungen, die kontinuierlich oder wiederholt in die aquatische Umwelt freigesetzt werden, vermutet werden könnten, wurde argumentiert, dass $DegT_{50,309}$ als Persistenzmaß verwendet werden sollte. Unsere Experimente unterstützen diese Hypothese jedoch nicht direkt, da wir die kürzesten und am wenigsten variablen «lag phases» in Suspensionen mit einer mikrobiellen Gemeinschaft aus einer unberührten Umgebung (CMP10) bestimmt haben. *Daher und in Anbetracht des derzeitigen Mangels an Verständnis für die beobachtete Variabilität der* «lag phases» *scheint die Verwendung von* $DT_{50,309}$ *-Werten zur Bewertung der Persistenz der vorsichtigere und umweltschonendere Ansatz zu sein.*

Ergebnisse für Studien vom Typ OECD 308. In den modifizierten Studien vom Typ OECD 308 konnten wir das Verhalten von 42 Verbindungen in mindestens einer der beiden Sediment-Wasser-Systeme beobachten. 38 davon wurden eindeutig aus den Testsystemen entfernt, wobei Biotransformation höchstwahrscheinlich der dominante Abbauprozess für 36 Verbindungen war, während abiotische Transformation wiederum der vorherrschende Abbauprozess für die beiden Verbindungen Hydrochlorothiazid und Irbesartan zu sein schien. Es gab zwei sehr bemerkenswerte Unterschiede zwischen den Ergebnissen der modifizierten Studien vom Typ OECD 308 und den Ergebnissen der Studien vom Typ OECD 309. Erstens waren die Abweichungen zwischen Wiederholungen in den modifizierten Studien des Typs OECD 308 vernachlässigbar klein, obwohl jeder Konzentrations-Zeit-Punkt aus unabhängigen, parallel betriebenen Testgefässen stammte. Zweitens beobachteten wir kaum «lag phases», wobei nur eine Verbindung eine «lag phase» von mehr als 10 Tagen aufwies. Es war auch sehr interessant festzustellen, dass die aus den modifizierten Experimenten vom Typ OECD 308 abgeleiteten $DT_{50,TS,mod308}$-Werte für die meisten Prüfsubstanzen keine signifikanten Unterschiede zwischen der Rhein- und der CMP-Studie aufwiesen. Die Ausnahme bildeten drei künstliche Süßstoffe (Acesulfam, Cyclamat und Saccharin), die eine erhöhte Biotransformation in dem mit Rheinsediment inkubierten System aufwiesen. Die Konzentrations-Zeitreihen aus Experimenten mit Rhein- und CMP-Sedimenten ergaben, dass dieselben 11 Verbindungen am schnellsten abgebaut wurden, d.h., Fenoxycarb, Atenolol, Sulfamethoxazol, Bezafibrat, Trimethoprim, Trinexapac-ethyl, Valsartan, Levetiracetam, Iprovalicarb und Fenhexamid ($DT_{50,TS,mod308}$ ≤10 Tage) und dieselben fünf Verbindungen am langsamsten abgebaut wurden, d.h. Aliskiren, Atazanavir, Citalopram, Carbamazepin und Lamotrigin. Letztere sind größtenteils Verbindungen, die ein starke Sorption aufweisen - bei Aliskiren, Atazanavir, Citalopram, Azoxystrobin, sowie bei Sitagliptin und Lamotrigin im Falle des CMP-Sediments, wurde bis zum Ende der Biotransformationsexperimente eine Akkumulation von >70 % der ursprünglich aufgestockten Substanzmasse in der Sedimentschicht beobachtet.

Für 19 Verbindungen war ein Vergleich zwischen den Ergebnissen von Standard-OECD-308-Studien und den hier durchgeführten modifizierten OECD-308-Typ-Studien möglich. Der auffälligste Unterschied war, dass die aus den Standard-OECD-308-Studien abgeleiteten $DT_{50,TS,std308}$-Werte in der Regel höher waren, unabhängig davon ob bei den Standard-OECD-308-Studien der NER als Ausgangsverbindung betrachtet wurde oder nicht. Wir interpretieren diese Unterschiede zwischen den Standard- und den modifizierten Studien so, dass sie hauptsächlich auf den höheren Sedimentgehalt und die geringere Homogenität der Sedimentschicht in den Standardstudien zurückzuführen sind, d. h. auf ein Sediment-Wasser-Verhältnis von 1:3 oder 1:4 (v/v) im Vergleich zu den modifizierten Studien mit einem Sediment-Wasser-Verhältnis von 1:10 (v/v). In der Tat waren bei mehr als der Hälfte der Verbindungen, für die regulatorische Daten verfügbar waren, zu Zeitpunkten, die mit dem Ende der modifizierten OECD 308-Studien übereinstimmten, mehr als 70 % der ursprünglichen Masse der Verbindung an das Sediment sorbiert (teilweise irreversibel).

Im Einklang mit den Zielen dieses Projekts haben wir die Standard-Halbwertszeiten ($DT_{50,w,mod308}$ und $DT_{50,TS,mod308}$) durch die Ableitung von $k'_{bio,lab}$ ergänzt, das dann auch zur Berechnung der kompartimentspezifischen Transformationshalbwertszeiten, d.h. $DegT_{50,w,mod308}$ und $DegT_{50,sed,mod308}$, verwendet wurde. $k'_{bio,lab}$ wurde nur aus den modifizierten OECD 308-Experimenten abgeleitet, da die große Variabilität zwischen den Wiederholungen und die langen «lag phases», die in den Studien des OECD 309-Typs beobachtet wurden, die Ableitung von $k'_{bio,lab}$ aus den letzteren Daten fragwürdig machten. Für die Ableitung von $k'_{bio,lab}$ aus Daten der modifizierten OECD 308-Experimente haben wir das Modellierungskonzept von Honti et al. (2016) angepasst, welches Transformations- und Sorptionsprozesse in einem Zwei-Kompartiment-System beschreibt. Insbesondere nahmen wir aufgrund der relativ dünnen Sedimentschicht und der konstanten Belüftung der Wassersäule während der Experimente des modifizierten OECD 308-Typs an, dass die Sedimentschicht vollständig aerob ist. Wir verwendeten Bayes'sche Parameterschätzung, um das Modell für einzelne Rhein- und CMP-Experimente separat und für beide Experimente gemeinsam zu kalibrieren. Die gemeinsame Anpassung wurde durchgeführt, um zu überprüfen, ob das Modell die experimentellen Daten aus beiden Biotransformationsstudien mit einem Satz substanzspezifischer Parameter anpassen kann.

Wie bereits bei den $DT_{50,TS,mod308}$ -Werten beobachtet, waren die aus den Daten der Rhein-Experimente abgeleiteten mittleren $k'_{bio,lab}$-Werte höher als die aus den Daten der CMP-Experimente abgeleiteten. Dennoch war es möglich, für 38 Verbindungen $k'_{bio,lab}$-Werte abzuleiten, die für beide Experimente gültig waren. In Übereinstimmung mit früheren Ergebnissen für eine begrenzte Anzahl von Verbindungen ergab der Vergleich der individuellen Kalibrierung mit der gemeinsamen Kalibrierung, dass die gemeinsame Modelllösung statistisch vorzuziehen war und dass die aus der gemeinsamen Kalibrierung abgeleiteten $k'_{bio,lab}$-Werte erheblich weniger unsicher waren als die Werte aus individuellen Kalibrierungen.

Vergleich der Halbwertszeiten in verschiedenen Testsystemen und zwischen verschiedenen Halbwertszeitindikatoren. Auf der Grundlage aller verfügbaren Ergebnisse haben wir die verschiedenen Dissipations- und Abbauhalbwertszeiten verglichen, die auf der Grundlage von Studien vom Typ OECD 309 sowie von Standard- und modifizierten Studien vom Typ OECD 308 berechnet wurden. Die wichtigsten Ergebnisse lauten wie folgt:

1. Der Vergleich der Dissipationshalbwertszeiten mit den Abbauhalbwertszeiten bestätigt, dass die Dissipationshalbwertszeiten in Wasser ($DT_{50,w}$) in den meisten Fällen deutlich kürzer waren als die Abbauhalbwertszeiten in Wasser ($DegT_{50,w}$). Eine Persistenzbewertung auf der Grundlage von $DT_{50,w}$ wäre daher weniger konservativ, erscheint aber nicht gerechtfertigt, da $DT_{50,w}$ den stark systemspezifischen Phasentransfer und die wahrscheinlich universelleren Transformationsprozesse in einen Topf wirft. Vielmehr sollte die Persistenzabschätzung in Wasser auf der Basis von $DegT_{50,w}$ erfolgen, welche ausschließlich die Entfernung der Verbindung aus der Wasserphase durch Biotransformation beschreibt.

2. Im Allgemeinen schien die Biotransformation in Standard- und modifizierten OECD 308-Typ- Studien stabiler zu sein als in Suspensionsversuchen, was durch kurze «lag phases» und geringe Variabilitäten innerhalb der Studien belegt wird. Vergleicht man den beobachteten Substanzverlust aus Standard- und modifizierten OECD 308-Typ-Studien, so scheint die Biotransformation in modifizierten Systemen verstärkt zu sein. Unsere Ergebnisse deuten darauf hin, dass dies höchstwahrscheinlich darauf zurückzuführen ist, dass (i) die Verbindungen im modifizierten System aufgrund des höheren Wasser-Sediment-Verhältnisses besser bioverfügbar sind, und (ii) größere Teile des Sediments in den modifizierten im Vergleich zu den Standardstudien vom Typ OECD 308 mit Sauerstoff angereichert sind, was zu einer verbesserten Homogenität im Sedimentkompartiment der modifizierten Studien vom Typ OECD 308 führt. Betrachtet man die Ergebnisse der OECD

309-Studien und vergleicht die Ergebnisse der modifizierten OECD 308-Studien mit denen der Standard-OECD 308-Studien, so kommt man zu dem Schluss, dass die modifizierten OECD 308-Studien im Vergleich zu den bestehenden OECD 309- und OECD 308-Studien eine bessere Interpretierbarkeit aufweisen und am besten geeignet zu sein scheinen, Informationen über die aerobe Biotransformation zu liefern. Bei der Standardisierung der Versuchsbedingungen, um ein klares Signal für die aerobe Biotransformation zu erhalten, muss jedoch berücksichtigt werden, dass die Variabilität in realen Umgebungen (z. B. das Vorhandensein von anaeroben Redoxbedingungen in tieferen Sedimentschichten oder unter stagnierenden oder eutrophierten Bedingungen) durch diese Versuchsanordnung nicht abgedeckt wird.

Studie im Rheineinzugsgebiet zur Bewertung der Biotransformation im Feld

Analysemethoden und Modellierungsansatz. Um die Biotransformation im Feld zu bewerten, wurde das Rheineinzugsgebiet als Fallstudie verwendet. Zu diesem Zweck konnten wir Proben verwenden, die im Rahmen der SMPC-Kampagne (*Sondermessprogramm Chemie*) der IKSR (Internationale Kommission zum Schutz des Rheins) genommen wurden. Konkret haben wir Proben aus zwei Wasserpaketen verwendet, die während zweier Jahreszeiten im Jahr 2017 (P1: März bis April, P3: Juli) rheinabwärts verfolgt und an 14 Stellen im Rhein beprobt wurden, sowie Proben aus 6 großen Zuflüssen für dieselben Jahreszeiten. In diesen Proben haben wir 36 Stoffe quantifiziert, für die eine kontinuierliche und konstante Emission aus Kläranlagen in den Rhein angenommen werden konnte und für die wir aufgrund früherer Messungen oder des Verbrauchs ein nachweisbares Vorkommen im Rheineinzugsgebiet erwarteten. Von diesen Stoffen überschnitten sich 28 mit Stoffen, für die in diesem Projekt ebenfalls Biotransformationsdaten in Laborsimulationsstudien generiert worden waren. Die Quantifizierung erfolgte mittels HPLC-MS/MS unter Verwendung eines Triple-Quad-Massenspektrometers, das für 14 Verbindungen Bestimmungsgrenzen unter 1 ng L^{-1} und für die meisten Analyten (35 Verbindungen) unter 10 ng L^{-1} ergab. Die höchsten LOQs wurden bei 50 ng L^{-1} für Oxypurinol und Benzotriazol festgestellt. Die gemessenen Konzentrationen wurden durch Multiplikation mit den während der jeweiligen Probenahmekampagnen gesammelten Abflussdaten in Massenflüsse umgerechnet.

Für die Schätzung der Biotransformationsratenkonstanten im Rheineinzugsgebiet haben wir ein zuvor entwickeltes Modell verwendet, das die Schätzung einer durchschnittlichen, bioverfügbaren und Biomassen-normalisierten Biotransformationsratenkonstante ($k'_{bio,field}$) durch Kalibrierung anhand gemessener Stoffflüsse ermöglicht. Da frühere Durchläufe des Modells starke Wechselwirkungen zwischen $k'_{bio,field}$ und zwei anderen Parametern gezeigt hatten, die gleichzeitig kalibriert werden (k_{esc}, das die Emissionen charakterisiert, und K_{oc}, welcher das Sorptionsverhalten beschreibt), wurde in diesem Projekt besonderes Augenmerk auf die verbesserte Schätzungen für diese beiden Parameter gelegt. Für K_{oc} wurde dies durch die Durchführung spezieller Sorptionsexperimente für die untersuchten Verbindungen und eine Reihe von relevanten Sedimenten erreicht. Der "Entweichungsfaktor", k_{esc}, ist ein dimensionsloser Faktor, der den Anteil der vermarkteten Wirkstoffe beschreibt, der in das Fließgewässernetz gelangt. Er wurde als Verhältnis zwischen den vermarkteten Pro-Kopf-Mengen und den Abwasserflüssen aus Kläranlagen berechnet und ermöglicht somit die Berücksichtigung länder- und jahresspezifischer Verbrauchsdaten bei der Berechnung der Stoffemissionen in den Rhein. Für die Schätzung von k_{esc} wurden die jährlichen Verbrauchsdaten von Arzneimitteln für Deutschland (für den Zeitraum 2010- 2018) und die Schweiz (für 2014-2016) verwendet, die von IQVIA zur Verfügung gestellt wurden. Für einige Wirkstoffe konnten wir dank der vierteljährlichen Verkaufsdaten auch jährliche und saisonale Trends untersuchen. Zur Berechnung der Abwasserflüsse aus Kläranlagen wurden die gemessenen Abwasser-Konzentrationen aus drei Schweizer und zwei deutschen (Baden-Württemberg, Nordrhein-Westfalen) Überwachungskampagnen herangezogen und mit

den verfügbaren Einleitungsdaten multipliziert. Die Qualität dieser Daten war unterschiedlich, da die Schweizer Daten meist aus Mischproben stammten, während die deutschen Daten meist aus Stichproben gewonnen wurden. Während die meisten Kampagnen eher kurze Zeiträume von einigen Wochen bis zu einigen Monaten abdecken, erstreckte sich eine Kampagne über einen Zeitraum von mehr als 10 Jahren.

Das verwendete Rheinmodell basiert auf Flussabschnitten, in denen die Verteilung und Umwandlung als Funktionen der physikalischen Eigenschaften des Abschnitts und der Sorptions-/Biotransformationseigenschaften des Wirkstoffs beschrieben wird. Das Verhalten der Wirkstoffe im gesamten Einzugsgebiet wird dann simuliert, indem mehrere Flussabschnitte entsprechend der Topologie des Flussnetzes miteinander verbunden werden. Dieses Modell wurde in einem Kalibrierungsverfahren verwendet, wobei das Modell versucht, den simulierten Massenfluss an die Beobachtungen aus den SMPC-Kampagnen anzupassen, indem es die Parameter k_{esc}, K_{oc} und $k'_{bio,field}$ anpasst. Wir verwendeten wiederum Bayes'sche Parameterschätzung statt, um das Modell zu kalibrieren. Dadurch erhielten wir (i) das angepasste Flussprofil für den Rhein und (ii) Verteilungen für alle drei kalibrierten Parameter, einschließlich $k'_{bio,field}$.

Da der Ansatz der expliziten Modellierung offensichtlich ein kompliziertes Modell erfordert, das auf verschiedenen, schwer zu beweisenden Annahmen über die physikalischen Eigenschaften der einzelnen Flussabschnitte aufbaut und bis zu einem gewissen Grad unter der schwachen Identifizierbarkeit der Parameter leidet, haben wir auch das alternative Konzept des Benchmarking zur Ableitung von Geschwindigkeitskonstanten ausprobiert. Beim Benchmarking wird das Verhalten einer bestimmten Verbindung von Interesse im Vergleich zu einer Benchmark-Verbindung bewertet, von der angenommen wird, dass sie sich nicht umwandelt, dieselben Prozesse des Verbleibs (z. B. Sorption) durchläuft und ähnliche Emissionsmuster aufweist. Um das Benchmarking auf unsere Daten anzuwenden, haben wir einen bereits bestehenden Benchmarking-Ansatz für Seen (Zou et al. 2014) konzeptionell erweitert, um ihn auf Flusssysteme anwenden zu können.

Geschätzte Biotransformationsratenkonstanten im Feld. Die Verbrauchsdaten zeigten länderspezifische Unterschiede für einige Verbindungen (z.B. Metoprolol, Mefenaminsäure) sowie saisonale Trends für Clarithromycin (Antibiotikum, erhöhter Verbrauch im ersten Quartal des Jahres), Fexofenadin (zur Behandlung von Allergiesymptomen, erhöhter Verbrauch im zweiten Quartal des Jahres) und Phenazon (möglicherweise auch aufgrund der Verwendung als Tierarzneimittel). Die Entweichungsfaktoren waren in der Schweiz und in Deutschland für die meisten Verbindungen ähnlich, was aufgrund der recht ähnlichen Abwasserbehandlungstechnologien auch zu erwarten war. Leider wiesen die Schätzungen der Entweichungsfaktoren in den fünf beteiligten Studien immer noch eine recht große Variabilität zwischen den einzelnen Proben auf, was sich letztlich in einer Unsicherheit bei der Schätzung der Biotransformationsratenkonstanten im Feld niederschlug. Diese Variabilität konnte nur als Zufall betrachtet werden, da wir keine signifikanten deterministischen Beziehungen zwischen den Entweichungsfaktoren und potenziellen Einflussfaktoren, die durch Daten abgedeckt wurden, wie z. B. die Größe der Kläranlage und die Jahreszeit, fanden. Zu den potenziellen Unsicherheitsquellen für die Schätzung der Entweichungsfaktoren gehörten das Fehlen vierteljährlicher Verbrauchsdaten, Interpolationen oder Extrapolationen für Jahre ohne Verbrauchsdaten, fehlende Abwassereinleitungsdaten für den Beobachtungszeitraum, Unsicherheiten bei den angeschlossenen Einwohnern pro Kläranlage und andere Eintragsquellen als die Kläranlage (z. B. über Regenwasserüberläufe oder aus Produktions- und Formulierungsanlagen).

Bei der Kalibrierung erzielte das Modell im Allgemeinen gute Übereinstimmungen mit den aus den SMPC-Proben abgeleiteten Massenflüssen. Auch die resultierenden Verteilungen von $k'_{bio,field}$ zeigten, dass dieser Abbauparameter zweiter Ordnung aus Felddaten geschätzt werden kann, wobei der Interquartilsbereich in der Regel weniger als eine Größenordnung abdeckt. Die

extremen Quantile (außerhalb des Interquartilsbereichs) lagen jedoch oft bei 3-4 Größenordnungen. Im Großen und Ganzen überlappten die Verteilungen von $k'_{bio,field}$ zwar bis zu einem gewissen Grad zwischen den einzelnen Verbindungen, wiesen aber dennoch signifikante Unterschiede zwischen Untergruppen von Verbindungen auf. Daher wurde erwartet, dass ein Vergleich mit experimentellen Werten, die in Laborexperimenten ermittelt wurden, zumindest qualitative Ähnlichkeiten zwischen der Persistenz im Labor und im Rheineinzugsgebiet aufzeigen könnte.

Interessant war auch, dass für viele Verbindungen $k'_{bio,field}$ in P3 (Juli 2017) höher war als in P1 (März - April 2017). Für die Phototransformation wurde der Effekt der erhöhten Einstrahlung in P3 direkt im Modell berücksichtigt, und der Unterschied in $k'_{bio,field}$ zwischen P3 und P1 sollte daher hauptsächlich auf eine erhöhte Biotransformation zurückzuführen sein. Diese Effekte könnten direkt in Form einer höheren Bioaktivität aufgrund der höheren Temperatur oder indirekt in Form spezifischer Veränderungen der mikrobiellen Gemeinschaft während des Sommers auftreten, doch fehlten uns zusätzliche Informationen, um diese Annahmen zu prüfen.

Wir haben auch $k'_{bio,field}$-Werte in Halbwertszeiten umgerechnet, indem wir mittlere charakteristische Eigenschaften eines Flussabschnitts angenommen haben, der den "durchschnittlichen Rhein" von der Aaremündung bis Lobith repräsentiert. Die auf diese Weise berechneten Halbwertszeiten für das Gesamtsystem reichten für die verschiedenen Verbindungen von einer halben Stunde bis zu Tausenden von Tagen, während die Halbwertszeiten im Wasser den Bereich von 10 Stunden bis zu mehr als 10 000 Tagen abdeckten. In Anbetracht der Wasseraufenthaltszeit im Rhein (weniger als 9 Tage, durchschnittlich 4-5 Tage in allen Wasserparzellen des Rheineinzugsgebiets) deuten diese Zahlen darauf hin, dass die meisten Verbindungen im Hauptkanal des Rheins nur sehr begrenzt oder gar nicht abgebaut werden. Das Modell deutet vielmehr darauf hin, dass die Biotransformation hauptsächlich in kleinen bis mittelgroßen Flüssen stattfindet, da diese (i) den größten Teil der Emissionen aufnehmen (die meisten Kläranlagen befinden sich an kleinen und mittelgroßen Flüssen), (ii) weniger Wasser pro Einheit Sedimentoberfläche haben, was in Übereinstimmung mit der k'_{bio}-Hypothese die Gesamthalbwertszeit des Systems verringern sollte, und (iii) ihr Sediment aufgrund der schwächeren Resuspensionskapazität der flacheren Strömung wahrscheinlich länger sedimentiert bleibt.

Benchmarking auf der Grundlage von Felddaten. Das Benchmarking-Modell ergab für die meisten Verbindungen akzeptable Übereinstimmungen mit den beobachteten relativen Konzentrationsverhältnissen. Dennoch erwiesen sich die distanz-spezifischen Ratenkonstanten aus dem Benchmarking-Verfahren als ebenso unsicher wie $k'_{bio,field}$. Die beiden Verfahren haben jedoch keine gemeinsamen Annahmen, so dass sie möglicherweise frei von den systematischen Fehlern des jeweils anderen sind. Eine Umrechnung der distanz-spezifischen Ratenkonstanten in Halbwertszeiten ($DL_{50,benchmark}$) unter Verwendung der mittleren Fliessgeschwindigkeit ergab, dass mit dem Benchmarking-Verfahren Halbwertszeiten im Rhein zwischen etwa einem halben und sechzig Tagen bestimmt werden können. Die Berechnung von Halbwertszeiten aus distanzspezifischen Ratenkonstanten wirkt sich auf die Verbindungen je nach ihren Sorptionseigenschaften unterschiedlich aus. Stark sorbierende Verbindungen werden vermutlich aufgrund ihrer stärkeren Affinität zum Eintritt in das Flussbett langsamer transportiert, so dass ihre Halbwertszeiten möglicherweise unterschätzt werden. Die Nützlichkeit des Benchmarking wird daher durch die Notwendigkeit einer Benchmark-Verbindung eingeschränkt, die den physikalisch-chemischen Eigenschaften der Zielverbindungen stark ähnelt und nicht umgewandelt wird. Auf der Grundlage der unabhängig ermittelten Halbwertszeiten aus dem Benchmarking scheint $DT_{50,TS,mod308}$ eine konservative Schätzung der Dissipation im Feld zu sein, aber es besteht nur eine geringe Korrelation zwischen $DL_{50,benchmark}$- und $DT_{50,TS,mod308}$-Werten.

Vergleich der Biotransformation in Laborsystemen und im Rheineinzugsgebiet

Daten aus Simulationsstudien zur Biotransformation, insbesondere aus modifizierten Studien vom Typ OECD 308, und aus der Feldstudie im Rheineinzugsgebiet ermöglichten die Ableitung verschiedener Persistenzindikatoren, d. h. verschiedener Halbwertszeiten und k'_{bio}-Werte, die jeweils auf spezifische Weise die Abbaubarkeit einer Verbindung beschreiben. Diese Daten wurden daher verwendet, um der Frage nachzugehen, welche dieser Indikatoren am besten geeignet sind, die Ergebnisse von Laborstudien mit dem Verhalten von Stoffen in einem realen, großräumigen System wie dem Rheineinzugsgebiet in Beziehung zu setzen. Zu diesem Zweck haben wir Halbwertszeiten und k'_{bio} -Werte, die aus modifizierten Experimenten vom Typ OECD 308 abgeleitet wurden, direkt mit Werten verglichen, die aus der Feldstudie im Rheineinzugsgebiet abgeleitet wurden, und zwar sowohl in Bezug auf absolute als auch auf relative Werte. Im Folgenden wird nur der Vergleich auf der Grundlage von aus P3-Daten abgeleiteten Geschwindigkeitskonstanten erörtert, da die Wassertemperaturen im Rhein während der P3- Kampagne (Juli 2017) mit den Temperaturen während der Biotransformationssimulationsstudien vergleichbar waren und weil die P3-Daten für die meisten Verbindungen ein deutlicheres Biotransformationssignal erkennen ließen.

Zunächst verglichen wir die Halbwertszeiten für die Dissipation $DT_{50,w.mod308}$, die in modifizierten Studien vom Typ OECD 308 mit Inokulum aus dem Rhein beobachtet wurden, mit den Halbwertszeiten für den Abbau $DegT_{50,w,field}$ aus der P3-Kampagne. Diese beiden Parameter zeigten in der Tat eine statistisch signifikante, mäßige Korrelation (R^2 = 0,5, Pearson's r = 0.71) und streuten um die 1:1-Linie. Wir stellten jedoch fest, dass mehrere Verbindungen kürzere $DT_{50,w.mod308}$ als $DegT_{50,w,field}$ aufwiesen, und dass dies insbesondere bei Verbindungen mit höheren K_{oc}-Werten der Fall war. *Dies bestätigt die Erkenntnisse aus dem Vergleich von Dissipations- und Abbauhalbwertszeiten aus Laborstudien. Die Verwendung von $DT_{50,w,mod308}$ als Persistenzindikator kann zu einer Unterschätzung der Umweltpersistenz einer Verbindung führen, die mit zunehmenden K_{oc}-Werten steigt.*

Als Nächstes verglichen wir die für die modifizierten Studien vom Typ OECD 308 berechneten Abbauhalbwertszeiten $DegT_{50,w,mod308}$ mit Inokulum aus dem Rhein mit den aus der P3-Kampagne abgeleiteten Abbauhalbwertszeiten $DegT_{50,w,field}$. In diesem Fall wurden beide Abbauhalbwertszeiten - im Labor und im Feld - auf der Grundlage der jeweiligen k'_{bio}-Werte der Verbindungen berechnet. Die beiden Parameter zeigten eine statistisch signifikante Korrelation mit einer recht hohen erklärten Varianz (R^2 = 0,79, Pearson's r = 0.89). Dementsprechend fanden wir bei einem direkten Vergleich der $k'_{bio,lab}$- Werte aus modifizierten Studien vom Typ OECD 308 mit Rhein-Inokulum ($k'_{bio,lab,R}$) mit den $k'_{bio,field}$- Werten, die aus P3-Daten abgeleitet wurden, ebenfalls eine statistisch signifikante Korrelation, jedoch mit etwas geringerer erklärter Varianz (R^2 = 0,5, Pearson's r = 0.71). In absoluten Zahlen war der Abbau im Feld jedoch für alle Verbindungen schneller als der Abbau im Laborsystem mit Rheininokulum. Diese Ergebnisse stimmen mit früheren Ergebnissen derselben Autoren für eine viel kleinere Gruppe von Verbindungen überein (Honti et al. 2018). Dieser absolute Unterschied von oft mehr als einer Größenordnung zwischen Feld- und Laborsystemen kann auf tatsächliche Unterschiede in der Aktivität der mikrobiellen Biomasse zwischen dem Labor- und dem Feldsystem zurückzuführen sein, aber auch auf die Verwendung des TOC als sehr grobe Annäherung an die Biomasse. *Dennoch deutet die gute Qualität der Korrelationen darauf hin, dass k'_{bio}-Werte oder daraus abgeleitete Abbauhalbwertszeiten tatsächlich die Übertragung von Labor- auf Feldwerte unterstützen können. Die Korrelation könnte mit einer präziseren Messung der aktiven oder gar abbauenden Biomasse in aquatischen Systemen weiter verbessert werden.*

Da sich die Halbwertszeiten für den Abbau im Gesamtsystem ($DT_{50,TS}$) leichter aus den Laborstudien vom Typ OECD 308 ableiten lassen als die Abbauhalbwertszeiten im Wasser, welche die Auswirkungen des Phasentransfers zwar vollständig ausschliessen, deren Bestimmung aber eine kompliziertere inverse Modellierung erfordert, haben wir schließlich auch die Halbwertszeiten für den Abbau im Gesamtsystem ($DT_{50,TS,mod308}$), die für die modifizierten Studien vom Typ OECD 308 mit Inokulum aus dem Rhein berechnet wurden, mit den Halbwertszeiten für den Abbau im Gesamtsystem ($DegT_{50,TS,field)}$ verglichen, die aus der P3-Kampagne abgeleitet wurden. Daraus ergab sich eine statistisch signifikante, moderate Korrelation (R^2 =0,41, Pearson's r= 0.64). In Übereinstimmung mit den obigen Ergebnissen für die Abbauindikatoren haben wir auch wiederum festgestellt, dass die $DT_{50,TS,mod308}$-Werte im Allgemeinen höher sind als die $DegT_{50,TS,field}$-Werte, und zwar im Durchschnitt um etwa eine Größenordnung.

Insgesamt gibt es keine allgemeingültige Antwort auf die Frage, wie gut die aus Laborstudien abgeleiteten Persistenzindikatoren das beobachtete Abbauverhalten im Feld vorhersagen können. Wir können dies im Bezug auf grobe Kategorien, relativem und absolutem Verhalten betrachten. Was die Kategorien anbelangt, so erwiesen sich Verbindungen, die in den Laborsimulationsstudien durchweg als schwer abbaubar eingestuft wurden, auch im Feld als persistent. In ähnlicher Weise zeigten Verbindungen, die in den Laborsimulationsstudien durchweg in hohem Maße abgebaut wurden, während der P3-Kampagne auch im Feld einen deutlich beobachtbaren Abbau. In Bezug auf das relative Verhalten ergaben die aus den modifizierten OECD 308-Testsystemen abgeleiteten Gesamtsystem-Halbwertszeiten sowie die k'_{bio}-Werte mäßige, statistisch signifikante Korrelationen zwischen Labor- und Felddaten. *Interessanterweise waren die Korrelationen stärker, wenn die Persistenzindikatoren auf der Grundlage des k'_{bio}-Konzepts abgeleitet wurden, was darauf hindeutet, dass k'_{bio} und die daraus abgeleiteten Halbwertszeiten in der Tat eine genauere Übersetzung zwischen Labor- und Feldhalbwertszeiten ermöglichen, zumindest in relativer Hinsicht, als die Halbwertszeiten für den Gesamtsystemabbau.* Der absolute Vergleich zwischen den aus Laborexperimenten abgeleiteten Persistenzindikatoren und der Feldstudie deutet darauf hin, dass die Biotransformation in den modifizierten Experimenten vom Typ OECD 308 generell langsamer verläuft als für das Rheineinzugsgebiet modelliert. Dieser absolute Unterschied könnte jedoch auch aus der Tatsache resultieren, dass die mikrobielle Abbauaktivität nicht mit dem TOC-Wert skaliert. *Wir empfehlen daher, weitere Methoden zur verbesserten Charakterisierung der aktiven oder abbauenden Biomasse zu erforschen, um das k'_{bio}-Konzept neu zu bewerten, da es das theoretische Potenzial hat, die Abschätzung der Persistenz im Feld aus laborgestützten Simulationsstudien weiter zu verbessern.*

1 Introduction

Synthetic substances entering surface water bodies bear the potential to harm the aquatic environment. Chemicals that are persistent, i.e., recalcitrant toward biotic and abiotic degradation, are of special concern as they can distribute widely, reach high concentrations, and result in environmental exposure that is difficult to control and reverse (Cousins et al. 2019; Boethling et al. 2009). It is therefore crucial to easily and robustly assess persistence of chemicals in laboratory experiments to ideally prevent the release of persistent chemicals into the environment. Unfortunately, the relationship between persistence estimates derived from laboratory experiments and actual persistence in the field is often unclear, particularly in the case of microbial biotransformation (McLachlan, Zou, and Gouin 2017). To remedy this translation gap, there is a need to (i) better understand how biotransformation observed in laboratory experiments compares to biotransformation in the field, and (ii) to define data evaluation procedures that help relating outcomes of laboratory-based studies to compound behavior in the field.

Today, persistence assessment of organic chemicals is an integral part of many international regulatory frameworks. In Europe, for example, chemical regulations aim to protect human and environmental health through early identification of chemicals with hazardous properties, and prescribe how to assess a chemical's persistence based on half-lives derived from standardized OECD transformation simulation studies (EFSA 2014; CHMP 2006; EP&C 2006). Two OECD test guidelines are relevant for chemicals that are not readily biodegradable and may enter surface waters: the OECD 308 test guideline, which targets transformation in aquatic water/sediment systems, and the OECD 309 test guideline, which assesses transformation in the pelagic water body (OECD 2002, 2004).

However, since the introduction of both guidelines, professionals in industry and academia involved in biotransformation and persistence assessment have been raising concerns regarding the performance and environmental relevance of those so-called simulation studies (Honti and Fenner 2015; Shrestha et al. 2016; McLachlan, Zou, and Gouin 2017). OECD 308 biotransformation experiments are to be carried out in the dark under stagnant conditions with a 2-3 cm thick sediment layer covered by a shallow water column to yield a water-sediment ratio of 3:1 to 4:1 (v/v) (OECD 2002). Major points of criticism refer to (i) the recommended water-sediment ratio, which does not reflect conditions in most natural surface water bodies and shifts compound mass distribution excessively toward the sediment phase, and (ii) a lack of standardization which leads to variability in test conditions (e.g. redox conditions in the sediment layer, system geometry) (Shrestha et al. 2016; Honti and Fenner 2015; Honti et al. 2016; Coll et al. 2020). OECD 309 studies are carried out in natural water without or with some suspended sediment (OECD 2004). This test system is being criticized for its vaguely standardized test conditions (e.g., pelagic/ suspension test, light/ dark) (Honti et al. 2018), and its highly variable outcomes (Seller et al. 2020).

Shrestha et al. (2016) suggested that some of the aforementioned shortcomings of OECD 308 studies could be addressed by increasing the water-sediment ratio and by ensuring full aeration and some agitation of the test system. While the former was expected to shift the compound mass from being sorbed to sediment more towards the aqueous phase and hence increase the fraction of compounds being available for degradation, the latter modification, in combination with a thinner sediment layer, was expected to reduce anoxic zones in the sediment and hence increase reproducibility and interpretability of the observed transformation signal. Indeed, for four test compounds, both mineralization and the ratio of CO_2 to non-extractable residues (NER) in the sediment were increased in such a modified OECD 308-type experiment, suggesting that

contact of the compounds with sediment was more likely to lead to biotransformation than to (irreversible) sorption (Shrestha et al. 2016). These results indicated that the modified setup allowed for improved observation of biotransformation. However, the study was limited to only four compounds whose test concentrations were far above levels commonly measured in the aquatic environment, which may significantly alter biotransformation kinetics (Hammershøj et al. 2019; Li and McLachlan 2019). Therefore, the behavior of such a modified OECD 308-type experimental setup should be evaluated further with a broader set of test compounds at environmentally relevant concentration levels.

While changing the design of experimental test systems might improve their interpretability and repeatability, it will not answer the question of how and to what extent outcomes of such laboratory studies relate to observations of degradation in actual field situations. Indeed, guidance on how to translate outcomes of biotransformation simulation studies to predict a compound's actual biotransformation behavior in the environment is mostly missing (Honti and Fenner 2015; Honti et al. 2016). In the context of regulatory persistence assessment, today's common practices stipulate the derivation of half-lives from laboratory tests. Indeed, half-lives derived from OECD 309 pelagic simulation studies at low compound concentration levels were shown to reasonably represent compound behavior in a deep lake with little exchange between water body and sediment layer (Li and McLachlan 2020). In rivers, in contrast, half-lives depend on the hydraulic exchange between stream channel and sediment and vary greatly even within one stream (Radke and Maier 2014; Jaeger, Posselt, et al. 2019). Also, it is important to note that dissipation half-lives (DT_{50}) derived from biotransformation studies in water-sediment systems, lump together transformation and phase transfer processes, and are dependent on the geometry of the experimental system, the sediment-water ratio and the physicochemical properties of the employed water and sediment (Honti and Fenner 2015). As a consequence, it remains unclear to what extent DT_{50} values derived from laboratory experiments predict compound behavior in actual river systems.

One method that is increasingly being highlighted and discussed as potentially helpful in overcoming some of the issues involved in interpreting degradation behaviour across systems is the so-called benchmarking approach (McLachlan, Zou, and Gouin 2017). The hypothesis behind benchmarking is that the relative degradation behaviour between chemicals is more conserved than absolute measures of persistence, which are influenced by a number of system-specific factors such as biomass concentration and activity, temperature, solid phase concentrations and many more. Assuming that assumption to be true, benchmarking could support persistence assessment in at least two ways. First, when attempting to evaluate degradation in the field, cumbersome mass balance considerations may be circumvented by evaluating a compounds concentration relative to an appropriate stable benchmark (Zou, MacLeod, and McLachlan 2014; Zou, Radke, Kierkegaard, and McLachlan 2015; Zou, Radke, Kierkegaard, MacLeod, et al. 2015). Second, it might be assumed that chemicals would exhibit equal relative persistence or at least equal rank order of persistence in laboratory study setting and in the field. Hence, benchmarking could potentially help to translate outcomes of laboratory studies into behaviour in the field. However, all of the potential applications described above rely on the assumption that system-specific differences influencing the observed DT_{50} (i.e., phase transfer, bioavailability etc.) are filtered out by comparing the compound's behavior to the behavior of a benchmark chemical. This seems at best questionable given that different chemicals show different responses to system-specific differences such as the water-sediment ratio, pH, temperature etc.

In order to eliminate some of the most influential system-specific differences affecting biotransformation kinetics in water-sediment systems, Honti et al. (2016) introduced a data evaluation framework that derives a second-order biotransformation rate constant (k'_{bio}) from

biotransformation study outcomes. k'_{bio} is corrected for the substance's bioavailability, assuming that only compound mass that is not adsorbed to sediment particles is available for biotransformation, and thus allows disentangling biotransformation from phase transfer processes and bioavailability limitations. Further, k'_{bio} is normalized to the amount of organic carbon in the sediment and water compartment, taking, (i) the organic carbon as a proxy that is assumed to be proportional to degrader biomass, and (ii) assuming a compound's potential for biotransformation to depend on its contact with degrader biomass. It has been suggested that such a bioavailability-corrected and biomass-normalized second-order rate constant is a more robust indicator of a substance's biotransformation potential. Thus, k'_{bio} could allow unifying observations from different water-sediment systems, including OECD 308/ 309 tests and natural rivers; at least indirectly by using k'_{bio} as a parameter to compare a compound of interest with a selected benchmark chemical (Honti et al. 2016; Honti et al. 2018).

So far, it has been demonstrated that it was indeed possible to derive bioavailability-corrected and biomass-normalized second-order rate constants that validly described biotransformation across different laboratory test systems ($k'_{bio,lab}$), i.e., OECD 308/ 309 studies, for three exemplary compounds (Honti et al. 2016). Subsequent attempts to compare $k'_{bio,lab,308}$ values derived from standard OECD 308 tests to $k'_{bio,field}$ values inferred from field observations in the Rhine catchment remained inconclusive (Honti et al. 2018). This was partly attributed to the limited number of compounds, i.e., four, for which this comparison was possible, but partly also to the large uncertainties of the $k'_{bio,field}$ estimates. To actually derive a compound's $k'_{bio,field}$ values from concentration patterns measured in a river system, its emission rates into the river system, as well as its other relevant environmental fate properties, i.e., organic carbon-water partitioning coefficient (K_{oc}) and susceptibility towards abiotic transformation (i.e., hydrolysis and phototransformation), need to be known as accurately as possible. Otherwise, uncertainty in emission, sorption, and transformation can compensate for each other's effect, which prevents an accurate determination of $k'_{bio,field}$ (Honti et al. 2018). Unfortunately, however, there is a lack of experimentally derived and hence accurately known environmental fate properties for most wastewater-relevant substance classes (e.g., pharmaceuticals and industrial chemicals) since their determination is not required by the respective regulations or data are not publicly accessible (Oelkers and Floeter 2019).

Against this scientific background, the objective of our study was to more thoroughly assess how outcomes from laboratory biotransformation studies compare to biotransformation observed in the field, and to use these insights to derived recommendations on how to conduct and evaluate OECD 308 and 309-type studies to yield outcomes that are as relevant to the aquatic environment as possible. More specifically, the aims of the project were:

1. To improve the test design for laboratory studies on transformation in surface water and water/sediment-systems to reduce variability in study outcomes and to improve their interpretability re. biotransformation;
2. To provide guidance and a tool to evaluate laboratory study results from OECD 308-type studies regarding biotransformation, including additional (meta)data requirements needed for the improved evaluation;
3. To compare different persistence indicators derived from laboratory studies (i.e., DT_{50}, $DegT_{50}$, k'_{bio}) to persistence indicators derived by measurements and modeling in a river catchment.

To fulfill the specific aims of the project, we, first, studied biotransformation in laboratory experiments for a broad set of >40 test compounds at environmentally relevant concentration levels in both standard and modified OECD 308 and 309-type systems. We then systematically compared half-lives and biotransformation rate constants observed in laboratory test systems

and in the field for a subset of 28 compounds frequently detected in wastewater treatment plant (WWTP) effluents, surface water bodies, and even ground- and drinking water resources (Neumann M 2019; Anliker et al. 2020; Singer et al. 2010; Singer et al. 2016; Li and McLachlan 2019; Li et al. 2017; Ruff et al. 2015) in the Rhine river catchment by measuring compound fluxes in the main channel of the Rhine and its major tributaries. Biotransformation kinetics in both types of studies - in the field and in the laboratory - were evaluated, first, by deriving half-lives, and, second, by adapting the model frameworks of Honti et al. (2016, 2018) to determine both $k'_{bio,lab}$ and $k'_{bio,field}$ values. In order to reduce uncertainties of both $k'_{bio,lab}$ and $k'_{bio,field}$, we conducted complementary sorption, hydrolysis and phototransformation experiments, which provided prior estimates for Bayesian parameter inference when calibrating the k'_{bio}-models. Hence, besides addressing the main aims of our study, we gathered consistently derived biotransformation, hydrolysis, phototransformation, and sorption information for >28 compounds of high environmental relevance.

2 Evaluation of Aquatic Biotransformation in Laboratory Test Systems

We conducted a set of different biotransformation simulation studies by employing experimental setups within and beyond standards of OECD 308/309 studies. OECD 309-type studies were performed as suspension tests containing 1 and 10 g solids L^{-1}. Further, we conducted modified OECD 308-type studies in which the sediment-water ratio was changed to higher water contents compared to standard OECD 308 studies, i.e., we used a sediment-water ratio of 1:10 (v/v) instead of 1:3 to 1:4 (v/v) (see Chapter 2.1.4.4).

All experiments were conducted with water and sediment sampled from the agriculture and wastewater effluent impacted river Rhine (Mumpf, Switzerland), as well as with water and sediment sampled from the pristine Cressbrook Mill Pond (CMP, Derbyshire, UK).

Suspensions are referred to with a code indicating sampling site, sediment concentration in g L^{-1}, and sampling time in case of Rhine suspensions. The lower sediment suspensions are R1-Fall, R1-Spring, and CMP1, the higher biomass suspensions are R10-Fall, and CMP10. Sampling of the Rhine was done twice, i.e., in fall and in spring, to obtain environmental samples with comparable physicochemical properties (Table 2) but different microbial communities. This investigation of seasonality was done in 1 g solids L^{-1} suspensions to be consistent with current OECD 309 standards. Since the OECD 309 guideline does not specify whether sediment should be kept in suspension via magnetic stirrer or orbital shaker. Therefore, for the purpose of comparison, both setups, horizontal shaker and magnetic stirrer, were employed to keep fine CMP sediment in suspension (CMP1/10 and CMP1/10-Stirrer, respectively). In case of Rhine inoculum, the sediment was kept in suspension via orbital shaking exclusively. Modified OECD 308-type experiments were performed with sediment and water sampled from the Rhine in spring, referred to as mod308R, as well as with water and sediment sampled from CMP, i.e., mod308CMP.

In each study, we followed the fate of 43 test compounds covering a broad range of different biotransformation and sorption behavior (Table 1). Test compounds were spiked to the test systems in mixture to an environmentally relevant concentration of 1 µg L-1 each. Primary biotransformation and sorption behavior of the test compounds was investigated (i) by measuring the compounds' concentration in the water phase over time during OECD 309-type studies, and (ii) by measuring the compounds' concentration in both sediment and water phase over time during modified OECD 308-type studies.

The performance of the here conducted biotransformation simulation studies was then evaluated by deriving different parameters describing a compound's persistence and by systematically comparing those parameters across experiments. Finally, compound behavior in modified OECD 308/309-type studies was compared to compound behavior in standard OECD 308 studies for 19 compounds for which information was available.

2.1 Materials and Methods

2.1.1 Test Compounds

Chemicals of known environmental relevance, i.e., often measured in wastewater treatment plant effluents or surface water bodies (Ruff et al. 2015; Jaeger, Posselt, et al. 2019; Zou, Radke, Kierkegaard, MacLeod, et al. 2015; Singer et al. 2010; Singer et al. 2016), were selected as test compounds with the additional goal of covering a broad range of non-volatile compounds with different transformation and sorption behavior. Of the 43 test compounds listed in Table 1, 36

were selected for the first two experiments with Rhine sediment (R1/10-Fall) and were complemented with additional 7 compounds for the following experiments (R1-Spring, CMP1/10, CMP1/10-Stirrer, mod308R, and mod308CMP). The final set of test compounds included 24 pharmaceuticals, 15 pesticides, 3 artificial sweeteners, and 1 industrial chemical. All chemicals were available from Sigma-Aldrich, TRC-Canada, TCI-Europe, or USP-Rockville. Own isotope-labelled standards, which were used for quantification during chemical analysis, were available for 36 compounds (Table 1) and had been purchased from TRC-Canada, C/D/N Isotopes, or Novartis.

As indicated in Table 1, regulatory data describing compound behavior in standard OECD 308 studies was available with sufficient data quality for a subset of 19 compounds. Regulatory data was used to compare and evaluate the performance of modified OECD 308-type studies in comparison to standard OECD 308 studies. Further, Table 1 lists test compounds whose biotransformation behavior was not only assessed in laboratory studies but also in the natural environment, i.e., the Rhine river catchment (see Chapter 4), referred to as field compounds.

Table 1: Selected test compounds

Selected test compounds and their isotope-labelled standards used for chemical analysis. N.a. indicates that an isotope-labelled standard was not available for this study. The column Abbr. shows abbreviations used for compound names. The column "regulatory data available" indicates for which compounds we considered data reported during standard OECD 308 experiments used for regulatory purposes.

Compound	Abbr.	CAS ID	Isotope-labelled standard	Field compounds	Regulatory data available
5-Methylbenzotriazole	5BM	136-85-6	5-Methylbenzotriazole-D_6	yes	no
Acesulfame	ACE	55589-62-3	Acesulfame-D_4	yes	no
Aliskiren	ALI	173334-57-1	Aliskiren-D_6	yes	yes
Atazanavir	ATA	198904-31-3	Atazanavir-D_5	yes	yes
Atenolol	ATE	29122-68-7	Atenolol-D_7	yes	no
Azoxystrobin	AZO	131860-33-8	Azoxystrobin-D_4	no	yes
Bezafibrate	BEZ	41859-67-0	Bezafibrate-D_4	yes	no
Bicalutamide	BIC	90357-06-5	Bicalutamide-D_4	yes	no
Carbamazepine	CAR	298-46-4	Carbamazepine-D_8	yes	no
Carbendazim	CBA	10605-21-7	Carbendazim-D_4	no	yes
Citalopram	CIT	59729-33-8	Citalopram-D_6	yes	no
Clarithromycin	CLA	81103-11-9	n.a.	yes	no
Clopidogrel carboxylic acid	CLO	144457-28-3	n.a.	yes	no
Cyclamate	CYC	139-05-9	Cyclamate-D_{11}	yes	no

Compound	Abbr.	CAS ID	Isotope-labelled standard	Field compounds	Regulatory data available
Diclofenac	DIC	15307-86-5	Diclofenac-D_4	yes	no
Dimethenamid	DIM	87674-68-8	Dimethenamid-D_3	no	yes
Diuron	DIU	330-54-1	Diuron-D_6	no	yes
Fenhexamid	FEN	126833-17-8	Fenhexamid-D_3	no	yes
Fenoxycarb	FOC	72490-01-8	n.a.	no	no
Fexofenadine	FEX	83799-24-0	Fexofenadine-D_6	yes	no
Fipronil	FIP	120068-37-3	Fipronil-$^{13}C_2{}^{15}N_2$	no	yes
Gabapentin	GAB	60142-96-3	Gabapentin-D_4	yes	no
Hydrochlorothiazide	HYD	58-93-5	Hydrochlorothiazide-$^{13}CD_2$	yes	yes
Imidacloprid	IMI	138261-41	Imidacloprid-D_4	no	yes
Iprovalicarb	IPR	140923-17	n.a.	no	yes
Irbesartan	IRB	138402-11-6	Irbesartan-D_4	yes	no
Isoproturon	ISO	34123-59-6	Isoproturon-D_6	no	yes
Lamotrigine	LAM	84057-84-1	Lamotrigine-$^{13}C_3D_3$	yes	no
Levetiracetam	LEV	102767-28-2	Levetiracetam-D_3	yes	no
Lidocaine	LID	137-58-6	Lidocaine-D_{10}	yes	yes
Mefenamic acid	MEF	61-68-7	Mefenamic acid-D_3	yes	no
Mesotrione	MES	104206-82-8	Mesotrione-D_3	no	yes
Metoprolol	MTO	37350-58-6	Metoprolol-D_7	yes	no
Napropamide	NAP	15299-99-7	n.a.	no	yes
Picoxystrobin	PIC	117428-22-5	n.a.	no	yes
Saccharin	SAC	81-07-2	Saccharin-D_4	yes	no
Sitagliptin	SIT	486460-32-6	Sitagliptin-D_4	yes	no
Sulfamethoxazole	SUL	723-46-6	Sulfamethoxazole-D_4	yes	no
Terbuthylazine	TER	5915-41-3	Terbuthylazine-D_5	no	yes
Trimethoprim	TRI	738-70-5	Trimethoprim-D_9	yes	no
Trinexapac-ethyl	TNE	95266-40-3	n.a.	no	yes
Valsartan	VAL	137862-53-4	Valsartan-$^{15}N^{13}C_5$	yes	yes

Compound	Abbr.	CAS ID	Isotope-labelled standard	Field compounds	Regulatory data available
Venlafaxine	VEN	93413-69-5	Venlafaxine-D_6	yes	no

2.1.2 Environmental Sampling

Water and sediment for biotransformation experiments were sampled from the agriculture and wastewater effluent impacted river Rhine (Mumpf, Switzerland) and from the pristine Cressbrook Mill Pond (CMP, Derbyshire, UK). In compliance with the OECD 308 guideline, sampling sites were chosen to strongly differ in texture and TOC content of the sediment (OECD 2002). The coarse textured sediment from the Rhine (~73% sand, ~20% silt, ~7% clay) had a TOC content of 0.7%, while the much finer sediment of CMP (45% sand, 49% silt, 5% clay) had a TOC content of 10%. Sampling of sediment and water from the river Rhine was done in September 2018 (R1/10-Fall) and in March 2019 (R1-Spring). CMP was sampled in August 2019 (CMP1/10, CMP1/10-Stirrer).

For modified OECD 308-type experiments, sediment samples were taken with a stainless-steel shovel from the 5 to 10 cm upper layer of the bottom sediment at the respective sampling site. For modified OECD 309-type suspension tests, only the upper 1 cm of sediment was sampled by carefully sucking the surface layer of the bottom bulk sediment through a tube (Ø= 2 cm) connected to a drill pump (see Annex A.1, Figure A1). Water samples from the respective sites were taken in plastic containers. Environmental samples were then cooled during transport from the sampling sites to the laboratory (transportation time: 2 h Rhine samples and 3 days CMP samples) and then directly filled into experimental containers. An acclimation period (24 h up to 7 days) to reach stable pH and O_2-content in the water phase was applied prior to adding the test substances. Further details on the environmental sampling are listed in Table 2.

Table 2: Environmental sampling collection records

	Rhine Fall	Rhine Spring	CMP
Sampling Date	19.09.2018	04.03.2019	12.08.2019
Location	Mumpf am Rhein, Switzerland; shallow littoral zone	Mumpf am Rhein, Switzerland; shallow littoral zone	Cressbrook, Derbyshire UK
Water depth	~1 m	~1 m	
Depth of sampled sediment layer	~1 cm	~1 cm for R1-Spring ~5 cm for mod308R	~5 cm
Grain size distribution of sediment	70% sand, 23% silt, 7% clay	73% sand, 20% silt, 7% clay	45% sand, 49% silt, 5% clay
pH water	8.05	8	8.12
Temperature water	21.7°C	11°C	9°C
Dissolved O_2 water	8.6 mg L^{-1}	8.03 mg L^{-1}	7.46 mg L^{-1}

2.1.3 Experimental Setup of OECD 309-type Studies

2.1.3.1 Test System and Test Conditions

1 L glass bottles were filled with 600 mL water and amended with sediment to obtain 1 and 10 g solids L^{-1} suspensions (wet weight), respectively. The OECD 309 guideline does not further specify whether sediment should be kept in suspension via magnetic stirrer or orbital shaker. Shrestha et al. (2016) found that a magnetic stirrer grinds coarse-textured sediment, resulting in a drastic change of grain size distribution and the continuous formation of new surfaces that can increase sorption. Therefore, the sandy Rhine sediment was kept in suspension exclusively via orbital shaking. For comparison purposes, both setups, horizontal shaker and magnetic stirrer, were employed to keep fine CMP sediment in suspension (CMP1/10 and CMP1/10-Stirrer, respectively). Experimental containers were loosely capped with cotton plugs to ensure air exchange but to avoid potential contamination via deposition (see Annex A.1, Figure A2).

All experiments were carried out at room temperature (22±2°C) in the dark. The pH values of the water phase during the Rhine and CMP experiments were at 8±0.2 and 8.4±0.3, respectively (average of 12 measurements).

Test substances were dissolved in ethanol (EtOH) and spiked to the suspensions to a final concentration of 1 µg L^{-1} each, resulting in a solvent addition of 0.04% (v/v); the OECD 309 guideline allows for a solvent addition of up to 1% (v/v) (OECD 2004). Chemical dissipation from the water phase was followed during up to 63 days.

2.1.3.2 Experimental Replicates and Sacrificial Sampling

R1/10-Fall was performed with 8 experimental replicates. The number of replicates was then increased to 14 for R1-Spring, and to 18 for CMP1/10. Sacrificial sampling of whole experimental vessels was necessary for further microbial analysis (not reported here, for further information, see Seller et al. (2020). Therefore, monitored concentration-time series of chemical dissipation end at different time points in each experimental replicate. Still, at least two replicates were monitored for more than 54 days in each experiment.

2.1.3.3 Sampling and Sample Processing for Chemical Analysis

Concentrations of test compounds in the water phase of biotransformation experiments were monitored by taking subsamples of 1.5 mL from each experimental replicate. For the biotransformation experiments, sampling was done after 0, 1, 4, 7, 14, 28, 35, 42, 49, 56, and 63 days during R1/10-Fall, after 0, 1, 4, 7, 14, 21, 28, 35, 42, 57, and 63 days during R1-Spring, and after 0, 2, 4, 7, 13, 20, 27, 34, 45, and 54 days during CMP1/10.

Subsamples were transferred to 2 mL Eppendorf tubes and centrifuged at 20’000 g for 10 min. 500 µL of supernatant were transferred to 2 mL glass vials and spiked with a mixture containing all internal standards to a concentration of 500 ng L^{-1}. Samples were then stored at -20°C until chemical analysis, which was performed within one month after the end of the respective experiment.

2.1.3.4 Differences to Regulatory OECD 309 Suspension Tests

In comparison to regulatory OECD 309 suspension tests, our here presented setup was modified by:

a) Increasing the sediment content beyond OECD 309 standards, which limit sediment addition to ≤1 g solids L^{-1}.

b) Spiking unlabelled test compounds in mixture.

c) Considering only one test concentration, which was at the lower end of recommendations in the OECD 309 guideline, i.e., 1 µg L^{-1}.

2.1.4 Experimental Setup of Modified OECD 308-type Studies

2.1.4.1 Test System and Test Conditions

Biotransformation experiments were conducted in 1 L amber glass bottles (i.e., Ø = 10 cm) with a water-sediment ratio of 10:1 (v/v), which translates to 780 mL water covering a 1 cm thick sediment layer, i.e., 30 g_{dw} (dry weight) of CMP sediment and 100 g_{dw} of Rhine sediment. The water column was aerated with wet air pumped through a syringe ending 1.5 cm above the sediment surface to avoid disturbing its upper layer as shown in Figure 1 and Annex A.1, Figure A3.

Figure 1: Experimental setup and system geometry of modified OECD 308-type studies

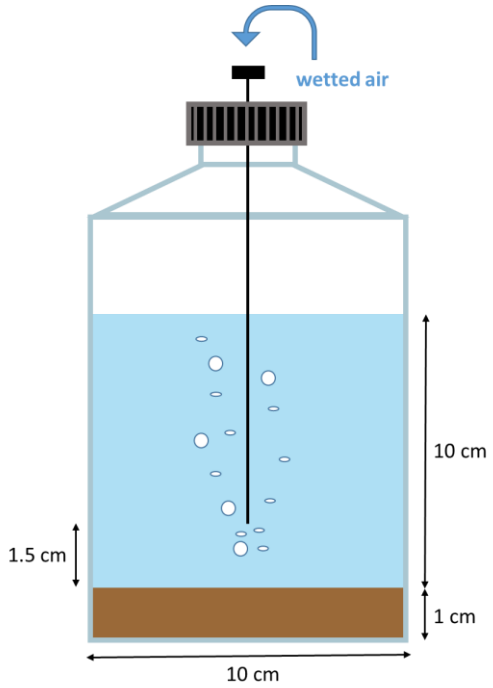

Source: own figure, Eawag

An acclimation period of 7 days was applied to reach stable pH and O_2-concentration in the water phase before starting biotransformation experiments. Average water phase O_2-concentrations of 12 measurements during the Rhine and CMP experiments were at 7±0.9 and 7.9±0.3 mg L^{-1}, respectively. All experiments were carried out at room temperature (22±2°C) in the dark. The pH values of the water phase during the Rhine and CMP experiments were at 8±0.1 and 8.5±0.37, respectively (12 measurements). Both values are within 0.3 pH units of field conditions during environmental matrix sampling (Table 2).

Test substances were dissolved in EtOH and spiked in mixture to a concentration of 1µg L^{-1} each, resulting in a solvent addition of 0.04% (v/v). Their fate in the experimental batches was followed over a time period of >54 days.

2.1.4.2 Experimental Replicates and Sacrificial Sampling

A total of 18 replicates was set up for each modified OECD 308 study. To determine chemical concentrations in both the sediment and the water phase, two replicates were sacrificed at nine sampling time points throughout >54 days.

2.1.4.3 Sampling and Sample Processing for Chemical Analysis

During the Rhine study, duplicates were sacrificed after 1, 5, 8, 15, 22, 29, 36, 50, and 64 days. During the CMP study, duplicates were sacrificed after 2, 4, 7, 13, 20, 27, 34, 45, and 54 days. To determine starting concentrations (C_0), only subsamples of the water phase were taken from each experimental replicate since it can be assumed that diffusion into the sediment layer followed by sorption processes can be neglected within the first few minutes after substance spike.

To determine compound concentrations in the water phase of the experimental vessels, aliquots of 1.5 mL were taken from the water phase, centrifuged at 20'000 g for 10 min, and the supernatant was transferred into HPLC vials where a mix of ISTDs was added to a concentration of 500 ng L^{-1} to account for losses during chemical analysis.

To determine compound concentrations in the sediment, the supernatant water was decanted from the experimental vessels and the remaining bulk sediment was homogenized by manual stirring. Sediment was then lyophilized and aliquots of 6 and 2 g of Rhine and CMP sediment, respectively, were homogenized with 0.5 g diatomaceous earth and transferred into 11 mL stainless-steel cells of an accelerated solvent extractor ASE 350 unit from Dionex, which were equipped with glass fiber- and cellulose filters at the bottom. A mixture of nanopure water, methanol, and acetone (50:25:25 v/v/v) was used as extraction solvent for pressurized liquid extraction (PLE) during two extraction cycles of 5 min each at 80°C and 1500 psi. PLE extracts were evaporated to 1 mL using a Synocore Polyvap (Büchi). Remaining extracts were centrifuged at 20'000 g for 15 min and 500 µL of supernatant were transferred to HPLC vials and amended with the ISTDs mix to a concentration of 1 µg L^{-1}.

Absolute compound recoveries after extraction and evaporation were quantified by spiking several portions of Rhine and CMP sediment with a known amount of test substances 24 hours prior to extraction. Table 3 lists total compound recoveries and coefficients of variation (CV) derived from spiking triplicate portions of Rhine and CMP sediment to 83 and 250 ng $g_{sediment}^{-1}$, respectively. While recoveries are good to acceptable for most compounds in the Rhine sediment, recoveries were decreased when extracting CMP sediment. This was due to heavy ion suppression during chemical analysis from co-extracted matrix. Furthermore, for compounds undergoing rapid biotransformation reactions such as atenolol, bezafibrate, fenoxycarb, sulfamethoxazole, trinexapac-ethyl or valsartan, poor recoveries can be speculated to partially result from compound removal via biotransformation reactions occurring in the sediment within 24 h after substance spike prior to extraction. Nevertheless, the here presented method was the best compromise found that allowed to process both CMP and Rhine samples by consistently applying the same extraction method.

Table 3: Compound recoveries from sediment extraction

Total compound recoveries from sediment extraction and their coefficient of variation (CV) calculated from triplicate samples. N.d. indicates bad recovery due to significant ion suppression in extracted CMP samples.

	Rhine sediment		CMP sediment	
Compound	**Recovery (%)**	**CV (%)**	**Recovery (%)**	**CV (%)**
5MB	61	3	100	4
ACE	79	3	83	3
ALI	78	5	79	5
ATA	67	5	39	6
ATE	79	2	n.d.	n.d.
AZO	89	4	55	5
BEZ	60	5	n.d.	n.d.
BIC	77	2	59	3
CAR	78	8	101	5
CBA	74	4	89	2
CIT	64	3	62	6
CLO	68	3	83	2
CYC	74	3	69	3
DIC	74	9	83	3
DIM	88	4	75	4
DIU	80	5	60	2
FEN	64	5	n.d.	n.d.
FEX	88	4	100	2
FIP	60	3	n.d.	n.d.
FOC	35	12	n.d.	n.d.
GAB	47	5	n.d.	n.d.
HYD	101	8	97	3
IMI	75	2	71	3
IPR	69	4	n.d.	n.d.
IRB	82	6	91	6
ISO	81	3	66	2
LAM	94	2	99	5
LEV	59	4	73	2
LID	65	2	66	6
MEF	77	8	79	12
MES	54	3	n.d.	n.d.
MTO	80	9	84	5
NAP	87	2	55	8

	Rhine sediment		CMP sediment	
Compound	Recovery (%)	CV (%)	Recovery (%)	CV (%)
PIC	83	2	45	12
SAC	73	5	n.d.	n.d.
SIT	80	7	69	5
SUL	80	6	n.d.	n.d.
TER	84	6	80	4
TNE	87	8	n.d.	n.d.
TRI	79	2	67	4
VAL	45	5	n.d.	n.d.
VEN	72	2	64	6

2.1.4.4 Differences to Regulatory OECD 308 Studies

In comparison to regulatory OECD 308 studies, our here presented setup was modified by:

a) Decreasing the sediment-water ratio to 1:10 (v/v). This resulted in a sediment layer of 1 cm covered by a 10 cm water column (i.e., 780 mL).

b) Modified OECD 308-type experiments were conducted at a temperature of 22±2°C, while standard OECD 308 studies are conducted at 20°C.

c) Ensuring full aeration of the supernatant water column (optional in OECD 308 guideline) (OECD 2002). Based on oxygen profiles measured in the sediment layer of standard and modified OECD 308-type studies by Shrestha et al. (2016), we further assume our experimental setup of modified OECD 308-type studies resulted in mostly aerobic conditions in the sediment layer.

d) Considering one test concentration (i.e., 1 µg L^{-1}), which was lower than concentration levels commonly applied in regulatory OECD 308 studies.

e) Spiking unlabeled test compounds in mixture.

f) Working with unlabeled compounds in modified OECD 308-type studies did not allow us to monitor the formation of non-extractable residues (NER). However, PLE treatment of sediment samples can be assumed to have resulted in a much more efficient extraction of parent compound mass compared to standard OECD 308 studies, i.e., batch extraction methods such as 12 h solvent extraction at room temperature (Loeffler et al. 2020).

2.1.5 Abiotic Control Experiments

To distinguish biotransformation from phase transfer processes in experimental vessels, abiotic controls were set up alongside the respective biotransformation experiments, i.e., modified OECD 308-type studies and OECD 309-type studies. Water and sediment were sterilized by two times autoclaving (each cycle: 120°C for 20 min); beyond that the experimental setup of abiotic controls was identical to the setup of the respective biotransformation experiment. To identify which compounds are susceptible toward removal via hydrolysis, test compounds were additionally spiked into experimental vessels containing sterilized water only. To ensure sterile conditions, abiotic experiments were conducted over a time period of <20 days. Compound concentrations were determined in the water phase only.

2.1.6 Chemical Analysis

All samples, i.e., water phase samples from OECD 309-type studies, modified OECD 308-type studies, the respective abiotic control experiments, as well as sediment extracts from modified OECD 308-type studies were analyzed with the same analytical method using an Agilent 6495C Triple Quad Mass Spectrometer coupled to an Agilent HPLC 1290 (binary pump) system. 100 µL of each sample were injected on a reversed phase column (Acquity UPLC HSS T3, 1.8 µm, 2.0 x 100 mm, Waters) equipped with a precolumn (Acquity UPLC HSS T3, 1.8 µm, 2.1 x 5 mm, Waters). Separation was performed following a gradient of water and methanol both acidified with 0.1% formic acid at a flow rate of 500 µL min^{-1} (0-2 min 100% water, 2-18.5 min linear gradient to 5% water, 18.5-22 min kept at 5% water, 22.5-24.5 min switch to 100% water). Ionization in positive and negative mode (switching mode) was achieved by electrospray ionization. Analytes were detected using Triple Quad dynamic MRM mode. Test compounds and 36 internal standards were identified by measuring two transitions each. Calibration samples covered a range from 2.5 to 1500 ng L^{-1} for quantification of compounds in the water phase samples from biotransformation experiments and abiotic control experiments. In case of sediment extracts from biotransformation experiments and sorption experiments (see Chapter 3), calibration samples covered a range from 2.5 ng L^{-1} to 40 µg L^{-1}.

The MassHunter Quantitative Analysis software tool was used for data evaluation. For each analyte, quantification was done with the most intense transition, the second transition was used for qualification. An exception was cyclamate; only one transition could be measured, which was therefore used as quantifier. Limits of quantification (LOQ) were in all cases below 25 ng L^{-1} (i.e., <2.5% of initially spiked concentrations).

2.1.7 Deriving Total System Half-Lives ($DT_{50,TS,309}$) from OECD 309-type Studies

Compound residues in each experimental replicate as a function of time were fitted to a first-order degradation model considering lag phases to be consistent with data evaluation recommendations in regulatory frameworks where the same data evaluation procedure is called modified hockey-stick model (FOCUS 2006; OECD 2004). Here, we defined the total system degradation half-life ($DegT_{50,TS,309}$) as the time interval needed to reach 50% primary degradation, once compound dissipation has started. In contrast, the total system half-life ($DT_{50,TS,309}$) was defined as the sum of $DegT_{50,TS,309}$ and the length of the lag phase (t_{lag}).

Total parent compound residues in experimental systems at a given time were calculated from measured water phase concentrations, considering a sediment-water partitioning coefficient derived from sorption experiments. System-specific sediment-water partitioning coefficients K_d (L kg^{-1}) were calculated from the compound concentrations measured in the water phase of the abiotic sorption controls and the total suspended solids concentration TSS (kg L^{-1}) (Equation (1)), assuming constant partitioning behavior (i.e., K_d) throughout the experiment. K_d values were calculated individually for each time point of sampling from the abiotic sorption controls (2, 4, 10 days) and an average of those was used as the final K_d (Table 7).

$$K_d(t) = \frac{(C_{0,abiotic} - C_{t,abiotic})}{C_{t,abiotic}\ TSS} \quad (1)$$

The dissolved fraction f_{aq} of the total parent compound residue in the test system can be calculated as a function *of* K_d *and* TSS according to Equation (2).

$$f_{aq} = \frac{1}{1 + K_d \ TSS} \quad (2)$$

At equilibrium, the total compound residue in the system at each time point $C_{TS}(t)$ can be calculated from the measured parent compound concentration in the water phase $C_{w,eq}(t)$ and the dissolved fraction f_{aq}.

$$C_{TS}(t) = \frac{C_{w,eq}(t)}{f_{aq}} \quad (3)$$

C_{TS} was plotted as a function of incubation time and fitted to a first-order degradation model with lag phases t_{lag} (Equation (4)) using the software R (Version: 3.6.2). Degradation rate constants k (d^{-1}) were calculated individually for each experimental replicate.

$$C_{TS}(t) = \begin{cases} C_0 & \text{for } t < t_{lag} \\ C_0 \ \exp\left(-k \cdot \left(t - t_{lag}\right)\right) & \text{for } t > t_{lag} \end{cases} \quad (4)$$

$DegT_{50,TS,309}$, $DT_{50,TS,309}$ and k were related as shown in Equation (5) and Equation (6).

$$DegT_{50,TS,309} = \frac{\ln(2)}{k} \quad (5)$$

$$DT_{50,TS,309} = DegT_{50,TS,309} + t_{lag} \quad (6)$$

2.1.8 Deriving Half-Lives ($DT_{50,w,308}$ and $DT_{50,TS,308}$) from Standard and Modified OECD 308-type Studies

A first-order degradation model considering lag phases was fitted to total parent compound residues in the experimental vessels over time in standard and modified OECD 308-type studies. Model equations provided in Chapter 2.1.7. Our here applied first-order degradation model is called a modified hockey-stick model of the FOCUS guidance on estimating persistence and degradation kinetics from environmental fate studies (FOCUS 2006). We here defined the total system half-life ($DT_{50,TS,308}$) as the sum of the time interval needed to reach 50% compound removal from the experimental vessels after onset of degradation plus the length of the lag phase. To calculate dissipation half-lives from the water column ($DT_{50,w,308}$), Equation (4) was fitted to concentration measurements in the water phase only. Modelled transformation kinetics cover biotic and abiotic compound transformation; compounds susceptible to removal via abiotic hydrolysis are listed in Table 5.

In case of modified OECD 308-type studies, to account for uncertainties in our data due to potential compound mass losses during sample handling and LC/MS analysis, we only considered compound mass dissipation >15% from the test vessels during biotransformation experiments to indicate actual transformation. Therefore, we could only reliably calculate transformation rate constants >0.003 d^{-1} and hence $DT_{50,TS,mod308}$ of <230 days.

In order to enable a comparison between $DT_{50,TS,308}$ values derived from standard and modified OECD 308-type studies, $DT_{50,TS,std308}$ from standard studies were calculated via two different approaches. Generally speaking, in case of standard OECD 308 studies conducted with ^{14}C-radiolabelled substances, radioactivity detected in the sediment layer may stem from reversibly sorbed parent compound and transformation products, but also include truly irreversibly bound

fractions because of compound incorporation into biomass or the formation of covalent bonds. The truly irreversibly bound fraction might not necessarily be equal to NER. These are operationally defined by the employed extraction procedure, which is not standardized in current regulatory guidelines (OECD 2002; Loeffler et al. 2020). Frequently used batch extraction methods (e.g., 12 h solvent extraction at room temperature), for instance, are known to provide comparably low extraction efficiencies (Loeffler et al. 2020).

Therefore, to account for uncertainty in extraction efficiencies and to compare to our own modified OECD 308-type studies, in which we only quantified parent compound mass, we calculated $DT_{50,TS,std308}$ from standard OECD 308-type studies in two ways, representing two possible extreme assumptions regarding extraction efficiencies. In the more conservative approach, we calculated total parent compound residues in standard OECD 308-type studies as the sum of NER, sediment-extracted and water phase parent compound. This approach is likely to overestimate parent compound $DT_{50,TS,std308}$, as NER not only includes non-extracted parent compound mass but also transformation products and truly irreversibly bound fractions. In the second approach, we calculated total parent compound residues in standard OECD 308-type studies as the sum of sediment-extracted and water phase parent compound only. With this second approach, sediment-bound parent compound mass may be underestimated in case of low and/ or varying efficiencies of extraction methods applied.

Working with unlabeled compounds in modified OECD 308-type studies did not allow us to monitor the formation of NER. However, PLE treatment of sediment samples can be assumed to have resulted in a much more efficient extraction of parent compound mass compared to standard OECD 308 studies (Loeffler et al. 2020). We further corrected measured parent compound concentrations in the sediment by dividing the extracted compound mass by the separately determined absolute recovery to account for losses during sample treatment.

In the following, $DT_{50,TS,mod308}$ derived from our modified studies were compared to both $DT_{50,TS,std308}$ derived from standard studies. It is to note that, while we calculated two types of $DT_{50,TS,std308}$ to account for differing efficiencies of different sediment extraction methods, we do not further address the question of how to interpret NER in this study.

2.1.9 Alternative Approaches to Evaluate Biotransformation Simulation Studies – the k'_{bio} -Concept

As outlined in Chapter 1, half-lives ($DT_{50,w}$ and $DT_{50,TS}$) from biotransformation studies in water-sediment systems may lump together transformation and phase transfer processes, and hence are dependent on the geometry of the experimental setup and the physicochemical properties of the employed water and sediment. In order to eliminate some of the most influential system-specific differences affecting biotransformation kinetics in water-sediment systems, Honti et al. (2016) introduced a data evaluation framework that derives a second-order biotransformation rate constant (k'_{bio}) from biotransformation study outcomes. k'_{bio} is corrected for the substance's bioavailability, assuming that only dissolved compound mass is available for biotransformation, and thus allows disentangling biotransformation from phase transfer. Further, k'_{bio} is normalized to the amount of degrader biomass available in a specific test system, assuming that a substance's potential for biotransformation depends on its contact with active degrader organisms or enzymes that can catalyze primary biotransformation reactions. It has been suggested that such a bioavailability-corrected and biomass-normalized second-order rate constant, which also allows to calculate compartment-specific transformation half-lives, i.e., $DegT_{50,w}$ and $DegT_{50,sed}$, should be a more robust indicator of a substance's biotransformation

potential and thus allow unifying observations from different water-sediment systems, including OECD 308/ 309 tests and natural rivers (Honti et al. 2016; Honti et al. 2018).

Yet, when aiming to calculate a second-order biotransformation rate constant based on data measured during biotransformation simulation studies ($k'_{bio,lab}$), deriving microbiological data describing the activity of specific degraders responsible for biotransformation of the here selected broad set of test chemicals would be challenging, if not impossible. Therefore, we here assume that organic carbon content in the experimental systems could be considered a suitable proxy for degrader biomass since organic carbon and bacterial activity have previously been found to correlate in river sediments (Fischer, Wanner, and Pusch 2002). However, such an assumption renders it impossible to explain large differences between experimental replicates from biotransformation simulation studies, as this was the case for most compounds in the 309-type studies conducted here (see Chapter 2.2). Hence, we only used data from modified OECD 308-type studies to further explore the k'_{bio}-concept and to derive compartment-specific transformation half-lives (see Chapter 2.3).

2.1.9.1 Deriving $k'_{bio,lab}$ Values and Compartment-Specific Transformation Half-Lives ($DegT_{50,w,mod308}$ and $DegT_{50,sed,mod308}$) from Modified OECD 308-type studies

We adapted the model framework of Honti et al. (2016) to describe transformation and sorption processes in the two-compartment system employed for modified OECD 308-type studies. Here, we define the settled sediment layer including pore water as the first compartment, and the supernatant water column, which we assume not to contain any suspended particles, as the second compartment. Other than in the model framework of Honti et al. (2016), we assume a fully mixed aerobic sediment layer (assumption based on oxygen profiles measured by Shrestha et al. (2016) in modified OECD 308-type studies). Test compounds are assumed to be either in dissolved phase in the water compartment (i.e., neglecting association with dissolved organic carbon), or in sorbed or dissolved state in the sediment compartment. All transformation processes, i.e., abiotic hydrolysis or biotransformation, are assumed to follow first-order kinetics in both compartments. To describe compound removal via biotransformation, the model allows to derive a $k'_{bio,lab}$ value normalized to degrader biomass. As suggested in Honti et al. (2016), we used TOC measured in the sediment and water compartment of the experimental vessels as a proxy for degrader biomass and thereby assume that the fraction of active degraders relative to total bacterial biomass is the same in both laboratory inocula. Dispersion and diffusion processes following Fick's law connect sediment and water compartments. Sorption equilibrium in the sediment is assumed to be reached instantaneously and the sediment compartment itself is treated as a fully mixed reactor, i.e., transformation processes are assumed to take place synchronously and to the same rate throughout the entire sediment. This is in line with recommendations given in the FOCUS Guidance Document on Estimating Persistence and Degradation Kinetics from Environmental Fate Studies (FOCUS 2006). Following those model assumptions, compound dissipation from the water and sediment compartment can be described as:

$$\frac{dP_w}{dt} = -\left(k_{hydro} + k'_{bio,lab}\ TOC_w\right) P_w - D_p \frac{\frac{P_w}{z_w} - \frac{P_{w,sed}}{z_{sed}}}{\frac{z_{sed}}{2}} \quad (7)$$

$$\frac{dP_{sed}}{dt} = -\left(k_{hydro} + k'_{bio,lab}\ TOC_{sed}\right) \frac{1}{1 + K_{oc}\ f_{oc,sed}\ \frac{\rho_b}{\theta}} P_{sed} + D_p \frac{\frac{P_w}{z_w} - \frac{P_{w,sed}}{z_{sed}}}{\frac{z_{sed}}{2}} \quad (8)$$

with P_w and P_{sed} as parent compound in the water and sediment compartment, respectively, and $P_{w,sed}$ as parent compound in the pore water [ng L^{-1}]. The dissolved fraction of parent compound in the sediment compartment is calculated considering the compounds' K_{oc} values [L kg^{-1}], the sediments organic carbon fraction ($f_{oc,sed}$), sediment bulk density (ρ_b) in kg L^{-1}, and sediment porosity (Θ). Rate constants k_{hydro} [d^{-1}] and $k'_{bio,lab}$ [L (g OC d)$^{-1}$] describe abiotic and biotic transformation, respectively. TOC in water (TOC_w) and sediment (TOC_{sed}) are given in g OC L^{-1}. Parameters z_w and z_{sed} describe the height of the water and sediment compartment [cm], respectively, in the experimental vessels of the biotransformation simulation studies. D_p is a diffusion/dispersion coefficient in $cm^2\ s^{-1}$. A list of all parameters that need to be monitored during biotransformation simulation studies in order to derive $k'_{bio,lab}$ is provided in Annex A.1, Table A1.

According to the model framework, the transformation rate constant of parent compound residues in the supernatant water column (k_w) can be derived according to Equation (9), and transformation in the bulk sediment layer (k_{sed}) can be derived according to Equation (10).

$$k_w = k_{hydro} + k'_{bio,lab} \cdot OC_w \tag{9}$$

$$k_{sed} = (k_{hydro} + k'_{bio,lab} \cdot OC_{sed}) \cdot \frac{1}{1+Koc \cdot foc,sed \cdot \frac{\rho}{\theta}} \tag{10}$$

Compartment-specific transformation half-lives in the water ($DegT_{50,w,mod308}$) and sediment layer ($DegT_{50,sed,mod308}$) can be calculated as:

$$DegT_{50,w,mod308} = \frac{\ln(2)}{k_w} \tag{11}$$

$$DegT_{50,sed,mod308} = \frac{\ln(2)}{k_{sed}} \tag{12}$$

All equations were implemented in C++ and solved by fitting the model to averaged data of the duplicate vessels sampled at each time point. We used a Bayesian parameter estimation framework to calibrate the model for individual Rhine and CMP experiments separately, and jointly across both experiments. The joint fit was performed to verify whether the model can fit experimental data from both biotransformation studies with one set of substance-specific parameters, i.e., k_{hydro}, $k'_{bio,lab}$, and K_{oc}. Further, we compared estimated values and uncertainties of the individual and joint calibration procedure. Parameter priors for most observed quantities were set to equal the mean and standard deviation of experimentally determined values. A prior for k_{hydro} was based on abiotic hydrolysis control experiments, D_p was derived from abiotic sorption control experiments, K_{oc} priors for pesticides were taken from data provided in the Pesticides Properties Database of the University of Hertfordshire, K_{oc} priors for our other test compounds were calculated from our own sorption experiments (see Chapter 3). The only fixed input to the model were Z_w and Z_{sed} with 10 and 1 cm, respectively. For the unknown $k'_{bio,lab}$ parameter we applied a vague, uniform prior distribution ranging from 0 to 100000. A lognormal distribution was given to all other priors. Experiment-specific priors are listed in Table 4, substance-specific priors are listed in Table 5.

Posterior parameter distributions were sampled by Markov chain Monte Carlo sampling based on the classical Metropolis algorithm with 25000 iterations, the first 10000 dedicated to burn-in.

Please note, that the OECD Analyser provides a software interface that allows to evaluate data from standard OECD 308 studies based on the same concepts presented here. However, it has to be noted that the OECD Analyser does not yet allow to perform a joint model fit between two standard OECD 308 studies.

Table 4: Experiment-specific priors

Experiment specific priors used for parameter estimation with their mean and their respective standard deviation (sd).

	Rhine		CMP	
	mean	sd	mean	sd
OC_w (mg L^{-1})	2.2	1	4	2
OC_{sed} (g L^{-1})	0.89	0.4	3.8	1.9
$f_{oc,sed}$ (%)	0.7	0.14	10	2
Θ (-)	0.49	0.1	0.85	0.2
ρ (g cm^{-3})	1.27	0.13	0.38	0.04

Table 5: Substance-specific priors

Susbstance specific priors used for parameter estimation with their mean and their respective standard deviation (sd).

Compound	K_{oc} [L kg^{-1}]		D_p (cm^2 d^{-1}) Rhine		D_p (cm^2 d^{-1}) CMP		k_{hyd} [d^{-1}]	
	mean	sd	mean	sd	mean	sd	mean	sd
5MB	126	56	0.28	0.12	1.95	1.76	0.0008	0.00008
ACE	23	1	0.09	0.06	0.09	0.09	0.00001	0.000001
ALI	3750	1090	n.d.	n.d.	2.1	2.25	0.00001	0.000001
ATA	7200	7200	n.d.	n.d.	1.32	1.37	0.00001	0.000001
ATE	109	109	0.39	0.32	1.6	1.45	0.00001	0.000001
AZO	589	200	n.d.	n.d.	1.42	1.3	0.00001	0.000001
BEZ	36	18	0.09	0.1	0.31	0.3	0.00001	0.000001
BIC	977	943	0.3	0.22	1.43	1.23	0.00001	0.000001
CAR	473	473	0.19	0.18	1	0.67	0.00001	0.000001
CBA	223	23	0.44	0.47	1.9	1.77	0.00001	0.000001
CIT	24200	7120	2.13	1.06	4.99	6.2	0.00001	0.000001
CLO	72	64	0.02	0.02	0.58	0.66	0.00001	0.000001
CYC	2	1	0.08	0.06	0.09	0.09	0.00001	0.000001
DIC	169	66	0.14	0.11	0.47	0.51	0.00001	0.000001
DIM	227	137	0.16	0.13	0.81	0.56	0.00001	0.000001
DIU	680	200	0.26	0.2	1.26	0.93	0.00001	0.000001
FEN	475	300	0.18	0.06	0.96	1	0.00001	0.000001

FEX	2440	998	n.d.	n.d.	1.58	1.3	0.00001	0.000001
FIP	727	300	0.45	0.46	0.45	0.46	0.0047	0.00047
FOC	1816	600	1.33	0.7	2.73	2.76	0.00001	0.000001
GAB	151	95	0.55	0.46	0.3	0.3	0.00001	0.000001
HYD	99	7	0.23	0.25	2.61	3.47	0.031	0.0031
IMI	225	150	0.19	0.16	0.95	0.78	0.00001	0.000001
IPR	106	40	0.02	0.05	0.24	0.38	0.00001	0.000001
IRB	70	35	0.48	0.49	2.8	2.6	0.111	0.01
ISO	122	100	0.13	0.15	0.5	0.3	0.00001	0.000001
LAM	292	89	0.26	0.15	1.74	1.59	0.00001	0.000001
LEV	45	9	0.02	0.04	0.09	0.09	0.00001	0.000001
LID	66	15	0.2	0.15	0.95	0.68	0.00001	0.000001
MEF	286	143	0.19	0.13	0.95	0.7	0.00001	0.000001
MES	122	100	0.14	0.1	0.73	0.68	0.00001	0.000001
MTO	176	116	0.36	0.2	1.7	1.6	0.00001	0.000001
NAP	839	400	0.22	0.03	1.23	1.48	0.00001	0.000001
PIC	965	200	0.55	0.29	1.47	1.21	0.00001	0.000001
SAC	22	22	0.08	0.05	0.09	0.09	0.00001	0.000001
SIT	7720	1590	0.98	0.3	2.57	2.69	0.005	0.0005
SUL	10	7	0.22	0.14	0.63	0.51	0.00001	0.000001
TER	231	100	0.21	0.18	1.2	0.97	0.00001	0.000001
TNE	280	200	0.19	0.16	0.67	0.67	0.009	0.0009
TRI	11000	11000	0.75	0.12	3.2	3.1	0.00001	0.000001
VAL	4	2	0.05	0.05	0.09	0.09	0.00001	0.000001
VEN	3830	1090	0.62	0.39	1.88	1.85	0.00001	0.000001

2.2 Biotransformation in OECD 309-type studies

2.2.1 Identifying Compound Removal Pathways

Biotransformation was distinguished from hydrolysis and sorption by comparing biotransformation experiments with their abiotic controls. Comparing biotransformation experiments with control experiments in sterile water indicated susceptibility toward hydrolysis at pH values relevant for the conducted tests (i.e., pH 7-8) for six compounds, i.e., irbesartan, hydrochlorothiazide, fipronil, sitagliptin, trinexapac-ethyl, and 5-methylbenzotriazol. However, the latter four compounds had a dissipation rate from sterile water systems ≤0.005 d^{-1} (i.e., $DT_{50,abiotic}$ ≥139 days, Table 5), suggesting that biotransformation may be the dominant removal pathway in case of compound dissipation from the experimental systems. In case of hydrochlorothiazide and irbesartan, substances losses in sterile controls were comparable to those in biologically active biotransformation experiments; hence, we conclude in line with

previous research (Li and McLachlan 2019; Mbah 2005) that both compounds' dissipation was mostly attributable to abiotic transformation.

Compound removal from the water phase due to sorption was only relevant in CMP10 experiments (except for citalopram in R1-Spring), likely due to the high TOC content of the pond sediment. Highest affinity for sediment was observed for citalopram, followed by trimethoprim, fenoxycarb, and sitagliptin (for K_d values see Table 7). Analytical issues with water phase samples occurred for five test substances, which were therefore excluded from further analysis, i.e., aliskiren, atazanavir, azoxystrobin, clarithromycin, and fexofenadine. For carbamazepine, all dissipation from the water phase in CMP10 was exclusively attributable to sorption; carbamazepine is resistant towards biotransformation. For the remaining 35 test compounds, dissipation from experimental vessels could be assigned at least partially to biotransformation.

2.2.2 Shaker vs. Stirrer Experiments

We gathered strongly differing results when testing two experimental setups to keep CMP sediment in suspension, i.e., orbital shaker and magnetic stirrer. In agreement with the results of Shrestha et al. (2016), results of CMP1/10-Stirrer revealed that keeping sediment in suspension via magnetic stirrer led to grinding of particles and continuously increased sorption of chemicals, which made differentiation between transformation and sorption difficult. Changes in grain size distribution are presented in Table 6.

Table 6: Grain size distribution of CMP sediment

Grainsize distribution of CMP sediment prior the experiments, after 54 days on an orbital shaker, and after 54 days suspended by a magnetic stirrer.

	Grain size	Start of experiment	54 days, orbital shaker	54 days, magnetic stirrer
	<0.04 µm	2.11	2.45	6.09
	0.04-2 µm	1.25	1.35	3.79
	2-4 µm	3.04	3.26	8.17
clay	-4 µm	**6.40**	**7.07**	**18.06**
	4-8 µm	6.82	7.51	17.25
	8-16 µm	11.04	13.28	22.79
	16-31 µm	15.74	20.61	19.23
	31-62.5 µm	15.30	18.67	11.34
silt	4-62.5 µm	**48.90**	**60.07**	**70.61**
	62.5-125 µm	10.29	11.82	6.04
	125-250 µm	7.35	6.59	2.99
	250-500 µm	11.90	7.61	2.04
	500-1000 µm	15.16	6.84	0.26
	1000-2000 µm	-	-	-
sand	62.5-2000 µm	**44.70**	**32.85**	**11.33**

While sorption equilibrium was typically reached within less than 2 days in the abiotic controls, sorption in the biotransformation experiments with magnetic stirrer seemed to have continued to increase beyond the duration of the abiotic control experiments. This is best illustrated by comparing removal of persistent compound carbamazepine from the water phase of stirred and shaken systems. Outcomes of data evaluation as outlined in Chapter 2.1.7 indicated an almost 50% loss of carbamazepine from the stirred biotransformation systems compared to less than 10% loss from the shaken systems. Comparison of carbamazepine removal in stirred and shaken systems is shown in Figure 2. In the stirred system, the total system dissipation rate constant (k) was calculated to be 0.012 d^{-1} (R^2 = 0.94), resulting in an alleged $DegT_{50,TS,309}$ of 57.7 days. Due to the compounds previously determined resistance towards transformation, this loss could only be assigned to increased sorption to the grinded sediment. Based on these results, an experimental setup in which sediment is kept in suspension via orbital shaking appeared more appropriate to clearly distinguish biotransformation from phase transfer. Data from stirrer experiments was therefore not used for further data analysis.

Figure 2: Carbamazepine residues in shaken and stirred systems

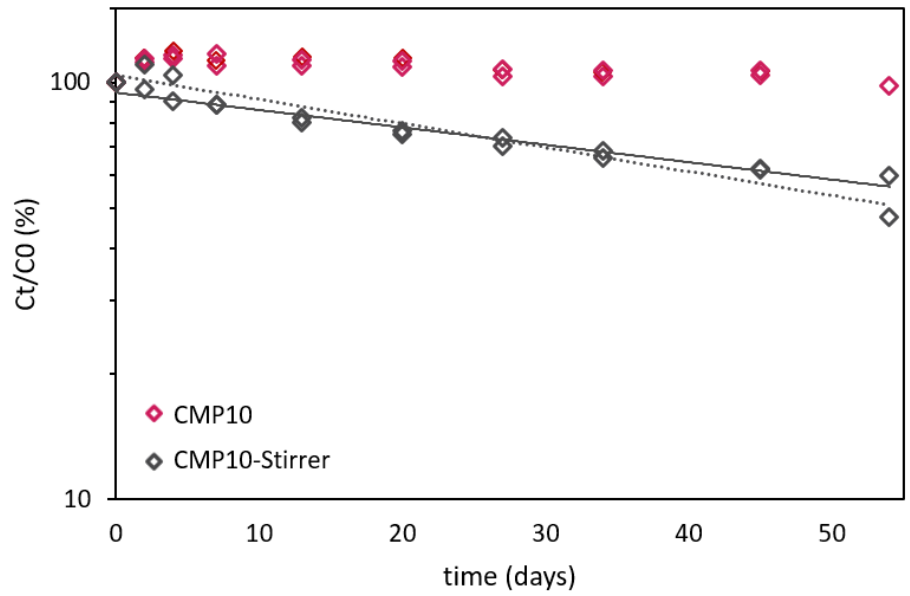

Carbamazepine residues in shaken (red diamonds) and stirred systems (grey diamonds). Diamonds represent calculated CTS at each time point in four experimental replicates of CMP10 and two experimental replicates of CMP10-Stirrer. Dashed and solid lines are modelled 1st order kinetic fits to each of the CMP10-Stirrer replicates. Ct/C0 is the portion of the spiked amount still remaining after the given time.
Source: Seller et al. 2020 (Figure SI3)

2.2.3 Concentration-Time Series

Generally, compound dissipation via biotransformation was faster in suspensions with increased sediment content. Least compound losses were observed in CMP1 and R1-Fall - only six substances showed up to 50% removal by the end of those experiments - while dissipation of most substances could be observed in R1-Spring, R10-Fall and CMP10. Those observations suggest that the extent of compound removal via biotransformation is influenced by the amount of sediment-borne biomass, but also by the microbial test communities' composition or activity. The latter two parameters have been demonstrated to undergo seasonal variations in surface waters (Gilbert et al. 2012; Staley et al. 2015; Sun et al. 2017), which agrees with our findings of

varying biotransformation capacities in environmental samples sourced during different seasons.

Besides interstudy variations, we observed drastic differences between replicates of the same study once biotransformation of compounds reached a detectable range. We expressed intrastudy variations as the spread between maximum and minimum concentrations of one compound in different replicates at the same time point. Especially during R1-Spring and R10-Fall, intrastudy variations increased over time; in R1-Spring, the average spread between trajectories increased from 270 ng L^{-1} after 13 days to 430 ng L^{-1} after 28 days. Intrastudy variations in biotransformation kinetics were lowest in CMP10 with a spread of less than 90 ng L^{-1} regardless of the time point. Described inter- and intrastudy variations are exemplarily illustrated for the three compounds atenolol, carbendazim, and diuron in Figure 3. A compilation of concentration-time series of all compounds during OECD 309-type suspension tests are shown in Annex A.2 Figure A4.

Figure 3: Water phase concentrations of atenolol, carbendazim, and diuron in suspension tests

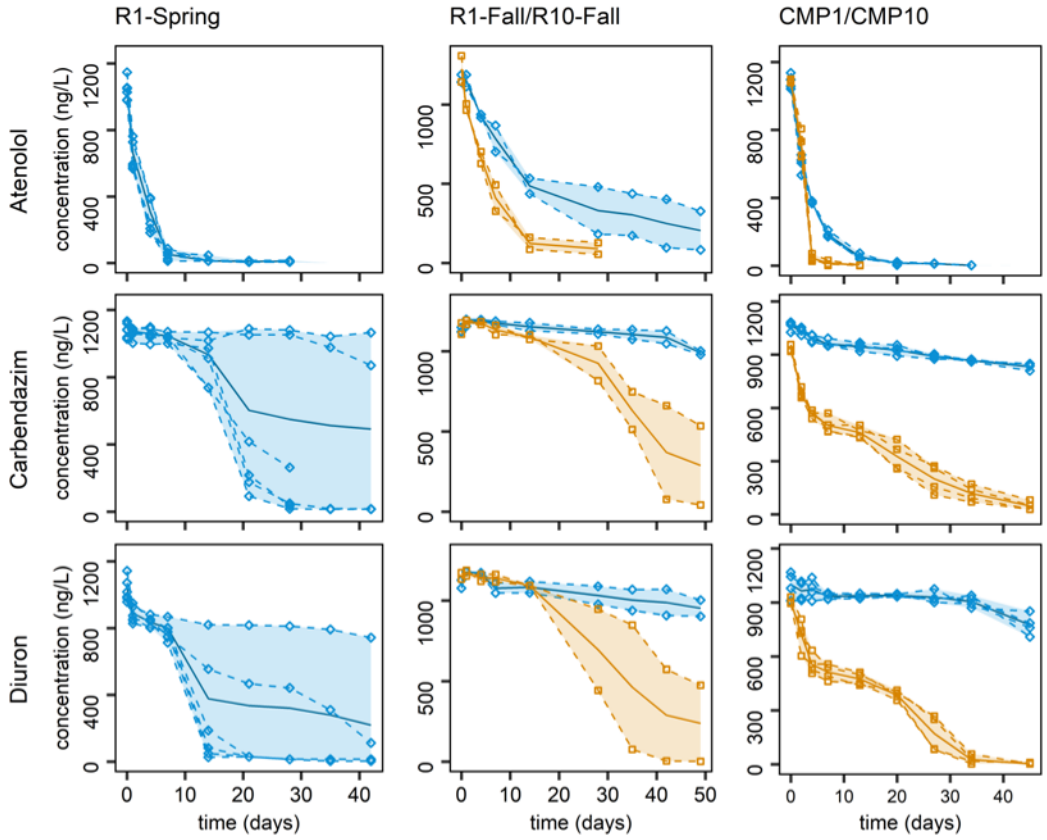

Suspensions containing 1 g solids L^{-1} are colored in blue with measured data represented as diamonds, and suspensions containing 10 g solids L^{-1} are shown in yellow with measured data represented as squares. Measurement points belonging to the same experimental replicate are connected with dashed lines. The solid line shows the average concentration calculated from the plotted experimental replicates, shaded areas indicate the spread of the concentrations measured at the same time point.

Source: Seller et al. 2020 (Figure 1)

Generally, little variation was observed for rapidly degrading compounds, i.e., atenolol, bezafibrate, and fenoxycarb. Literature suggests that those compounds are biotransformed by

enzymes widespread among bacteria (Achermann et al. 2018; Kern et al. 2010; Helbling et al. 2010; Johnson et al. 2015), supporting our observation that biotransformation readily occurred in different suspension tests. However, inter- and intrastudy variations in chemical removal indicate that most of our test compounds seem to have been transformed by enzymes less widespread or only expressed under specific conditions. Rare enzymes have a lower probability of occurrence at lower inoculum concentrations and their emergence in different test systems strongly depends on how the microbial community evolves over time (Martin et al. 2017; Goodhead et al. 2014; Johnson et al. 2015; Jaeger, Coll, et al. 2019). Coherently, a previous study in activated sludge showed that biotransformation of acesulfame, phenylureas (i.e., diuron and isoproturon in our study), and carbendazim strongly depends on the solids retention time and hence community composition, suggesting a need for enzyme activities not always present in activated sludge (Achermann et al. 2018). In our study, increasing sediment borne biomass by employing 10 g solids L^{-1} suspensions increased the likelihood of providing sufficient specific degraders/ enzymes to yield observable dissipation of most compounds from water-sediment suspensions; however, significant inter- and intra-study variations could still occur (see Chapter 2.2.4).

2.2.4 Lag Phases and Half-Lives ($DT_{50,TS}$ and $DegT_{50,TS,309}$)

We further aimed to reflect how observed varying biotransformation capacity of microbial test communities influences metrics for persistence assessment of chemicals derived from biotransformation kinetics in suspension tests (i.e., $DegT_{50,TS,309}$ and $DT_{50,TS,309}$). Therefore, we fitted the kinetic model described in Chapter 2.1.7 to trajectories derived from those studies in which we observed significant compound removal, i.e., R1-Spring, R10-Fall, and CMP10.

To account for sorption, system-specific sediment-water partitioning coefficients K_d were calculated from data of abiotic sorption control experiments. Derived K_d values describing the compounds sorption behavior during CMP10 are shown in Table 7. Citalopram was the only compound for which sorption appeared to be a significant removal pathway from the water phase during Rhine experiments, i.e., with a K_d of 100±20 L kg^{-1} in R1-Spring. Lag phases, half-lives and evaluation statistics derived when fitting the first-order degradation model to data from the biotransformation experiments are provided in Table 8.

Table 7: Sediment-water partitioning coefficients K_d of test compounds in CMP10

Sediment-water partitioning coefficients Kd of test compounds in CMP10, calculated as given in Equation (1). Kd values were calculated individually for each time point of sampling from the abiotic sorption controls (2, 4, 10 days), listed values present their average and standard deviation.

Compound	K_d (L kg^{-1}) in CMP10
5-Methylbenzotriazole	94±52
Acesulfame	0±1
Atenolol	53±9
Bezafibrate	0±1
Bicalutamide	54±13
Carbamazepine	20±4
Carbendazim	76±24

Compound	K_d (L kg^{-1}) in CMP10
Citalopram	625±138
Clopidogrel carboxylic acid	0±1
Cyclamate	0±1
Diclofenac	0±1
Dimethenamid	0±1
Diuron	29±6
Fenhexamid	17±4
Fenoxycarb	307±43
Fipronil	49±6
Gabapentin	1±1
Imidacloprid	9±3
Iprovalicarb	10±11
Isoproturon	7±7
Lamotrigine	42±17
Levetiracetam	0±1
Lidocaine	14±8
Mefenamic acid	19±8
Mesotrione	0±1
Metoprolol	56±13
Napropamide	32±9
Picoxystrobin	29±18
Saccharin	0±1
Sitagliptin	166±57
Sulfamethoxazole	14±19
Terbuthylazine	20±10
Trimethoprim	307±112
Trinexapac-ethyl	0±1
Valsartan	0±1
Venlafaxine	69±15

Table 8: Biotransformation kinetic parameters

Rate constants k (d^{-1}), lag phase (days), and half-lives (days) calculated as described in Chapter 2.1.7 together with their geometric mean, standard deviation (sd) and coefficient of variation (CV, %). n indicates how many data points were available with a clear deviation from their initial substance concentration, i.e. more than 10% substance loss and hence used for estimating k. In case lag phases exceed the duration of the experiments, no information on biotransformation kinetics could be obtained, i.e., k and $DegT_{50,TS,309}$ values could not be calculated.

		R1-Spring							R10-Fall					CMP10						
		Rep1	Rep2	Rep3	Rep4	mean	sd	CV	Rep1	Rep2	mean	sd	CV	Rep1	Rep2	Rep3	Rep4	mean	sd	CV
5MB	k	0.228	0.117	0.068	0.008	0.06	0.09	151						0.034	0.022	0.036	0.039	0.03	0.01	23
	R^2	0.99	0.99	0.9	0.95									0.97	0.88	0.99	0.98			
	n	4	5	4	4									6	6	7	7			
	lag phase	12	13	27	16	16.1	6.9	43						9	0	5	7	5.25	3.86	74
	$DegT_{50,309}$	3	6	10	87	11.2	40.4	361						20	32	19	18	21.6	6.55	30
	$DT_{50,TS,309}$	15	19	37	103	32.3	40.8	126						29	32	24	25	28.1	4.04	14
ACE	k	n.a.	0.015	n.a.	n.a.				0.002	n.a.				0.019	0.019	0.028	0.038	0.02	0.01	36
	R^2		0.98						0.77					0.99	0.97	0.96	0.99			
	n		6						3					3	4	4	4			
	lag phase	>63	13	>42	>42				2.5	>63				27	18	26	31	25	5.45	22
	$DegT_{50,309}$		46						347					36	36	25	18	27.6	8.85	32
	$DT_{50,TS,309}$	>63	59	>42	>42				349	>63				63	54	51	49	54	6.18	11
ATE	k	0.452	0.452	0.31	0.329	0.38	0.08	20	0.161	0.16	0.16	0	0.4	0.896	0.994	1.206	1.137	1.05	0.14	13
	R^2	0.99	0.99	0.97	0.98				0.99	0.98				0.99	1	1	0.99			
	n	4	5	4	4				6	6				5	4	3	5			
	lag phase	0	0	0	0	0	0.	0	0.2	0	0.10	0.14	141	1.5	1.3	1	1	1.18	0.24	21
	$DegT_{50,309}$	2	2	2	2	2	0	0	4	4	4.00	0	0	1	1	1	1	1	0	0
	$DT_{50,TS,309}$	2	2	2	2	2	0	0	5	4	4.47	0.71	16	2	2	2	2	2	0	0
BEZ	k	0.291	0.418	0.247	0.314	0.31	0.07	23						0.279	0.403	0.48	0.484	0.4	0.1	24
	R^2	0.99	0.98	0.99	0.99									0.96	0.96	0.98	0.97			
	n	4	5	5	5									5	5	5	5			
	lag phase	0	0	0	0	0	0	0						0	0	0	0	0	0	0

		R1-Spring							R10-Fall					CMP10						
		Rep1	Rep2	Rep3	Rep4	mean	sd	CV	Rep1	Rep2	mean	sd	CV	Rep1	Rep2	Rep3	Rep4	mean	sd	CV
	$DegT_{50,309}$	2	2	3	2	2.21	0.5	23						2	2	1	1	1.41	0.58	41
	$DT_{50,TS,\ 309}$	2	2	3	2	2.21	0.5	23						2	2	1	1	1.41	0.58	41
BIC	k	0.025	0.034	n.a.	0.23	0.06	0.12	200						0.083	0.064	0.087	0.058	0.07	0.01	20
	R^2	0.94	0.98		0.96									0.95	0.96	0.97	0.95			
	n	8	6		4									5	7	7	7			
	lag phase	7	18	>42	32	15.9	12.5	79						5.4	2	3	3	3.14	1.45	46
	$DegT_{50,309}$	28	20		3	11.9	12.8	107						8	11	8	12	9.59	2.06	22
	$DT_{50,TS,\ 309}$	35	38	>42	35	36	1.73	5						14	13	11	15	13.2	1.71	13
CBA	k	0.294	0.23	0.017	n.a.	0.1	0.15	138	0.005	0.111	0.02	0.07	318	0.077	0.087	0.063	0.056	0.07	0.01	20
	R^2	0.99	0.99	1					0.99	0.76				0.98	0.98	0.98	0.98			
	n	3	4	2					6	5				6	7	6	8			
	lag phase	13	13	29	>42	>17	9.24	54	0	14	7.00	9.9	141	17	11	13	6	11	4.57	42
	$DegT_{50,309}$	2	3	41		6.3	22.2	355	139	6	28.88	94.1	326	9	8	11	12	9.87	1.83	18
	$DT_{50,TS,309}$	15	16	70	>42	>25.6	31.5	123	139	20	52.73	84.2	160	26	19	24	18	21.5	3.86	18
CIT	k	0.055	0.116	0.113	0.033	0.07	0.04	60						0.052	0.031	0.048	0.058	0.05	0.01	25
	R^2	0.85	0.83	0.88	0.93									0.88	0.84	0.83	0.95			
	n	9	11	8	5									5	6	6	6			
	lag phase	0	0	0	9	2.25	4.5	200						12	4	7	7	6.96	3.32	48
	$DegT_{50,309}$	13	6	6	21	9.96	7.14	72						13	22	14	12	14.8	4.57	31
	$DT_{50,TS,309}$	13	6	6	30	10.9	11.3	104						25	26	21	19	22.6	3.3	15
CLO	k	0.011	0.015	0.009	0.01	0.01	0	24	0.023	0.023	0.02	0	0	0.023	0.037	0.03	0.027	0.03	0.01	21
	R^2	0.95	0.91	0.95	0.98				0.97	0.98				0.93	0.94	0.97	0.95			
	n	10	11	5	6				5	6				7	8	10	8			
	lag phase	0	0	5.6	0	1.4	2.8	200	32	28	29.93	2.83	9	2.4	5.6	0	0	2	2.65	133
	$DegT_{50,309}$	63	46	77	69	62.6	13.2	21	30	30	30.00	0	0	30	19	23	26	24.2	4.65	19
	$DT_{50,TS,309}$	63	46	83	69	63.8	15.3	24	62	58	59.97	2.83	5	33	24	23	26	26.2	4.51	17
CYC	k	0.11	0.083	0.018	0.016	0.04	0.05	117	0.04	0.043	0.04	0	5	0.019	0.023	0.042	0.016	0.02	0.01	50

		R1-Spring							R10-Fall					CMP10						
		Rep1	Rep2	Rep3	Rep4	mean	sd	CV	Rep1	Rep2	mean	sd	CV	Rep1	Rep2	Rep3	Rep4	mean	sd	CV
	R^2	0.99	0.96	0.94	0.76				0.99	0.79				0.99	0.98	0.93	0.94			
	n	4	7	7	8				5	7				4	5	5	8			
	lag phase	4	0.2	0	0	1.05	1.97	188	33	14	21.49	13.4	63	16	14	19	3	10.6	6.98	66
	$DegT_{50,,309}$	6	8	39	43	16.8	19.7	117	17	16	16.49	0.71	4	36	30	17	43	29.8	11.03	37
	$DT_{50,TS,309}$	10	9	39	43	19.7	18.3	93	50	30	38.73	14.1	37	52	44	36	46	44.1	6.61	15
DIC	k	0.026	0.027	0.008	0.007	0.01	0.01	78	0.012	0.021	0.02	0.01	40	0.024	0.041	0.032	0.034	0.03	0.01	22
	R^2	0.99	0.96	1	0.77				0.93	0.85				0.95	0.96	0.96	0.97			
	n	8	7	2	6				9	9				7	7	9	10			
	lag phase	7	14	35	4	10.8	14	129	0	4	2.00	2.83	141	0.6	5.2	2	0	1.95	2.32	119
	$DegT_{50,309}$	27	26	87	99	49.6	38.7	78	58	33	43.75	17.7	40	29	17	22	20	21.6	5.1	24
	$DT_{50,TS,309}$	34	40	122	103	64.3	44.3	69	58	37	46.32	14.9	32	29	22	24	20	23.5	3.86	16
DIM	k	0.016	0.021	0.012	0.01	0.01	0	34	0.01	0.018	0.01	0.01	42	0.028	0.034	0.029	0.031	0.03	0	9
	R^2	0.96	0.97	1	0.94				0.91	0.96				0.99	0.99	0.99	0.98			
	n	8	7	2	6				8	11				8	9	9	10			
	lag phase	2	9.6	27	2.4	5.9	11.7	197	0	0	0	0	0	0.1	0	0	0	0.03	0.05	200
	$DegT_{50,309}$	43	33	58	69	48.8	15.9	33	69	39	51.9	21.2	41	25	20	24	22	22.7	2.22	10
	$DT_{50,TS,309}$	45	43	85	72	58.7	20.6	35	69	39	51.9	21.2	41	25	20	24	22	22.7	2.22	10
DIU	k	0.382	0.318	0.037	0.007	0.07	0.19	256	0.042	0.255	0.1	0.15	146	0.098	0.042	0.061	0.047	0.06	0.03	43
	R^2	0.99	0.99	0.97	0.84				0.85	0.99				0.94	0.88	0.88	0.93			
	n	3	3	8	6				7	4				5	7	7	7			
	lag phase	7	7	0	2	4	3.56	89	14	24	18.3	7.07	39	12	0	2	3	4.25	5.32	125
	$DegT_{50,309}$	2	2	19	99	9.31	46.4	498	17	3	7.14	9.9	139	7	17	11	15	11.8	4.43	37
	$DT_{50,TS,309}$	9	9	19	101	19.9	44.6	225	31	27	28.9	2.83	10	19	17	13	18	16.6	2.63	16
FEN	k	0.091	0.073	0.041	0.053	0.06	0.02	36	0.034	0.037	0.04	0	6	0.104	0.103	0.103	0.1	0.1	0	2
	R^2	0.99	0.99	0.96	0.95				0.98	0.96				0.99	0.99	0.99	0.99			
	n	9	8	7	9				10	11				8	6	8	7			
	lag phase	1.7	0	0	0	0.43	0.85	200	0	0	0	0	0	0	0	0	2	0.5	1	200
	$DegT_{50,309}$	8	9	17	13	11.2	4.11	37	20	19	19.5	0.71	4	7	7	7	7	7	0	0

		R1-Spring							R10-Fall					CMP10						
		Rep1	Rep2	Rep3	Rep4	mean	sd	CV	Rep1	Rep2	mean	sd	CV	Rep1	Rep2	Rep3	Rep4	mean	sd	CV
	$DT_{50,TS,309}$	9	9	17	13	11.6	3.83	33	20	19	19.5	0.71	4	7	7	7	9	7.45	1	13
FOC	k	0.381	0.409	0.417	3.707	0.7	1.65	236	4.195	1.115	2.16	2.18	101	2.244	1.861	1.221	4.312	2.17	1.34	62
	R^2	0.99	0.99	0.98	0.99				0.99	0.99				1	1	1	0.99			
	n	4	4	3	4				3	3				3	3	3	3			
	lag phase	0	0	1	0.9	0.48	0.55	116	0.8	0	0.4	0.57	141	2	2	1.5	2	1.86	0.25	13
	$DegT_{50,309}$	2	2	2	0.2	1.12	0.9	80	0.2	1	0.45	0.57	126	0	0	1	0	0.25	0.5	200
	$DT_{50,TS,309}$	2	2	3	1.1	1.91	0.78	41	1	1	1	0	0	2	2	2	2	2	0	0
FIP	k	0.01	0.011	0.005	0.007	0.01	0	35	n.a.	0.012				0.044	0.048	0.05	0.044	0.05	0	6
	R^2	0.95	0.94	0.91	0.89					0.77				0.92	0.82	0.87	0.89			
	n	10	11	5	6					11				8	8	9	10			
	lag phase	0	0	0	2	0.5	1	200	>63	0				0	0	0	0	0	0	0
	$DegT_{50,309}$	69	63	139	99	87.9	34.8	40		58				16	14	14	16	15	1.15	8
	$DT_{50,TS,309}$	69	63	139	101	88.4	34.9	39	>63	58				16	14	14	16	15	1.15	8
GAB	k	0.023	0.019	0.02	0.018	0.02	0	11	0.015	0.02	0.02	0.00	20	0.014	0.017	0.018	0.018	0.02	0	11
	R^2	0.94	0.91	0.88	0.95				0.95	0.97				0.94	0.89	0.99	0.96			
	n	8	8	7	7				9	8				7	8	7	9			
	lag phase	2.4	0	0	1.1	0.88	1.14	130	0.7	5	1.87	3.04	163	2	0	4	0	1.5	1.91	128
	$DegT_{50,309}$	30	36	35	39	34.8	3.74	11	46	35	40.1	7.78	19	50	41	39	39	42	5.25	12
	$DT_{50,TS,309}$	33	36	35	40	35.9	2.94	8	47	40	43.4	4.95	11	52	41	43	39	43.5	5.74	13
IMI	k	n.a.	n.a.	n.a.	n.a.				n.a.	n.a.				0.009	0.012	0.013	0.008	0.01	0	23
	R^2													0.97	0.94	0.84	0.92			
	n													5	7	10	8			
	lag phase	>63	>63	>42	>42				>63	>63				0	1	0	1	0.5	0.58	115
	$DegT_{50,309}$													77	58	53	87	67.4	16	24
	$DT_{50,TS,309}$	>63	>63	>42	>42				>63	>63				77	59	53	88	67.9	16.1	24
IPR	k	0.115	0.092	0.004	0.013	0.03	0.06	205	0.009	0.022	0.01	0.01	65	0.08	0.059	0.115	0.118	0.09	0.03	32
	R^2	0.99	0.98	0.99	0.94				0.91	0.81				0.91	0.9	0.97	0.97			

		R1-Spring							R10-Fall					CMP10						
		Rep1	Rep2	Rep3	Rep4	mean	sd	CV	Rep1	Rep2	mean	sd	CV	Rep1	Rep2	Rep3	Rep4	mean	sd	CV
	n	5	6	3	8				10	7				6	7	5	6			
	lag phase	10	6	5.4	0	5.35	4.11	77	1	0	0.5	0.71	141	0	0	3	2	1.25	1.5	120
	$DegT_{50,309}$	6	8	173	53	25.8	78.4	304	77	32	49.6	31.8	64	9	12	6	6	7.9	2.87	36
	$DT_{50,TS,309}$	16	14	179	53	38.2	77.8	204	78	32	50	32.5	65	9	12	9	8	9.39	1.73	18
ISO	k	0.307	0.239	0.035	0.021	0.09	0.14	168	0.028	0.092	0.05	0.05	89	0.052	0.03	0.067	0.031	0.04	0.02	42
	R^2	0.99	0.99	0.99	0.97				0.96	0.98				0.96	0.99	0.98	0.91			
	n	13	5	3	3				6	6				6	8	8	9			
	lag phase	13	13	33	28	19.9	10.3	52	28	31	29.5	2.12	7	7	3	17	0	6.75	7.41	110
	$DegT_{50,309}$	2	3	20	33	7.93	14.8	187	25	8	14.1	12.02	85	13	23	10	22	16	6.48	40
	$DT_{50,TS,309}$	15	16	53	61	29.7	24.2	81	53	39	45.5	9.9	22	20	26	27	22	23.6	3.3	14
LAM	k	n.a.	n.a.	n.a.	n.a.				0.004	n.a.				0.008	0.007	0.008	0.008	0.01	0	6
	R^2													0.92	0.92	0.93	0.94			
	n								2					5	4	6	8			
	lag phase	>63	>63	>42	>42				30	>63				6	9	0	0	3.75	4.5	120
	$DegT_{50,309}$								173					87	99	87	87	89.9	6	7
	$DT_{50,TS,309}$	>63	>63	>42	>42				203	>63				93	108	87	87	93.4	9.91	11
LEV	k	0.371	0.229	0.827	0.406	0.41	0.26	63	0.046	0.101	0.07	0.04	57	0.207	0.128	0.131	0.165	0.15	0.04	24
	R^2	0.98	0.99	0.99	0.97				0.98	0.91				0.95	0.93	0.94	0.94			
	n	5	5	4	5				9	5				5	6	6	6			
	lag phase	2	0.3	4	2.7	1.6	1.54	97	0	1	0.5	0.71	141	3	1.2	1.4	3	1.97	0.98	50
	$DegT_{50,309}$	2	3	1	2	1.86	0.82	44	15	7	10.3	5.66	55	3	5	5	4	4.16	0.96	23
	$DT_{50,TS,309}$	4	3	5	4	3.94	0.82	21	15	8	11	4.95	45	6	7	7	7	6.74	0.5	7
LID	k	0.027	0.015	0.016	0.019	0.02	0.01	29	0.013	0.02	0.02	0.00	31	0.026	0.038	0.023	0.037	0.03	0.01	25
	R^2	0.94	0.92	0.89	0.86				0.92	0.95				0.98	0.97	0.99	0.98			
	n	9	7	5	6				10	10				8	8	8	9			
	lag phase	0	0	8	0	2	4	200	0	0	0	0	0	0	0.4	1	0	0.35	0.47	135
	$DegT_{50,309}$	26	46	43	36	36.9	8.88	24	53	35	43.1	12.7	30	27	18	30	19	22.9	5.92	26

		R1-Spring							R10-Fall					CMP10						
		Rep1	Rep2	Rep3	Rep4	mean	sd	CV	Rep1	Rep2	mean	sd	CV	Rep1	Rep2	Rep3	Rep4	mean	sd	CV
	$DT_{50,TS,309}$	26	46	51	36	38.5	11.1	29	53	35	43.1	12.7	30	27	19	31	19	23.5	6	26
MEF	k	0.111	0.079	0.017	0.016	0.04	0.05	120						0.056	0.078	0.066	0.079	0.07	0.01	16
	R^2	0.98	0.97	0.94	0.81									0.97	0.97	0.99	0.98			
	n	4	5	7	8									8	7	7	7			
	lag phase	7	6	1.3	0	3.58	3.44	96						2	3	5	4	3.31	1.29	39
	$DegT_{50,309}$	6	9	41	43	17.6	20	114						12	9	11	9	10.2	1.5	15
	$DT_{50,TS,309}$	13	15	42	43	24.4	16.5	68						14	12	16	13	13.7	1.71	12
MES	k	0.033	0.036	0.011	0.028	0.02	0.01	45	0.097	0.082	0.09	0.01	12	0.115	0.1	0.097	0.094	0.1	0.01	9
	R^2	0.88	0.9	0.78	0.85				0.97	0.95				0.99	0.99	0.99	0.98			
	n	10	9	7	9				10	7				8	8	9	10			
	lag phase	0.3	0	0	0	0.08	0.15	200	3	0.6	1.34	1.7	126	2	1	2	1	1.41	0.58	41
	$DegT_{50,309}$	21	19	63	25	28.2	20.8	74	7	8	7.48	0.71	9	6	7	7	7	6.74	0.5	7
	$DT_{50,TS,309}$	21	19	63	25	28.2	20.8	74	10	9	9.49	0.71	7	8	8	9	8	8.24	0.5	6
MTO	k	0.108	0.113	0.074	0.064	0.09	0.02	28	0.057	0.045	0.05	0.01	17	0.189	0.243	0.289	0.229	0.23	0.04	18
	R^2	0.93	0.92	0.98	0.96				0.98	0.94				0.96	0.96	0.96	0.96			
	n	6	6	8	9				7	8				6	6	6	6			
	lag phase	0.6	0	1.4	0	0.5	0.66	133	2	0	1	1.41	141	0	0	0	0	0	0	0
	$DegT_{50,309}$	6	6	9	11	7.73	2.45	32	12	15	13.4	2.12	16	4	3	2	3	2.91	0.82	28
	$DT_{50,TS,309}$	7	6	11	11	8.44	2.63	31	14	15	14.5	0.71	5	4	3	2	3	2.91	0.82	28
NAP	k	0.052	0.031	0.007	0.035	0.03	0.02	74	0.004	0.014	0.01	0.01	94	0.022	0.025	0.01	0.018	0.02	0.01	37
	R^2	0.9	0.93	0.94	0.99				0.76	0.83				0.95	0.94	0.94	0.99			
	n	8	11	5	2				6	7				6	5	6	5			
	lag phase	0	0	3.5	35	9.63	17	177	28	14	19.8	9.9	50	5	10	8	14	8.65	3.8	44
	$DegT_{50,309}$	13	22	99	20	27.4	40.5	148	173	50	93	87	94	32	28	69	39	39.4	18.6	47
	$DT_{50,TS,309}$	13	22	103	55	35.7	40.7	114	201	64	113	96.9	85	37	38	77	53	48.9	18.7	38
PIC	k	0.088	0.083	0.027	0.023	0.05	0.04	76	0.008	0.0031	<0.01	0	70	0.033	0.024	0.016	0.018	0.02	0.01	35
	R^2	0.99	0.94	0.79	0.78				0.5	0.86				0.91	0.91	0.84	0.9			

		R1-Spring							R10-Fall					CMP10						
		Rep1	Rep2	Rep3	Rep4	mean	sd	CV	Rep1	Rep2	mean	sd	CV	Rep1	Rep2	Rep3	Rep4	mean	sd	CV
	n	11	11	9	9				10	11				8	8	9	9			
	lag phase	0	0	0	0	0	0	0	0	0	0	0	0	2.1	0	0	0	0.53	1.05	200
	$DegT_{50,309}$	8	8	26	30	15	11.7	78	87	224	139	96.9	69	21	29	43	39	31.8	9.93	31
	$DT_{50,TS,309}$	8	8	26	30	15	11.7	78	87	224	139	96.9	69	23	29	43	39	32.5	9.15	28
SAC	k	0.134	0.126	0.029	0.06	0.07	0.05	69	0.286	0.177	0.22	0.08	34	0.017	0.079	0.054	0.017	0.03	0.03	91
	R^2	0.99	0.99	0.84	0.65				0.94	0.95				0.75	0.88	0.92	0.71			
	n	4	4	5	5				3	5				6	4	8	6			
	lag phase	6.4	6.6	7	14	8.02	3.68	46	35	35	35	0	0	5	26	19	6	11	10.2	93
	$DegT_{50,309}$	5	6	24	12	9.64	8.73	91	2	4	2.83	1.41	50	41	9	13	41	21.1	17.4	83
	$DT_{50,TS,309}$	12	12	31	26	18.5	9.74	53	37	39	38	1.41	4	46	35	32	47	39.5	7.62	19
SIT	k	0.081	0.059	0.068	0.033	0.06	0.02	35						0.065	0.056	0.059	0.06	0.06	0	6
	R^2	0.99	0.83	0.89	0.69									0.99	0.98	0.98	0.99			
	n	11	10	8	8									7	7	8	8			
	lag phase	0	1	0	1	0.5	0.58	115						3	3.4	2	3	2.8	0.6	21
	$DegT_{50,309}$	9	12	10	21	12.3	5.48	45						11	12	12	12	11.7	0.5	4
	$DT_{50,TS,309}$	9	13	10	22	12.7	5.92	47						14	16	14	15	14.7	0.96	7
SUL	k	0.023	0.05	0.032	0.035	0.03	0.01	33	0.027	0.057	0.04	0.02	54	0.275	0.101	0.114	0.102	0.13	0.08	63
	R^2	0.18	0.47	0.57	0.49				0.88	0.96				0.93	0.94	0.93	0.91			
	n	10	11	8	9				10	11				7	9	9	9			
	lag phase	0	0	0	0	0	0	0	0	0	0	0	0	1.5	0	0	0	0.38	0.75	200
	$DegT_{50,309}$	30	14	22	20	20.7	6.61	32	26	12	17.7	9.9	56	3	7	6	7	5.45	1.89	35
	$DT_{50,TS,309}$	30	14	22	20	20.7	6.61	32	26	12	17.7	9.9	56	4	7	6	7	5.86	1.41	24
TER	k	n.a.	n.a.	n.a.	n.a.				n.a.	n.a.				0.007	0.015	0.009	0.007	0.01	0	42
	R^2													0.96	0.97	0.92	0.97			
	n													4	4	7	6			
	lag phase	>63	>63	>42	>42				>63	>63				5	20	2	0	6.75	9.07	134
	$DegT_{50,309}$													99	46	77	99	76.8	25.1	33

		R1-Spring							R10-Fall					CMP10						
		Rep1	Rep2	Rep3	Rep4	mean	sd	CV	Rep1	Rep2	mean	sd	CV	Rep1	Rep2	Rep3	Rep4	mean	sd	CV
	$DT_{50,TS,309}$	>63	>63	>42	>42				>63	>63				104	66	79	99	85.6	17.7	21
TRI	k	0.18	0.153	0.071	0.045	0.1	0.06	67						0.146	0.329	0.338	0.222	0.25	0.09	37
	R^2	0.96	0.97	0.87	0.79									0.99	0.99	0.96	0.98			
	n	5	5	8	9									5	4	5	4			
	lag phase	1.5	0	0	0	0.38	0.75	200						3	3	3	3	3	0	0
	$DegT_{50,309}$	4	5	10	15	7.4	5.07	68						5	2	2	3	2.78	1.41	51
	$DT_{50,TS,309}$	5	5	10	15	7.83	4.79	61						8	5	5	6	5.89	1.41	24
TNE	k	0.131	0.127	0.062	0.077	0.09	0.03	37	0.06	0.059	0.06	0	1	0.289	0.264	0.291	0.268	0.28	0.01	5
	R^2	0.99	0.99	0.97	0.95				0.98	0.96				0.99	0.99	0.99	0.99			
	n	5	6	8	9				8	8				6	5	5	5			
	lag phase	0.5	0	0	0	0.13	0.25	200	3	3.4	3.19	0.28	9	0	0	0	0	0	0	0
	$DegT_{50,309}$	5	5	11	9	7.05	3	43	12	12	12	0	0	2	3	2	3	2.45	0.58	24
	$DT_{50,TS,309}$	6	5	11	9	7.38	2.75	37	15	15	15	0	0	2	3	2	3	2.45	0.58	24
VAL	k	0.193	0.271	0.111	0.189	0.18	0.07	36	0.047	0.115	0.07	0.05	65	0.082	0.099	0.101	0.086	0.09	0.01	10
	R^2	0.99	0.98	0.97	0.95				0.95	0.97				0.88	0.96	0.94	0.93			
	n	5	5	9	9				6	4				6	6	5	6			
	lag phase	0	0	0	0	0	0	0	24	26	25	1.41	6	3	1	3	1	1.73	1.15	67
	$DegT_{50,309}$	4	3	6	4	4.12	1.26	31	15	6	9.49	6.36	67	8	7	7	8	7.48	0.58	8
	$DT_{50,TS,309}$	4	3	6	4	4.12	1.26	31	39	32	35.3	4.95	14	11	8	10	9	9.43	1.29	14
VEN	k	0.005	0.008	0.021	0.011	0.01	0.01	71	0.029	0.023	0.03	0	16	0.009	0.012	0.012	0.008	0.01	0	20
	R^2	0.9	0.85	0.92	0.94				0.87	0.96				0.9	0.95	0.91	0.81			
	n	8	10	7	6				9	11				6	6	7	7			
	lag phase	0	3.3	0	2.4	1.43	1.69	118	0	0	0	0	0	2	3	0	1	1.5	1.29	86
	$DegT_{50,309}$	139	87	33	63	70.8	44.8	63	24	30	26.8	4.24	16	77	58	58	87	68.9	14.4	21
	$DT_{50,TS,309}$	139	90	33	65	72	44.7	62	24	30	26.8	4.24	16	79	61	58	88	70.4	14.5	20

Lag phases are commonly observed in laboratory biotransformation tests (Comber 2010; Li and McLachlan 2019; Ott et al. 2020); here, lag phases occurred to various extents for all compounds, except for bezafibrate, and ranged from ~1 day to up to more than 63 days, depending on compound and experiment. Lag phases were generally shorter in tests carried out with 10 g solids L^{-1}, especially in CMP10. Further, we observed intrastudy variations of lag phases, which were most significant in R1-Spring; differences between replicates were greater than 20 days for five compounds (i.e., acesulfame, bicalutamide, carbendazim, dimethenamid, and isoproturon). As discussed previously, biotransformation of at least three of those has been hypothesized to depend on the emergence of specific enzymes.

However, current regulatory guidelines do not specify how to consider lag phases when assessing a substance's persistence, i.e., whether $DegT_{50,309}$ or $DT_{50,TS,309}$ are to be used as decisive persistence measure (ECHA 2017; FOCUS 2006). Since lag phases are a sign of microbial adaptation and reduced lag phases could be speculated for compounds continuously or repeatedly released to the aquatic environment (e.g., pharmaceuticals, or pesticides), it has been argued that $DegT_{50,309}$ should be used as persistence metric (Ahtiainen, Aalto, and Pessala 2003; Poursat et al. 2019; Birch et al. 2017; Blunt et al. 2018). However, our experiments do not directly support this hypothesis as we determined shortest and least variable lag phases in suspensions employing a microbial community sourced from a pristine environment (CMP10). Therefore, and in light of the current lack of understanding of observed variability in lag phases, the use of $DT_{50,TS,309}$ values to assess persistence would seem the more cautious and environmentally protective approach. It needs to be noted though that $DT_{50,TS,309}$ of a given compound can range from a few days to over 100 days due to the combined effect of varying lag phases and $DegT_{50,309}$ - see e.g., 5-methylbenzotriazole, carbendazim, diuron, or iprovalicarb in Figure 3 or Table 8. Similarly, variations in half-lives of one or two orders of magnitude have previously been observed in different OECD 308 or OECD 309 studies for several of our test compounds, including acesulfame, diclofenac, trimethoprim, and venlafaxine (Fahlman et al. 2018; Li and McLachlan 2019; Coll et al. 2020).

Interstudy variations depend on origin and sampling period of the microbial test community and may be considered an indicator of strong fluctuations in biotransformation potential of a compound under spatially and temporally varying conditions of natural aquatic environments (Gilbert et al. 2012; Staley et al. 2015; Sun et al. 2017). Intrastudy variations on the other hand, i.e., experimental replicates drifting apart over the time course of an experiment, make the interpretation of biotransformation study outcomes challenging, especially when persistence is assessed by comparing a derived half-life to persistence cut-off values defined in regulatory frameworks.

2.3 Biotransformation in Modified OECD 308-type Studies

2.3.1 Identifying Removal Pathways

As described in Chapter 2.2.1, comparing biotransformation experiments with control experiments in sterile water allowed identifying the six compounds irbesartan, hydrochlorothiazide, fipronil, sitagliptin, trinexapac-ethyl, and 5-methylbenzotriazol to be susceptible towards hydrolysis at environmentally relevant pH (i.e., pH 7-8), yet with rather low hydrolysis rate constants, i.e., ≤0.005 d^{-1} for the latter four compounds (Table 5).

Several test compounds showed high affinity toward the sediment, i.e., accumulation of >70% of initially spiked compound mass in the sediment layer by the end of biotransformation experiments was observed for aliskiren, atazanavir, azoxystrobin, citalopram, and sitagliptin, as well as for lamotrigine in case of CMP sediment. Consistently, experimentally determined K_{oc} values of those compounds are rather high (see Chapter 3).

Due to analytical issues, we were not able to measure compound residues in the sediment for clarithromycin, fenhexamid, fipronil, and mesotrione in case of CMP experiments, and for clarithromycin, aliskiren, atazanavir, and azoxystrobin in case of Rhine experiments.

Overall, we were able to observe the behavior of 42 compounds in at least one modified OECD 308-type system; five compounds appeared to be rather recalcitrant toward removal from the test systems with $DT_{50,TS,mod308}$ >100 days, and 38 compounds dissipated from the test systems with $DT_{50,TS,mod308}$ <100 days. In case of compound dissipation, we assume biotransformation to be the dominant removal pathway for 36 compounds, while abiotic transformation may be the dominant removal pathway for the two compounds hydrochlorothiazide and irbesartan.

2.3.2 Concentration-Time Series

Residues measured in duplicates sacrificed at each sampling time point were generally in good agreement, with an average difference of 4 and 3% of initially spiked compound mass for residues measured in the water phase and the sediment layer, respectively. Hence, in contrast to OECD 309-type studies (see Chapter 2.2.3 and Chapter 2.2.4), intrastudy variations between experimental replicates appear to be negligible in modified OECD 308-type studies. Exemplary residue-time series are shown for acesulfame, isoproturon and terbuthylazine in Figure 4. A compilation of residue-time series for all test compounds is shown in Annex A.2, Figure A5.

Figure 4: Residues of acesulfame, isoproturon, and terbuthylazine in modified OECD 308-type studies

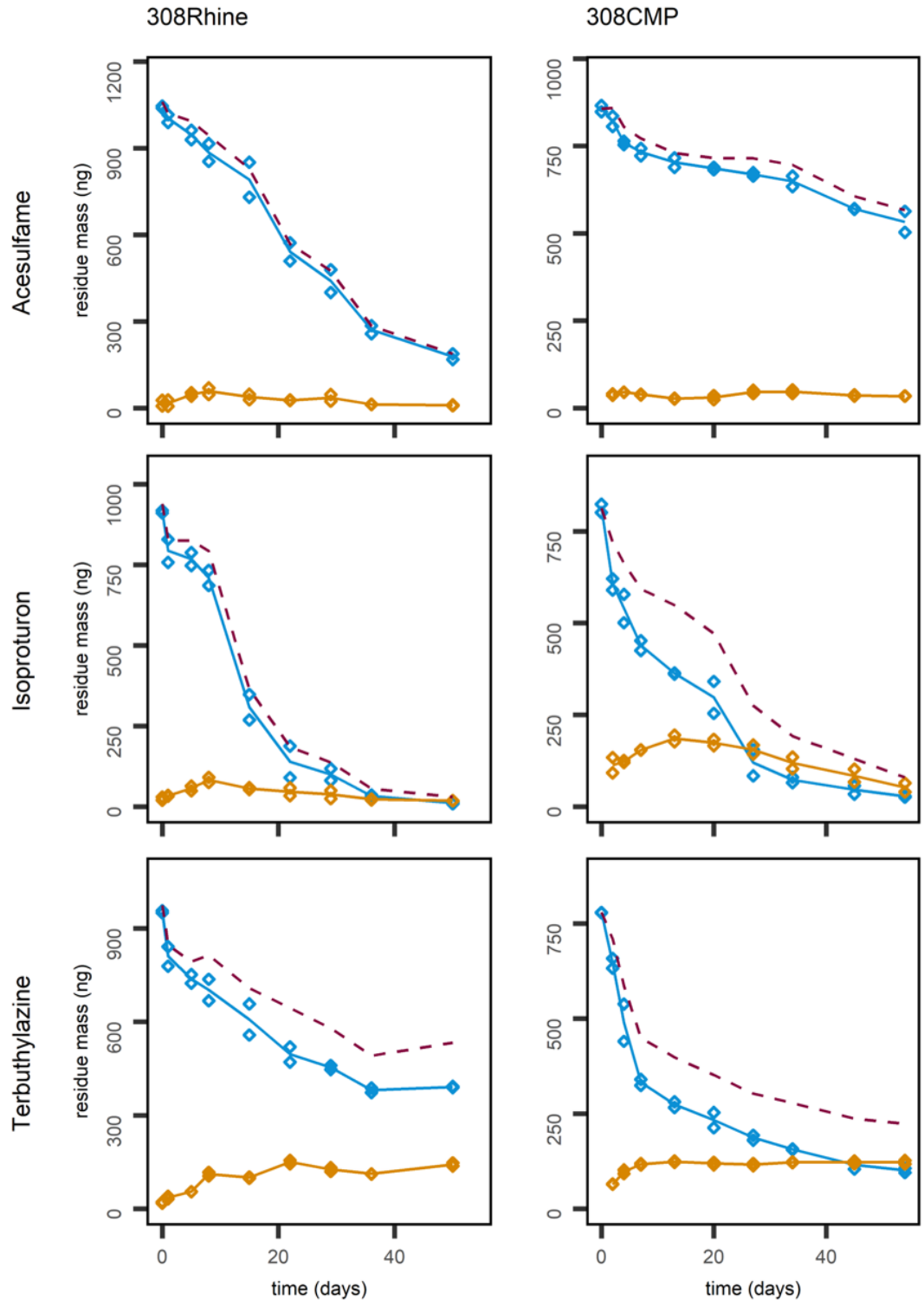

Residues of acesulfame, isoproturon and terbuthylazine measured in the water phase (blue diamonds) and sediment (yellow diamonds) over the time course of modified OECD 308-type studies. Solid lines show the average between residues measured in the sampled duplicates at each time point in the water phase and sediment, respectively. Dotted line shows the average total compound residues as a sum of residues in the water phase and sediment.

Source: own figure, Eawag

2.3.3 Lag Phases and Half-Lives ($DT_{50,w,mod308}$ and $DT_{50,TS,mod308}$)

The negligible differences between compound residues measured in the water phase and the sediment of sacrificed samples (Figure 4) justified fitting the first-order degradation model to the averaged compound residues in sacrificed duplicates over time. Model fits were generally good with maximum standard errors <5%. Derived $DT_{50,w,mod308}$, $DT_{50,TS,mod308}$ and further statistical model parameters are given in Table 9 and Table 10. Lag phases >2 days were observed for 14 compounds, however, only isoproturon had a lag phase >10 days in CMP experiments. $DT_{50,w,mod308}$ ranged from 0.8 to 73 days. $DT_{50,TS,mod308}$ ranged from ≤2 days (e.g., fenoxycarb and atenolol) to >230 days (e.g., carbamazepine, citalopram, and lamotrigine).

As evident from Table 10, $DT_{50,TS,mod308}$ values derived from modified OECD 308-type experiments did not differ significantly between the Rhine- and the CMP study for the majority of test compounds. Both studies identified the same 11 compounds as most rapidly degrading, i.e., fenoxycarb, atenolol, sulfamethoxazole, bezafibrate, trimethoprim, trinexapac-ethyl, valsartan, levetiracetam, iprovalicarb, fenhexamid, and irbesartan with $DT_{50,TS}$ ≤10 days. Consistently, those same compounds had also shown rapid biotransformation in previous research in activated sludge of WWTPs (Achermann et al. 2018). In contrast, aliskiren, atazanavir, citalopram, carbamazepine, and lamotrigine were consistently identified as the most persistent compounds with $DT_{50,TS}$ >100 days in both modified OECD 308-type systems.

Noticeable interstudy differences between $DT_{50,TS,mod308}$ occurred for the three artificial sweeteners, i.e., acesulfame, cyclamate and saccharin. $DT_{50,TS,mod308}$ values of all three sweeteners were roughly one order of magnitude higher in CMP experiments compared to Rhine experiments. In case of acesulfame, previous research demonstrated bacterial evolution toward an increased capacity to metabolize the artificial sweetener in WWTPs (Kahl et al. 2018; Kleinsteuber et al. 2019). Further, it has been shown that WWTP discharge can affect a microbial communities biotransformation capacity in rivers and lakes such that the sweetener acesulfame - previously considered persistent - can be biotransformed (Coll et al. 2020). At the time of environmental sampling for the here conducted biotransformation experiments, none of the target compounds were measured in water samples from CMP. However, several compounds, including the three artificial sweeteners, were quantifiable in water samples from the Rhine at concentrations of up to 250 ng L^{-1} (i.e., acesulfame). We hence speculate that pre-exposure to the artificial sweeteners of the microbial test community sourced from the Rhine resulted in an enhanced ability to biotransform those compounds resulting in shorter $DT_{50,TS,mod308}$ in Rhine experiments.

Contrariwise, the three compounds 5-methylbenzotriazole, bicalutamide, and fexofenadine had shorter $DT_{50,TS,mod308}$ values in CMP than in Rhine experiments. For those compounds, differences in $DT_{50,TS,mod308}$ were clearly linked to the compounds' differing sorption behavior during the biotransformation studies. Even though the CMP sediment had a much higher TOC content, the three compounds appeared to sorb more strongly to the Rhine sediment. Hence, their bioavailability was decreased in Rhine experiments. Literature on those compounds' sorption behavior suggests that their distribution between water and sediment not only depends on the sediments TOC content but also its pH, ionic strength, or clay and mineral content(Xu et al. 2021; Hart et al. 2004; Azuma et al. 2017). In fact, in case of bicalutamide and fexofenadine, we indeed derived higher K_{oc} values in our own sorption experiments described in Chapter 3 when

employing sediment or soil with a rather low TOC content, supporting the hypothesis that sorption of those compounds is driven by sediment properties other than TOC content.

Table 9: $DT_{50,w,mod308}$ in modified OECD 308-type studies

$DT_{50,w,mod308}$ (days) in both modified OECD 308-type studies, i.e., employing sediment and water from the Rhine or CMP, respectively. Mean $DT_{50,w,mod308}$ show the geometric mean of $DT_{50,w,mod308}$ of the two studies (i.e., mod308R and mod308CMP), together with the standard deviation (sd) and the coefficient of variation (CV, %). N.d. indicates that $DT_{50,w,mod308}$ could not be determined based on the here presented data. Lag phases are given in days, σ describes the standard model error in %.

Comp.	Study	$DT_{50,w,mod308}$	mean $DT_{50,w,mod308}$	sd $DT_{50,w,mod308}$	CV $DT_{50,w,mod308}$	Lag phase	σ	R^2
5MB	Rhine	7.7	5.9	2.3	38	0	7	0.99
	CMP	4.5				0	8	0.97
ACE	Rhine	22.8	40.9	35.6	87	2.7	3	0.98
	CMP	73.2				0.2	6	0.93
ALI	Rhine	n.d.	n.d.	n.d.	n.d.	n.d.	n.d.	n.d.
	CMP	5.2				0	8	0.97
ATA	Rhine	n.d.	n.d.	n.d.	n.d.	n.d.	n.d.	n.d.
	CMP	6.8				2	7	0.98
ATE	Rhine	1.8	2	0.4	17	0.2	0	1
	CMP	2.3				0.7	0	1
AZO	Rhine	n.d.	n.d.	n.d.	n.d.	n.d.	n.d.	n.d.
	CMP	6.1				0	7	0.97
BEZ	Rhine	2.5	2.6	0.2	8	0	7	0.97
	CMP	2.8				0	6	0.98
BIC	Rhine	14.3	8.8	6.3	72	0	5	0.99
	CMP	5.4				0	2	1
CAR	Rhine	63.1	35.9	30.2	84	0	6	0.85
	CMP	20.4				0	5	0.81
CBA	Rhine	7.8	6.8	1.3	19	0	6	0.98
	CMP	6				0	7	0.97
CIT	Rhine	0.8	1	0.4	35	0	8	0.95
	CMP	1.3				0	5	0.99
CLO	Rhine	22.3	22.4	0.1	1	6.6	2	1
	CMP	22.5				0	5	0.94
CYC	Rhine	5.4	11.2	12.7	113	0	7	0.97
	CMP	23.4				0.5	5	0.98
DIC	Rhine	13.2	17.9	7.9	44	3.2	5	0.99
	CMP	24.4				0	5	0.95
DIM	Rhine	16.6	12.2	5.4	44	0	6	0.99
	CMP	9				0	5	0.98
DIU	Rhine	5.5	5.5	0	0	0	8	0.95
	CMP	5.5				0	9	0.94
FEN	Rhine	5.9	5.7	0.2	4	0	7	0.98
	CMP	5.6				0	2	1
FOC	Rhine	1.2	1.2	0	0	0.5	6	0.99

Comp.	Study	$DT_{50,w,mod308}$	mean $DT_{50,w,mod308}$	sd $DT_{50,w,mod308}$	CV $DT_{50,w,mod308}$	Lag phase	σ	R^2
	CMP	1.2				0.6	0	1
FEX	Rhine	8.2	6.7	2	30	2.8	8	0.97
	CMP	5.4				1	2	1
FIP	Rhine	10.8	7.1	4.3	61	0	10	0.99
	CMP	4.7				0.1	4	0.99
GAB	Rhine	34.6	37.9	4.9	13	0	3	1
	CMP	41.5				0	9	0.85
HYD	Rhine	25.5	18.6	8.4	45	0	5	0.99
	CMP	13.6				0	8	0.94
IMI	Rhine	27.8	15.7	13.4	85	0	5	0.94
	CMP	8.9				0	10	0.95
IPR	Rhine	9.3	8.1	1.6	19	4.4	4	0.99
	CMP	7.1				1.2	3	0.99
IRB	Rhine	8.4	6.3	2.6	42	1.7	6	0.98
	CMP	4.7				0.5	4	0.99
ISO	Rhine	11.2	10.6	0.8	8	3.5	6	0.98
	CMP	10				0	7	0.97
LAM	Rhine	26.6	14.3	13.4	93	0	5	0.81
	CMP	7.7				0	13	0.91
LEV	Rhine	4.6	5	0.6	11	3.1	12	0.96
	CMP	5.4				0.6	2	1
LID	Rhine	20.8	13.8	8.2	59	0	5	0.96
	CMP	9.2				0	14	0.89
MEF	Rhine	8.1	9.2	1.7	18	2.7	6	0.98
	CMP	10.5				0	4	0.98
MES	Rhine	5.2	3.5	2.1	59	0	4	1
	CMP	2.3				0.5	2	1
MTO	Rhine	4.8	3.8	1.3	34	2.1	10	0.96
	CMP	3				0.2	2	1
NAP	Rhine	18.5	12.6	7.0	55	0	5	0.98
	CMP	8.6				0	13	0.87
PIC	Rhine	9.3	6.8	3.1	46	0	4	0.99
	CMP	4.9				0	7	0.98
SAC	Rhine	9.2	22	30.5	139	7.2	6	0.99
	CMP	52.4				0	6	0.9
SIT	Rhine	1	1.7	1.4	82	0	15	0.84
	CMP	3				0	4	0.99
SUL	Rhine	4.3	3.5	1	28	0	5	0.99
	CMP	2.9				0.5	3	0.99
TER	Rhine	28.7	16.4	13.6	83	0	5	0.92
	CMP	9.4				0	10	0.95
TRI	Rhine	3.9	2.9	1.2	41	1.7	7	0.98
	CMP	2.2				0.2	0	1
TNE	Rhine	5	4.2	1	23	2.7	5	0.99
	CMP	3.6				1.5	1	1

Comp.	Study	$DT_{50,w,mod308}$	mean $DT_{50,w,mod308}$	sd $DT_{50,w,mod308}$	CV $DT_{50,w,mod308}$	Lag phase	σ	R^2
VAL	Rhine	4.4	5.4	1.6	29	2.6	12	0.95
	CMP	6.6				2.8	7	0.97
VEN	Rhine	6	5	1.3	27	0	8	0.99
	CMP	4.1				0	10	0.97

Table 10: $DT_{50,TS,mod308}$ in modified OECD 308-type studies

$DT_{50,TS,mod308}$ (days) in both modified OECD 308-type studies, i.e., employing sediment and water from the Rhine or CMP, respectively. Mean $DT_{50,TS,mod308}$ show the geometric mean of $DT_{50,TS,mod308}$ of the two studies (i.e., mod308R and mod308CMP), together with the standard deviation (sd) and the coefficient of variation (CV, %). N.d. indicates that $DT_{50,TS,mod308}$ could not be determined based on the here presented data. $DT_{50,TS}$ and lag phases are given in days, σ describes the standard model error in %.

Comp.	Study	$DT_{50,TS,mod308}$	mean $DT_{50,TS,mod308}$	sd $DT_{50,TS,mod308}$	CV $DT_{50,TS,mod308}$	Lag phase	σ	R^2
5MB	Rhine	20.5	11.3	10.1	90	0	5	0.97
	CMP	6.2				0	10.8	0.95
ACE	Rhine	24	47.1	48.3	103	3.6	2.9	0.98
	CMP	92.3				2.1	3.7	0.93
ALI	Rhine	n.d.	n.d.	n.d.	n.d.	n.d.	n.d.	n.d.
	CMP	220				2.5	4.2	0.59
ATA	Rhine	n.d.	n.d.	n.d.	n.d.	n.d.	n.d.	n.d.
	CMP	348				9.4	1.5	0.81
ATE	Rhine	1.8	2	0.4	17	0.2	0	1
	CMP	2.3				0.6	0.2	1
AZO	Rhine	n.d.	n.d.	n.d.	n.d.	n.d.	n.d.	n.d.
	CMP	37.6				0	6.3	0.61
BEZ	Rhine	2.8	3.7	1.5	40	0	6.8	0.97
	CMP	4.9				2.7	1.8	1
BIC	Rhine	41	19	22.8	120	2.1	3.7	0.97
	CMP	8.8				0	3.3	0.99
CAR	Rhine	>230	>230	n.d.	n.d.	2.5	4.1	0.32
	CMP	>230				0	2.8	0.06
CBA	Rhine	15.8	15.2	0.8	5	0	6	0.97
	CMP	14.7				0	10	0.93
CIT	Rhine	>230	>230	n.d.	n.d.	0	5.2	0.78
	CMP	>230				3.6	2.4	0.07
CLO	Rhine	25	25.2	0.4	1	0	4.9	0.95
	CMP	25.5				0	4.9	0.97
CYC	Rhine	6.5	12.6	12.8	101	3.2	4.4	0.99
	CMP	24.6				3.3	4.5	0.98
DIC	Rhine	24.4	30	8.9	30	8	2.6	0.99
	CMP	37				0	4.5	0.94
DIM	Rhine	18.4	14.6	4.8	33	0	3.6	0.99
	CMP	11.6				0.7	4.5	0.99

Comp.	Study	$DT_{50,TS,mod308}$	mean $DT_{50,TS,mod308}$	sd $DT_{50,TS,mod308}$	CV $DT_{50,TS,mod308}$	Lag phase	σ	R^2
DIU	Rhine	8	10.4	3.9	37	3.3	6.2	0.98
	CMP	13.5				0	7.9	0.95
FEN	Rhine	8.6	n.d.	n.d.	n.d.	1.9	6.1	0.98
	CMP	n.d.				n.d.	n.d.	n.d.
FEX	Rhine	38.4	18.5	20.9	113	0	11.2	0.79
	CMP	8.9				0	7.7	0.96
FIP	Rhine	24	n.d.	n.d.	n.d.	1.8	3.9	0.99
	CMP	n.d.				n.d.	n.d.	n.d.
FOC	Rhine	1.1	1	0.1	14	0.8	0.6	1
	CMP	0.9				0.1	0.8	1
GAB	Rhine	40	n.d.	n.d.	n.d.	0	2	0.99
	CMP	n.d.				n.d.	n.d.	n.d.
HYD	Rhine	26	23	4	18	0	4.9	0.99
	CMP	20.3				0	4.9	0.96
IMI	Rhine	56.4	40.8	19	47	0	5.8	0.92
	CMP	29.5				0	4.7	0.88
IPR	Rhine	9.7	8.3	1.8	22	4.7	4.2	0.99
	CMP	7.1				1.2	2.7	1
IRB	Rhine	10	8.9	1.4	16	0	3.6	0.99
	CMP	8				0	7.9	0.96
ISO	Rhine	12.8	19.7	12.4	63	4.2	5.6	0.98
	CMP	30.4				15.6	3.1	0.99
LAM	Rhine	102	n.d.	n.d.	n.d.	0	5.7	0.73
	CMP	>230				4	0.58	0.17
LEV	Rhine	5	5.4	0.6	11	2.7	6.3	0.99
	CMP	5.8				1.2	1.7	1
LID	Rhine	45.8	50.9	7.6	15	0	5.9	0.97
	CMP	56.6				0	12.1	0.52
MEF	Rhine	10.7	13.6	4.7	34	4.1	5.4	0.98
	CMP	17.3				0	5.9	0.97
MES	Rhine	5.5	n.d.	n.d.	n.d.	0	4	0.99
	CMP	n.d.				n.d.	n.d.	n.d.
MTO	Rhine	6.1	9.7	6.5	67	0	5.2	0.98
	CMP	15.3				0.8	6.9	0.96
NAP	Rhine	46	50.3	6.3	13	2.9	2.8	0.98
	CMP	54.9				0	5.8	0.83
PIC	Rhine	43.8	38.6	6.9	18	1.8	16.3	0.91
	CMP	34				0	6.2	0.83
SAC	Rhine	9.5	22.3	30.3	136	7.2	3	1
	CMP	52.4				0	5.74	0.9
SIT	Rhine	118	85.2	40	47	0.1	5.7	0.98
	CMP	61.5				0	5.8	0.84
SUL	Rhine	4.4	3.6	1.1	30	0	5.8	0.91
	CMP	2.9				0.5	3.5	0.99

Comp.	Study	$DT_{50,TS,mod308}$	mean $DT_{50,TS,mod308}$	sd $DT_{50,TS,mod308}$	CV $DT_{50,TS,mod308}$	Lag phase	σ	R^2
TER	Rhine	45	39.3	7.5	19	0	5.8	0.91
	CMP	34.4				0	6.4	0.91
TNE	Rhine	5	4.2	1	23	2.8	5.3	0.99
	CMP	3.6				1.5	1	1
TRI	Rhine	4.7	4.2	0.7	17	0.1	2.3	1
	CMP	3.7				0.3	1.3	1
VAL	Rhine	3.3	4.6	2.1	47	0	4.1	0.99
	CMP	6.3				1.6	5.4	0.98
VEN	Rhine	46.7	n.d.	n.d.	n.d.	0	5.8	0.9
	CMP	n.d.				n.d.	n.d.	n.d.

2.3.4 $k'_{bio,lab}$ Values and Compartment-Specific Half-Lives ($DegT_{50,w,mod308}$ and $DegT_{50,sed,mod308}$)

The model framework developed to estimate biotransformation rate constants in modified OECD 308-type biotransformation experiments could be fitted to data of 38 and 42 compounds from individual Rhine and CMP experiments, respectively, with good quality. Estimated $k'_{bio,lab}$ values varied from 0.01 to 50898 $L((g\ OC)d)^{-1}$. It has to be noted, that $k'_{bio,lab}$ values below 0.1 and above 100 $L((g\ OC)d)^{-1}$ are subject to identifiability issues because of little or very fast transformation during the experiments. Still, those extreme values can be used to identify rapidly biotransformed and rather persistent compounds.

For most compounds, mean $k'_{bio,lab,R}$ values derived from data of Rhine experiments exclusively were higher than those derived from data of CMP experiments only. Nevertheless, it was possible to derive $k'_{bio,lab,joint}$ values that were valid across both experiments for 38 compounds, as demonstrated by the good fit to the data when jointly fitting the data from both experiments (exemplary compounds in Figure 5, a compilation of model fit to measured compound residues for all compounds in Annex A.2, Figure A6). Table 11 and Figure 6 show the $k'_{bio,lab}$ posteriors derived via individual and joint model fitting.

In line with the results of Honti et al. (2016), comparing the individual fits to the joint fit revealed that the joint model solution was statistically preferable (comparison based on Akaike Information Criterion). Further, for the majority of compounds (i.e., 29 out of 38 compounds), $k'_{bio,lab,joint}$ values derived from the joint fit were considerably less uncertain than values from individual fits (coefficients of variation in Table 11).

Posterior distributions for other substance- and system-specific parameters are mostly similar for the joint fit as they were for the individual fits and are centred around the priors. This means that the joint fit did not improve the parameters' identifiability, however, there were also no inconsistencies between these parameters and the data.

Figure 5: Model fits to experimental data

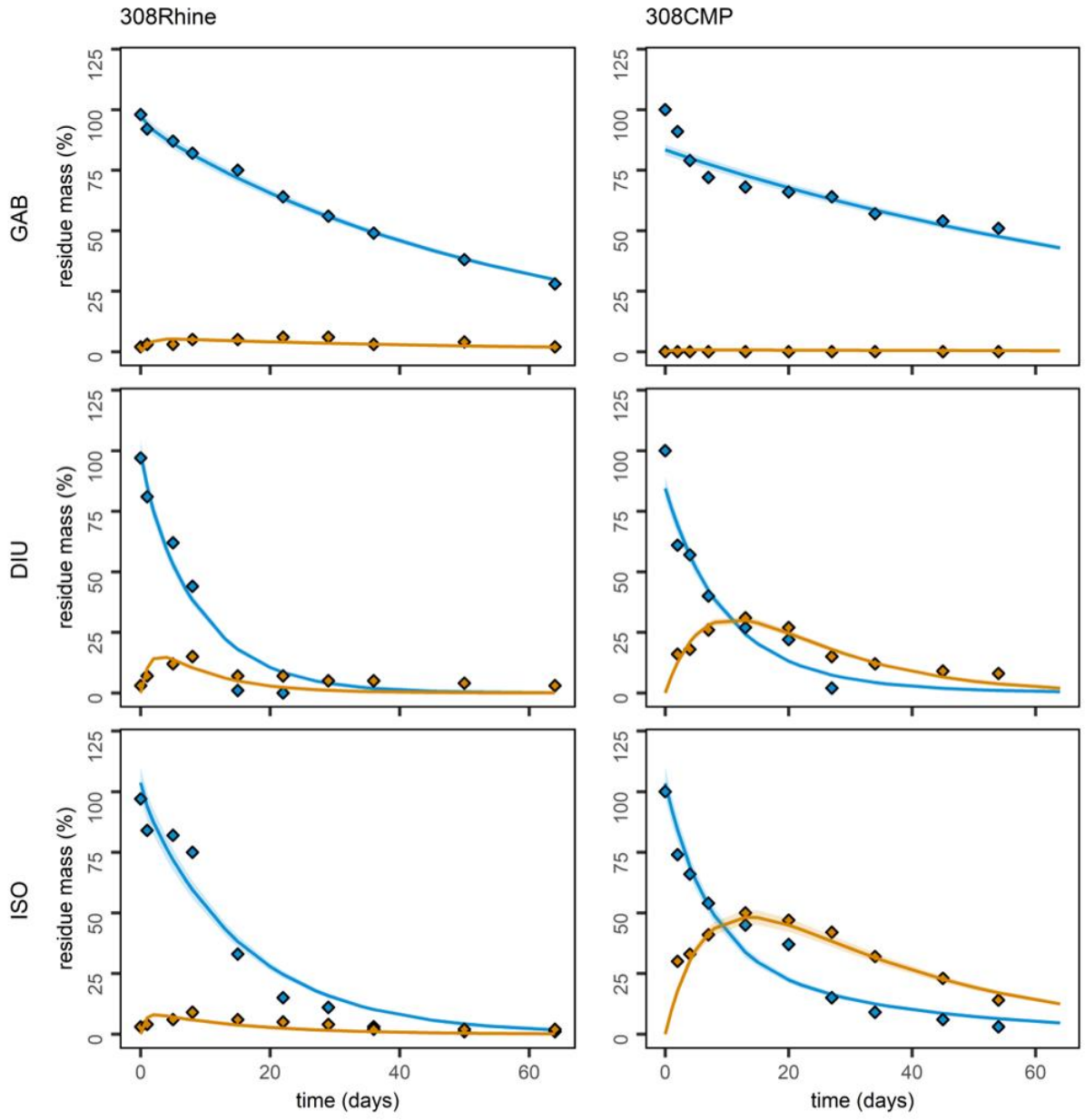

Model fits to experimental data when using $k'_{bio,lab,joint}$ to predict residue-time series. Average residues measured in the water phase and sediment of experimental duplicates are shown as blue and yellow diamonds, respectively. Solid lines show the model fit to the data.

Source: own figure, Eawag

Table 11: $k'_{biol,lab}$ values

$k'_{bio,lab}$ values in $L((g\ OC)d)^{-1}$ with their mean value, standard deviation (sd), and coefficient of variation (CV, %) derived via individually fitting data from CMP and Rhine modified OECD 308-type experiments ($k'_{bio,lab,CMP}$ and $k'_{bio,lab,R}$, respectively) and joint data fitting ($k'_{bio,lab,joint}$).

	$k'_{bio,lab,CMP}$			$k'_{bio,lab,R}$			$k'_{bio,lab,joint}$		
Comp.	**mean**	**sd**	**CV**	**mean**	**sd**	**CV**	**mean**	**sd**	**CV**
5MB	12.21	14.4	118	4.32	6.28	145	1.39	0.8	57

	$k'_{bio,lab,CMP}$			$k'_{bio,lab,R}$			$k'_{bio,lab,joint}$		
ACE	0.04	0.02	50	6.71	4.75	71	0.64	0.34	54
ALI	0.07	0.04	57	n.a.	n.a.	n.a.	n.a.	n.a.	n.a.
ATA	2.16	2.32	107	n.a.	n.a.	n.a.	n.a.	n.a.	n.a.
ATE	40.03	25.55	64	102.3	33.69	33	17.79	3.47	20
AZO	1.75	1.49	85	n.a.	n.a.	n.a.	n.a.	n.a.	n.a.
BEZ	50898	26695	53	133.8	66.2	49	57.24	27.55	48
BIC	17.94	6.72	37	1.21	0.37	30	3.65	1.35	37
CAR	0.01	0.01	100	0.05	0.03	55	0.003	0.003	89
CBA	2.24	3.31	148	2.63	3.75	135	1.14	0.47	41
CIT	0.96	0.99	103	0.49	0.52	105	0.24	0.25	105
CLO	0.13	0.07	54	14.21	8.86	62	2.51	1.62	65
CYC	3.71	3.24	87	55.1	26.27	48	5.49	1.73	31
DIC	0.17	0.1	59	1.76	0.85	48	1.49	0.74	50
DIM	2.86	2.34	82	4.44	3.38	76	1.4	0.45	32
DIU	3.9	2.8	72	22.06	16.81	76	4.53	2.03	45
FEN	9.42	7.41	79	20.95	10.36	49	16.2	5.89	36
FEX	16.38	7.2	44	n.a.	n.a.	n.a.	n.a.	n.a.	n.a.
FIP	49375	26566	54	0.9	0.43	48	1.13	0.43	38
FOC	5.73	2.57	45	50390	26777	53	155.9	53.23	34
GAB	0.03	0.02	67	0.81	0.54	67	0.8	0.39	49
HYD	0.04	0.03	75	0.5	0.5	100	0.04	0.02	57
IMI	0.29	0.25	86	0.44	0.32	72	0.23	0.08	34
IPR	17.64	12.5	71	36.3	22.9	63	23.71	10.51	44
IRB	0.18	0.19	106	0.27	0.33	125	0.08	0.07	94
ISO	0.43	0.27	63	15.78	10.42	66	1.09	0.48	44
LAM	0.01	0.01	100	0.2	0.09	45	0.02	0.01	62
LEV	22.21	15.43	69	128.6	82.16	64	50.2	20.5	41
LID	0.12	0.06	50	0.53	0.41	77	0.16	0.05	34
MEF	2.12	1.85	87	6.71	4.16	62	3.39	1.46	43
MES	52.98	35.29	67	47.92	21.86	46	28.34	6.31	22
MET	2.68	2.03	76	46.71	38.01	81	5.01	2.74	55
NAP	0.36	0.4	111	0.96	0.31	33	0.4	0.16	40
PIC	3.74	2.19	59	1.1	0.6	54	0.97	0.31	32
SAC	1.62	1.09	67	34.76	18.68	54	4.18	2.2	53
SIT	4.38	2.67	61	1.19	0.84	71	0.34	0.23	68
SUL	41.16	29.58	72	60.13	30.9	51	38.6	17.9	46
TER	0.26	0.14	54	0.43	0.23	54	0.25	0.09	37

	$k'_{bio,lab,CMP}$			$k'_{bio,lab,R}$			$k'_{bio,lab,joint}$		
TNE	29.58	21.16	72	64.24	36.8	57	55.4	16.02	29
TRI	49.7	2.97	6	59.06	26.9	46	48.8	12.6	26
VAL	6.07	2.45	40	115.3	54	47	43.1	13.01	30
VEN	0.24	0.31	129	2.4	2.03	85	0.47	0.34	74

Figure 6: Posterior distribution of $k'_{bio,lab}$

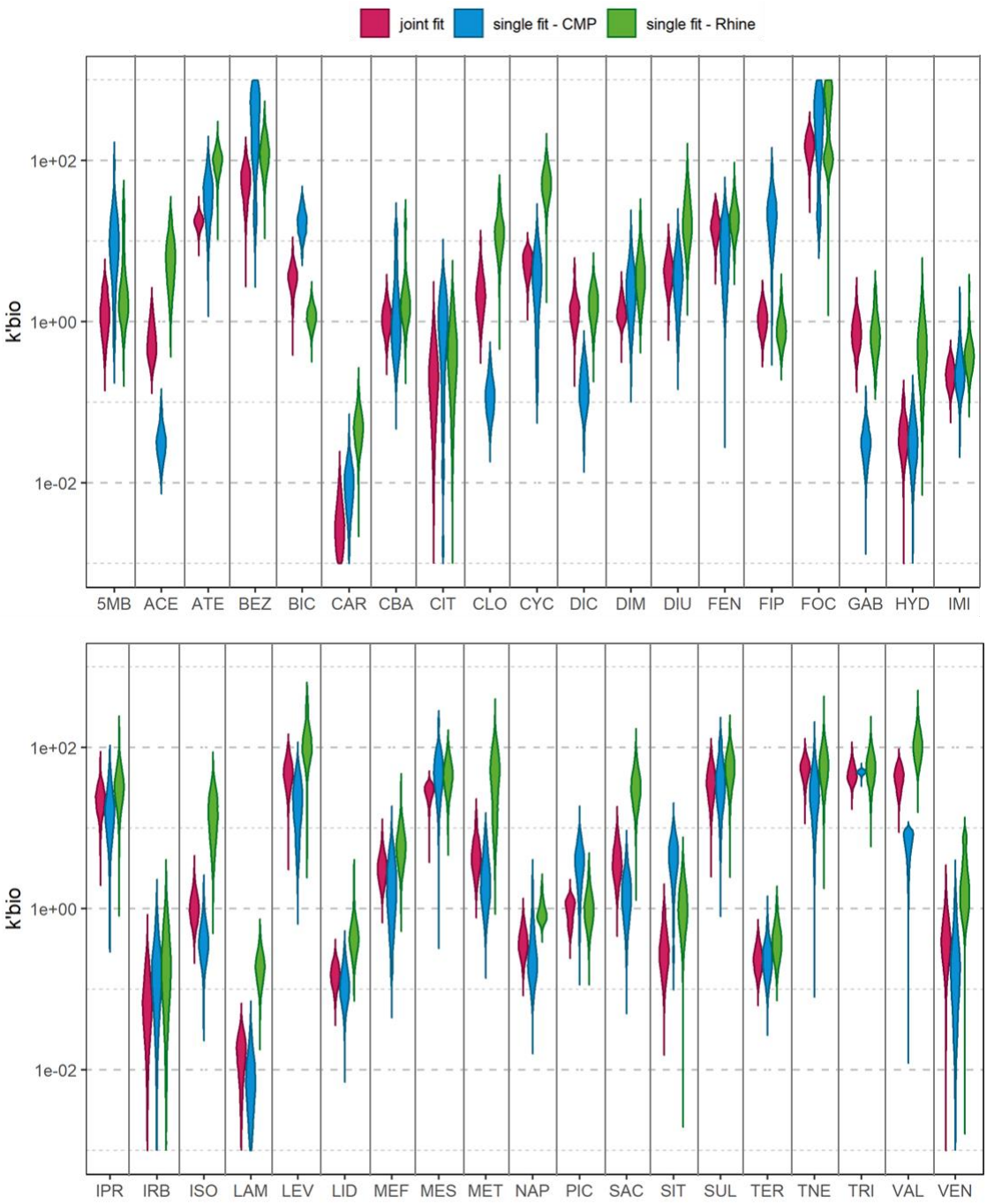

Posterior distributions of $k'_{bio,lab}$ values in $L((g\ OC)d)^{-1}$.

Source: own figure, Eawag

Table 12 shows compartment-specific half-lives (i.e., $DegT_{50,w,mod308}$ and $DegT_{50,sed,mod308}$) calculated with the $k'_{bio,lab}$, k_{hydro}, and K_{oc} posteriors from the joint model fit. Figure 7 further shows a comparison of $DegT_{50,w,mod308}$ and $DegT_{50,sed,mod308}$ for each of the two biotransformation studies. The color-code used in Figure 7 (as well as in Figures 10-11, and Figures 21-26) indicates the compounds affinity toward sorption by dividing the test compounds into different groups based on their calibrated K_{oc} values rounded to integers. In case of our test compounds, the calibrated $logK_{oc}$ values range from 1 to 4.

Further, it has to be noted that $DegT_{50,sed,mod308}$ describes degradation in the bulk sediment, which not only depends on the compounds' intrinsic biotransformation potential (as expressed by $k'_{bio,lab}$ and k_{hydro}) but also on the compounds' bioavailability, i.e., its presence in the pore water of the bulk sediment. As evident from Figure 7, compound transformation in the water phase is slower than in the bulk sediment, i.e., $DegT_{50,w,mod308} >> DegT_{50,sed,mod308}$ for the majority of compounds. This difference may be explained by the differing amounts of degrader biomass (i.e., TOC as a proxy for degrader biomass) in the two compartments. Only for six compounds, i.e., citalopram, hydrochlorothiazide, irbesartan, sitagliptin, trimethoprim, and venlafaxine, $DegT_{50,sed,mod308}$ and $DegT_{50,w,mod308}$ are in a comparable range. In case of irbesartan and hydrochlorothiazide, similar transformation half-lives in both compartments may result from the compounds' susceptibility towards abiotic transformation, which would explain why their $DegT_{50,w,mod308}$ and $DegT_{40,sed,mod308}$ do not depend on the TOC concentration in the respective compartments. The other four compounds have a rather high K_{oc} values ($logK_{oc}$ ~4) and strongly sorb to the sediment in the test system. Therefore, those compounds are barely bioavailable in the sediment layer, which obviously results in increased $DegT_{50,sed,mod308}$ values that converge towards their $DegT_{50,w,mod308}$.

Note that, due to the identifiability limits for $k'_{bio,lab}$ values of < 0.1 $L((g\ OC)d)^{-1}$, transformation half-lives greater than 3000 and 1700 days in the CMP and Rhine study, respectively, are subject to large uncertainties. Nevertheless, they can be seen as an indicator for high persistence of the respective compound.

Table 12: $DegT_{50,w,mod308}$ and $DegT_{50,sed,mod308}$ in modified OECD 308-type studies

$DegT_{50,w,mod308}$ and $DegT_{50,sed,mod308}$ in CMP and Rhine experiments, calculated from $k'_{bio,lab,joint}$. Half-lives are given with their mean and standard deviation (sd) in days. The coefficient of variation (CV) is given in %, it has to be noted that the CVs listed in this table are not comparable to the CVs listed in Tables 8-9 as those describe variations between different experiments while the CV given here is a measure for model uncertainties.

	$DegT_{50,w}$ – CMP			$DegT_{50,sed}$ – CMP			$DegT_{50,w}$ – Rhine			$DegT_{50,sed}$ – Rhine		
	mean	sd	CV	mean	sd	CV	mean	sd	CV	mean	sd	
5MB	108.8	62.5	57	2.56	7.53	294	179.2	102.9	58	4.78	12.9	269
ACE	270.3	145.6	54	0.76	1.78	234	489.8	263.9	54	2.25	4.06	182
ATE	9.7	1.9	19	0.01	0.02	200	17.7	3.5	20	0.03	0.05	167
BEZ	3	1.5	50	0.01	0.02	200	5.5	2.6	47	0.03	0.05	167
BIC	47.4	17.5	37	15.02	57.8	385	86.2	31.8	37	26.4	98.4	373
CAR	31226	27920	89	1418862	4651491	327	41297	36925	89	616998	1755711	285
CBA	151.6	61.8	41	1.8	10.82	600	275.1	112.2	41	3.51	14.5	413
CIT	714	747.1	105	1277	5931	464	1287.2	1346.9	105	2215	10265	463
CLO	69	44.7	65	0.85	1.91	224	125.4	81.2	65	1.73	3.6	208
CYC	31.5	9.9	31	0.03	0.04	133	57.3	18	31	0.14	0.18	129
DIC	116.5	58.3	50	3.02	9.99	328	211.5	109	52	5.55	16.78	302
DIM	123.8	40.2	32	1.32	3.05	231	224.8	72.9	32	2.54	5.61	221
DIU	38.2	17.1	45	1.9	7.29	384	69.5	31.2	45	3.42	12.04	352
FEN	10.7	3.9	36	0.91	2.79	306	19.4	7.1	36	1.61	4.78	297
FIP	152.6	57.8	38	3.75	16.79	448	277	104.9	38	6.79	26.85	395
FOC	1.1	0.4	36	0.08	0.29	362	2.0	0.7	0.35	0.13	0.5	385
GAB	216.7	106.3	49	2.32	5.03	217	393.1	192.8	49	4.92	9.62	196
HYD	29	16.5	57	27.1	126	465	29	16.5	57	37.8	106.7	282

IMI	741.4	254.3	34	15.2	40.03	263	1336.2	458.2	34	28.33	69.5	241
IPR	7.3	3.2	44	0.04	0.1	250	13.3	5.9	44	0.08	0.17	213
IRB	7.1	6.7	94	8.17	22.22	271	7.1	6.7	94	10.35	20.95	202
ISO	158.6	70.4	44	2.3	6.27	273	287.7	127.7	44	4.56	10.82	237
LAM	9770	6032.6	62	172.3	751.7	436	15912.7	9825.5	62	321.5	1191	370
LEV	3.4	1.4	41	0.01	0.03	300	6.3	2.6	41	0.03	0.06	200
LID	1094.7	368.9	34	6.71	21.79	325	1964.7	662	34	14.5	35.8	247
MEF	51.1	21.9	43	1.72	4.57	271	92.8	39.9	43	3.13	7.94	254
MES	6.1	1.4	23	0.04	0.06	150	11.1	2.5	23	0.07	0.12	171
MET	34.6	18.9	55	2.76	7.16	259	62.8	34.4	55	4.9	12.43	254
NAP	428.7	173.1	40	27.2	83.1	305	775.5	313.1	40	48.4	142.4	294
PIC	178.6	56.8	32	9.5	52.59	564	324.1	103	32	16.8	85.1	506
SAC	41.4	21.8	53	0.12	0.21	175	75.3	39.5	52	0.32	0.52	163
SIT	107.4	72.8	68	236.4	1309	554	118.8	80.6	68	405	2209	545
SUL	4.5	2.1	47	0.01	0.01	100	8.2	3.8	46	0.03	0.04	133
TER	694.3	257.7	37	10.4	31.3	301	1252.1	464.7	37	19.97	53.1	266
TNE	3	0.9	30	0.07	0.13	186	5.3	1.5	28	0.13	0.24	185
TRI	3.6	0.9	25	2.9	16	552	6.5	1.7	26	5.01	27.6	551
VAL	4	1.2	30	0.004	0.01	250	7.3	2.2	30	0.02	0.02	100
VEN	369.9	272	74	84.2	391	464	669.5	492.4	74	147	671.5	457

Figure 7: Comparison of $DegT_{50,w,mod308}$ and $DegT_{50,sed,mod308}$

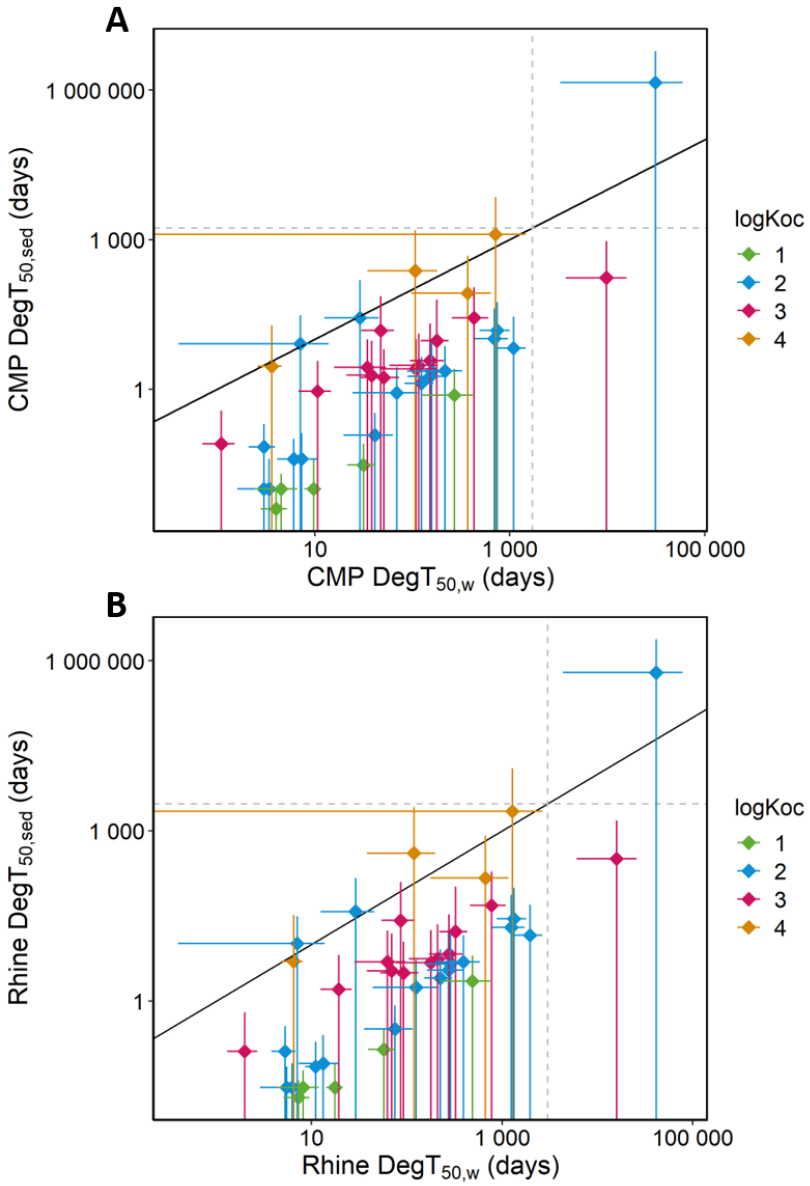

Comparison between $DegT_{50,w,mod308}$ and $DegT_{50,sed,mod308}$ (A) in case of CMP study and (B) in case of Rhine study. Diamonds are colored with respect to their calibrated rounded $logK_{oc}$ values. The 1:1 lines are plotted as solid black lines in both graphs. The dashed grey lines indicate the cut-off for identification of the compartment-specific half-lives, i.e., $DegT_{50,w,mod308}$ and $DegT_{50,sed,mod308}$ calculated with a $k'_{bio,lab,joint}$ <0.1 $L((g\ OC)d)^{-1}$.

Source: own figure, Eawag

2.4 Half-Lives ($DT_{50,w,std308}$ and $DT_{50,TS,std308}$) in Standard OECD 308 Studies

In addition to our own biotransformation studies, we further fitted the first-order degradation model to data listed in regulatory dossiers describing the fate of a subset of 19 compounds (Table 1) in standard OECD 308 studies. As outlined in Chapter 2.1.8, two different approaches were used to calculate total compound residues in standard OECD 308 studies; first, by considering the formation of NER as a transformation process, and second, by estimating total compound residues accounting for both extractable and non-extractable residues in the

sediment. Derived $DT_{50,w,std308}$, $DT_{50,TS,std308}$ and further statistical model parameters are given in Table 13 and Table 14. $DT_{50,w,std308}$ values ranged from 1 to 86 days (Table 13). Lag phases were generally low, i.e. <12 days. $DT_{50,TS,std308}$ values derived from standard OECD 308 studies were rather high with 12 out of 19 compounds having $DT_{50,TS,std308}$ >100 days (Table 14).

More than half of the compounds for which regulatory data was available had >70% of their initial compound mass sorbed (partially irreversible) to the sediment by the end of the respective regulatory OECD 308 studies. Those observations suggest that compound mass distribution shifts significantly toward the sediment during standard OECD 308 studies - i.e., in systems employing a sediment-water ratio of 1:3 or 1:4 (v/v) - compromising the compounds' availability for biotic and abiotic transformation.

Table 13: $DT_{50,w,std308}$ in standard OECD 308 studies

$DT_{50,w,std308}$ (days) in different standard OECD 308 studies, i.e., employing sediment and water sampled from various locations. Mean $DT_{50,w,std308}$ show the geometric mean of $DT_{50,w,std308}$ calculated from the respective studies available for each compound together with their standard deviation (sd) and the coefficient of variation (CV, %). Lag phases are given in days, σ describes the standard model error in %.

Comp.	Test system	$DT_{50,w,std308}$	mean $DT_{50,w,std308}$	sd $DT_{50,w,std308}$	CV $DT_{50,w,std308}$	Lag phase	σ	R^2
ALI	Rohrspitz	4.6	2.6	2.2	83	0	10	0.97
	Espelwater	1.5				0	8	0.98
ATA	Goose aerob	2.7	5.1	4.9	97	0	11	0.94
	Golden aerob	9.7				0	13	0.97
AZO	Warinton	3.1	3.0	0.1	5	0.2	34	1
	Old Basing	2.9				0	21	0.96
CBA	Unter Widdersheim	5.7	7.9	3.7	47	0	7	0.96
	Bickenbach	10.9				0.6	4	0.99
DIM	Anwil	20.5	17.5	4.0	23	0	5	1
	Rhine	14.9				0	8	0.99
DIU	River Erft	7.4	6.6	1.1	17	0	7	0.98
	Hönniger Weiher	5.8				0	8	0.97
FEN	Hönniger Weiher	2.4	3.0	1.2	41	0	10	0.96
	Angler Weiher	5				0	4	1
	Lake Hönniger	2.5				0	20	0.93
	Lake Stanley	2.7				0	6	0.96
FIP	Iron Hatch	27.1	12.1	9.4	78	0.1	12	0.95
	Ongar	21.4				0	5	0.9
	Pondwater	6				5.8	39	0.98
	TS97/07	12.2				0	5	0.99
	TS97/08	6.1				0	10	0.96
HYD	LowOM	18.6	17.4	1.7	10	0	10	0.97
	HighOM	16.2				0	5	0.94
IMI	Ijenzdoorm	13.4	33.3	37.8	114	0	9	0.99
	Lienden	86.1				0	6	0.93
	Stilwell	31.9				0	6	0.71
IPR	Hönniger Weiher	1	1.5	0.9	61	0.8	28	0.53
	Anglersee	2.3				0	25	0.75
ISO	River Nidda	29	25.3	7.5	29	0	7	0.98

	Gravel Pit	35				3	9	0.98
	Bury Pond	18				0	11	0.88
	Emperor Lake	22.4				0	5	0.85
LID	Humsterbach	20.1	30.8	19.2	62	0	5	0.95
	Pfalzwater	47.2				0	12	0.94
MES	Swiss Lake aerob	10.6	8.3	2.9	35	0	4	1
	Calwich	6.5				0	2	1
NAP	Sandy Loam System	5.2	6.1	1.4	23	0	8	0.97
	Clay Loam System	7.2				0	6	0.98
PIC	(-phenyl) Virginia	7.3	9.0	1.9	22	0	12	0.95
	(-pyridin) Virginia	8.2				0	10	0.95
	(-phenyl) Old Basin	11.8				0	8	0.97
	(-pyridin) Old Basin	9.2				0	17	0.79
TER	Rhine	20.6	21.4	1.2	6	0	5	0.91
	Anwil	22.3				0	5	0.91
TNE	River	3.4	4.2	1.2	29	0	2	1
	Pond	5.1				0.3	3	0.99
VAL	Pond	9.8	14.2	7.6	53	0	4	0.98
	River	20.5				0.1	11	0.93

Table 14: $DT_{50,TS,std308}$ in standard OECD 308 studies

$DT_{50,TS,std308}$ (days) in different standard OECD 308 studies, i.e., employing sediment and water sampled from various locations. Mean $DT_{50,TS,std308}$ show the geometric mean of $DT_{50,TS,std308}$ calculated from the respective studies available for each compound together with their standard deviation (sd) and the coefficient of variation (CV, %). Lag phases are given in days, σ describes the standard model error in %. The heading "Extractable parent compound plus NER" indicates that total compound residues in the sediment were calculated by considering extractable and non-extractable residues as parent compound residues. The heading "extractable parent compound only" indicates that total compound residues only considers the extractable fraction of compound mass in the sediment as parent compound residues.

Comp.	Test system	Extractable parent compound plus NER							Extractable parent compound only						
		$DT_{50,TS,std308}$	mean $DT_{50,TS,std308}$	sd $DT_{50,TS,std308}$	CV $DT_{50,TS,std308}$	Lag phase	σ	R2	$DT_{50,TS,std308}$	mean $DT_{50,TS,std308}$	sd $DT_{50,TS,std308}$	CV $DT_{50,TS,std308}$	lag phase	σ	R2
ALI	Rohrspitz	403.5	821	897	109	1.4	4.4	0.53	56	61	7	12	0.5	7.6	0.93
	Espelwater	1672				2.2	1.9	0.34	66				0	11	0.85
ATA	Goose aerob	192	165	36	22	10	2.7	0.95	56	77	36	47	5.8	1.7	0.99
	Golden aerob	141				4.6	2.1	0.97	107				0.3	5.4	0.92
AZO	Warinton	193.7	217	36	16	0	6	0.87	162	179	25	14	0	5.5	0.91
	Old Basing	244				0	6.9	0.85	197				0	6.9	0.9
CBA	Unter Widdersheim	341.5	203	156	77	3.1	2.7	0.86	72	34	40	117	0.5	5.4	0.95
	Bickenbach	121.2				0	4.3	0.91	16				2.55	4	0.99
DIM	Anwil	123.3	94	36	38	2.4	3.4	0.96	36	31	7	23	3.8	1.6	0.99
	Rhine	72.1				0	5.5	0.98	26				0	2.9	0.95
DIU	River Erft	151.8	266	223	84	7.4	5.8	0.93	52	97	91	94	13	7.7	0.95
	Hönniger Weiher	467.4				0	5.7	0.42	181				0	5.8	0.66
FEN	Hönniger Weiher	93.7	109	58	53	0	5.8	0.71	15	10	4	38	0	5.8	0.99
	Angler Weiher	58.5				0	5.3	0.88	10				0	3.6	0.99
	Lake Hönniger	194				0	5.8	0.2	13				0	7.1	0.99
	Lake Stanley	131				0	5.8	0.31	6				0	7.3	0.99
FIP	Iron Hatch	70.1	32	21	67	0	5.5	0.91	60.6	28	18	65	0	6.6	0.92
	Ongar	40.2				0	6.2	0.95	34.2				0	6.3	0.96
	Pondwater	15.8				3	4.5	0.99	14				3.6	0.8	0.99
	TS97/07	21.1				0	5.4	0.99	19.5				0	5.2	0.98

	TS97/08	33.8				0	4.4	0.99	30.2				0	4.9	0.99
HYD	LowOM	38.4	50	19	38	0	4.6	0.97	31.5	32	1	4	0	4.7	0.97
	HighOM	65.2				0	5.9	0.95	33.5				0	4.4	0.96
IMI	Ijenzdoorm	221.3	230	11	5	0	4.8	0.95	29.6	70	48	69	0.6	3.2	0.99
	Lienden	243.3				0	2.8	0.99	124				0	5.3	0.93
	Stilwell	227.2				4.5	1.3	0.94	93.4				2.6	3.2	0.93
IPR	Hönniger Weiher	79	64	19	30	0.3	5.4	0.96	33.2	23	12	52	1.9	3.8	0.99
	Anglersee	52				0	4.9	0.97	16.1				0	2.5	0.99
ISO	River Nidda	283.7	203	149	73	30	8.14	0.57	69.9	98	78	79	0	5.7	0.92
	Gravel Pit	115.2				1.7	4.07	0.94	66.6				2.8	2.9	0.99
	Bury Pond	122.7				0	5.76	0.75	87.8				0	5.8	0.82
	Emperor Lake	427.1				2.1	3.69	0.61	229				0.9	4.9	0.81
LID	Humsterbach	1091.5	546	579	106	3.1	6.8	0.09	243	186	71	38	0	5.8	0.86
	Pfalzwater	273.2				1.9	3.8	0.97	143				3.8	2	0.99
MES	Swiss Lake aerob	36.1	49	22	45	0	14.45	0.78	10.6	8	3	34	0	3.7	0.99
	Calwich	67.7				0	5.7	0.57	6.6				0.3	2.1	0.99
NAP	Sandy Loam System	368	350	25	7	2.5	2.5	0.86	272	238	45	19	0	2.4	0.93
	Clay Loam System	332.1				0	4.6	0.64	208				0	6.7	0.65
PIC	(-phenyl) Virginia	62.8	58	7	12	2.2	3.6	0.98	56.3	53	6	11	1.8	5.4	0.96
	(-pyridin) Virginia	65.6				4.9	4.9	0.97	58.9				0	5.6	0.93
	(-phenyl) Old Basin	55.8				12	4.2	0.98	50.8				4.9	5.9	0.96
	(-pyridin) Old Basin	49.5				5.9	3.9	0.98	45.7				2.1	5	0.97
TER	Rhine	262.3	298	53	18	0	3	0.9	78.5	92	20	22	0	2.5	0.99
	Anwil	337.5				0	4.1	0.72	107				0	5.3	0.97
TNE	River	6.8	11	8	70	0	12.9	0.94	3.9	5	1	23	0.1	3.9	0.99
	Pond	17.7				0	9.1	0.83	5.4				0.4	5.4	0.99
VAL	Pond	18.7	25	10	41	0.2	21	0.76	13.2	19	9	49	3.2	7.1	0.97
	River	33.1				0.4	19.6	0.74	26				0	4.9	0.91

2.5 Comparing Outcomes of Different Biotransformation Simulation Studies

2.5.1 Comparison of $DT_{50,w}$ in Standard- and Modified OECD 308-type Studies

Figure 8 shows $DT_{50,w,std308}$ derived from standard OECD 308 studies compared to $DT_{50,w,mod308}$ derived from modified OECD 308-type studies. Generally, $DT_{50,w,std308}$ and $DT_{50,w,mod308}$ varied from <1 to ~100 days. For 12 out of 20 compounds compared, the highest water phase dissipation half-life was amongst the $DT_{50,w,std308}$ values. However, when considering the spread between $DT_{50,w}$ calculated from data of both modified OECD 308-type studies, there does not seem to be a clear trend when comparing $DT_{50,w,std308}$ and $DT_{50,w,mod308}$.

It has to be noted that dissipation from the water phase captures both, sorption and transformation processes. Hence, deriving a hypothesis regarding the differences in biotransformation behavior between standard and modified OECD 308-type studies is not possible based on the comparison of $DT_{50,w,std308}$ and $DT_{50,w,mod308}$ only.

Figure 8: $DT_{50,w}$ in standard- and modified OECD 308-type studies

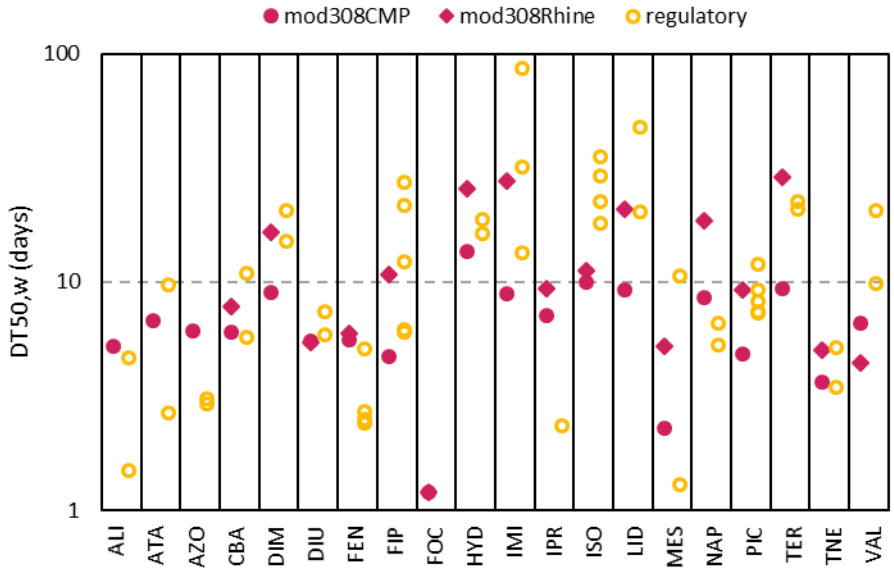

Comparison of $DT_{50,w,std308}$ derived from data of standard OECD 308 studies and $DT_{50,w,mod308}$ derived from modified OECD 308-type studies.
Source: own figure, Eawag

2.5.2 Comparison of $DT_{50,TS}$ in OECD 308/309-type Experiments

In the following, we discuss the comparison between $DT_{50,TS,mod308}$, $DT_{50,TS,309}$ and $DT_{50,TS,std308}$. In this context, it has to be noted that the standard OECD studies were conducted with radiolabeled substances. Therefore, in the sediment layer, it was possible to differentiate between reversibly sorbed compound mass and NER. However, the ratio between extractable and truly non-extractable residues in the sediment depends on the extraction method applied (see Chapter 2.1.8), which was generally less thorough than the one used in the modified OECD 308-type studies. For the detailed comparison between standard OECD 308 studies and modified OECD

308/309-type studies presented in Chapter 2.5.2.1, any NER was considered as parent compound, which results in conservative $DT_{50,TS,std308}$ estimates.

If only compound mass extracted from the sediment was considered as parent compound, i.e., formation of NER was considered equivalent to mineralization, derived half-lives ($DT_{50,TS,std308(NER = min)}$) are shorter (see Table 12). Figure 9 shows a comparison between $DT_{50,TS,mod308}$ and $DT_{50,TS,std308(NER= min)}$. As methods applied to extract compound residues from the sediment were less thorough in standard OECD 308 studies compared to sediment extraction methods used to treat samples from modified OECD 308-type studies, differences between $DT_{50,TS,mod308}$ and $DT_{50,TS,std308(NER= min)}$ are smaller than shown in Figure 10. Nevertheless, the longest half-life for 16 out of the19 compounds compared was observed in one of the standard OECD 308 studies. $DT_{50,TS,mod308}$ and $DT_{50,TS,std308(NER= min)}$ were most similar for compounds susceptible toward abiotic hydrolysis, i.e., fipronil, hydrochlorothiazide, picoxystrobin, and trinexapac-ethyl (see Table 5).

Figure 9: $DT_{50,TS,mod308}$ in comparison to $DT_{50, TS,std308(NER= min)}$

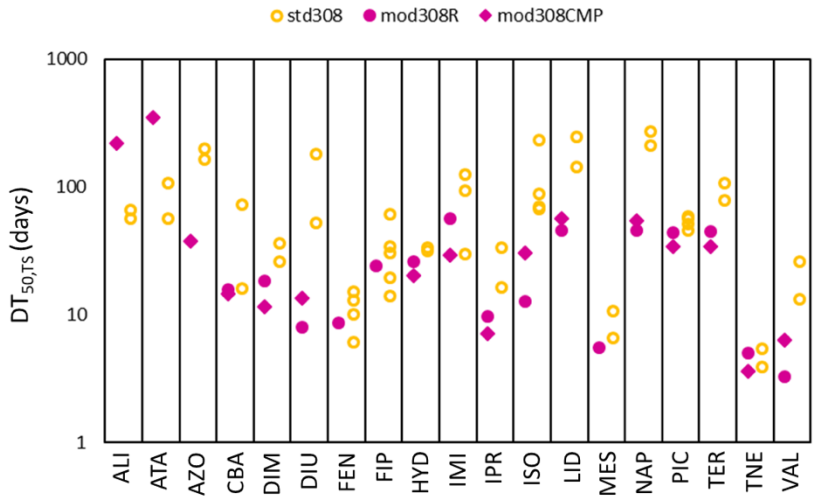

Source: own figure, Eawag

2.5.2.1 Comparison of $DT_{50,TS}$ derived from Standard and Modified OECD 308-type Systems

Generally, $DT_{50,TS,std308}$ values derived from standard OECD 308 studies, i.e., systems employing a sediment-water ratio of 1:3 or 1:4 (v/v), were rather high, with 12 out of 19 compounds having $DT_{50,TS,std308}$ >100 days (Figure 10), exceeding the typical duration of OECD 308 studies (OECD 2002). Compared to standard OECD 308 studies, compound dissipation appeared to be much faster in modified OECD 308-type studies, resulting in $DT_{50,TS,mod308}$ of 13 compounds being up to one order of magnitude lower. When comparing $DT_{50,TS,mod308}$ and $DT_{50,TS,std308}$ of aliskiren and atazanavir, it has to be noted that $DT_{50,TS,mod308}$ are subject to rather large uncertainties as the model extrapolated those values far beyond the duration of the experiments; nevertheless, biotransformation of the two compounds is minimal in both modified and regulatory biotransformation experiments.

Other than for the majority of compared compounds, $DT_{50,TS,std308}$ and $DT_{50,TS,mod308}$ for hydrochlorothiazide, fipronil, picoxystrobin, and trinexapac-ethyl did not differ that strongly. For these compounds, we assume that contribution or, in case of hydrochlorothiazide, even dominance of abiotic transformation processes may cause those more similar dissipation

kinetics, as our sterile control experiments indicated those compounds' susceptibility toward hydrolysis (see Table 5).

Interstudy variabilities between different standard OECD 308 studies were significant for 7 out of 19 compounds (i.e., CV >50% between $DT_{50,TS,std308}$ values from different studies). Further, when comparing interstudy variabilities of standard OECD 308 studies to interstudy variabilities of modified OECD 308-type studies, CVs of $DT_{50,TS,std308}$ were higher than CVs of $DT_{50,TS,mod308}$ for 8 of the 13 compounds for which at least two $DT_{50,TS}$ values were available from both standard and modified OECD 308-tpye studies (Table 10 and Table 14). While several parameters (e.g., viability of the microbial test community, oxygen saturation, or pH) can influence the outcomes of biotransformation simulation studies, interstudy variabilities can also be caused by differences in the fractions of compound mass sorbed to sediment and therefore unavailable for biotransformation. The fact that compromised bioavailability due to sorption may be a key factor explaining differences in the extent of biotransformation observed in standard OECD 308 studies was previously shown for different homologues of linear alkylbenzene sulfonates (Lara-Martin et al. 2007). The TOC content of the sediment employed in the here considered standard OECD 308 studies varied from 0.3 to 5.4%, depending on compound and study. Strikingly, the difference in TOC content was much greater between the sediments employed in the modified OECD 308-type studies, i.e., 0.7 and 10% TOC in Rhine and CMP sediment, respectively; however, this >10-fold difference in TOC did not result in in similar or even larger interstudy variabilities in $DT_{50,TS,mod308}$. Further in line with the hypothesis that sorption differences contributing importantly to interstudy variability, we observed after 54-60 days of experiment, accumulation in the sediment of >70% of the initial compound mass for 3 of the 19 compounds (i.e., atazanavir, aliskiren, and azoxystrobin) in case of modified OECD 308-type experiments, while this was the case for more than half of the test compounds in case of standard OECD 308 studies. These observations suggest that, due to the lower sediment-water ratio, larger portions of compound mass are present in the water phase of modified OECD 308-type studies and, hence, bioavailable. As a consequence, differences in TOC content less strongly affected observed $DT_{50,TS,mod308}$ values.

Figure 10: **$DT_{50,TS}$ of test compounds in OECD 309-type suspension tests, modified OECD 308-type studies, and in standard OECD 308 studies**

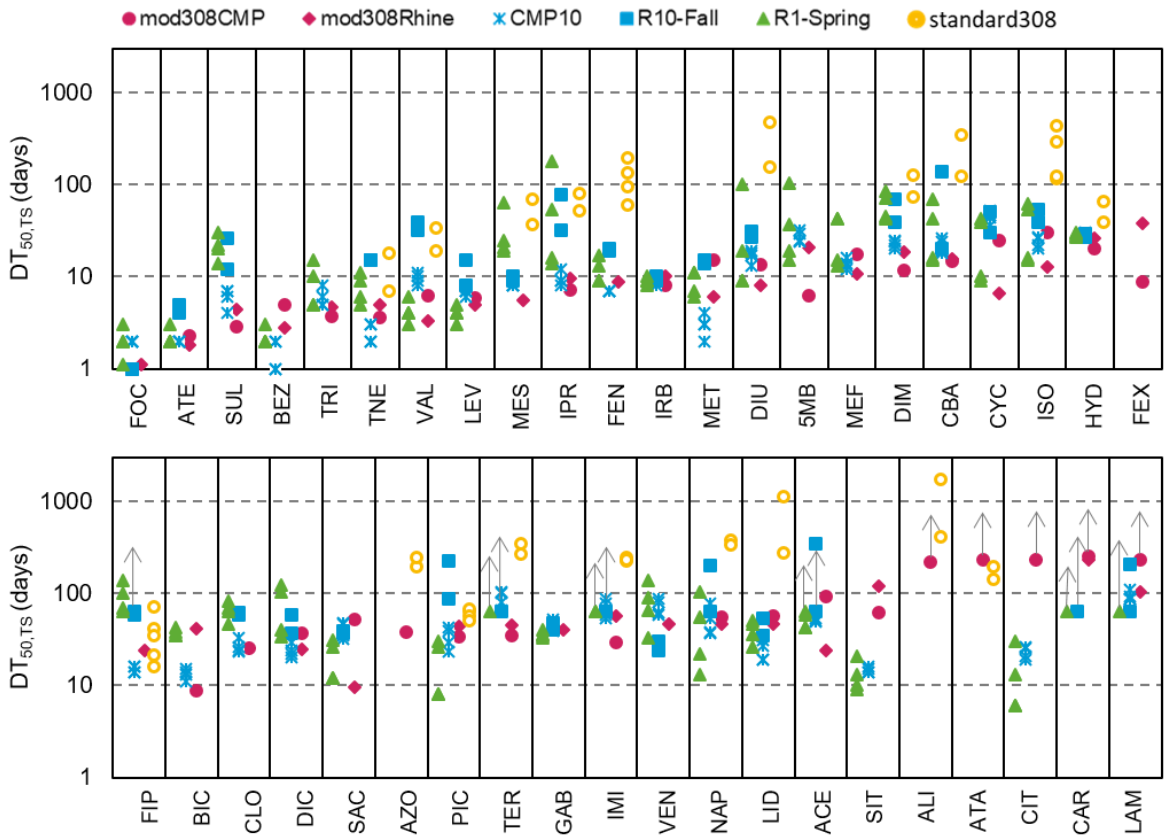

$DT_{50,TS}$ of test compounds in OECD 309-type suspension tests containing 1 g solids L^{-1} (R1-Spring), suspension tests containing 10 g solids L^{-1} (CMP10 and R10-Fall), modified OECD 308-type studies employing a sediment-water ratio of 1:10 (v/v) (mod308CMP and mod308Rhine), and in standard OECD 308 studies employing a sediment-water ratio of 1:3 or 1:4 (standard308) and considering NER to be parent compound. In case of suspension tests, note that different $DT_{50,TS}$ values belonging to the same study indicate inter-replicate variabilities. $DT_{50,TS}$ values marked with upward pointing arrows cannot be considered as definite values because either $DT_{50,TS}$ values were >230 days, or lag phases exceeded the duration of biotransformation experiments, meaning that the $DT_{50,TS}$ values shown are minimal estimates. Standard errors of the degradation models were <12%.
Source: Seller et al. 2021 (Figure 1)

Furthermore, we assume that aeration of the water column throughout the time course of the modified OECD 308-type studies may have resulted in a mostly aerobic sediment layer. This assumption is based on the measurements of oxygenation profiles in different sediment layers of regulatory- and modified OECD 308-type studies presented in Shrestha et al. (2016). While in regulatory OECD 308 studies, only the upper ~1.5mm of the sediment layer are aerobic, O_2 appeared to reach deeper sediment layers in aerated modified OECD 308-type studies. For most compounds, aerobic biotransformation is suggested to be a more important removal pathway than anaerobic transformation. Hence, we hypothesize – in line with the results of Shrestha et al. (2016) – that biotransformation is indeed significantly enhanced in modified OECD 308-type experiments. Consistently, our results indicate that in modified systems contact between compounds and sediment appears to lead more often to transformation rather than sorption compared to in the standard setup.

It has to be noted that increasing the ratio of water to sediment in the experimental vessels and ensuring mostly aerobic conditions were not the only modifications applied to the test design of standard OECD 308 studies that may have caused the observed decrease of $DT_{50,TS,mod308}$ in modified studies. In case of modified OECD 308-type studies, all test compounds were spiked in a mixture to an environmentally relevant concentration (i.e., 1 µg L^{-1}), which is lower than compound concentrations commonly applied during standard OECD 308 experiments (i.e., up to mg L^{-1} range) (Coll et al. 2020). So far, there is no experimental evidence that spiking test compounds to OECD test systems in low concentration mixture alters their biotransformation kinetics (Hammershøj et al. 2019). However, the concentration level at which biotransformation tests are performed has been shown to influence transformation kinetics. For example, Hammershøj et al. (2019) showed that a gradual increase of initial compound concentration in OECD 309 pelagic tests inhibits biotransformation of carbohydrates. Likewise, Li et al. (2019) and Coll et al. (2020) reported shorter half-lives at lower test concentrations of several pharmaceuticals and food additives, including gabapentin in pelagic tests and acesulfame, carbamazepine, and diclofenac in standard OECD 308 tests. Yet, pelagic tests with acesulfame, atenolol, and metoprolol indicated a more rapid compound dissipation from experimental vessels operated at higher concentration levels (Li and McLachlan 2019). Hence, there is still a lack of understanding how outcomes of biotransformation simulation studies are affected by test concentrations. However, with regard to predicting a compound's behavior in the aquatic environment based on laboratory experiments, it appears reasonable to apply test compounds close to their concentrations commonly measured in surface waters.

Further, the temperature at which biotransformation experiments were performed slightly varied between standard and modified OECD 308-type studies. The here considered standard OECD 308 studies were performed at 20°C, while modified OECD 308-type studies were performed at 22±2°C. Based on the Arrhenius equation, a temperature difference of 10°C roughly results in half-lives differing by a factor of 2.5. As we observed differences of up to one order of magnitude between $DT_{50,TS,std308(NER = parent)}$ and $DT_{50,TS,mod308}$, it is reasonable to assume that a temperature difference of 2°C between standard and modified OECD 308-type studies did not cause the observed differences and did not strongly influence the comparison between $DT_{50,TS,mod308}$ and $DT_{50,TS,std308}$ significantly.

Finally, system geometry may influence compound behavior, i.e., sorption behavior, in standard and modified OECD 308-type studies. Unfortunately, parameters describing system geometry, i.e., diameter of the test vessel and actual height of the sediment layer and water column, are mostly not reported for standard OECD 308 studies. Therefore, in the frame of this study, we could not determine influence of system geometry on compound behavior in different standard and modified OECD 308-type studies.

It should be kept in mind, that the standard OECD 308 studies were conducted radiolabeled and the analytical methods relying on detection of radioactivity with less thorough extraction and less sophisticated substance specific analytical techniques than for the modified tests, however being able to determine NER. The above evaluation (Fig. 10) is based on considering NER completely as parent compound. If the approach was taken to disregard NER (i.e. to consider them to be the equivalent of mineralized) the outcome looks different, with half-lives $DT_{50,TS,std308(NER = min)}$ being shorter (see Table 10 and Figure 9 above).

2.5.2.2 Comparison of $DT_{50,TS}$ in OECD 308 and OECD 309-type Water-Sediment Studies

Figure 10 further shows $DT_{50,TS,309}$ values derived from the compounds' dissipation kinetics in suspension tests containing 1 and 10 g solids L^{-1}. In case of suspension tests, Figure 10 does not only show differences between different studies but also intrastudy variations, which were most significant in case of R1-Spring. Even though $DT_{50,TS,309}$ from suspension tests vary significantly and range from ~1 to >100 days, they generally indicate faster compound dissipation from suspension test systems than from regulatory OECD 308 systems.

$DT_{50,TS,mod308}$ values derived from modified OECD 308-type systems are within the same range as the variable $DT_{50,TS,309}$ values derived from suspension tests. Interestingly, interstudy differences of $DT_{50,TS,mod308}$ were less significant than the intrastudy variations (i.e., differences in $DT_{50,TS,309}$ derived from experimental replicates) observed during suspension tests containing 1 g solids L^{-1} (i.e., R1-Spring, Figure 10). Only the two compounds citalopram and sitagliptin dissipated significantly slower from modified OECD 308-type systems than from suspension test systems. Both compounds accumulated in the bed sediment of modified OECD 308-type studies, i.e., with >70% of the initial compound mass being detected in the sediment layer by the end of the experiments. Even though both compounds have been shown to undergo biotransformation, e.g. in activated sludge(Henning et al. 2019; Beretsou et al. 2016), their bioavailability and hence biotransformation appears to be reduced in the presence of increased amounts of sediment, which is consistent with them belonging to the group of test compounds exhibiting the highest K_{oc} values, i.e., $\log K_{oc} \sim 4$ (see Chapter 3).

Generally, most similar $DT_{50,TS,mod308}$ and $DT_{50,TS,309}$ values were observed for rapidly dissipating compounds, i.e., atenolol, bezafibrate, fenoxycarb, and trimethoprim. Despite their different sorption behavior in abiotic sorption control experiments (i.e., sorption to bed sediment in case of fenoxycarb, trimethoprim, and atenolol), they rapidly dissipated from the test systems, most likely because removal from the water phase via biotransformation was faster than the establishment of sorption equilibrium with the sediment layer. Further, $DT_{50,TS,mod308}$ and $DT_{50,TS,309}$ values dwere similar in all test systems for compounds whose removal is dominated by abiotic transformation, i.e., irbesartan and hydrochlorothiazide, whose susceptibility toward hydrolysis was shown in previous research(Li and McLachlan 2019; Mbah 2005) and further confirmed by our own abiotic control experiments.

2.5.3 Comparison of $DegT_{50,w,mod308}$ and $DT_{50,w,mod308}$ in Modified OECD 308-type Studies

Figure 11: $DegT_{50,w}$ and $DT_{50,w}$ in modified OECD 308-type studies

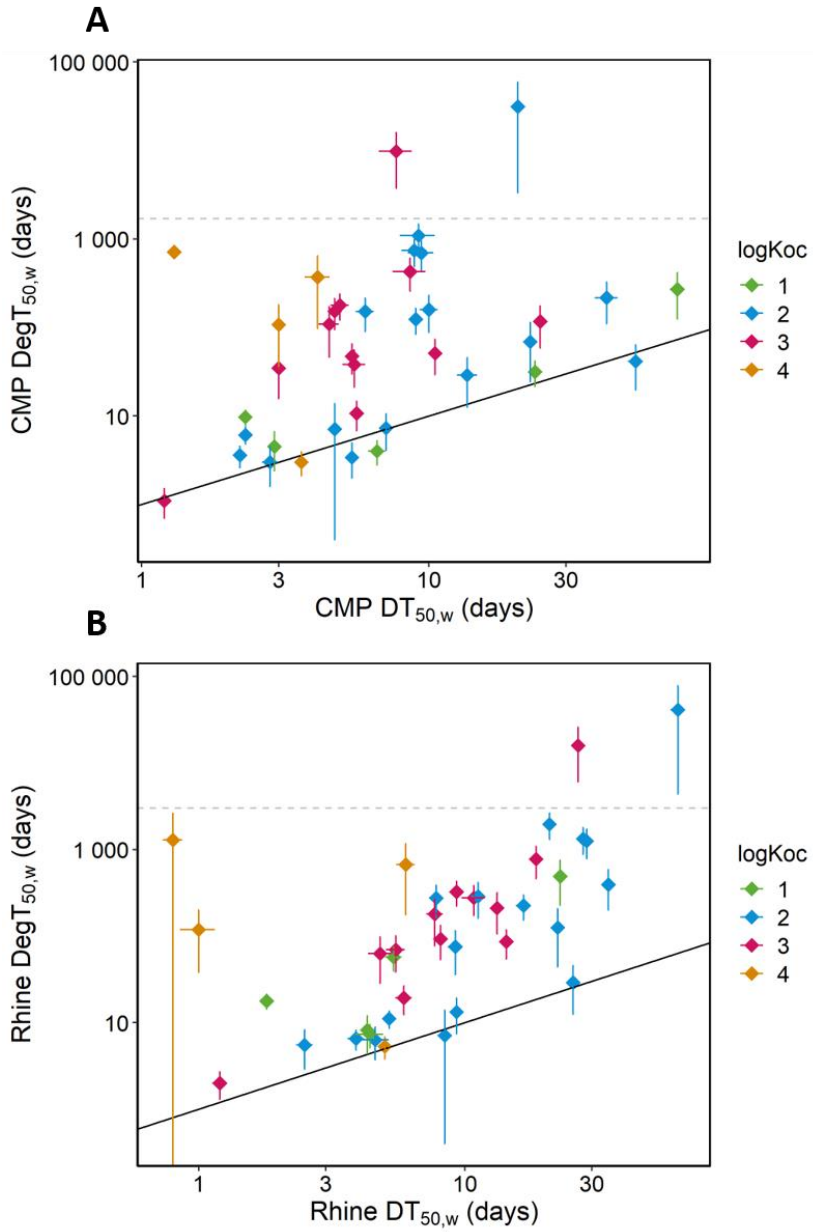

Comparison of $DT_{50,w}$ and $DegT_{50,w}$ in modified OECD 308-type studies. Linear correlations between x- and y-axis have a R^2 of 0.007 and 0.54 in case of plot (A) and (B), respectively. Diamonds are colored with respect to their calibrated rounded $logK_{oc}$ values. The 1:1 lines are plotted as solid black lines in both graphs. The dashed grey lines indicate the cut-off for identification of $DegT_{50,w}$, i.e., $DegT_{50,w}$ calculated with a $k'_{bio,lab}$ >0.1 $L((g\ OC)d)^{-1}$.

Source: own figure, Eawag

Figure 11 compares values for $DegT_{50,w,mod308}$ and $DT_{50,w,mod308}$ derived from data of modified OECD 308-type studies. $DT_{50,w,mod308}$ and $DegT_{50,w,mod308}$ were derived as described in Chapter 2.1.8 and Chapter 2.5.1, respectively. In line with the results of Honti et al. (2015), $DegT_{50,w,mod308}$ were in most cases longer than $DT_{50,w,mod308}$. $DT_{50,w,mod308}$ lump together phase transfer and transformation processes, hence, short $DT_{50,w,mod308}$ may result from rapid transformation or sorption, or a combination of both. $DegT_{50,w,mod308}$ disentangle transformation from phase

transfer processes and describes compound removal from the water phase via transformation; its values are therefore up to two orders of magnitude higher than $DT_{50,w,mod308}$. This significant difference between the two quantities indicates that the assessment of a compound's persistence may result in rather different persistence classification, depending on whether $DegT_{50,w,mod308}$ or $DT_{50,w,mod308}$ values are compared against pre-defined persistence cut-off values.

The strong influence of dispersion and sorption processes on $DT_{50,w,mod308}$ is further highlighted by the rather low correlation between the two quantities, i.e., $DegT_{50,w,mod308}$ and $DT_{50,w,mod308}$. This is especially true in case of the CMP study, for which we did not find any statistically significant relationship between $DegT_{50,w,mod308}$ and $DT_{50,w,mod308}$, as indicated by a R^2 of <0.01 (Figure 11A). An R^2 of 0.54 indicates a somewhat stronger relationship between $DegT_{50,w,mod308}$ and $DT_{50,w,mod308}$ in case of modified OECD 308-type studies in inoculum sampled from the Rhine (Figure 11B). As the CMP sediment has a much higher TOC content than the Rhine sediment, it is likely that compound dissipation from the water phase during the CMP study is driven by sorption to the organic carbon of the sediment. During the modified OECD 308-type employing Rhine sediment, in contrast, sorption has most likely contributed comparably less to most compounds' dissipation from the water phase, which is why transformation leaves a more visible signal in the $DT_{50,w,mod308}$ values, resulting in a stronger correlation between $DegT_{50,w,mod308}$ and $DT_{50,w,mod308}$. Exceptions from the latter are the two compounds sitagliptin and citalopram; while we calculated the shortest two $DT_{50,w,mod308}$ for those compounds from the data of the Rhine experiments, their $DegT_{50,w,mod308}$ were rather long. However, as discussed previously, >70% of those compounds initial mass accumulated in the sediment layer in the experimental vessels over the time course of both modified OECD 308-type studies (see Chapter 2.3.1). In fact, $DT_{50,w,mod308}$ in both studies were <10 days for all four compounds having a $logK_{oc}$ vale of ~4, including citalopram and sitagliptin. Hence, for strongly sorbing compounds, phase transfer processes dominate compound removal from the water phase, even in biotransformation simulation studies employing sediments with low TOC content.

2.5.4 Comparison of $DegT_{50,sed,mod308}$ and $DT_{50,TS,mod308}$ in Modified OECD 308-type Studies

Figure 12 shows a comparison between $DT_{50,TS,mod308}$ and $DegT_{50,sed,mod308}$ derived from data of modified OECD 308-type studies as described in Chapter 2.1.8 and Chapter 2.5.1, respectively. We compare $DegT_{50,sed,mod308}$ with $DT_{50,TS,mod308}$, since we assume that a compounds removal from experimental vessels is driven by its biotransformation in contact with sediment-borne biomass.

As evident from Figure 12, $DegT_{50,sed,mod308}$ are mostly shorter than $DT_{50,TS,mod308}$ since $DT_{50,TS,mod308}$ values are a combination of both rather rapid transformation in the sediment and slower transformation in the water phase (Table 12). Hence, $DT_{50,TS,mod308}$ values are always dependent on the experimental setup. Honti et al. (2015) showed that a change in the sediment-water ratio from 1:3 to 1:4 can alter $DT_{50,TS,std308}$ by 40%. Phase transfer processes are further dependent on the properties of the employed sediment, therefore, it has to be noted that each biotransformation simulation study employing a different sediment will result in different outcomes. $DegT_{50,sed,mod308}$, on the other hand, disentangles transformation from phase transfer processes and is therefore more representative of a compound's actual propensity to be degraded by biotic and abiotic transformation.

$DT_{50,TS,mod308}$ and $DegT_{50,sed,mod308}$ values appeared to be moderately correlated in case of modified OECD 308-type experiments performed in inoculum sampled from the Rhine, i.e., R^2 =0.7. However, it has to noted that $DT_{50,TS,mod308}$ are between one and two orders of magnitude higher than $DegT_{50,sed,mod308}$ and the correlation does not follow the 1:1 line shown in Figure 12. Half-lives of compounds with a rather high K_{oc} value appear to be closer to the 1:1 line, which seems to be consistent with the finding that their $DegT_{50,w,mod308}$ and $DegT_{50,sed,mod308}$ values are rather similar (Table 12). Similarly, the two compounds being removed dominantly through abiotic transformation, i.e., hydrochlorothiazide and irbesartan, have similar values for $DegT_{50,sed,mod308}$ and $DT_{50,TS,mod308}$.

In case of the CMP study, the relationship between $DT_{50,TS,mod308}$ and $DegT_{50,sed,mod308}$ is statistically not significant with R^2 = 0.065. This reduced correlation of half-lives derived from CMP data highlights the influence of dispersion and sorption processes on $DT_{50,TS,mod308}$. In fact, abiotic sorption controls showed that long time periods were needed to reach sorption equilibrium between the sediment and water phase in the experimental vessels containing CMP sediment, i.e., >20 days. In case of Rhine sediment, partitioning equilibrium was reached within <7 days. Hence, phase transfer processes obviously take less time and are less influential on compound half-lives in test systems employing sandy sediment with low TOC content. Nevertheless, compounds with rather high K_{oc} values, as well as the two compounds being removed through abiotic transformation, had again a $DegT_{50,sed,mod308}$ that was comparable with their $DT_{50,TS,mod308}$ in the CMP study.

Figure 12: $DT_{50,TS,mod308}$ and $DegT_{50,sed,mod308}$ in modified OECD 308-type studies

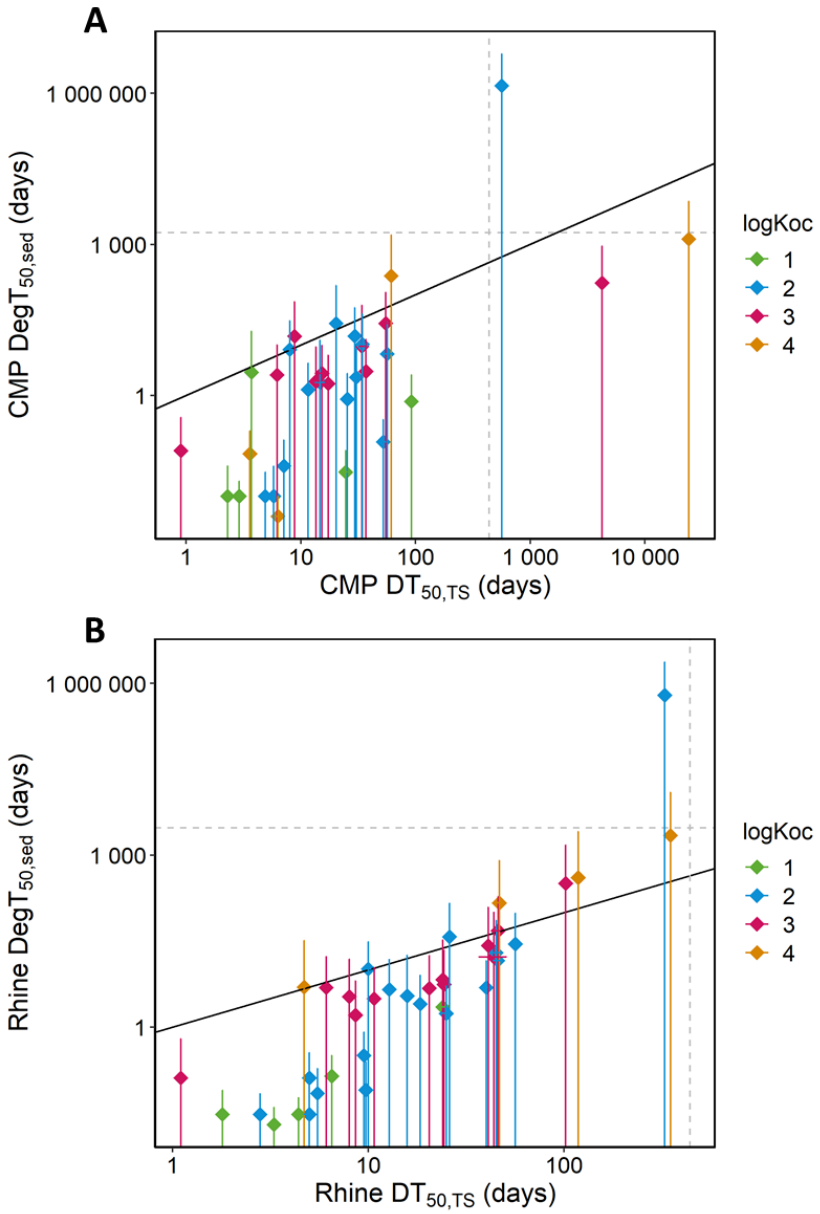

Comparison of $DT_{50,TS,mod308}$ and $DegT_{50,sed,moe308}$ in modified OECD 308-type studies. Linear correlations between x- and y-axis have a R^2 have a R^2 of 0.065 and 0.74 in case of plot (A) and (B), respectively. Diamonds are colored with respect to their calibrated logKoc values. The 1:1 lines are plotted as solid black lines in both graphs. The dashed grey lines indicate the cut-off for identification of $DegT_{50,sed,mod308}$, i.e., $DegT_{50,sed,mod308}$ calculated with a $k'_{bio,lab}$ >0.1 $L((g\ OC)d)^{-1}$, as well as the cut-off for reliable $DT_{50,TS,mod308}$.

Source: own figure, Eawag

3 Complementary Sorption and Phototransformation Experiments

In Chapter 4, the model framework of Honti et al. (2018) is used to determine biotransformation rate constants in the field ($k'_{bio,field}$), which, in Chapter 5, are then compared to biotransformation rate constants derived from modified OECD 308-type laboratory experiments ($k'_{bio,lab}$) introduced in the previous Chapter 2. In Chapter 4, a slightly updated version of the Rhine model is used which also considers abiotic transformation processes, i.e., hydrolysis and phototransformation. Overall, the updated Rhine model has five compound-specific parameters which have to be calibrated: k_{esc} characterizing emissions, K_{oc} describing sorption behaviour, and three transformation rate constants capturing biotransformation, abiotic hydrolysis and phototransformation, i.e., $k'_{bio,field}$, k_{hydro}, and k_{photo}, respectively. Since initial runs of the model indicated that there are strong interactions between these parameters, it is essential to have as accurate and precise as possible priors for those parameters.

Therefore, we conducted a set of complementary experiments capturing the compounds' susceptibility towards phototransformation and their sorption behavior in sediments. The compounds' susceptibility towards abiotic hydrolysis was estimated based on the sterile controls performed alongside the biotransformation simulation studies (see Chapter 2.1.5).

The complementary sorption and phototransformation experiments were performed for those compounds that were investigated in both laboratory studies and field, i.e., 28 compounds including 14 pharmaceuticals, 3 artificial sweeteners and 1 industrial chemical (Table 1).

3.1 Materials and Methods

3.1.1 Sorption Experiment

3.1.1.1 Experimental Setup

Sorption experiments were performed using an experimental procedure based on methods outlined in Davis and Janssen (2020). With our sorption experiments, we aimed to capture the variability of a compound's K_{oc} when exposed to different environmental conditions, as they might occur in a catchment as large as the one of the Rhine river. Hence, two sediments from Cressbrook Mill Pond (UK) and the Rhine river (sampled at Mumpf, Switzerland), as well as one standardized soil, LUFA 2.1, were selected based on differing properties such as pH, organic carbon content, and grain size distribution (Table 15). Prior to the experiment, the sediments and soil were sieved to a particle size of ≤1mm, freeze-dried in the case of the sediments, and sterilized by autoclaving to avoid compound loss from the experimental vessels due to biotransformation.

Table 15: Properties of sediments/soil chosen for sorption experiments

Location	pH	Organic carbon content [%]	Grain size distribution
Pond (CMP)	6.58 ± 0.04	10	45% sand, 49% silt, 5% clay
Rhine River	7.48 ± 0.13	0.5	73% sand, 20% silt, 7% clay
LUFA 2.1	5.01 ± 0.06	0.7	85.3% sand, 9.1% silt, 5.6% clay

The experiments were conducted in two stages: First, to observe the adsorption kinetics of the test substances to determine the time needed to reach sorption equilibrium. In the second stage, adsorption isotherm tests were performed using five concentrations of the test compounds spanning two orders of magnitude (0.3 to 30 µg L^{-1}), with an equilibration time of 16 hours (determined from the first experimental stage).

Based on available sorption data from literature, phase transfer behavior observed in the biotransformation experiments, and predicted sorption behavior based on chemical properties, the test substances were divided into separate groups according to their expected degree of sorption. Grouping the compounds allowed them to be tested using different sediment-water ratios in the experimental setup; compounds with very low sediment-water distribution coefficients (K_d) require higher amounts of sediment in the test system so that differences between initial and equilibrium concentrations can be detected. Conversely, compounds with high K_d require lower amounts of sediment, such that the degree of sorption is not too high and the equilibrium concentration in the water phase can still be measured despite analytical limits. Thus, testing highly-sorbing compounds separately from weakly-sorbing compounds helped to avoid these potential issues. Further, compounds for which we previously experienced analytical challenges were tested individually. Grouping of the compounds is shown in Figure 13.

Figure 13: Compound grouping for sorption experiments

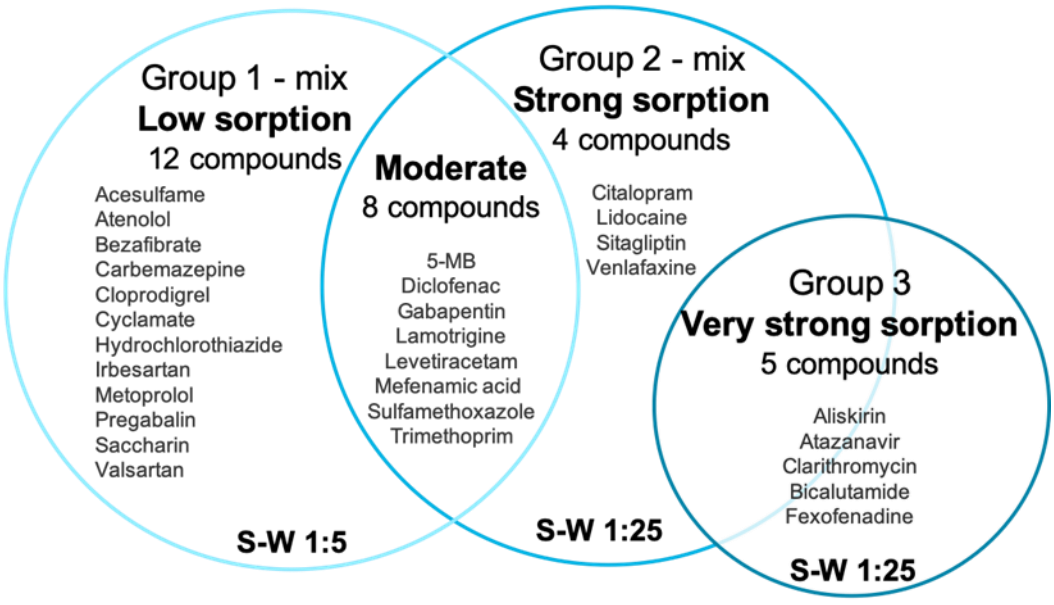

Groups of compounds to be spiked together in sorption experiments, with the corresponding sediment-water ratio used in stage 1.
Source: own figure, Eawag

Table 16 shows the applied sediment-water ratios in the sorption experiments of stage 2. As several compounds of Mix 1 sorbed rather strongly to the pond sediment, experiments with this mix were done twice, i.e., in vials containing a sediment-water ratio of 1:5 and 1:25, respectively.

Table 16: Sediment-water ratios applied during sorption isotherm experiments

Sediment-water ratios chosen for sorption isotherm experiments, based on results from preliminary sorption equilibrium time tests.

	Pond	Rhine river	LUFA 2.1
Mix 1	1:25 1:5	1:2	1:2
Mix 2	1:50	1:5	1:5
Aliskiren	1:50	1:25	1:25
Atazanavir	1:50	1:5	1:5
Bicalutamid	1:50	1:25	1:25
Clarithromycin	1:25	1:5	1:5
Fexofenadine	1:50	1:5	1:5

In order to streamline the process, stage 1 experiments were conducted using the LUFA soil and pond sediment only, while stage 2 was done with all three matrices. As the LUFA soil and Rhine sediment had a similar organic carbon content, the time to reach equilibration was not expected to be significantly different between these two, while the lower pH of the LUFA soil may influence sorption kinetics. As the Rhine river sediment was not tested in stage 1, the same sediment-water ratio as for the LUFA soil was used for stage 2 experiments, as it was expected that a similar degree of sorption would occur due to the similar organic carbon contents of the two matrices.

Both experimental stages followed the same general protocol. Sacrificial samples were prepared in LC vials, to which either 20, 40, 200 or 500 mg of sediment (dry weight) were added according to the desired sediment-water ratio. In stage 1, vials were prepared in duplicate for each sampling time point (0, 4, 8, 24, and 48 h). The sediments were autoclaved at 120°C in order to sterilize them, and 950 µL of 10 mM $CaCl_2$ were added to each vial, whereafter they were placed on a horizontal shaker at 250 rpm overnight to allow the $CaCl_2$ solution to equilibrate with the sediment. After this equilibration period, 50 µL of a spike solution of each compound mixture were spiked into the vials to reach a total initial volume of 1 mL and concentration of 1 µg L^{-1}. Vials were then placed back on the horizontal shaker and removed at each specified time point. The water phase was separated from the sediment via centrifugation (20000 g for 10 min) and the resulting supernatant was stored at -20°C until analysis with LC-MS. Additional samples were prepared to test the stability of the compounds in the soil supernatant. In these samples, the $CaCl_2$ supernatant was removed via centrifugation after overnight equilibration and the test compounds were spiked into the supernatant and analyzed at time points of 0 and 48 hours. This served to assess hydrolysis and/or sorption of the test compounds to the glass vials, as well as to account for matrix effects from the soil supernatant.

Stage 1 results were assessed to determine the time required for the sorption equilibrium to be reached. It was found that 8 hours was sufficient for most compounds to reach equilibrium, however an equilibration time of 16 hours was then chosen to be sure that the equilibrium was reached, as well as for practical reasons. Stage 2 was then conducted in the same manner as stage 1, but instead of sampling at different times, the test vials were spiked to one of the 5 test

concentrations (0.3, 1, 3, 10, or 30 µg L^{-1}) of the respective compound mixture, and all vials were removed and processed after an equilibration time of 16 hours.

Initial spiking concentrations were determined by spiking triplicate samples of 950 µL $CaCl_2$ solution to the intended test concentrations, using the same working solutions containing the test compounds as in stage 1 and stage 2 of the sorption experiments.

3.1.1.2 Data Analysis

To fit a linear model to determine K_d, the concentration in the sediment was calculated by subtracting the equilibrium water concentration from the initial concentration, assuming all compound losses from the water phase were due to sorption to the sediment, rather than being related to hydrolysis or sorption to the test vessel (experimentally confirmed with hydrolysis control samples). To express the sorbed fraction relative to the sediment mass rather than volume, it is multiplied by the sediment:water ratio:

$$C_{sed}^{eq} = \left(C_{aq}^{0} - C_{aq}^{eq}\right)\frac{V}{m} \quad (13)$$

where C_{sed}^{eq} is the concentration, or amount, of compound sorbed to the sediment (µg kg^{-1}), C_{aq}^{0} is the initial concentration measured in the water, C_{aq}^{eq} is the equilibrium concentration in the water (µg L^{-1}), V is the initial volume of water in the test system (L), and m is the mass of sediment used in the test system (kg). The distribution coefficient, K_d, is defined as the ratio of compound in the sediment and water phases,

$$K_d = \frac{C_{sed}^{eq}}{C_{aq}^{eq}} \quad (14)$$

which could then be calculated by fitting a linear regression model using R (R Core Team, 2020) where the slope of the line is the distribution coefficient K_d (L kg^{-1}).

$$C_{sed}^{eq} = K_d\, C_{aq}^{eq} \quad (15)$$

K_d values determined from the linear regression model were converted to K_{oc} by dividing by the fraction of organic carbon in each sediment (Table 15). Besides fitting a linear regression model to the experimental data, we further derived Freundlich isotherms. However, the Freundlich coefficient n_F^{-1} ranged from 0.5 to 1.3, nevertheless, most compounds exhibited linear behavior with n_F^{-1} not being statistically different from 1.

3.1.1.3 Sorption Experiments for Positively charged Compounds

Several test compounds are, at least partially, positively charged at the pH of our experiments, e.g., aliskiren, citalopram, clarithromycin, sitagliptin, or venlafaxine. We therefore hypothesized that they not only strongly sorb to the sediment but also associate with dissolved organic carbon (DOC) in the water phase of the experiments. Heat treatment to sterilize soils, i.e., autoclaving, can result in a release of carbon from the sediment to the water phase and therefore increase the DOC. In our experiments, this phenomenon seemed to be especially critical for the pond sediment and the LUFA soil. For those matrices, the initially derived K_{oc} values were up to one log-unit lower than what was observed in the Rhine sediment, most likely due to not properly accounting for the amount of compounds sorbed to the DOC in the water phase.

Therefore, we repeated stage 2 sorption experiments for the strongly sorbing, partially positively charged compounds in “washed” pond sediment and LUFA soil. In this context,

washing the sediment means that we exchanged the $CaCl_2$ supernatant in the experimental vials three times after autoclaving and were so able to reduce the DOC content in the water phase by a factor of 10 in case of pond sediment and by a factor of 4 in case of LUFA soil. It has to be noted that the TOC of the sediment slightly decreased during this washing procedure, however, this loss was measured and accounted for when calculating K_{oc} values. Otherwise, the experimental protocol followed the methods outlined above for stage 2 sorption experiments.

3.1.2 Phototransformation Experiments

3.1.2.1 Experimental Setup

Phototransformation experiments were conducted with the goal to semi-quantitatively assess whether direct or indirect phototransformation may be a relevant pathway for removal of the respective compounds from the aquatic environment. Phototransformation kinetics were determined (i) in buffered nanopure water (5 mM phosphate buffer, pH=8), (ii) in buffered nanopure water amended with pony lake fulvic acid (PLFA) to a dissolved organic matter (DOM) concentration of 10 mg L^{-1}, and (iii) in sterile water from the Rhine and CMP (i.e., DOM concentrations of 2.2 and 1.2 mg L^{-1}, respectively). Field compounds were spiked into different test waters in mixture to individual concentrations of 1 µg L^{-1}. 40 µM furfuryl alcohol (FFA) were added to determine the concentration of the reactive oxygen species $^1O_2$. To monitor the light flux during the experiment, a para-nitroanisole/ pyridine (PNA/Pyr) actinometer was used with initial PNA and Pyr concentrations of 10 µM and 0.5 mM, respectively. Phototransformation experiments were then carried out in quartz tubes (25 mL, inner diameter 1.5 cm), which were positioned in a water bath (25°C) at an angle of 30°, 40 cm below the light source of a solar simulator (Heraeus model Suntest CPS+) equipped with a xenon arc lamp. Subsamples of 500 µL were taken from each quartz tube before irradiation, and during an additional 5 time points within 4 hours of experiment. Subsamples were spiked with the ISTDs mix to a concentration of 500 ng L^{-1} prior to analysis.

Dark control samples were set up for each test condition and were used to account for hydrolysis or other non-photochemical losses of the test compounds. Dark controls were kept in 2 mL amber glass vials covered with aluminum foil, and were immersed in the water bath shielded from the light source to be otherwise exposed to the same experimental conditions as the irradiated samples.

3.1.2.2 Data Analysis

Phototransformation data were analyzed to determine the reaction order and decay rates for FFA, PNA and all test compounds. Peak areas (FFA, PNA) or concentrations (test compounds) were plotted against exposure time according to zero order (C vs. t), first order ($\ln[C\ C_0^{-1}]$ vs. t) and second order (C^{-1} vs. t) kinetics, were C is the concentration of the reactive species at time t, and C_0 is the initial concentration. The reaction order was determined based on which plot resulted in the best linear relationship according to the regression coefficient (R^2), and the relative standard error of the slope.

In the case of first-order kinetics, the first-order integrated rate law (Equation (16) was used to determine the observed pseudo-first order reaction rate constant, k_{obs}, in units of $time^{-1}$.

$$\ln\frac{C}{C_0} = -k_{obs}t \qquad (16)$$

The observed rate constant for FFA degradation, $k_{obs,FFA,}$ was used to calculate the steady-state concentration of $^1O_2$, in mol L^{-1}, in each sample tube from the solar simulator according to equation 13, using the known bimolecular reaction rate constant of FFA with singlet oxygen, $k_{r,FFA}$ (1.07 x108 $M^{-1}s^{-1}$ at 25°C) determined previously (Appiani et al. 2017).

$$[^1O_2]_{ss} = \frac{k_{obs,FFA}}{k_{r,FFA}} \quad (17)$$

PNA degradation data was used to assess whether the light conditions were stable over the course of the experiment, based on the R^2 value and standard error of the slope from the first-order linear regression. From the PNA data, the photon fluence rate of the solar simulator was calculated according to equation 14,

$$E^0_{p,250-400nm} = \frac{k_{obs,PNA}}{2.303 \cdot \phi_{PNA/pyr} \cdot \sum_{\lambda=250nm}^{400nm}(f_{p,\lambda} \cdot \epsilon_{PNA,\lambda})} \quad (18)$$

with $E^0_{p,250-400nm}$(E $m^{-2}s^{-1}$) being the photon fluence rate between 250-400 nm, $k_{obs,PNA}$ (s^{-1}) the observed reaction rate constant of PNA degradation, $\phi_{PNA/pyr}$ the quantum yield of PNA degradation with Pyr ($\phi_{PNA/pyr} = 0.29[Pyr] + 0.00029 = 0.00043$, (Laszakovits et al. 2016)), $f_{p,\lambda}$ the fraction of the relative light spectrum for each wavelength and $\varepsilon_{PNA,\lambda}$ (m^2 mol^{-1}) the molar absorption coefficient of PNA (Dulin and Mill 1982). The photon fluence rate (E^0) of the solar simulator was then compared with the E^0 measured for natural sunlight in Zurich, Switzerland (August 2013).

Rate constants calculated from first-order regression (Equation 12) were considered statistically significant when k_{obs} was statistically significant from 0, with R^2>0.7 and relative standard error <100%. For compounds that decayed but did not exhibit clear first-order kinetics (i.e. k_{obs} >0 but R^2<0.7), rate constants were not reported, and the decay was described instead as % loss over the time of the experiment. Loss from hydrolysis or other non-photochemical processes observed from dark controls was also described as % loss over time. T-tests (α=0.05) were performed to determine whether observed compound loss was statistically significant, as well as to determine if any loss could be attributed to hydrolysis or sorption to the test vessels rather than phototransformation.

3.2 Results

3.2.1 Experimentally Determined K_d and K_{oc} Values

An example of the measured isotherm data and modelled fits is shown for metoprolol in Figure 14. Results were first assessed by comparing the measured concentrations in the water at equilibrium (after 16 hours) to the initial water concentrations (Figure 14a). The dotted black line shows the 1:1 relationship, i.e., delineating no difference between the equilibrium and initial concentrations, and hence the limiting case where no sorption is observed. Conversely, compounds that sorbed more strongly fell further below this line. The data was visualized first before being fitted with either the linear or Freundlich isotherm model to get an idea of the quality of the data and whether or not the modelled fits would be reliable. In general, the linear sorption model fitted the data well with R^2 greater than 0.7 for most compounds, and was thus sufficient to describe the sorption behavior within the considered concentration range.

For some weakly sorbing compounds, measured concentrations were slightly above the 1:1 line, which would indicate that the measured concentration at equilibrium was higher than the measured initial concentration. As this is not possible, we assume that these compounds sorb so little that the difference in concentration lies within the uncertainty of the analytical method.

Figure 14: Outcomes of sorption experiments in case of metoprolol

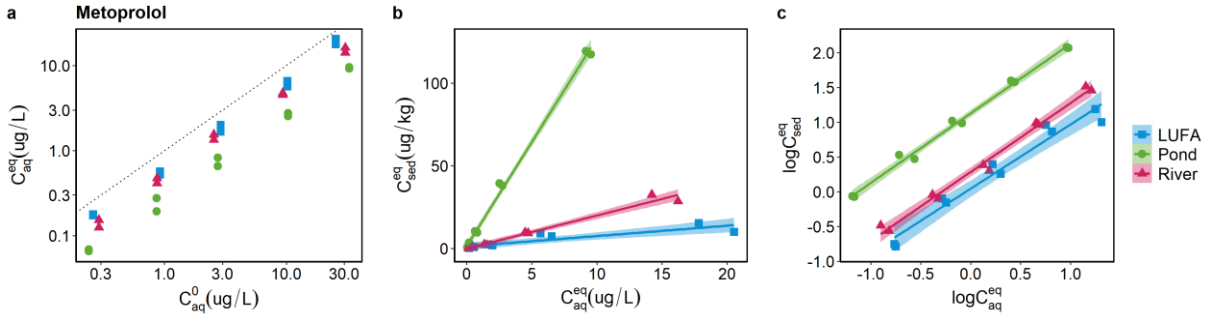

Results for Metoprolol showing a) water concentration at equilibrium vs. initial water concentration on log scale, with measured data (points) and lines representing the mean of two replicates, as well as a 1:1 reference line (dotted black line), b) linear modelled isotherm, and c) Freundlich modelled isotherm (not used here). Both isotherms show measured data (points) and linear regression model with 95% confidence interval.
Source: own figure, Eawag

Table 17summarizes the K_d and K_{oc} values derived from stage 2 sorption experiments. Please note that we here present values from experiments with washed pond sediment and LUFA soil for aliskiren, atazanavir, citalopram, clarithromycin, fexofenadine, sitagliptin, and venlafaxine. It is worth noting that washing the sediment indeed brought LUFA K_{oc} values closer to the Rhine values, but did not seem to have a strong effect on the K_{oc} values derived from the pond experiments.

Table 17: Sorption parameters from linear isotherm model

K_d and K_{oc} values (L kg^{-1}) are listed with their respective standard errors. K_{oc} values are calculated from K_d based on the f_{oc} indicated for each sediment. Regression parameters are not determined (n.d.) if the fit for K_d was poor with R^2 <0.7. K_d values found to be negative but with R^2>0.7 are listed as less than the lowest positive K_d for that matrix.

Compound	Matrix	K_d	K_{oc}	R^2
5MB	LUFA 2.1	n.d.	n.d.	n.d.
	Pond	16.9±0.4	154±3	0.99
	Rhine	0.9±0.1	110±20	0.99
ACE	LUFA 2.1	n.d.	n.d.	n.d.
	Pond	2.3±0.1	20.6±0.6	0.99
	Rhine	0.17±0.06	21±7	0.85
ALI	LUFA 2.1	29.6±10.1	3445.8±1809	0.99
	Pond	35±2	320±16	0.95
	Rhine	32±3	4040±310	0.99
ATA	LUFA 2.1	61.9±11.7	7197.3±2088.6	0.99
	Pond	24±2	217±16	0.89
	Rhine	<0.17	<21	0.73
ATE	LUFA 2.1	n.d.	n.d.	n.d.
	Pond	8.6±0.3	78±2	0.99
	Rhine	1.1±0.2	140±20	0.93

Compound	Matrix	K_d	K_{oc}	R^2
BEZ	LUFA 2.1	n.d.	n.d.	n.d.
	Pond	3.9±0.2	35±2	0.97
	Rhine	n.d.	n.d.	n.d.
BIC	LUFA 2.1	4±2	570±240	0.71
	Pond	26±2	240±21	0.87
	Rhine	n.d.	n.d.	n.d.
CAR	LUFA 2.1	n.d.	n.d.	n.d.
	Pond	6.36±1.7	63.6±16	0.81
	Rhine	n.d.	n.d.	n.d.
CIT	LUFA 2.1	163.1±11	18968.6±1891	0.85
	Pond	286±10	2596±90	0.97
	Rhine	230±160	28550±20500	0.97
CLA	LUFA 2.1	16.6±7.7	1931.4±1373	0.99
	Pond	n.d.	n.d.	n.d.
	Rhine	40±11	5020±1390	0.99
CLO	LUFA 2.1	n.d.	n.d.	n.d.
	Pond	5.6±0.2	51±2	0.97
	Rhine	0.8±0.2	100±30	0.98
CYC	LUFA 2.1	<0.62	<88	0.82
	Pond	n.d.	n.d.	n.d.
	Rhine	n.d.	n.d.	n.d.
DIC	LUFA 2.1	n.d.	n.d.	n.d.
	Pond	10.5±0.3	95±3	0.99
	Rhine	1.5±0.2	190±20	0.99
FEX	LUFA 2.1	25.7±19.9	2982.2±3593	0.99
	Pond	37.8±0.7	344±6	0.99
	Rhine	14±1	1710±150	0.98
GAB	LUFA 2.1	1.5±0.2	210±20	0.95
	Pond	6.8±0.2	62±2	0.99
	Rhine	1±0.1	130±20	0.92
HYD	LUFA 2.1	0.7±0.1	100±20	0.86
	Pond	9.1±0.2	83±2	0.99
	Rhine	0.7±0.1	90±10	0.97
IRB	LUFA 2.1	n.d.	n.d.	n.d.
	Pond	6.3±0.2	57±2	0.98
	Rhine	n.d.	n.d.	n.d.
LAM	LUFA 2.1	2.8±0.4	390±50	0.76
	Pond	22.4±0.5	204±5	0.99
	Rhine	1.7±0.2	220±20	0.99
LEV	LUFA 2.1	0.42±1.9	38.7±274.6	0.92
	Pond	4.1±1.9	41.4±19.6	0.86
	Rhine	0.44±1.9	55.1±243.7	0.95
LID	LUFA 2.1	0.55±1.8	50.6±253	0.88
	Pond	7.9±1.8	79.6±18	0.97
	Rhine	0.21±1.7	66.3±225	0.89
MEF	LUFA 2.1	25±6	3570±830	0.99
	Pond	38±2	348±14	0.96
	Rhine	2±1	250±140	0.97

Compound	Matrix	K_d	K_{oc}	R^2
MTO	LUFA 2.1	0.6±0.1	90±20	0.79
	Pond	12.6±0.2	114±2	0.99
	Rhine	2±0.1	250±20	0.97
PRE	LUFA 2.1	1.8±0.2	250±30	0.96
	Pond	6.1±0.2	55±2	0.99
	Rhine	1.4±0.1	170±20	0.90
SAC	LUFA 2.1	<0.62	<88	0.85
	Pond	n.d.	n.d.	n.d.
	Rhine	<0.17	<21	0.79
SIT	LUFA 2.1	56.3±17	6543.9±3099	0.99
	Pond	59±2	536±21	0.97
	Rhine	70±20	8730±2160	0.98
SUL	LUFA 2.1	n.d.	n.d.	n.d.
	Pond	1.7±0.1	15.4±0.9	0.98
	Rhine	n.d.	n.d.	n.d.
TRI	LUFA 2.1	60.21±51.4	7001.2±9174	0.93
	Pond	97±4	884±34	0.97
	Rhine	n.d.	n.d.	n.d.
VAL	LUFA 2.1	n.d.	n.d.	n.d.
	Pond	4.4±0.1	39.6±0.9	0.99
	Rhine	n.d.	n.d.	n.d.
VEN	LUFA 2.1	37.8±21	4389.5±3772	0.98
	Pond	29±1	262±9	0.98
	Rhine	25±4	3160±350	0.94

3.2.2 Definition of Sorption Priors for k'_{bio}-Modelling

As outlined above (Introduction to Chapter 3), the sediment sorption coefficient K_{oc} is a model parameter that is required when deriving $k'_{bio,field}$ and $k'_{bio,lab}$ from model calibration. Since it is uncertain itself, for each compound and K_{oc} value, a prior distribution was derived and used in model calibration. For compounds that were included in our own sorption experiments (i.e., compounds that were investigated in both laboratory studies and field), priors were determined based on those experimental results. For compounds studied exclusively in the laboratory (i.e., pesticides) or in the field, K_{oc} values were collected from literature.

The prior distribution for K_{oc} was assumed to be lognormal due to the rather high variability of experimentally determined K_{oc} values and the fact that only positive values are meaningful for this quantity. The two parameters of the lognormal distribution, the mean and the standard deviation (not the mean and stdandard deviation of the log-transformed values) were specified based on all available K_{oc} values for each compound.

a) Special conditions were determined for priors calculated from sorption experiments. If Koc was negative due to failure of the model fitting or lack of sorption, those values were excluded from calculation. Based on the number of remaining estimates, the following decisions were made:

b) If 2 or 3 Koc estimates were available (out of the 3 experiments with the different sediment types), we determined their mean and standard deviation and assigned a lognormal prior

with the corresponding parameters. When CV (ratio of standard deviation and mean) exceeded 1, the standard deviation was reduced to a set CV of 1.

c) If only one Koc estimate was available, that single Koc value was assumed to be the mean of the lognormal prior and CV was set to 1.

d) In case of acids (cyclamate, mefenamic acid, valsartan) featured in sorption experiments, we only used Koc measurement from the Rhine sediment to determine the prior because the pH of the Rhine sediment differed by one to two pH units from the other matrices tested. In that case, the prior mean was set to the estimated mean and CV was set to 0.5. For other compounds with measured Koc values, if the result from the Rhine sediment was discarded due to uncertain measurement results, CV was also set to 0.5.

The above-mentioned limits for CV had to be introduced due to the asymmetric nature of the lognormal distribution. Extreme quantiles quickly widen with increasing standard deviation. For CV=1 (when standard deviation is the same as the mean), the 95% confidence range already covers two orders of magnitude. Higher confidence range would effectively cancel the information content of the prior K_{oc} values.

K_{oc} values from the sorption experiments are summarized in Table 18, alongside literature values.

Table 18: K_{oc} vlaues from literature and from own sorption experiments

Means and standard deviations (sd) for Koc (L kg^{-1}) from literature and experiments. Prior values used in the model are highlighted in red.

Comp.	Literature values		Sorption experiments	
	mean	sd	mean	sd
5MB	87	87	126	56
ACE	3	3	23	1
ALI	1790	1480	3750	424
AMI	34	34		
ATA	1880	1730	7200	7200
ATE	17	17	109	109
BEN	57	57		
BEZ	288	288	36	18
BIC	263	263	977	943
CAR	473	473	NA	NA
CIT	6920	6920	24200	7120
CLA	59	59	3910	2970
CLO	1640	1340	72	64
CYC	2	2	2	1
DIC	733	521	169	66
FEX	14600	14600	2440	998
GAB	4	4	151	95
HYD	31	31	99	7

Comp.	Literature values		Sorption experiments	
	mean	sd	mean	sd
IRB	7760	7760	70	35
LAM	537	537	292	89
LEV	7	7	45	9
LID	251	251	66	15
MEF	475	475	286	143
MTO	58	58	176	116
MOC	31	31		
OXC	87	87		
PHE	39	39		
PRE	2	2	191	167
PRO	501	501		
RAN	309	309		
SAC	15	15	22	22
SIT	23400	234	7720	1590
SUL	37	37	10	7
TRI	3040	3040	11000	11000
VAL	1890	1890	4	2
VEN	427	427	3830	901

3.2.3 Phototransformation Rate Constants

Phototransformation experiments allowed identifying compounds that might potentially undergo phototransformation reactions in the aquatic environment. We ensured constant light emission during the experiments and the photon fluence rate (E^o) was 3.73x10^{-4} Es m^{-2}s^{-1}. In comparison, E^o for natural sunlight in Zürich (August 2013) can be estimated to be 7.82x10-4 Es m^{-2}s^{-1}, indicating that the light emitted by the solar simulator in this experiment was approximately half of the strength of peak summer sunlight in central Europe. The irradiance spectra of the solar simulator and natural sunlight used in these calculations showed a good overlap indicating that the solar simulator suitably mimicked the spectral output of natural sunlight. The decay of FFA in the experimental vessels demonstrated that $^1O_2$ steady-state concentrations were constant over the course of the experiments and difference in $^1O_2$ concentrations between the test waters scaled with the respective DOM content as expected.

During our phototransformation experiments (4 hours, pH=8), we determined direct phototransformation as a relevant removal pathway (i.e., concentration decrease >20%) for five field compounds, i.e., diclofenac, hydrochlorothiazide, aliskiren, atazanavir, and sulfamethoxazole, with the first two compounds showing the most rapid transformation as illustrated in Figure 15.

Indirect phototransformation appeared to be a less significant removal pathway and was statistically significant only for four compounds, i.e., carbamazepine, clopidogrel carboxylic acid, lidocaine, and mefenamic acid, with mefenamic acid showing the greatest susceptibility towards

indirect phototransformation. It has to be noted that there was no compound removal via indirect phototransformation from the two natural waters tested, i.e., from the Rhine and CMP samples, but only from the test water amended with PLFA to a DOM concentration of 10 mg L^{-1}. Even at this elevated DOM concentrations, which is at the upper limit of what is commonly observed in natural rivers (Ejarque et al. 2017), the maximum observed rate for indirect phototransformation was <0.067 d^{-1} (mefenamic acid).

Figure 15: Compound dissipation via direct phototransformation

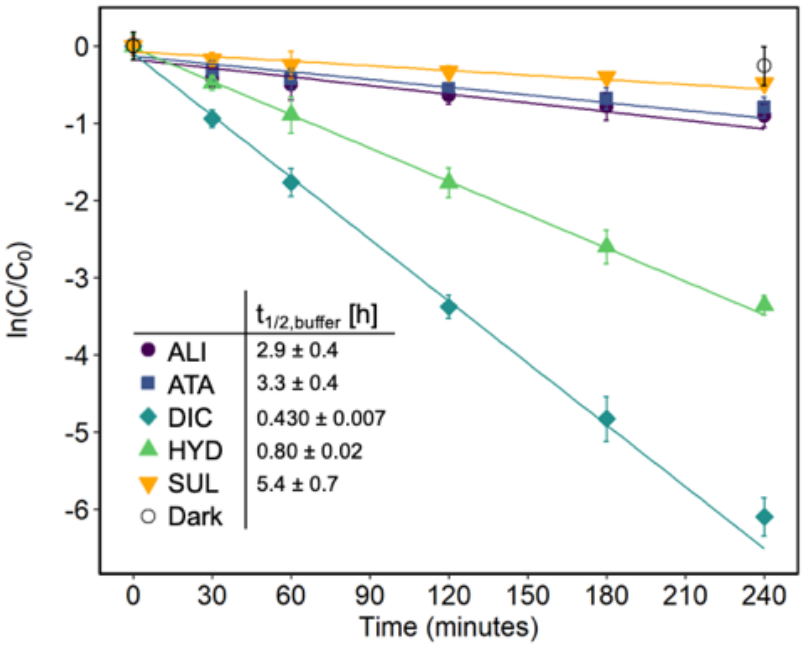

Compound dissipation of aliskiren, atazanavir, diclofenac, hydrochlorothiazide, and sulfamethoxazole from pH-bufferd nanopure water due to direct phototransformation.
Source: own figure, Eawag

3.2.4 Definition of Phototransformation Priors for $k'_{bio,field}$-Modelling

Due to the fact that no compound removal via indirect phototransformation was measured in the water samples containing natural water, i.e., sampled from the Rhine and CMP, we chose to neglect indirect phototransformation as a removal pathway in the Rhine model.

On the other hand, we considered direct phototransformation in the Rhine model by deriving a prior for k_{photo} that captures diclofenac's direct phototransformation at the aquatic environment's surface within the Rhine river catchment during the SMPC sampling campaigns in 2017 (see Chapter 4). We therefore followed the methods outlined in Tixier et al. (2003). Briefly, we used the GCSOLAR software to calculate a pseudo-first-order rate constant based on diclofenac's quantum yield and its absorbance spectrum, which were previously determined by Davis et al. (2017). GCSOLAR further allowed to consider season, latitude, time of day, depth in water body, and ozone layer as parameters influencing the compounds phototransformation rate constant. However, since GCSOLAR estimates are derived under the assumption of a perfectly clear sky, we further corrected the prior phototransformation rate constant for reduced sunlight during their hydraulic residence time in the Rhine. Thereby, we considered the

theoretical global radiation in Germany and the actually measured global radiation at Frankfurt am Main (Germany) during March and July 2017. Hence, we derived two prior rate constants describing diclofenac's phototransformation at the water surface, one for each of the two sampling campaigns considered for the Rhine model (see Chapter 4); k_{photo} of diclofenac was estimated to be 0.7 and 2.2 d^{-1} during spring and summer 2017, respectively.

For the other four compounds that showed susceptibility towards direct phototransformation, we then multiplied the prior phototransformation rate constant for diclofenac with a factor describing the respective compound's rate constant relative to diclofenac's rate constant as measured in our direct phototransformation experiments, i.e., 0.53, 0.14, 0.13, 0.08 for hydrochlorothiazide, aliskiren, atazanavir, and sulfamethoxazole, respectively. Prior distributions used to account for direct phototransformation within the Rhine during two seasons, i.e., spring and summer, are shown in Table 19.

Table 19: Phototransformation priors

Prior distributions used to describe direct phototransformation at the water surface in the Rhine catchment for compounds whose susceptibility toward direct phototransformation has been shown in laboratory phototransformation experiments.

	k_{photo} (d^{-1})	
	P1	**P3**
DIC	0.7±0.07	2.2±0.2
HYD	0.37±0.04	1.16±0.1
ALI	0.098±0.01	0.31±0.03
ATA	0.091±0.009	0.28±0.03
SUL	0.056±0.006	0.17±0.02

4 Rhine Field Study

4.1 Rhine Modelling

4.1.1 Introduction

In the PIdent-I project (Fenner et al. 2016) field data from the Rhine campaign of Ruff et al. (2015) were modeled to assess degradation in the Rhine for seven compounds with biotransformation considered as the sole loss pathway. For this purpose, a Rhine catchment model was developed that allowed estimating an average bioavailability and biomass-normalized biotransformation rate constant in the Rhine catchment ($k'_{bio,field}$) (Honti et al., 2018). This study highlighted that credible information about the emission and sorption properties of the compounds were crucial for the estimation of $k'_{bio,field}$ with tolerable uncertainty.

The specific aim of the new Rhine Field study carried out in this project was to more broadly assess the practical use of field measurements in estimating persistence indicators. The specific objectives to reach this aim, were (i) to reduce uncertainty as much as possible by improving the accuracy of emission data and sorption / abiotic transformation parameters, and (ii) to extend the set of compounds. We were fortunate to obtain access to the samples taken as part of the SMPC campaign (*Sondermessprogramm Chemie*) of ICPR (International Commission for the Protection of the Rhine). In SMPC, four water parcels have been followed down the Rhine during each season of 2017. The water parcels have been sampled at 14 locations along the Rhine and in 6 large tributaries. In those samples, we quantified a set of substances for which a continuous and constant emission could reasonably be assumed, and used the Rhine catchment model to estimate transformation rate constants ($k'_{bio,field}$) with sufficient precision for those substances.

4.1.2 Methods

The methodological approach was as follows: First, suitable substances were selected from the SMPC compound inventory based on the expected stability of emissions, sufficient detectability, and the availability of consumption data and WWTP effluent concentrations. It has to be emphasized that although the selected set of compounds strongly overlapped with the set used in laboratory studies (see Chapter 2.1.1), it was not the same due to the different requirements of the two studies. Then, the selected compounds were quantified from the SMPC samples to determine fluxes at the monitoring locations. Afterwards, emission estimates were made, which, together with dedicated measurements of sorption parameters provided prior parameter distributions for the catchment-scale water quality model.

4.1.2.1 Substance Selection

The initial set of potentially interesting substances contained 42 pharmaceutical active ingredients (APIs), 3 artificial sweeteners, 2 corrosion inhibitors, and 1 biocide. This starting list was compiled based on a review of available consumption data and field concentrations measured during the Ruff et al. (2015) measurement campaign carried out in 2011.

Selection criteria for target substances were as follows:

1. Data availability: consumption data, measured concentrations in WWTP effluents
2. Expected detectable presence in the Rhine catchment based on previous measurements or consumption relative to known measurable substances

Substances could be excluded from the initial list due to one of the following reasons (see Table 20):

3. Missing measured concentrations in WWTP effluents
4. Analytical issues with effluent measurements at WWTP
5. Not detectable in Rhine
6. Not included in SMPC measurement campaign

4.1.2.2 Substance Quantification

4.1.2.2.1 The SMPC Dataset and Sample Preparation

For chemical analysis, samples of two of the four campaigns carried out in the frame of the SMPC were used. The P1 campaign was sampled between 19.3.2017 and 6.4.2017 in the Rhine and its catchment, and P3 was sampled between 10.7.2017 and 27.7.2017. Additionally, samples from three stations (Weil am Rhein, Bischoffsheim and Bimmen) from the two other campaigns (P2 and P4) were analyzed as well to evaluate fluctuations among the water parcels. Samples were stored at -20°C after sampling. After thawing, 10 ml of sample was centrifuged (4000 rpm, room temperature, 20 min) to remove any particulate matter. Exactly 1 ml of supernatant was transferred and was spiked with isotope-labelled internal standards at a concentration of 100 ng L^{-1} to account for compound losses and instrument fluctuations.

4.1.2.2.2 Measurement with Liquid Chromatography coupled Mass Spectrometry

The system consisted of an Agilent Triple Quad Mass spectrometer (Agilent 6496 B) coupled with an Agilent HPLC system (1290 Infinity II, Autosampler, Column Oven, Pump). 100 µl of the samples was injected and separated on a reversed phase column (Acquity UPLC HSS T3, 1.8 µm, 2.0 x 100 mm, Waters) equipped with a precolumn (Acquity UPLC HSS T3, 1.8 µm, 2.1 x 5 mm, Waters). The following gradient of water (Solvent A) and methanol (solvent B) both acidified with 0.1% formic acid at a flow rate of 500 µl/min was used.: 0-1 min 100% A, 1-18.5 min linear gradient to 5 % A, 18.5-22.0 kept at 5 % A, 22.5 switch to 100 % A and kept constant to reequilibrate for 2 min.

Analyte detection was performed using a triple quad in dynamic MRM mode. Ionization was performed by electrospray ionization (3.5 kV in positive, 3.9 kV in negative mode, mass resolution 0.7 Da). 40 compounds and 35 isotope-labeled standards were analyzed by measuring two transitions each (Quantifier and Qualifier) with a minimum dwell time of 10.12 ms and a cycle time of 650 ms.

4.1.2.2.3 Quality Controls and Data Treatment

Data evaluation was performed using MassHunter Quantitative Analysis (Version B.08.00). For each analyte, quantification was performed on the more dominant transition. The qualifier control was in all cases between 80 – 120 % tolerance. LOQs (limit of quantification) were determined and were below 1 ng L^{-1} for 14 compounds, and below 10 ng L^{-1} for the majority of analytes (35 compounds). Highest LOQs were detected at 50 ng L^{-1} for oxypurinol and benzotriazole.

For quantification, calibration samples were prepared covering a range from 0.1 ng L^{-1} to 1000 ng L^{-1}. Seven sites were spiked with 50 ng L^{-1} and 500 ng L^{-1} to determine the relative recovery which was determined between 80 and 120 % for all 40 compounds. Triplicate injection of the samples showed an average deviation of merely 3.9 % and triplicated sample preparation and measurement showed an average standard deviation of 4.5 %.

Additional calibration standards mixed externally (Neochema) were measured as well and compared to the quantified amount for 10 compounds. The comparison revealed less than 10 % deviation from the determined value.

4.1.2.3 Estimation of Emissions

The Rhine modeling from the PIdent-I project has shown that meaningful estimates of biotransformation rates crucially depended on good emission estimates (Honti et al. 2018). Thus, an improved emission estimation was carried out by incorporating all available and relevant data sources.

A complex sequence of loss processes occurs from amounts of APIs marketed (which are recorded in the national statistics) to actual emissions into surface waters (Delli Compagni et al. 2020). In the beginning are two parallel pathways, an „improper usage" pathway actually avoiding human consumption, which involves improper disposal (i.e. flushing in the toilet), emissions from pharmaceutical manufacturing and other industrial use, and a „proper usage" pathway, i.e., consumption, metabolism, and excretion. After entering the sewer system, APIs may undergo various chemical and biological transformations, particularly in the receiving WWTPs. The latter may sometimes be circumvented and APIs may enter surface waters without treatment in case of active combined sewer overflows (Launay, Dittmer, and Steinmetz 2016). To describe this series of processes in detail would require measurements after each stage. Yet, the majority of relevant studies concentrate on removal processes inside the WWTP (Kasprzyk-Hordern, Dinsdale, and Guwy 2009; Patrolecco, Capri, and Ademollo 2014; Oberoi et al. 2019), whereas only few target sewer networks themselves due to the difficulty of sampling and the high variability of sources and pollutant transport (Ort, Lawrence, Rieckermann, et al. 2010; Ort, Lawrence, Reungoat, et al. 2010).

To overcome this knowledge gap, we apply a lumped treatment to the series of processes between the marketed API amounts and the effluents from the WWTPs. We define the dimensionless „escape factor" (k_{esc}) as the proportion of the marketed APIs reaching the stream network. Thus, k_{esc} integrates all above-mentioned pathways in a single number that is theoretically between 0 (no emissions) and 1 (the entire marketed amount in the catchment reaches the rivers).

Assuming that the „proper usage" pathway dominates and metabolism and removal at the WWTP are the most important processes, k_{esc} can be defined in a process-oriented way as follows:

$$k_{esc} = k_{exc} (1 - k_{rem}) \quad (19)$$

where k_{exc} is the excreted fraction of the non-metabolized API from the body (dimensionless), and k_{rem} is the removal efficiency in the WWTP (dimensionless). There are literature data for both k_{exc} and k_{rem} for many compounds, yet these are rather uncertain (Singer et al. 2016). The simplified formulation of Equation (19) can be extended to desired complexity by adding factors representing e.g. transformation in the sewer system, deconjugation, the role of the „improper usage" pathway, etc. (Delli Compagni et al. 2020), yet in the absence of relevant data this does not contribute to a better estimation of emissions. A more practical approach is to express the connection between marketed amount and the effluent:

$$F_{eff} = f_{cons} N_{pop} k_{esc} \quad (20)$$

where F_{eff} is the flux of the API in the WWTP effluent (ng d^{-1}), f_{cons} is the mean daily dose over the entire population based on the marketed amount (ng $person^{-1}$ d^{-1}), and N_{pop} is the population connected to the WWTP (person). By rearranging we get:

$$k_{esc} = F_{eff} / (f_{cons} N_{pop}) \quad (21)$$

This formulation can be used to estimate k_{esc} from market statistics, WWTP effluent fluxes and connected population data. The task is to find the relevant values of f_{cons} and N_{pop} that can be used in combination with existing measurements of F_{eff}. F_{eff} can be estimated based on effluent concentrations and corresponding discharge measurements:

$$F_{eff} = C_{eff} Q_{eff} \quad (22)$$

where C_{eff} is the concentration of the API in the WWTP effluent (ng d^{-1} L^{-1}) and Q_{eff} is the corresponding discharge measurement (L d^{-1}).

While Equation (21) is applicable to most compounds, it does not work for some with missing or irrelevant consumption data (e.g., artificial sweeteners). In these cases, we refrained from using estimating k_{esc} and instead merged it with f_{cons}:

$$F_{eff} = F_{pce} N_{pop} \quad (23)$$

where $F_{pce} = f_{cons} k_{esc}$ is the per capita effluent flux (ng $person^{-1}$ d^{-1}). By rearrangement we get:

$$F_{pce} = F_{eff} / N_{pop} \quad (24)$$

Both equations (21) and (24) express the same mapping from consumption to WWTP effluent. The advantage of using the slightly more complicated Equation (21) is that k_{esc} does not contain the differences induced by country-specific consumption habits. Thus, assuming that treatment technology is similar in most WWTPs in the Rhine catchment, a single k_{esc} value can be used everywhere, while F_{pce} needs to be determined on a country-by-country basis.

4.1.2.3.1 Consumption Data

Annual consumption data of pharmaceuticals and artificial sweeteners were collected for Germany (for the period of 2010-2018) and Switzerland (for 2014-2016). Data source was IQVIA (formerly IMS Health, www.iqvia.com), provider was UBA and BAfU for Germany and Switzerland, respectively. Besides these recent datasets, Singer et al. (2016) provide estimations for the German and the Swiss consumption for 2009. For the years of 2017 and 2018, IQVIA provided quarterly consumption data for Germany. All consumption data referred to human medical usage. Therefore, although also listed, the data for artificial sweeteners could not be used because these compounds are used in large quantities by the food industry. For corrosion inhibitors, no consumption data were available. Analysis of consumption data revealed significant year-to-year and seasonal changes for numerous compounds. Long-term trends reflect the general market share of a specific API. Within a single year, consumption of course can vary around the long-term trends, but for certain compounds there can be a significant seasonal dependence in intake too (e.g., APIs mainly used in the allergy and flu season).

To get a precise estimate of k_{esc}, it was important to match f_{cons} to the quarterly period when effluent concentrations were measured. Therefore, we applied a multiplicative interpolation model of consumption dynamics that was applied to generate quarterly consumption from the annual data:

$$C(Y,Q) = [C_Y + S_C Q/4 (C_{Y+1} - C_Y)] f(Q) \quad (25)$$

where C(Y,Q) is consumption (kg $quarter^{-1}$) in the Q^{th} quarter of year Y, C_Y is the mean quarterly consumption in the given year Y (kg $quarter^{-1}$), C_{Y+1} is the mean quarterly consumption in the next year, and Q is the quarter index (1-4), S_C is the slope of the local annual trend (kg $year^{-1}$), and f(Q) is the seasonal multiplicator (dimensionless with the mean of 1 over all quarters). For

2017 -2018 for Germany, the exact quarterly consumption values provided by IQVIA were used without interpolation.

The consumption model in Equation (25) was fitted for each compound in two steps.

First, long-term trends were fitted for Switzerland and Germany separately by setting S_C for each year based on the annual consumption statistics (thereby assuming that f(Q) was always 1). This was an important step to extend consumption data for missing years, as WWTP effluent data covered numerous years outside the period of consumption data, As the Swiss data for 2009 were given as semi-closed intervals for some compounds by Singer et al. (2016), this year was included in the calculations in two alternative ways, depending on the type of estimation. Specific values were directly used for the consumption for 2009. When ranges were provided (e.g. consumption was higher than or equal to a given value), the final value for 2009 was decided based on a trend analysis. A linear regression was fitted to the available consumption data. The regression value for 2009 was accepted when it fell into the range specified by Singer et al. (2016), otherwise the limit value was used. Based on the position of data gaps, extrapolation or interpolation was used to fill in missing annual values between 2010 and 2018 (Table 22 and Table 23).

After estimating the long-term trends, the seasonality factors f(Q) were determined based on the quarterly consumption data for Germany (2017-2018). As these two years did not exactly align to the trends previously estimated from the longer annual statistics, we did not use the annual S_C for detrending, but used a moving average method (window width=4 quarters). Then, f(Q) could be determined from the ratio between the actual consumption and the trendline.

Seasonal variability was assumed to be country-independent, thus f(Q) determined from the German quarterly datasets of 2017-2018 was applied to all the other years both in the German and Swiss consumption time series.

There are several compounds with significant seasonal and year-to-year change in use. After market introduction of a pharmaceutical or other product, different trends may occur during commercial availability (take-off, expansion and decline). In special cases, the marketing may cease and the emissions afterwards gradually fall to zero. These phases can vary by country and year depending on actual regulations and current preferences. For the target compunds, we observed all kind of trends. The rate and direction of change was not always predictable for years with missing data from consumption data of previous or following years, or based on the trends and consumptions of other countries covering the same years. This meant that extrapolation and interpolation of annual consumption data might lead to high uncertainty in escape rate calculation. A good example for such a case is valsartan, which saw a dramatic decrease in consumption in the last two quarters of 2018 due to product recalls because of impurities. This change could not be estimated properly from the previous years.

4.1.2.3.2 WWTP Effluent Data

WWTP emission data were obtained from three Swiss and two German (Baden-Württemberg, Nordrhein-Westfalen) monitoring campaigns. Swiss data were provided by Eawag (as host institution for these studies), German data were provided by the Landesanstalt für Umwelt Baden-Württemberg and the LANUV (Landesamt für Natur, Umwelt und Verbraucherschutz Nordrhein-Westfalen). The Swiss samples were composite samples, collected at multiple intervals during a longer time span. The German data we used here was mostly from grab samples, taken at specific time points. Emitted fluxes were calculated as the product of sample concentrations with measured discharge.

Swiss monitoring campaigns:

1. CH1 campaign (Singer et al. 2016): Effluent concentration and corresponding discharge measurements from 6 WWTPs in Switzerland. Campaign period: March 2012. Samples were flow- or time-proportional 24-h composite samples collected and mixed flow-proportionally into 1-week composite samples.
2. CH2 campaign (Götz 2015): Effluent concentration and corresponding discharge measurements from 9 WWTPs in Switzerland. Campaign period: May to August 2013. Samples were flow- or time-proportional 24-h composite samples collected and mixed flow-proportionally into 3-day composite samples.
3. CH3 campaign (Schymanski et al. 2014): Effluent concentration measurements from 10 WWTPs in Switzerland. Discharges during the campaign period were not measured, so WWTP-specific long-term mean daily discharge values (Q24 [m3 d^{-1}]) provided by https://map.geo.admin.ch were used in effluent flux calculations. Campaign period: February 2010. Samples were flow-proportional 24-h composite samples.

German monitoring campaigns:

1. Baden-Württemberg (BW) campaign: Effluent concentration measurements from 6 WWTPs in Germany from the state of Baden-Württemberg Only yearly discharges were available for each WWTP, thus mean daily discharges were calculated and used in effluent flux calculations. Campaign period: June 2012- April2013. Samples were measured once each month: WWTPs with automatic samplers provided 24-h composite samples, in all other cases the samples were qualified grab samples (Qualifizierte Stichprobe (§ 2 AbwVO), i.e., a 10-minute composite sample of 5 grab samples taken every two minutes). Source: The Landesanstalt für Umwelt Baden-Württemberg compiled chemical data and load estimation within a special research project named “Spurenstoffinventar der Fließgewässer in Baden-Württemberg” (Inventory of micropollutants in rivers of Baden-Württemberg).
2. North Rhine-Westphalia (NRW) campaign: Effluent concentration and corresponding discharge measurements from 156 WWTPs in Germany from the state of North Rhine-Westphalia. Campaign period: 1999-2018 (we only used measurements from 2009 onward). Samples were qualified grab samples. Source: The official monitoring program conducted by LANUV measuring effluent concentrations and corresponding discharges at the outlet of the WWTPs.

The number of inhabitants actually connected to the WWTP is relevant to calculate F_{pce} [g (person yr)$^{-1}$]. We used served population data in F_{pce} calculation. Datasets of the two German campaigns contained information on served population for the WWTPs. For the Swiss WWTPs, served population data were collected from two sources. Data from 2005 were gained from Data for 2017 were collected from the webpage of BAFU (https://www.bafu.admin.ch/bafu/de/home/themen/wasser/fachinformationen/massnahmen-zum-schutz-der-gewaesser/abwasserreinigung/erhebung-angeschlossene-einwohner.html). Wherever it was possible, actual served population values from the year of the sampling campaign were used. In other cases, we determined them with interpolation from other years or – when data gaps were too frequent for interpolation – values from the closest available year were taken.

4.1.2.3.3 Pairing Consumption and Effluents

As mentioned earlier, due to the seasonality and trends in consumption, WWTP effluent measurements needed to be paired with the corresponding consumption estimate to reduce the uncertainty of k_{esc}.

Therefore, we applied the following algorithm:

1. If quarterly consumption data was available for the compound, estimated consumption for the corresponding year and month of the effluent concentration measurements were used by applying Equation (25);
2. If quarterly consumption data was not available, but annual was, annual consumption from the corresponding year of the effluent concentration measurements was used;
3. If there was no reliable or available consumption data for a compound, escape rates could not be calculated. Emissions were estimated based on F_{pce} from the year closest to that of the SMPC measurement campaign.

4.1.2.4 Sorption

The Rhine model (Honti et al. 2018) has three compound-specific parameters to be calibrated: k_{esc} characterizes emissions, K_{oc} the sorption behaviour, and $k'_{bio,field}$ the rate of biotransformation. Previous runs of this model have shown that there are strong interactions between these parameters. As k'_{bio} is the target parameter to be estimated, it becomes obvious that K_{oc} and k_{esc} are the two crucial parameters that define the degrees of freedom for k'_{bio} and affect its uncertainty. Therefore, it was highly important to improve the estimates of K_{oc} by performing dedicated sorption experiments with selected compounds and relevant sediments as described in Chapter 3, which allowed to improve the sorption prior estimates used for the Rhine model calibration.

4.1.2.5 Setting up the Rhine Model

The applied model was the one in Honti et al. (2018) extended with hydrolysis and direct phototransformation. The model is based on river reaches, where partitioning and transformation in an equilibrium state are described as functions of the physical properties of the reach and the sorption/biotransformation properties of the API. The APIs' behavior in the entire catchment is simulated by connecting multiple stream reaches following the topology of the stream network.

In every single reach, the output flux is calculated by assuming first-order kinetics:

$$F_{out} = F_{in} \exp(-\delta k_w \tau_w) \quad (26)$$

where F_{in} and F_{out} are the total incoming and outflowing fluxes of the parent compound for a single reach (kg d^{-1}), respectively, k_w ist he biotransformation rate constant in the water phase (d^{-1}, to be derived from $k'_{bio,field}$ by multiplication with the OC concentration in the water as per the suspended solids content), τ_w is the mean water residence time in the reach (d), and δ is a dimensionless modification factor that accounts for the sorption, storage and biotransformation activity of the settled sediment estimated again from the local OC content. The modification factor derives from the physical properties of the reach, and the sorption behaviour of the API:

$$\delta = 1 + (S / (SSC\, Z_w))/(Z_a/(K_d\, S) + 1) \quad (27)$$

where K_d is the sediment-water partitioning coefficient, SSC is the suspended sediment concentration (kg m^{-3}), S is the resuspendable sediment stock in the active layer (kg m^{-2}), and Z_a and Z_w are the depths of the active sediment layer and the water column (m), respectively.

Degradation processes other than biotransformation were non-negligible for a few compounds according to literature and other experimental results. We considered hydrolysis and direct phototransformation, both characterized by their respective first-order transformation rate constants. Hydrolysis affected the aqueous fractions both in water and sediment, while direct phototransformation applied to the aqueous fraction of the water column alone.

The total system hydrolysis rate is the following:

$$k_{hydr,ts} = k_{hydr} (f_{aq,w} (1-p_s) + f_{aq,s}\, p_s) \quad (28)$$

where $k_{hydr,ts}$ is the total system hydrolysis rate [d^{-1}], k_{hydr} is the hydrolysis rate of the aqueous fraction [d^{-1}], $f_{aq,w}=1/(1+ K_d\ SSC)$ and $f_{aq,s}=1/(1+S\ K_d/Z_a)$ are the aqueous fractions in water and sediment [-], $p_s=S/(Z/K_d + SSC\ Z + S)$ is the fraction of the compound being in the sediment [-].

The total system direct phototransformatio rate is:

$$k_{photo,ts} = k_{photo}\ f_{aq,w}\ \exp(-k_{ext}\ Z/2) \quad (29)$$

where $k_{photo,ts}$ is the total system hydrolysis rate [d_{-1}], k_{photo} is the surface hydrolysis rate of the aqueous fraction [d^{-1}], $k_{ext}=0.22+0.000011$ SSC is the estimated diffuse light attenuation constant [m^{-1}].

The mean physical properties for each reach were estimated based on drainage area and channel slope (see description in section S4 in the SI of Honti et al. (2018) or in the Annex A.3.1). Mean SSCs were derived from estimated channel geometry, flow velocity, and sediment grain size distribution. In reality, SSC is governed by discharge, season, the state of the upstream catchment, and the stage of flood pulses, which together make it highly dynamic. We had to neglect this variability as we had no information to model dynamic SSC in the entire stream network.

4.1.2.5.1 Calibration Procedure

Running the model is actually a calibration procedure, whereby the model tries to fit its simulated flux to the observations derived from the SMPC campaigns by adjusting the parameters k_{esc}, K_d, and $k'_{bio,field}$. The calibration procedure took place in a Bayesian framework.

The calculated k_{esc} and F_{pce} values presented in Table 26 and Table 27, and K_d (K_{oc}) data shown in Table 18 served as prior information for the inverse modeling of $k'_{bio,field}$ values. The prior distributions of k_{esc} were assumed to be lognormal with means and standard deviations derived from the unified pool of Swiss and German data. F_{pce}s kept their country-specific means and shared the same coefficient of variation. For estimation of the K_{oc} priors, see Chapter 3.2.2. The prior for $k'_{bio,field}$ was a uniform distribution over the technically feasible numerical range (10^{-4} to 10^{4} [L (d·g OC)$^{-1}$]) to warrant mathematical stability and to ease convergence.

The parameter posteriors were sampled by Markov chain Monte Carlo sampling. At least two parallel chains were launched with at least 4000 steps, out of which 3000 served the purpose of burn-in. Convergence was checked by comparing the non burn-in parts of the samples from the parallel chains. In case of convergence problems, additional chains were launched with their length determined on demand.

The model was run separately for the P1 and P3 sampling campaigns of SMPC. The outcome of inverse modeling is two-fold: (i) the fitted flux profile for the Rhine, and (ii) posterior marginal distributions (i.e. the projections of the joint posterior distribution into a single dimension for each parameter, which neglect cross-parameter dependence) for all three calibrated parameters, including $k'_{bio,field}$. From a persistence assessment perspective, the latter, and especially the posterior marginal distribution for k'_{bio} is the most important outcome of inverse modeling, but it needs to be remembered that is conditional on the prior distributions applied during calibration, the model structure and the observed flux data. From the posterior marginal distributions, means and uncertainty intervals can be extracted. The entire posterior can be used to analyze correlations among posterior parameters.

Nevertheless, it has to be noted that calibrated model parameters always carry a bias because parameter values are used by the calibration algorithm to compensate for the structural deficiencies of the model. For the very same reason, calibrated parameters may lose their

attributed meanings (e.g., the physical, chemical, or biological concepts behind them, which we use during model construction and the assignment of priors). Therefore, caution is required when interpreting posterior parameter distributions. For example, if a compound was actually formed out of others in the Rhine itself, this would decrease its $k'_{bio,field}$ or k_{hydr} or k_{photo} (if applicable). As a result, depending on the significance of mechanisms not represented in the model, calibrated parameters can contain biases up to a considerable proportion.

4.1.3 Concepts of Uncertainty used in Model Fitting

We treat uncertainty stemming from both inherent variability and from the lack of knowledge with the mathematical concept of probability as proposed by Reichert et al. (2015), which allows to deal with different sources of uncertainty in a unified framework.

Uncertainty obviously comes from different sources during modelling. First, modelling requires data about the drivers of the system (inputs) and reference observations about the system's behaviour (outputs) for calibration. These data are all potentially laden with truly random measurement errors. Models have uncertainty in their parameters and mathematical structures, namely that the mathematical equations may not properly represent the subject phenomenon and system properties manifested in the unknown model parameters may not be constant over time. These sources normally result in systematic deviations between modelled and observed behaviour due to the internal memory of model systems, which means that an error committed at a specific time influences later behaviour too.

To illustrate the dependency between the different sources of uncertainty, we use the case of "inverse modelling" for an OECD 308 or 309 experiment, i.e., a calculation in which a model is fitted to observations to learn about the model's parameters. This problem is mathematically equivalent to model calibration, yet the primary objective here is not to tune the model to the observed system to make predictions with it later on, but to estimate certain system-specific quantities through the parameters.

Strictly defined, input uncertainty can be neglected at the beginning, as the only inputs to the model are the time coordinates of observation, e.g., when the measurements are made. Outputs are the measurements of the different fractions at the observation times, and of course they contain observation uncertainty. We hypothesize that the model structure to be fitted to the observations is correct, so we reject the presence of structural model bias. Yet, parameters are still uncertain. In this situation, we can establish the following relationships (Reichert 2012):

$$Y_{obs} = Y_{real} + E_{obs} \quad (30)$$

where Y_{obs} is the observed output, Y_{real} is the true output, and E_{obs} is the observation error. As we do not consider a structural bias, we expect the model to simulate the true outputs, so

$$Y_{mod}(p) = Y_{real} \quad (31)$$

where $Y_{mod}(p)$ is the model's output, a function of model parameters p. This means, that

$$Y_{obs} = Y_{mod}(p) + E_{obs} \quad (32)$$

which can be rearranged to

$$E_{obs} = Y_{mod}(p) - Y_{obs} \quad (33)$$

From this it is obvious that observation error (which should be a random variable) becomes a function of model parameters. This is utilised in model fitting so the likelihood of a certain parameter combination, L(p), is calculated from the likelihood of differences between observed and modelled values:

$$L(p) = L(Y_{mod}(p) - Y_{obs}) \quad (34)$$

1. This conceptual framework means that for the calibrated model there are different uncertainty intervals:Parameters have their own uncertainty intervals,
2. which map into an uncertainty bound for the output (“parametric uncertainty”, the uncertainty of Y_{mod}, which is assumed to be equal to Y_{real}),
3. and the total uncertainty of output, including both parametric uncertainty and observation uncertainty (the uncertainty of Y_{obs}).

According to this setup, observed outputs have to lay mostly within the total uncertainty region if a model has been successfully calibrated. For the true outputs, however, it can be expected that they should lie within the narrower range represented by the parametric uncertainty range.

4.1.4 Results

The final list of substances selected to be quantified and modeled in the Rhine catchment contains 36 compounds out of the 48 initial candidates (Table 20). Most of the selected compounds (except: AMI, BEN, MOC, OXC, PHE, PRE, PRO, RAN, SAC) overlap with substance list for the laboratory studies (see Chapter 2.1.1). As before, we will refer to the compounds mostly by their abbreviations.

Table 20: List of substances, including information on selection for Rhine

Number code indicates the reason for rejection (where applicable).

#	Compound	Abbreviation	Type	Selected
1	5-Methyl-Benzotriazol	5MB	corrosion inhibitor	yes
2	Atenolol	ATE	pharmaceutical	yes
3	Acesulfam	ACE	artificial sweetener	yes
4	Aliskiren	ALI	pharmaceutical	yes
5	Amisulpride	AMI	pharmaceutical	yes
6	Atazanavir	ATA	pharmaceutical	yes
7	Benzotriazole	BEN	corrosion inhibitor	yes
8	Bezafibrat	BEZ	pharmaceutical	yes
9	Bicalutamid	BIC	pharmaceutical	yes
10	Carbamazepin	CAR	pharmaceutical	yes
11	Cetirizin	CET	pharmaceutical	no [2,4]
12	Citalopram	CIT	pharmaceutical	yes
13	Clarithromycin	CLA	pharmaceutical	yes
14	Clopidogrel carboxylic acid	CLO	pharmaceutical	yes
15	Cyclamat	CYC	artificial sweetener	yes
16	DEET	DEE	biocide	no[4]
17	Diclofenac	DIC	pharmaceutical	yes
18	Ephedrin	EPH	pharmaceutical	no[1]
19	Fexofenadin	FEX	pharmaceutical	yes
20	Gabapentin	GAB	pharmaceutical	yes

#	Compound	Abbreviation	Type	Selected
21	Hydrochlorothiazide	HYD	pharmaceutical	yes
22	Irbesartan	IRB	pharmaceutical	yes
23	Ketoprofen	KET	pharmaceutical	no[3]
24	Lamotrigin	LAM	pharmaceutical	yes
25	Levetiracetam	LEV	pharmaceutical	yes
26	Lidocaine	LID	pharmaceutical	yes
27	Mefenamic acid	MEF	pharmaceutical	yes
28	Metformin	MET	pharmaceutical	no[4]
29	Metoprolol	MTO	pharmaceutical	yes
30	Moclobemid	MOC	pharmaceutical	yes
31	Olmesartan	OLM	pharmaceutical	no[1]
32	Oxcarbazepin	OXC	pharmaceutical	yes
33	Oxypurinol	OXY	metabolite of a pharmaceutical	no[1]
34	Phenazon	PHE	pharmaceutical	yes
35	Pregabalin	PRE	pharmaceutical	yes
36	Primidon	PRI	pharmaceutical	no[4]
37	Propanolol	PRO	pharmaceutical	yes
38	Ranitidine	RAN	pharmaceutical	yes
39	Saccharin	SAC	artificial sweetener	yes
40	Sitagliptin	SIT	pharmaceutical	yes
41	Sotalol	SOT	pharmaceutical	no[4]
42	Sucralose-FA	SUC	artificial sweetener	no[4]
43	Sulfamethoxazole	SUL	pharmaceutical	yes
44	Tramadol	TRA	pharmaceutical	no[1,4]
45	Trimethoprim	TRI	pharmaceutical	yes
46	Valsartan	VAL	pharmaceutical	yes
47	Venlafaxine	VEN	pharmaceutical	yes
48	Verapamil	VER	pharmaceutical	no[4]

[1] Missing measured concentrations in WWTP effluents.
[2] Analytical problems with effluent measurements at WWTP.
[3] Not detectable in Rhine.
[4] Not included in SMPC measurement campaign.

4.1.4.1 Quantified Concentrations and Fluxes

Fluxes measured at defined places along the Rhine and its tributaries served as basis for calibration of model parameters. Fluxes were calculated separately from SMPC P1 and P3 campaigns by multiplying the corresponding discharge and concentration measurements at a location (Table 22- Table 25). Locations of SMPC measurements are listed in Table 21 and shown in Figure 16.

Table 21: SMPC sampling locations used in modeling

Location	Latitude (N)	Longitude (E)
Reckingen/Rhein	47.57312	8.322821
Brugg	47.51233	8.232322
Weil am Rhein	47.60849	7.586128
Karlsruhe	48.97475	8.24886
Mannheim	49.47729	8.535347
Mean of Worms right and left side	49.67046	8.360756
Kornsand	49.86547	8.353622
Bischofsheim	50.00194	8.363325
Mainz	50.009	8.274739
Koblenz/Rhein	50.33761	7.595596
Koblenz/Mosel	50.3565	7.560412
Bad Honnef	50.64898	7.206415
Düsseldorf-Rechts	51.18426	6.782214
Duisburg-Links	51.43047	6.716646
Dinslaken	51.56219	6.686062
Lobith	51.8489	6.113916

Figure 16: SMPC sampling locations down to the German-Dutch border

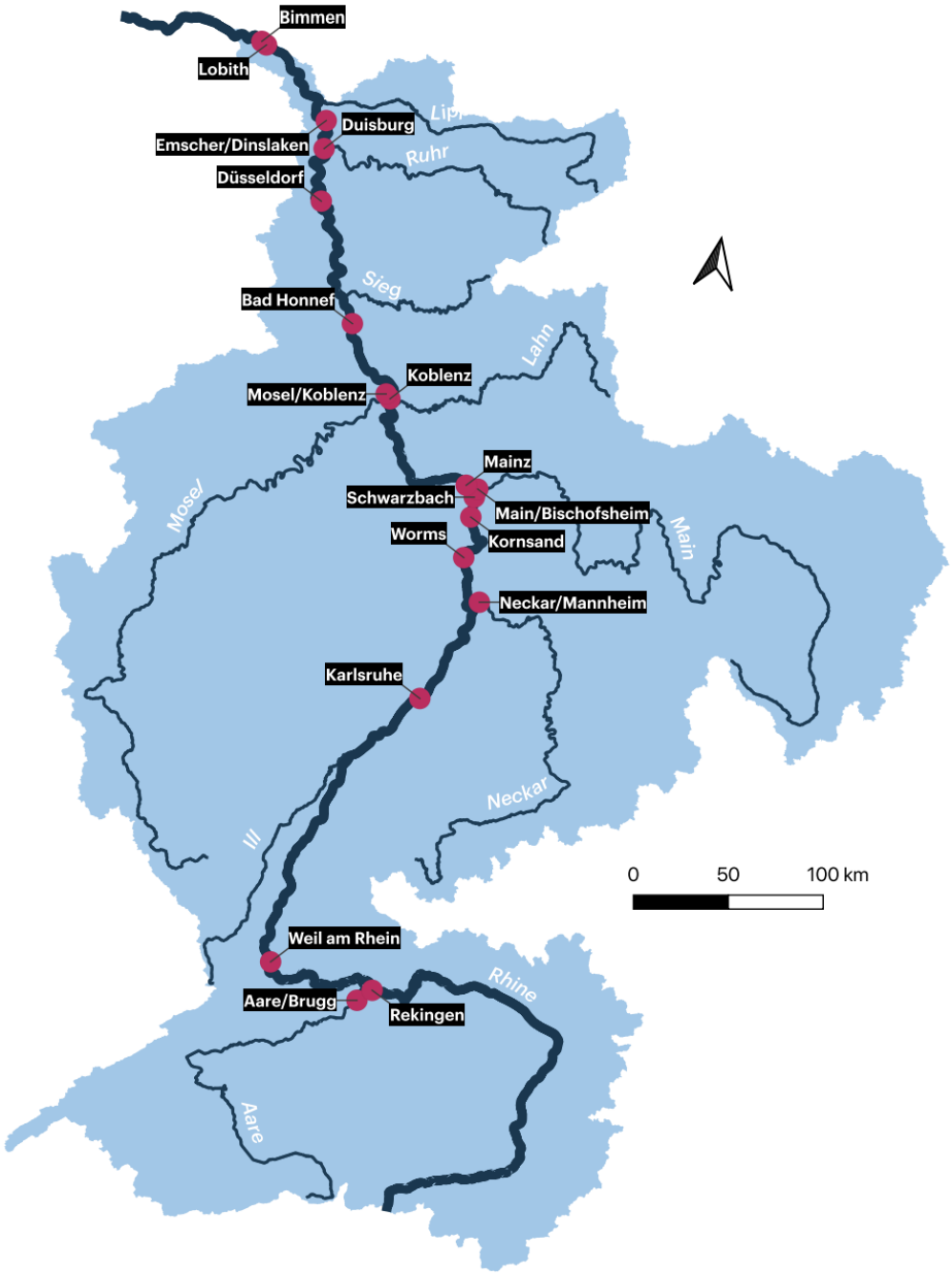

Source: own figure, BME

The measurements at locations (colored with red) where only grab samples were taken or where there was no measured discharge were discarded from flux calculations (see in Annex A.4, Table A3 - Table A6). The measurements from Bimmen were not used for further calculation and calibration because the location is affected by the incomplete mixing of a nearby WWTP effluent plume.

Concentration values in square brackets are above the calibration curve, therefore they are rough concentration estimations only. Nevertheless, these values were considered as precise concentration values during flux calculation. Concentration values in round brackets are between LOD (limit of detection) and LOQ (limit of quantification). These values were also

considered as precise concentration values in flux calculation. Empty cells indicate concentrations at or below LOQ. Empty cells were replaced by half of the LOQ for flux calculations (see in Annex A.4, Table A3 - Table A6).

4.1.4.2 Consumption

Constant, increasing, decreasing and mixed types of consumption trends were all detected (Table 22 and Table 23). Besides temporal changes, cross-country differences in per capita consumptions in Germany and Switzerland were also present. For example the annual consumptions of MET between 2014-2016 were almost four times higher in Germany than in Switzerland (in 2014 the German annual per capita consumption was 1.93 g, while in Switzerland it was 0.57 g). On the contrary, MEF was only consumed in Switzerland. Seasonal multiplicators (see Figure 17 and Table 26) were calculated for all compounds from the quarterly datasets of Germany (2017-2018) (Table 25).

Table 22: Annual per capita consumptions in Germany

Values marked in red values were extrapolated from German consumption data. NA indicates missing information. The column for 2009 shows either the numbers obtained by regression (in red) or an exact value from Singer et al. (2016) (in black). In escape rate calculations, only exact values from 2009 were used. (Source: IQVIA MIDAS Sales Data 2009 – 2018, with permission of IQVIA)

Year	2009	2010	2011	2012	2013	2014	2015	2016	2017	2018
Population	80 519 684	80 435 307	80 424 665	80 477 952	80 565 860	80 646 262	80 688 545	80 682 351	80 636 124	80 560 849
Compound	Annual consumption [g (capita, yr)$^{-1}$]									
5MB	NA	NA	NA	NA	NA	NA	NA	NA	NA	NA
ACE	NA	NA	NA	NA	NA	NA	NA	NA	NA	NA
ALI	0.2478	0.1852	0.2421	0.1655	0.1119	0.0914	0.0765	0.0655	0.0566	0.0493
AMI	0.0713	0.0708	0.0715	0.0709	0.0707	0.0722	0.0723	0.0734	0.0732	0.0725
ATA	0.0072	0.0081	0.0085	0.0088	0.0085	0.0074	0.0062	0.0051	0.0042	0.0033
ATE	0.0929	0.0872	0.0791	0.0714	0.0654	0.0600	0.0548	0.0500	0.0451	0.0407
BEN	NA	NA	NA	NA	NA	NA	NA	NA	NA	NA
BEZ	0.1917	0.1760	0.1650	0.1520	0.1405	0.1315	0.1226	0.1145	0.1060	0.0991
BIC	0.0102	0.0115	0.0122	0.0127	0.0132	0.0135	0.0132	0.0129	0.0128	0.0128
CAR	0.7982	0.7476	0.6980	0.6491	0.6075	0.5738	0.5462	0.5137	0.4872	0.4595
CIT	0.0911	0.0993	0.1194	0.1206	0.1160	0.1130	0.1060	0.1001	0.0948	0.0901
CLA	0.1853	0.1752	0.1719	0.1650	0.1698	0.1474	0.1488	0.1367	0.1280	0.1187
CLO	0.2459	0.2532	0.2470	0.2525	0.2662	0.2753	0.2695	0.2705	0.2745	0.2726
CYC	NA	NA	NA	NA	NA	NA	NA	NA	0.0000	0.0000
DIC	1.1374	1.1302	1.0918	1.0360	1.0300	1.0323	1.0482	1.0498	0.9775	0.9379
FEX	0.0343	0.0334	0.0362	0.0343	0.0374	0.0396	0.0401	0.0415	0.0403	0.0443
GAB	0.8701	0.9255	0.9823	1.0381	1.0844	1.1364	1.1436	1.1471	1.1496	1.1645
HYD	0.6323	0.6435	0.6446	0.6408	0.6328	0.6194	0.6028	0.5843	0.5609	0.5338
IRB	0.5574	0.5237	0.4947	0.4572	0.4395	0.4369	0.4297	0.4097	0.3877	0.3709
LAM	0.1145	0.1234	0.1326	0.1409	0.1511	0.1613	0.1719	0.1818	0.1911	0.2004
LEV	0.6626	0.8203	0.9755	1.1641	1.3574	1.5445	1.7037	1.8371	1.9369	2.0246
LID	0.1103	0.1171	0.1239	0.1238	0.1258	0.1289	0.1321	0.1229	0.0932	0.0936
MEF	0.0000	0.0000	0.0000	0.0000	0.0000	0.0000	0.0000	0.0000	0.0000	0.0000
MOC	0.0221	0.0212	0.0207	0.0197	0.0189	0.0185	0.0179	0.0173	0.0168	0.0164
MTO	1.9017	1.9333	1.9441	1.9510	1.9459	1.9290	1.8978	1.8577	1.7935	1.7459

Year	2009	2010	2011	2012	2013	2014	2015	2016	2017	2018
Population	80 519 684	80 435 307	80 424 665	80 477 952	80 565 860	80 646 262	80 688 545	80 682 351	80 636 124	80 560 849
Compound	Annual consumption [g (capita, yr)$^{-1}$]									
OXC	0.1982	0.1984	0.1967	0.1932	0.1921	0.1952	0.1954	0.1944	0.1924	0.1894
PHE	0.0343	0.0300	0.0265	0.0232	0.0207	0.0190	0.0183	0.0171	0.0162	0.0156
PRE	0.2043	0.2420	0.2663	0.2904	0.3109	0.3410	0.3786	0.4173	0.4389	0.4659
PRO	0.0496	0.0486	0.0477	0.0465	0.0458	0.0454	0.0447	0.0442	0.0434	0.0428
RAN	0.4730	0.4168	0.3695	0.3243	0.2898	0.2634	0.2424	0.2280	0.2201	0.2098
SAC	NA	NA	NA	NA	NA	NA	NA	NA	NA	NA
SIT	0.1169	0.1545	0.2291	0.2821	0.3165	0.4014	0.5298	0.5694	0.5965	0.6273
SUL	0.4340	0.4065	0.3608	0.3240	0.3125	0.2948	0.2765	0.2733	0.2737	0.2700
TRI	0.0928	0.0877	0.0786	0.0712	0.0688	0.0653	0.0616	0.0611	0.0615	0.0609
VAL	0.6944	0.7943	0.8583	1.0852	1.2841	1.4915	1.6861	1.8160	1.9202	1.8219
VEN	0.1481	0.1849	0.2173	0.2488	0.2708	0.2887	0.3029	0.3140	0.3220	0.3314

Table 23: Annual per capita consumptions in Switzerland

Values in red are extrapolated/interpolated from Swiss consumption. NA indicates missing information. The column for 2009 shows the lower range limit from Singer et al. (2016) (Source: IQVIA MIDAS Sales Data 2009 – 2018, with permission of IQVIA).

Year	2009	2010	2011	2012	2013	2014	2015	2016	2017	2018
Population	7 742 000	7 858 000	7 952 000	8 003 000	8 021 000	8 220 000	8 325 000	8 417 000	8 482 152	8 571 298
Compound	Annual consumption [g (capita, yr)$^{-1}$]									
5MB	NA	NA	NA	NA	NA	NA	NA	NA	NA	NA
ACE	NA	NA	NA	NA	NA	NA	NA	NA	NA	NA
ALI	NA	0.1912	0.1751	0.1603	0.1463	0.1308	0.1132	0.1018	0.0868	0.0731
AMI	NA	0.0529	0.0524	0.0521	0.0521	0.0509	0.0505	0.0499	0.0497	0.0492
ATA	NA	0.0407	0.0353	0.0302	0.0253	0.0201	0.0143	0.0104	0.0055	0.0009
ATE	NA	0.2409	0.2239	0.2083	0.1938	0.1742	0.1586	0.1434	0.1301	0.1156
BEN	NA	NA	NA	NA	NA	NA	NA	NA	NA	NA
BEZ	> 0.0646	0.0653	0.0616	0.0584	0.0554	0.0513	0.0478	0.0447	0.0416	0.0385
BIC	NA	0.0066	0.0063	0.0061	0.0058	0.0054	0.0054	0.0048	0.0047	0.0045
CAR	> 0.3229	0.4677	0.4435	0.4221	0.4027	0.3785	0.3481	0.3344	0.3109	0.2904

Year	2009	2010	2011	2012	2013	2014	2015	2016	2017	2018
Population	7 742 000	7 858 000	7 952 000	8 003 000	8 021 000	8 220 000	8 325 000	8 417 000	8 482 152	8 571 298
Compound	Annual consumption [g (capita, yr)$^{-1}$]									
CIT	> 0.0969	0.0925	0.0860	0.0801	0.0746	0.0676	0.0611	0.0558	0.0503	0.0448
CLA	> 0.1292	0.1991	0.1914	0.1849	0.1792	0.1675	0.1670	0.1535	0.1495	0.1430
CLO	> 0.1292	0.2039	0.1986	0.1945	0.1912	0.1860	0.1810	0.1762	0.1701	0.1657
CYC	NA	NA	NA	NA	NA	NA	NA	NA	NA	NA
DIC	> 0.6458	0.6026	0.5623	0.5256	0.4915	0.4474	0.4247	0.4123	0.3965	0.3803
FEX	NA	0.0549	0.0629	0.0711	0.0795	0.0851	0.0946	0.0995	0.1076	0.1145
GAB	> 0.3229	0.3481	0.3445	0.3428	0.3426	0.3345	0.3317	0.3276	0.3259	0.3230
HYD	> 0.1292	0.4524	0.4465	0.4431	0.4415	0.4307	0.4237	0.4195	0.4155	0.4106
IRB	> 0.9687	1.0527	1.0023	0.9581	0.9183	0.8682	0.7922	0.7761	0.7259	0.6831
LAM	> 0.1292	0.1617	0.1705	0.1800	0.1903	0.1969	0.2022	0.2126	0.2201	0.2278
LEV	> 0.3229	0.7858	0.8301	0.8780	0.9292	0.9629	0.9916	1.0416	1.0796	1.1181
LID	> 0.1292	0.1045	0.0808	0.0579	0.0355	0.0129	0.0132	0.0139	0.0144	0.0150
MEF	> 1.2916	2.6730	2.5280	2.3993	2.2816	2.1103	1.9944	1.8467	1.7325	1.6094
MOC	> 0.0129	0.0212	0.0203	0.0196	0.0189	0.0177	0.0172	0.0161	0.0154	0.0147
MTO	> 0.3229	0.6059	0.5957	0.5889	0.5846	0.5675	0.5575	0.5485	0.5416	0.5332
OXC	NA	0.1069	0.1085	0.1106	0.1132	0.1137	0.1137	0.1164	0.1177	0.1191
PHE	NA	NA	NA	NA	NA	NA	NA	NA	NA	NA
PRE	> 0.1292	0.1944	0.2268	0.2599	0.2937	0.3193	0.3512	0.3774	0.4080	0.4360
PRO	> 0.0969	0.0914	0.0862	0.0817	0.0775	0.0717	0.0731	0.0703	0.0644	0.0610
RAN	> 0.1292	0.1200	0.1114	0.1036	0.0962	0.0869	0.0808	0.0807	0.0771	0.0742
SAC	NA	NA	NA	NA	NA	NA	NA	NA	NA	NA
SIT	> 0.6452	0.5537	0.4661	0.3825	0.3013	0.2156	0.2358	0.2562	0.3613	0.5380
SUL	> 0.1292	0.4043	0.3962	0.3903	0.3862	0.3751	0.3627	0.3600	0.3527	0.3459
TRI	> 0.0323	0.0673	0.0660	0.0651	0.0645	0.0628	0.0607	0.0604	0.0592	0.0582
VAL	> 0.3229	0.7259	0.7504	0.7785	0.8096	0.8253	0.8367	0.8686	0.8897	0.9111
VEN	> 0.1292	0.2688	0.2694	0.2714	0.2746	0.2711	0.2728	0.2719	0.2738	0.2745

*No reliable consumption data.

**No consumption in Germany from 2005

Table 24: Quartely consumptions in Germany for 2017 and 2018

NA indicates missing information (Source: IQVIA MIDAS Sales Data 2009 – 2018, with permission of IQVIA).

	Quarterly consumption [kg]							
Compound	**QTR/3/17**	**QTR/6/17**	**QTR/9/17**	**QTR/12/17**	**QTR/3/18**	**QTR/6/18**	**QTR/9/18**	**QTR/12/18**
5MB	NA	NA	NA	NA	NA	NA	NA	NA
ACE	NA	NA	NA	NA	NA	NA	NA	NA
ALI	1173.6	1171.9	1101.0	1114.4	1015.4	1011.3	959.7	984.5
AMI	1445.1	1476.6	1470.6	1511.9	1429.2	1455.2	1450.2	1503.0
ATA	88.5	88.2	84.5	80.6	71.5	68.5	62.8	59.9
ATE	920.7	924.5	890.4	897.4	831.2	836.2	797.5	816.9
BEN	NA	NA	NA	NA	NA	NA	NA	NA
BEZ	2133.8	2158.8	2115.8	2140.1	2000.4	2023.0	1947.7	2012.9
BIC	255.9	255.0	259.9	264.3	257.2	257.6	256.4	259.9
CAR	9645.2	9881.8	9787.8	9973.9	9162.1	9317.3	9074.8	9467.0
CIT	1927.3	1908.1	1886.5	1920.4	1812.1	1819.8	1773.1	1855.6
CLA	3694.4	2090.5	1914.9	2621.9	3746.1	1863.6	1655.0	2299.7
CLO	5428.9	5545.8	5503.8	5659.4	5436.4	5580.9	5444.9	5500.6
CYC	NA	NA	NA	NA	NA	NA	NA	NA
DIC	19107.1	19922.6	19991.3	19797.9	18489.3	19469.0	18575.8	19025.1

Compound	Quarterly consumption [kg]							
	QTR/3/17	QTR/6/17	QTR/9/17	QTR/12/17	QTR/3/18	QTR/6/18	QTR/9/18	QTR/12/18
FEX	771.4	1091.5	765.9	618.8	764.9	1348.5	791.5	660.2
GAB	22536.3	23189.1	23102.7	23875.1	22852.0	23604.3	23187.0	24167.4
HYD	11223.1	11471.2	11114.5	11423.3	10809.4	11092.0	10711.3	10386.8
IRB	7797.9	7928.9	7673.0	7861.8	7347.7	7465.8	7388.7	7677.2
LAM	3665.8	3811.3	3865.8	4070.2	3848.7	4025.2	4028.0	4242.4
LEV	37423.2	38737.5	39033.8	40993.6	39196.3	40744.1	40607.9	42554.1
LID	1904.3	1847.0	1868.3	1897.6	1895.0	1865.4	1858.0	1918.1
MEF	0	0	0	0	0	0	0	0
MOC	335.4	340.4	336.5	343.3	328.9	333.9	321.7	340.3
MTO	35703.1	36578.4	35681.3	36654.7	34838.5	35623.7	34445.8	35743.4
OXC	3767.5	3876.3	3862.5	4008.7	3735.5	3840.3	3755.4	3928.5
PHE	345.9	318.9	327.4	316.7	340.6	286.5	306.8	319.4
PRE	8460.7	8758.1	8914.2	9254.5	9071.0	9331.6	9315.0	9817.0
PRO	865.9	879.5	868.8	886.5	852.2	872.4	841.4	880.3
RAN	4410.6	4405.4	4369.3	4562.8	4285.8	4238.7	4075.9	4301.5
SAC	NA	NA	NA	NA	NA	NA	NA	NA

	Quarterly consumption [kg]							
Compound	**QTR/3/17**	**QTR/6/17**	**QTR/9/17**	**QTR/12/17**	**QTR/3/18**	**QTR/6/18**	**QTR/9/18**	**QTR/12/18**
SIT	11546.4	12029.2	11955.3	12569.1	12112.8	12695.1	12488.7	13238.1
SUL	5657.1	5187.1	5528.5	5700.4	5647.7	5078.8	5263.4	5762.1
TRI	1262.0	1162.8	1244.3	1286.1	1268.2	1144.9	1192.0	1301.2
VAL	37256.2	38816.7	38392.9	40375.0	39153.7	40801.9	34563.6	32257.4
VEN	6328.9	6421.5	6483.7	6731.1	6457.2	6648.2	6616.6	6975.3

Figure 17: Decomposition of quarterly consumption time series into trend and seasonality components

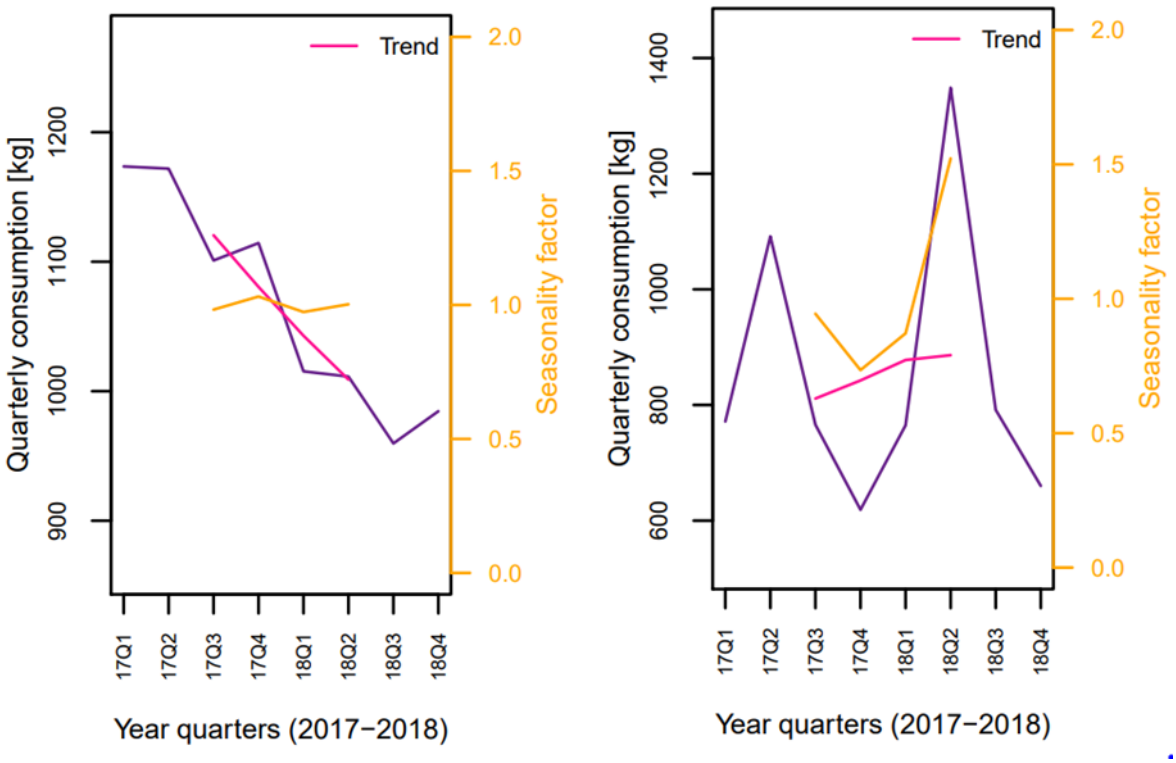

Quaterly consuption time series= dark purple line, trend= light purple line, and seasonality components= orange bar charts. Left figure: decomposition for a compound with low seasonality but strong annual trend (ALI). Right figure: decomposition for a compound with strong seasonality but weak subannual trend (FEX).

Source: own figure, BME

Table 25: Quarterly seasonal multiplicators

Q1: January-March, Q4: October-December

Compound	f(Q1)	f(Q2)	f(Q3)	f(Q4)
5MB*	NA	NA	NA	NA
ACE*	NA	NA	NA	NA
ALI	0.97	1.00	0.98	1.03
AMI	0.98	1.00	1.00	1.03
ATA	0.97	1.00	1.01	1.02
ATE	0.98	1.01	0.99	1.03
BEN*	NA	NA	NA	NA
BEZ	0.98	1.01	1.00	1.03
BIC	0.99	1.00	1.00	1.02

Compound	f(Q1)	f(Q2)	f(Q3)	f(Q4)
CAR	0.97	1.00	1.00	1.04
CIT	0.98	1.00	0.99	1.03
CLA	1.50	0.77	0.74	1.02
CLO	0.98	1.01	0.99	1.02
CYC*	NA	NA	NA	NA
DIC	0.96	1.03	1.02	1.02
FEX	0.87	1.52	0.94	0.73
GAB	0.98	1.01	1.00	1.02
HYD	0.98	1.02	0.99	1.02
IRB	0.97	1.00	0.99	1.03
LAM	0.97	1.00	1.00	1.04
LEV	0.98	1.00	0.99	1.03
LID	1.01	0.99	0.99	1.01
MEF**	NA	NA	NA	NA
MTO	0.98	1.01	0.99	1.02
MOC	0.99	1.01	1.00	1.02
OXC	0.97	1.00	1.00	1.04
PHE	1.08	0.92	1.00	0.98
PRE	0.99	1.00	1.00	1.02
PRO	0.98	1.01	0.99	1.02
RAN	0.99	1.00	0.99	1.04
SAC*	NA	NA	NA	NA
SIT	0.98	1.01	0.99	1.03
SUL	1.04	0.94	1.00	1.04
TRI	1.03	0.93	1.00	1.04
VAL***	0.98	1.01	0.99	1.02
VEN	0.98	1.00	1.00	1.03

*No reliable consumption data.

**No consumption in Germany from 2005.

***For VAL, trend fitting had to be manually corrected because of a sudden drop in consumption in the second half of 2018 in Germany.

Clarithromycin (CLA), Fexofenadine (FEX) and Phenazone (PHE) showed significant seasonal variability, for others seasonal changes were negligible. CLA is an antibiotic to cure bacterial infections related mainly to the respirotary system with highly increasing consumption in the first quarter of the year (+50%), and lower consumption in warmer months. FEX is mostly used to treat allergy symptoms. Accordingly, it has a peak (+52%) in consumption in the second quarter of the year. PHE is a pain reliever and fever reducing drug. It shows a moderate 10% increase in consumption in the first quarter of the year, which can be explained by its use because related illnesses are typical in colder seasons.

4.1.4.3 Emission Priors

Escape factors were calculated separately from the German and the Swiss datasets, depending on data availability. For all of the compounds with relevant consumption data, mean k_{esc} ($E[k_{esc}]$) values and standard deviations ($SD[k_{esc}]$) were estimated (Table 26). For Switzerland one mean escape rate with one standard deviation was calculated based on the 3 relevant studies (CH1, CH2, CH3) from individually calculated values. For Germany we calculated escape rates for the BW and NRW campaigns separately, and created the single countrywide value from their average. If escape rates could be determined for just one of the countries, the other country's value was used everywhere.

When it was possible to calculate escape rates for both countries for the same compound, the results could be compared. As it can be expected from its consumption-independent definition, escape rates of a given substance should be very similar in Switzerland and Germany given that wastewater treatment technologies are similar too. In most of the cases, they were indeed similar (for example, see CAR, HYD, VEN, SUL). Still, in a few cases, major differences were detected in escape rates between the two countries (e.g., ATE and GAB).

Moreover, for certain compounds (it was typical at: ALI, AMI, ATE, CIT, FEX, GAB, LID, PHE, SAC), some of the individual calculated escapes rate values are higher than 1, which would mean negative removal rates or excretion > 100%. This can be due to two reasons: (i) non-representative consumption data, including direct losses from production and formulation facilities or (ii) formation from other compounds, including metabolites.

Several sources of uncertainty were identified for k_{esc}. Lack of quarterly consumption data may increase uncertainty in escape rate calculations when the compound is subject to periodic fluctuations in consumption or strong uneven trends. Errors are also introduced with the interpolations or extrapolations for years lacking consumption data. Usage outside the human pharmaceutical domain (e.g. veterinary medicine) and production losses could not be included, causing a potential underestimation of consumption. This might be the case for e.g. PHE, for which veterinary use is known.

F_{pce}s are actually also used during the calculation of k_{esc} and are prone to numerous further sources of uncertainty. The proper quantification of effluent fluxes depends on representative effluent discharges, representative concentrations and reliable figures of the served population. These all may be compromised to some degree, particularly in those cases where grab sampling of effluents was used.

The uncertainty of k_{esc} and F_{pce}s could only be estimated by comparing estimates for the different campaigns. Individual values of $k_{esc} > 3$ were labelled as extreme outliers and discarded from the pool of estimates, as k_{esc} should be between 0 and 1 by definition. The range between 1 and 3 was allowed to accommodate for uncertainty stemming from seasonally or regionally variable consumption and errors in market data, WWTP effluents, etc. Less than 5% of k_{esc} estimates were discarded for any compound. The remaining estimates represented the uncertainty of k_{esc}.

Table 26: Consumption and escape rates

E: arithmetic means, SD: standard deviations, a: only annual consumption data.

Comp	Quarter of SMPC P1		Quarter of SMPC P3		Priors for Germany (GER)		Priors for Switzerland (CH)	
	Consumption GER [g (capita, yr)$^{-1}$]	Consumption CH [g (capita, yr)$^{-1}$]	Consumption GER [g (capita, yr)$^{-1}$]	Consumption CH [g (capita, yr)$^{-1}$]	E[k_{esc}]	SD[k_{esc}]	E[k_{esc}]	SD[k_{esc}]
ALI	0.058	0.084	0.055	0.079	NA	NA	0.638	0.522
AMI	0.072	0.048	0.073	0.050	0.669	0.624	0.584	0.418
ATA	0.004	0.005	0.004	0.003	NA	NA	0.597	0.216
ATE	0.046	0.127	0.044	0.123	0.305	0.444	0.501	0.355
BEZ	0.106	0.041	0.105	0.040	0.216	0.254	0.437	0.559
BIC	0.013	0.005	0.013	0.005	NA	NA	0.299	0.243
CAR	0.479	0.301	0.486	0.303	0.117	0.086	0.177	0.071
CIT	0.096	0.049	0.094	0.048	NA	NA	0.517	0.503
CLA	0.183	0.224	0.095	0.109	0.121	0.14	0.215	0.154
CLO	0.270	0.167	0.273	0.168	NA	NA	0.105	0.064
DIC	0.949	0.381	0.993	0.398	0.176	0.114	0.321	0.119
FEX	0.038	0.094	0.038	0.105	NA	NA	0.711	0.423
GAB	1.119	0.319	1.147	0.325	0.472	0.343	0.765	0.548
HYD	0.557	0.406	0.552	0.410	0.566	0.333	0.501	0.168
IRB	0.387	0.706	0.381	0.700	NA	NA	0.204	0.141
LAM	0.182	0.213	0.192	0.225	0.445	0.322	0.499	0.358
LEV	1.858	1.053	1.938	1.098	NA	NA	0.158	0.207
LID	0.095	0.015	0.093	0.015	NA	NA	0.722	0.546
MEF[a]	0.000	1.733	0.000	1.733	NA	NA	0.030	0.030
MTO	1.773	0.531	1.772	0.535	0.098	0.063	0.105	0.063
MOC	0.017	0.015	0.017	0.015	NA	NA	0.148	0.070
OXC	0.187	0.114	0.192	0.119	NA	NA	0.161	0.106
PHE	0.017	NA	0.016	NA	0.439	0.697	NA	NA

Comp	Quarter of SMPC P1		Quarter of SMPC P3		Priors for Germany (GER)		Priors for Switzerland (CH)	
	Consumption GER [g (capita, yr)$^{-1}$]	Consumption CH [g (capita, yr)$^{-1}$]	Consumption GER [g (capita, yr)$^{-1}$]	Consumption CH [g (capita, yr)$^{-1}$]	E[k_{esc}]	SD[k_{esc}]	E[k_{esc}]	SD[k_{esc}]
PRE	0.420	0.403	0.443	0.424	0.147	0.178	NA	NA
PRO	0.043	0.063	0.043	0.063	0.17*	0.09*	0.167	0.086
RAN	0.219	0.076	0.043	0.063	NA	NA	0.151	0.112
SIT	0.573	0.353	0.594	0.447	NA	NA	0.248	0.257
SUL	0.281	0.365	0.275	0.352	0.129	0.150	0.108	0.065
TRI	0.063	0.061	0.062	0.059	0.148	0.227	0.328	0.246
VAL	1.850	0.875	1.906	0.895	0.175	0.256	0.362	0.330
VEN	0.314	0.268	0.322	0.275	0.141	0.085	0.175	0.072

Table 27: Compounds without relevant consumption data

F_{pce}s and estimated escape rates, E: arithmetic mean, SD: standard deviation

Compound	Switzerland (2017) [g (capita, yr)$^{-1}$]		Germany (2017) [g (capita, yr)$^{-1}$]	
	E[F_{pce}]	SD[F_{pce}]	E[F_{pce}]	SD[F_{pce}]
5MB	0.823	0.165	0.12	0.087
ACE	2.606	1.873	1.037	0.4
BEN	0.503	0.292	1.219	0.846
CYC	0.124	0.282	0.098	0.328
SAC	0.171	0.183	0.177	0.223

4.1.4.3.1 Hydrolysis, Sorption and Phototransformation Priors used for the Rhine Model

Prior distributions describing the compounds sorption (K_{oc}), abiotic hydrolysis (k_{hydr}) and phototransformation (k_{photo}) behavior were taken from the experimental part of the project, i.e., Chapter 2 and Chapter 3 (Table 5, Table 18, and Table 19).

4.1.4.4 MCMC Outcomes, Convergence, Problematic Compounds

The model generally achieved good fits to the fluxes derived from the SMPC samples (see examples in Figure 18).

Figure 18: Modelled and measured fluxes for GAB and VAL in the P1 and P3 campaigns along the Rhine

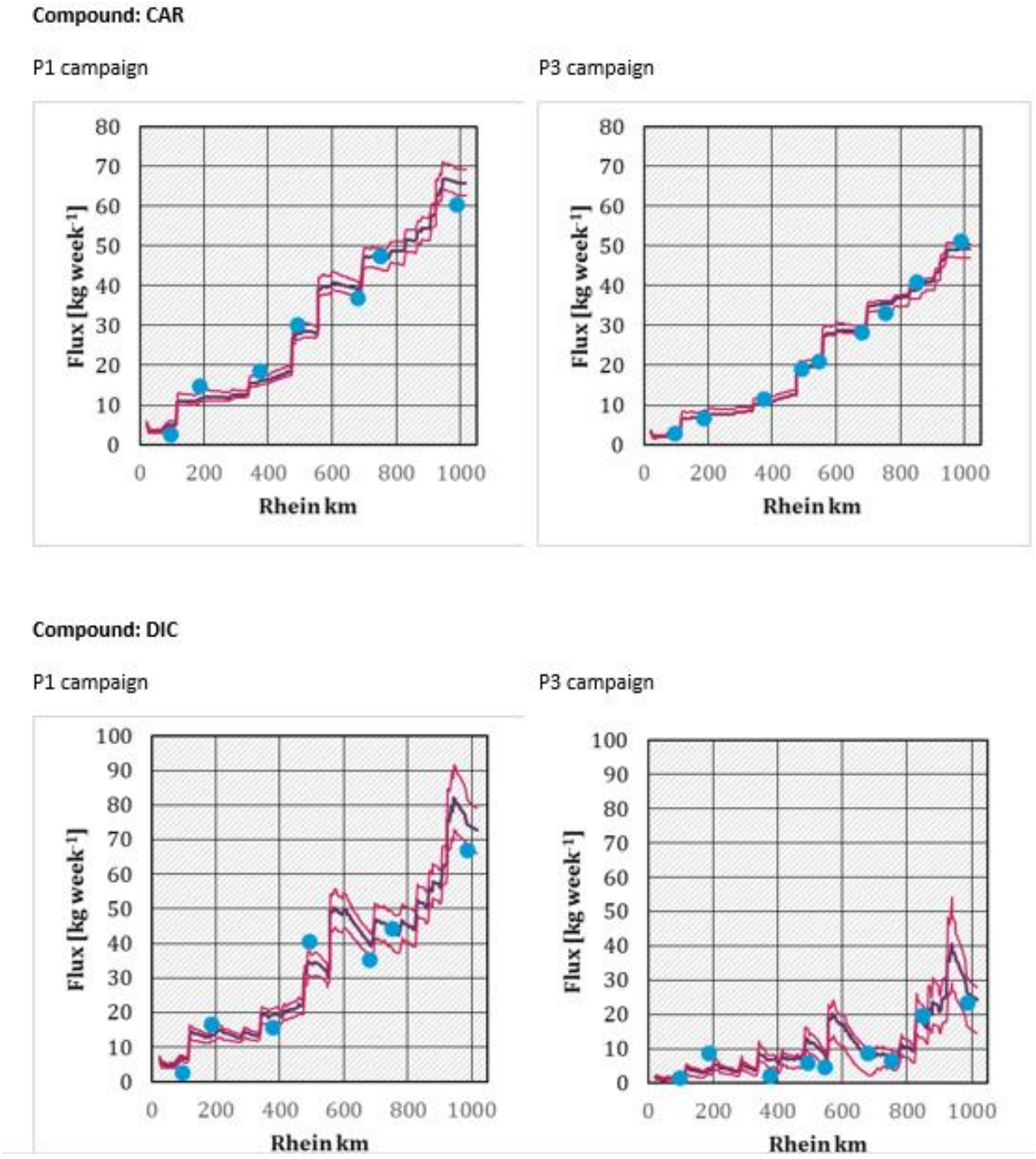

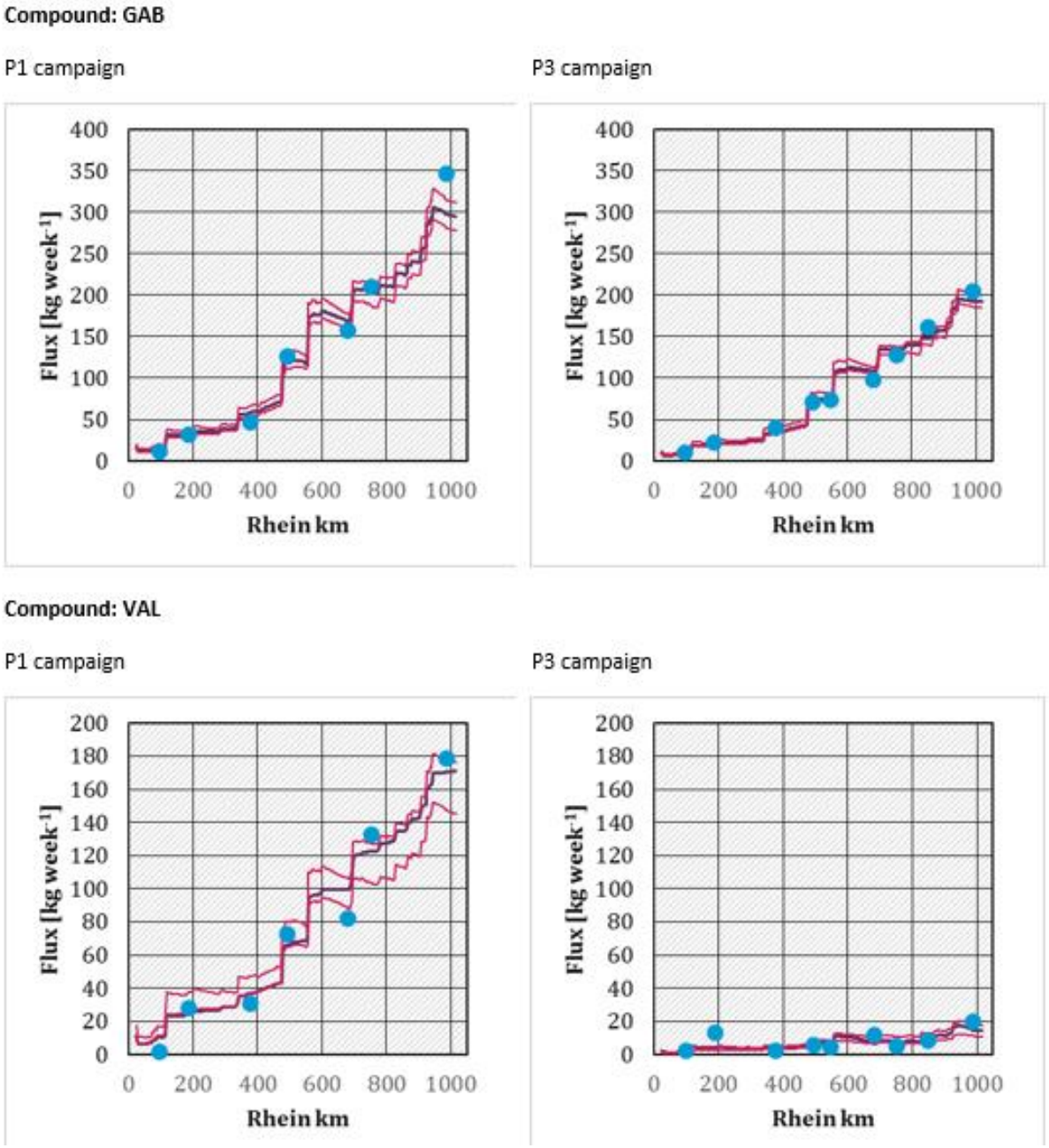

Thick dark purple line indicates the mean of the modelled flux. Light pink lines shows parametric uncertainty. Measured fluxes are indicated by blue dots.

Source: own figure, BME

4.1.5 Posterior Distributions of Rate Constants and Half-Lives in the Rhine

The posterior marginal distributions of $k'_{bio,field}$ showed that this second-order degradation parameter can be estimated from field data (see Figure 18, and Table 28 and Table 29 for mean values and distributions). The interquartile range (between 25-75% percentiles) usually covered an interval of less than one order of magnitude. However, the extreme quantiles (outside the interquartile range) often spanned over 3-4 orders of magnitude. This suggests that the posterior distributions were mostly very heavy tailed and that while estimating a minimally confident range (e.g. an 50% confidence interval) for $k'_{bio,field}$ is feasible and such a range can be relatively narrow, extreme values are disproportionally uncertain.

For many compounds, $k'_{bio,field}$ in P3 was higher than in P1 (Figure 19). We assume that this is due to the higher temperatures in summer compared to spring, which likely also leads to higher metabolic activities of the river microbial communities, yet lack additional information on the latter to test this assumption. For ACE, BEZ, CLA, DIC, HYD, IRB, MEF, PRO, SIT, TRI, and VAL, there was no overlap in the interquartile range, suggesting that degradation in P3 was significantly higher than degradation in P1 for these compounds. Another group, i.e., AMI, ATE, BIC, CYC, LID, MET, MOC, PRE, and SUL, showed a possible but not significant difference of the same kind. There were two counter-examples too: CAR and FEX showed significantly slower degradation in P3 than in P1. In both cases, it may be the consequence of mentioned uncertainty sources of the emission calculations (see Section 4.1.4.3) or/and the modelling. For example, CAR and FEX are both used in veterinary medicine which is an amount not included in the consumption estimates, because only human sales data are available, and the emissions from industrial point sources are also not represented in the datasets. FEX has also strong seasonal variability in consumption that leads to more uncertainty.

It has to be noted that $k'_{bio,field}$ values below 30 L (g OC d)$^{-1}$ practically mean that no degradation is observable along the Rhine due to the limited flow time, and, conversely, that the model is not able to differentiate k'_{bio} values above 1000 L (g OC d)$^{-1}$ as these all result in a complete removal between the monitoring locations of SMPC.

For the eight compounds with defined k_{hydr} and k_{photo} values (sections 3.2.2 and 3.2.4), the calibrated posteriors for these parameters were in close agreement with the priors (Table 30 and Table 31).

Figure 19: Degradation in SMPC P1 vs. P3: Modelled k'_{bio} values.

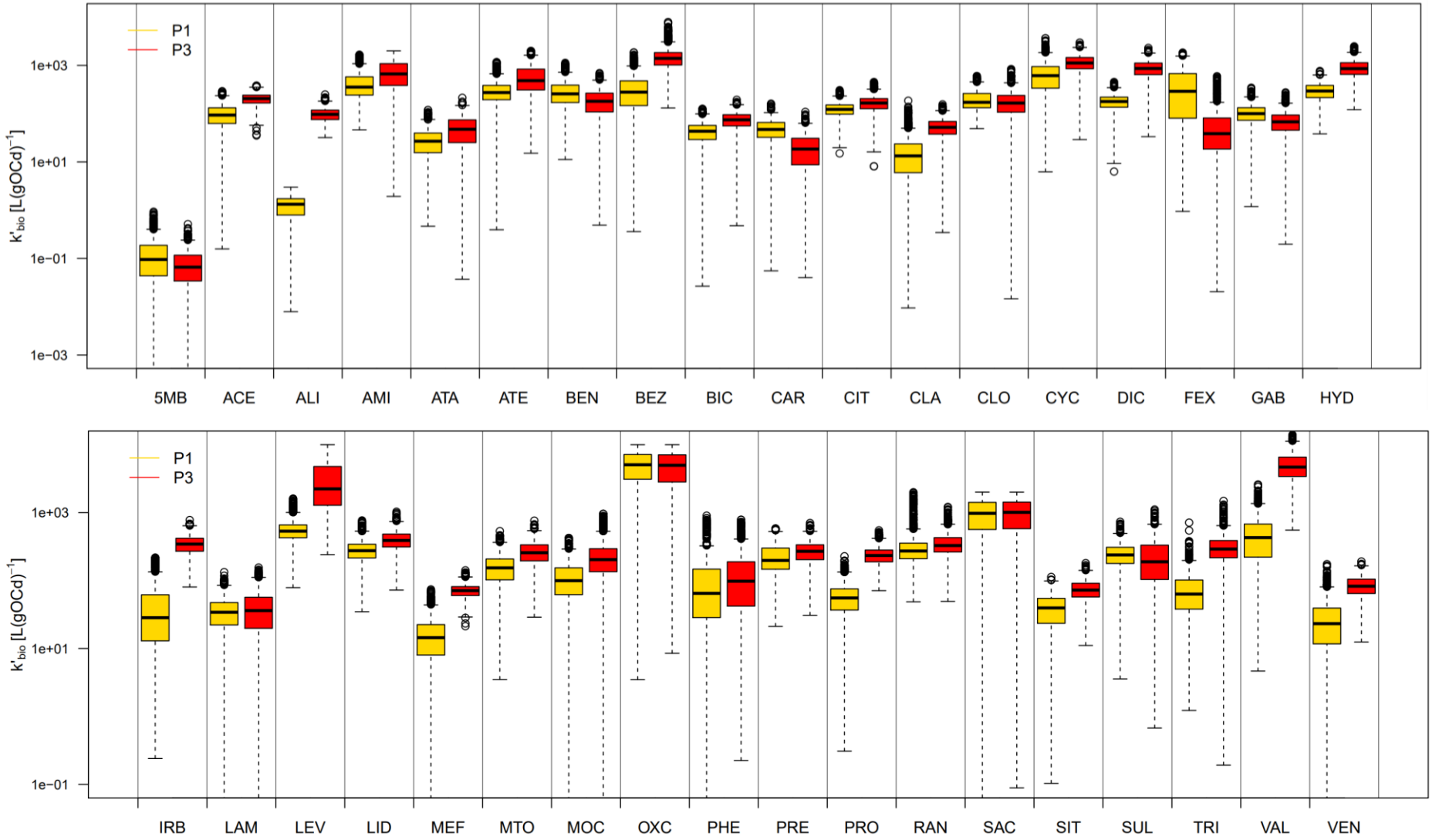

Source: own figure, Eawag

Table 28: k'_{bio} [L/(g OC, d)$^{-1}$] posteriors statistics from the P1 campaign

Minimum, maximum, arithmetic mean, standard deviation (SD) and 5th, 25th ,50th, 75th , 95th percentiles

Comp.	Min	Max	Mean	SD	5th perc.	25th perc.	50th perc.	75th perc.	95th perc.
5MB	0.00	0.9	0.14	0.13	0.01	0.04	0.10	0.19	0.37
ACE	0.16	292	99.5	51.5	22.7	62.6	93.4	132	188
ALI	0.01	3	1.3	0.6	0.20	0.8	1.3	1.7	2.4
AMI	46.2	1670	457	292	181	243	355	579	1048
ATA	0.46	119	30.1	19.54	4.93	15.6	26.9	39.7	67.7
ATE	0.39	1168	310	172	95.3	194	274	385	634
BEN	11	1130	312	214	78	170	257	390	823
BEZ	0.36	1862	344	272	39	147	279	478	885
BIC	0.03	126	44.6	22.1	11.2	29.1	43.3	57.1	84.9
CAR	0.06	161	49.0	24.0	12.2	32.3	47.1	65.7	85.0
CIT	15.0	307	127	43.1	63.4	97.7	123	152	205
CLA	0.01	186	18.4	18.7	1.06	6.00	13.3	23.6	54.3
CLO	49.0	603	210	113.8	91.7	132.6	172	262	459
CYC	6.24	3656	724	542	95.7	338	613	944	1872
DIC	6.32	454	181	68.9	68	136	179	220	294
FEX	0.94	1845	424	409	13.2	80.8	290	676	1243
GAB	1.19	345	107	49.6	37.4	72.8	100	133	204
HYD	38.1	766	304	123	129	215	294	385	522
IRB	0.24	217	49.1	53.9	2.67	13.0	28.4	61.7	186
LAM	0.06	133	35.9	19.2	7.71	22.3	34.2	47.4	70.2
LEV	78.6	1612	560	201	295	427	533	659	939
LID	34.77	768	286	102	143	215	275	342	471
MEF	0.04	74.1	16.5	11.5	1.97	8.02	14.4	22.5	39.2
MOC	0.01	423	115	71.9	24.5	62.0	99.6	154	251
MTO	3.50	534	161	77	53.9	103	154	208	301

Comp.	Min	Max	Mean	SD	5th perc.	25th perc.	50th perc.	75th perc.	95th perc.
OXC	3.49	9987	5081	2600	727	3106	5065	7167	9314
PHE	0.00	902	130	170	5.21	28.6	64.9	147	598
PRE	21.15	582	235	123.4	81.9	147	198	300	501
PRO	0.31	228	59.3	31.9	16.3	36.8	55.4	75.4	123
RAN	48.7	1994	325	231	140	210	272	355	650
SAC	0.01	1999	980	527	143	565	976	1415	1837
SIT	0.10	113	40.7	22.0	7.7	23.5	39.5	54.6	80.3
SUL	3.57	734	249	111	76.7	179	238	308	456
TRI	1.23	713	77.2	60.5	13.2	38.0	63.2	102	185
VAL	4.66	2588	505	376	72.4	222	428	678	1244
VEN	0.04	175	28.7	23.4	2.36	11.7	23.2	39.3	74.6

Table 29: k'_{bio} posteriors [L/(g OC, d)$^{-1}$] statistics from the P3 campaign

Minimum, maximum, arithmetic mean, standard deviation (SD) and 5th, 25th ,50th, 75th , 95th percentiles

Comp.	Min	Max	Mean	SD	5th perc.	25th perc.	50th perc.	75th perc.	95th perc.
5MB	0.00	0.51	0.09	0.07	0.01	0.03	0.07	0.12	0.23
ACE	35.3	382	206	57.8	111	166	205	242	305
ALI	31.9	250	99	31.9	54.7	75.6	97	118	157
AMI	1.93	1999	767	486	149	384	665	1086	1735
ATA	0.04	213	52.3	34.4	5.10	25.2	47.5	74.4	115
ATE	15.2	1992	622	420	163	309	483	838	1569
BEN	0.49	694	200.4	121.6	43.5	108.8	180.4	266	438
BEZ	131	7919	1564	837	659	1021	1397	1844	3146
BIC	0.48	194	75.7	28.8	29.4	55.8	74.5	95.1	123
CAR	0.04	109	21.8	16.3	1.89	8.74	18.5	30.9	53.1
CIT	8.12	454	169	64.4	70.7	127	166	206	278
CLA	0.34	156	54.3	24.6	16.8	37.6	52.1	68.9	98.9

Comp.	Min	Max	Mean	SD	5th perc.	25th perc.	50th perc.	75th perc.	95th perc.
CLO	0.01	836	189	123	35.0	107	166	239	405
CYC	29.0	2962	1177	459	497	853	1121	1457	2013
DIC	33	2302	902	363	368	645	861	1118	1592
FEX	0.02	597	78.7	105.4	5.40	18.5	38.5	81.3	305
GAB	0.20	276	74.3	42.2	18.8	45.3	67.6	93.7	155
HYD	121	2470	916	391	376	652	856	1137	1616
IRB	80	778	354	112	189	271	345	419	551
LAM	0.05	155	40.6	26.6	5.23	19.8	36.1	56.8	92.8
LEV	241	9993	3283	2500	870	1282	2235	4774	8658
LID	72.4	1030	403	129	210	313	389	483	631
MEF	21.3	141	71.8	17.1	45.0	60.3	71.1	81.4	101
MOC	0.03	956	244	169	59.1	135	203	294	627
MTO	28.9	762	267	108	111	195	257	336	455
OXC	8.50	9995	4976	2637	802	2825	4972	7082	9299
PHE	0.22	786	137	130	6.81	42.1	98.0	189	408
PRE	30.8	704	277	103	127	203	269	336	457
PRO	71.0	548	241	73.2	134	189	234	281	375
RAN	49.4	1209	357	143	179	263	328	428	622
SAC	0.09	1998	1008	523	155	581	1009	1427	1856
SIT	11.1	181	76.3	25.7	40.4	57.3	72.4	91	123
SUL	0.67	1110	244	192	35.2	104	189	332	659
TRI	0.19	1486	322	158	135	217	291	388	610
VAL	552	13997	5199	2482	2017	3400	4672	6546	10238
VEN	12.5	191	85.4	29.8	38.6	64.5	82.6	104.8	140

The posterior distributions of hydrolysis and direct phototransformation constants closely followed the prior distributions (see in Annex A.4, Table A7 and Table A8), which indicates that there was no strong evidence against the prior assumptions in the observed data.

Posterior $k'_{bio,field}$ values can be converted to half-lives upon assuming certain properties for the given reach. We performed the conversion for the mean characteristic section of the Rhine river, the „average Rhine“ (Aare mouth to Lobith) (for assumed average properties see Table 30).

Table 30: Properties of the characteristic Rhine reaches.

Reach	Z [m]	SSC [mg L^{-1}]	S [kg m^{-2}]	Z_a [m]
R	4.5	34	3.0	0.025

Total system and water half-lives showed significant variability, just like the k'_{bio} values they were derived from. Total system half-lives calculated for the characteristic Rhine reaches ranged from half an hour to thousands of days, while water half-lives covered the range from 10 hours to more than 10 000 days. Considering the mean flow time for all water parcels time in the Rhine (less than 9 days, 4-5 days on average across all water parcels entering the Rhine catchment), the mean $DegT_{50,ts}$ (36 days) suggests that most compounds showed very limited to no degradation in the river. Water half-lives ($DegT_{50w}$) were always longer than the total system half-lives, consistent with model assumptions (Table 31- Table 34).

Table 31: $DegT_{50,w}$ [d] statistics from the P1 campaign

Minimum, maximum, arithmetic mean, and 5th, 25th ,50th, 75th , 95th percentiles

	Min	Max	Mean	95th perc.	75th perc.	50th perc.	25th perc.	5th perc.
Comp.	R	R	R	R	R	R	R	R
5MB	2146	22463648	14756	270528	45629	20953	10661	5360
ACE	6.8	12681	20	87.8	31.9	21.4	15.1	10.6
ALI	665	252345	1546	9754	2515	1502	1153	844
AMI	1.2	43.2	4.4	11	8.2	5.6	3.4	1.9
ATA	16.8	4289	66.3	404	128	74.3	50.3	29.5
ATE	1.7	5070	6.4	20.9	10.3	7.3	5.2	3.1
BEN	1.8	178	6.4	25.6	11.7	7.8	5.1	2.4
BEZ	1.1	5546	5.8	51.7	13.6	7.1	4.2	2.3
BIC	15.8	74924	44.7	178	68.5	46.1	34.9	23.5
CAR	12.4	35983	40.7	164	61.7	42.4	30.4	23.5
CIT	6.5	133	15.7	31.4	20.4	16.3	13.2	9.7
CLA	10.8	211226	108	1888	333	150	84.5	36.7
CLO	3.3	40.7	9.5	21.8	15	11.6	7.6	4.3
CYC	0.5	320	2.8	20.9	5.9	3.3	2.1	1.1
DIC	4.4	316	11	29.2	14.7	11.2	9.1	6.8
FEX	1.1	2111	4.7	151	24.7	6.9	2.9	1.6
GAB	5.8	1677	18.7	53.4	27.4	19.9	15	9.8
HYD	2.6	52.3	6.6	15.4	9.3	6.8	5.2	3.8
IRB	9.2	8294	40.6	747	154	70.2	32.3	10.7
LAM	15	34499	55.5	259	89.6	58.4	42.1	28.4
LEV	1.2	25.4	3.6	6.8	4.7	3.7	3.0	2.1
LID	2.6	57.4	7	13.9	9.3	7.3	5.8	4.2
MEF	26.9	56050	121	1011	249	138	88.6	50.9
MOC	4.7	136138	17.3	81.5	32.2	20	13	8
MTO	3.7	570	12.4	37	19.4	13	9.6	6.6
OXC	0.2	572	0.4	2.7	0.6	0.4	0.3	0.2

PHE	2.2	673567	15.4	383	69.8	30.8	13.5	3.3
PRE	3.4	94.3	8.5	24.4	13.6	10.1	6.6	4
PRO	8.8	6475	33.6	122	54.2	36	26.4	16.3
RAN	1	40.9	6.1	14.3	9.5	7.3	5.6	3.1
SAC	1	164702	2	14	3.5	2	1.4	1.1
SIT	17.6	19269	49	261	84.9	50.4	36.5	24.8
SUL	2.7	559	8	26	11.2	8.4	6.5	4.4
TRI	2.8	1628	25.8	151	52.4	31.5	19.6	10.8
VAL	0.8	428	3.9	27.6	9	4.7	2.9	1.6
VEN	11.4	44338	69.6	847	170	85.9	50.7	26.7

Table 32: $DegT_{50,ts}$ [d] statistics from the P1 campaign

Minimum, maximum, arithmetic mean, and 5th, 25th ,50th, 75th , 95th percentiles

	Min	Max	Mean	95th perc.	75th perc.	50th perc.	25th perc.	5th perc.
Comp.	R	R	R	R	R	R	R	R
5MB	164	1714826	1127	20652	3483	1600	814	409
ACE	0.5	968	1.5	6.7	2.4	1.6	1.2	0.8
ALI	50.8	19264	118	745	192	115	88.1	64.4
AMI	0.1	3.3	0.3	0.8	0.6	0.4	0.3	0.1
ATA	1.3	327	5.1	30.9	9.8	5.7	3.8	2.2
ATE	0.1	387	0.5	1.6	0.8	0.6	0.4	0.2
BEN	0.1	13.6	0.5	2	0.9	0.6	0.4	0.2
BEZ	0.1	423	0.4	3.9	1	0.5	0.3	0.2
BIC	1.2	5720	3.4	13.6	5.2	3.5	2.7	1.8
CAR	0.9	2747	3.1	12.5	4.7	3.2	2.3	1.8
CIT	0.5	10.1	1.2	2.4	1.6	1.2	1	0.7
CLA	0.8	16125	8.3	144	25.4	11.4	6.4	2.8
CLO	0.3	3.1	0.7	1.7	1.1	0.9	0.6	0.3
CYC	0	24.4	0.2	1.6	0.5	0.2	0.2	0.1

DIC	0.3	24.1	0.8	2.2	1.1	0.9	0.7	0.5
FEX	0.1	161	0.4	11.5	1.9	0.5	0.2	0.1
GAB	0.4	128	1.4	4.1	2.1	1.5	1.1	0.7
HYD	0.2	4	0.5	1.2	0.7	0.5	0.4	0.3
IRB	0.7	633	3.1	57	11.7	5.4	2.5	0.8
LAM	1.1	2634	4.2	19.8	6.8	4.5	3.2	2.2
LEV	0.1	1.9	0.3	0.5	0.4	0.3	0.2	0.2
LID	0.2	4.4	0.5	1.1	0.7	0.6	0.4	0.3
MEF	2.1	4279	9.2	77.1	19	10.5	6.8	3.9
MOC	0.4	10393	1.3	6.2	2.5	1.5	1.0	0.6
MTO	0.3	43.5	0.9	2.8	1.5	1.0	0.7	0.5
OXC	0	43.7	0	0.2	0	0	0	0
PHE	0.2	51419	1.2	29.2	5.3	2.3	1	0.3
PRE	0.3	7.2	0.6	1.9	1	0.8	0.5	0.3
PRO	0.7	494	2.6	9.3	4.1	2.7	2	1.2
RAN	0.1	3.1	0.5	1.1	0.7	0.6	0.4	0.2
SAC	0.1	12573	0.2	1.1	0.3	0.2	0.1	0.1
SIT	1.3	1471	3.7	19.9	6.5	3.9	2.8	1.9
SUL	0.2	42.6	0.6	2	0.9	0.6	0.5	0.3
TRI	0.2	124	2	11.5	4	2.4	1.5	0.8
VAL	0.1	32.7	0.3	2.1	0.7	0.4	0.2	0.1
VEN	0.9	3385	5.3	64.7	13	6.6	3.9	2

Table 33: $DegT_{50,w}$ [d] statistics from the P3 campaign

Minimum, maximum, arithmetic mean, and 5th, 25th ,50th, 75th , 95th percentiles

	Min	Max	Mean	95th perc.	75th perc.	50th perc.	25th perc.	5th perc.
Comp.	R	R	R	R	R	R	R	R
5MB	3877	16267174	23341	200999	58389	30246	17065	8570
ACE	5.2	56.5	9.7	17.9	12.0	9.7	8.3	6.5

ALI	8.0	62.5	20.1	36.4	26.4	20.6	16.9	12.7
AMI	1.0	1035	2.6	13.4	5.2	3	1.8	1.1
ATA	9.3	53946	38.1	391	79.2	42	26.8	17.3
ATE	1.0	132	3.2	12.2	6.4	4.1	2.4	1.3
BEN	2.9	4075	10	45.9	18.3	11.1	7.5	4.6
BEZ	0.3	15.2	1.3	3.0	2.0	1.4	1.1	0.6
BIC	10.3	4188	26.3	67.9	35.7	26.8	21	16.3
CAR	18.3	49700	91.5	1056	228	108	64.6	37.6
CIT	4.4	246	11.8	28.2	15.7	12.0	9.7	7.2
CLA	12.8	5790	36.7	119	53.0	38.3	28.9	20.2
CLO	2.4	136750	10.6	57.0	18.6	12	8.3	4.9
CYC	0.7	68.7	1.7	4.0	2.3	1.8	1.4	1
DIC	0.9	59.7	2.2	5.4	3.1	2.3	1.8	1.3
FEX	3.3	97508	25.3	369	108	51.8	24.5	6.5
GAB	7.2	10102	26.9	106	44.0	29.5	21.3	12.9
HYD	0.8	16.5	2.2	5.3	3.1	2.3	1.8	1.2
IRB	2.6	24.8	5.6	10.5	7.4	5.8	4.8	3.6
LAM	12.8	40911	49.1	381	101	55.2	35.1	21.5
LEV	0.2	8.3	0.6	2.3	1.6	0.9	0.4	0.2
LID	1.9	27.5	5	9.5	6.4	5.1	4.1	3.2
MEF	14.1	93.5	27.8	44.4	33.1	28.1	24.5	19.8
MOC	2.1	67016	8.2	33.7	14.8	9.8	6.8	3.2
MTO	2.6	69	7.5	18	10.2	7.8	5.9	4.4
OXC	0.2	235	0.4	2.5	0.7	0.4	0.3	0.2
PHE	2.5	8879	14.6	293	47.4	20.4	10.6	4.9
PRE	2.8	64.8	7.2	15.7	9.8	7.4	5.9	4.4
PRO	3.6	28.1	8.3	14.9	10.6	8.5	7.1	5.3
RAN	1.6	40.4	5.6	11.1	7.6	6.1	4.7	3.2
SAC	1.0	22449	2	12.8	3.4	2	1.4	1.1
SIT	11	180	26.1	49.4	34.8	27.6	21.9	16.2
SUL	1.8	2956	8.2	56.7	19.2	10.6	6.0	3.0

TRI	1.3	10371	6.2	14.8	9.2	6.9	5.1	3.3
VAL	0.1	3.6	0.4	1.0	0.6	0.4	0.3	0.2
VEN	10.4	160	23.4	51.7	30.9	24.2	19.0	14.3

Table 34: $DegT_{50,ts}$ [d] statistics from the P3 campaign

Minimum, maximum, arithmetic mean, and 5th, 25th ,50th, 75th , 95th percentiles

Comp.	Min R	Max R	Mean R	95th perc. R	75th perc. R	50th perc. R	25th perc. R	5th perc. R
5MB	288	1208035	1733	14927	4336	2246	1267	636
ACE	0.4	4.2	0.7	1.3	0.9	0.7	0.6	0.5
ALI	0.6	4.6	1.5	2.7	2.0	1.5	1.3	0.9
AMI	0.1	76.8	0.2	1	0.4	0.2	0.1	0.1
ATA	0.7	4006	2.8	29.1	5.9	3.1	2.0	1.3
ATE	0.1	9.8	0.2	0.9	0.5	0.3	0.2	0.1
BEN	0.2	303	0.7	3.4	1.4	0.8	0.6	0.3
BEZ	0	1.1	0.1	0.2	0.1	0.1	0.1	0
BIC	0.8	311	2.0	5.0	2.7	2.0	1.6	1.2
CAR	1.4	3691	6.8	78.4	16.9	8.0	4.8	2.8
CIT	0.3	18.2	0.9	2.1	1.2	0.9	0.7	0.5
CLA	0.9	430	2.7	8.8	3.9	2.8	2.1	1.5
CLO	0.2	10155	0.8	4.2	1.4	0.9	0.6	0.4
CYC	0	5.1	0.1	0.3	0.2	0.1	0.1	0.1
DIC	0.1	4.4	0.2	0.4	0.2	0.2	0.1	0.1
FEX	0.2	7241	1.9	27.4	8.0	3.8	1.8	0.5
GAB	0.5	750	2.0	7.9	3.3	2.2	1.6	1
HYD	0.1	1.2	0.2	0.4	0.2	0.2	0.1	0.1
IRB	0.2	1.8	0.4	0.8	0.5	0.4	0.4	0.3
LAM	1	3038	3.6	28.3	7.5	4.1	2.6	1.6
LEV	0	0.6	0	0.2	0.1	0.1	0	0

LID	0.1	2.0	0.4	0.7	0.5	0.4	0.3	0.2
MEF	1.0	6.9	2.1	3.3	2.5	2.1	1.8	1.5
MOC	0.2	4977	0.6	2.5	1.1	0.7	0.5	0.2
MTO	0.2	5.1	0.6	1.3	0.8	0.6	0.4	0.3
OXC	0	17.4	0	0.2	0.1	0	0	0
PHE	0.2	659	1.1	21.8	3.5	1.5	0.8	0.4
PRE	0.2	4.8	0.5	1.2	0.7	0.5	0.4	0.3
PRO	0.3	2.1	0.6	1.1	0.8	0.6	0.5	0.4
RAN	0.1	3	0.4	0.8	0.6	0.5	0.3	0.2
SAC	0.1	1667	0.1	1.0	0.3	0.1	0.1	0.1
SIT	0.8	13.4	1.9	3.7	2.6	2.0	1.6	1.2
SUL	0.1	220	0.6	4.2	1.4	0.8	0.4	0.2
TRI	0.1	770	0.5	1.1	0.7	0.5	0.4	0.2
VAL	0	0.3	0	0.1	0	0	0	0
VEN	0.8	11.9	1.7	3.8	2.3	1.8	1.4	1.1

4.1.6 Discussion

4.1.6.1 Comparison of k_{esc} to other Literature Estimates

There are no literature values for k_{esc}, yet one of the factors that contribute to it, i.e., removal in WWTPs, is a frequent subject of research. Therefore, a short literature review was performed to collate measured removal rates of the study compounds from WWTPs reported in previous studies. Besides this, the CH1 study (Singer et al. 2016) contained removal and excretion rate estimates from which we reconstructed k_{esc} for comparison purposes, assuming that Equation (15) was valid (Table 35).

Table 35: Removal rates of WWTPs collected from literature and removal, excretion rate and escape rates from the CH1 study compared to mean escape rates calculated in this study

K_{esc} values are highlighted with red where we found very strong discrepancies between our and CH1 study estimates.

Compound	Literature	CH1 study	CH1 study	Estimate CH1 study	Prior for Germany	Prior for Switzerland
	k_{rem}	k_{rem}	k_{exc}	k_{esc}	$E[k_{esc}]$	$E[k_{esc}]$
5MB		NA	NA	NA	NA	NA
ACE	Scheurer et al. (2009): 0.41; Castronovo et al. (2016): 0.59-0.97; Falås et al. (2016): 0.80; Li et al. (2018): 0.15 ±0. 615,	NA	NA	NA	NA	NA
ALI		0.04	0.91	0.87	NA	0.64
AMI		0.09	0.77	0.70	0.67	0.58
ATA		0.05	0.30	0.29	NA	0.60
ATE	Fick et al. (2011): mean 0.51; Gurke et al. (2015) mean 0.226; Paxeus (2004): < 0.1; Vieno et al. (2005): 0.61; Castiglioni et al. (2006): summer (0.55), winter (0.1) ; Sipma et al. (2010). 0.0 to 0.97 for conventional activated sludge processes and 0.655–0.767 for MBR (from lit. summary)	0.22	0.83	0.65	0.31	0.50
BEN		NA	NA	NA	NA	NA

Compound	Literature k_{rem}	CH1 study k_{rem}	CH1 study k_{exc}	Estimate CH1 study k_{esc}	Prior for Germany $E[k_{esc}]$	Prior for Switzerland $E[k_{esc}]$
BEZ	Gurke et al. (2015) mean 0.488; Sipma et al. (2010): 0.21 to 0.993% for conventional activated sludge processes and 0.76–0.97 for MBR	0.61	0.77	0.30	0.21	0.43
BIC		0.03	0.65	0.63	NA	0.30
CAR	Fick et al. (2011): mean -0.03; -0.066;Paxeus (2004): <0.1-0.53; Ternes (1998): 0.07; Sipma et al. (2010): -1.22 to 0.58 for conventional activated sludge processes and -- 0.22–0.23 for MBR (from lit. summary)	0.25	0.26	0.20	0.12	0.18
CIT	Fick et al. (2011): mean 0.11	0.20	0.97	0.78	NA	0.52
CLA	Fick et al. (2011): mean 0.54	0.07	0.33	0.31	0.12	0.22
CLO		0.38	0.50	0.31	NA	0.11
CYC	Scheurer et al. (2009): >0.90; Li et al. (2018): 0.9684 ± 0.0247	NA	NA	NA	NA	NA
DIC	Fick et al. (2011): mean 0.28; Paxeus (2004): <0.1- 0.88; Ternes (1998): 0.69; Sipma et al. (2010). -1.43 to 0.8 for conventional activated sludge processes and -0.08–0.874 for MBR (from lit. summary)	0.87	0.16	0.02	0.18	0.32

Compound	Literature k_{rem}	CH1 study k_{rem}	CH1 study k_{exc}	Estimate CH1 study k_{esc}	Prior for Germany $E[k_{esc}]$	Prior for Switzerland $E[k_{esc}]$
FEX	Fick et al. (2011): mean 0.37	0.13	0.10	0.09	NA	0.71
GAB	Gurke et al. (2015) mean 0.064	0.92	1.00	0.08	0.47	0.77
HYD		0.09	1.00	0.91	0.57	0.50
IRB	Bayer et al. (2014): 0.16–0.40 (mean 0.29); Fick et al. (2011): mean 0.36	0.97	0.02	0.00	NA	0.20
LAM		0.11	0.10	0.09	0.45	0.50
LEV		0.45	0.66	0.36	NA	0.16
LID	Rúa-Gómez and Püttmann (2012): 0.13, 0.3, 0.37, 0.5 (MRFmicro-screen rotating drum filtersystem)	0.11	0.10	0.09	NA	0.72
MEF	Sipma et al. (2010). 0.0 to 0.51 for conventional activated sludge processes and 0.355–0.89 for MBR (from lit. summary)	NA	NA	NA	NA	0.03
MTO	Fick et al. (2011): mean 0.31; Gurke et al. (2015) mean -0.086; Paxeus (2004): <=0.1; Sipma et al. (2010). -0.01 to 0.77 for conventional activated sludge processes and 0.295–0.587 for MBR (from lit. summary)	0.23	0.11	0.09	0.10	0.11
MOC		0.09	0.01	0.01	NA	0.15

Compound	Literature k_{rem}	CH1 study k_{rem}	CH1 study k_{exc}	Estimate CH1 study k_{esc}	Prior for Germany $E[k_{esc}]$	Prior for Switzerland $E[k_{esc}]$
OXC	Gurke et al. (2015) mean 0.732	NA	NA	NA	NA	0.16
PHE		0.75	0.05	0.01	0.44	NA
PRE		0.92	1.00	0.08	0.15	NA
PRO	Gurke et al. (2015) mean -0.043; Sipma et al. (2010). 0.59 for conventional activated sludge processes and 0.655–0.776 for MBR (from lit. summary)	NA	NA	NA	0.17*	0.17
RAN	Fick et al. (2011): mean 0.85; Sipma et al. (2010): 0.247 to 0.422 for conventional activated sludge processes and 0.295–0.95 for MBR (from lit. summary)	0.22	0.30	0.23	NA	0.15
SAC	Scheurer et al. (2009): >0.94; Li et al. (2018): 0.9726 ± 0.0324	NA	NA	NA	NA	NA
SIT		0.02	0.79	0.78	NA	0.25

Compound	Literature k_{rem}	CH1 study k_{rem}	CH1 study k_{exc}	Estimate CH1 study k_{esc}	Prior for Germany $E[k_{esc}]$	Prior for Switzerland $E[k_{esc}]$
SUL	Fick et al. (2011): mean 0.73; Gurke et al. (2015) mean 0.424; Sipma et al. (2010): -1.38 to 0.99 for conventional activated sludge processes and 0.57–0.99 for MBR (from lit. summary)	0.22	0.20	0.16	0.13	0.11
TRI	Fick et al. (2011): mean 0.39; Gulkowska et al. (2008): -0.42,-0.17,-0.11, 0.62; Batt et al. (2006): 0.01 (conventional activated sludge), 0.50 (nitrifying activated sludge); Gurke et al. (2015) mean -0.106; Paxeus (2004): <0.1-0.4; Sipma et al. (2010): -0.4 to 0.404 for conventional activated sludge processes and 0.475–0.667 for MBR (from lit. summary)	0.09	0.60	0.55	0.15	0.33
VAL	Bayer et al. (2014): 0.94–0.98 (mean 0.96); Gurke et al. (2015) mean 0.244	0.91	1.00	0.09	0.18	0.36

Compound	Literature k_{rem}	CH1 study k_{rem}	CH1 study k_{exc}	Estimate CH1 study k_{esc}	Prior for Germany $E[k_{esc}]$	Prior for Switzerland $E[k_{esc}]$
VEN	Rúa-Gómez and Püttmann (2012): 0.23, 0.46, 0.48,0.49 (MRFmicro-screen rotating drum filtersystem); Fick et al. (2011): mean 0.21; Gurke et al. (2015) mean 0.077	0.19	0.46	0.37	0.14	0.18

The variability of k_{rem} estimates in Table 35 clearly shows that this parameter and therefore k_{esc} too have to be considered as case-specific (due to fluctuations in both momentary inflow and removal efficiency of WWTPs), and there is little hope to establish generally valid values with a small uncertainty range that would allow estimating the emission from a certain WWTP in a certain season without measurements. Long-term simultaneous measurements of in- and outflowing fluxes at numerous WWTPs may help to reduce the uncertainty of k_{rem} yet the inherent variability of other components of k_{esc} seems to be inescapable.

4.1.6.2 Variability of Emission

The k_{esc} estimates showed a large variability between the individual samples in the five involved studies. This variability could only be considered as randomness, as we found no significant deterministic relations between the individual k_{esc} estimates and potential influencing factors that were covered by data.

Specifically, there was no significant relation to WWTP size, although we initially expected the smaller plants to work somewhat less efficiently than the large ones. There appeared to be some weak connection between variability and the season of sampling in the Swiss campaigns, but the same did not show up in the German datasets and it turned out that the sampling of the WWTP size classes in Swiss campaigns were not evenly distributed seasonally, i.e., the few large plants were sampled in the spring, while smaller plants were sampled both in the spring and late summer.

4.1.6.3 $k'_{bio,field}$ in Rine vs. Removal in Rhine

We estimated removal rates in the Rhine from the estimated emissions and compared them to the modelled $k'_{bio,field}$ values (see in Annex A.4, Figure A9 and Table A9). Total emissions of all WWTPs were calculated from total consumption and maximum posterior probability value of k_{esc}. Removal is quantified as the proportion of total emissions that do not flow past Lobith (last measured point in SMPC campaign before the Rhine estuary). An overall – expected – tendency is that higher k'_{bio} means higher removal in the Rhine. Although both quantities used the same estimate for k_{esc}, there is no clean functional relationship. We assume that scattering originates to a large extent from the different sorption properties of the compounds because removal will be affected by sorption while $k'_{bio,field}$ has been normalized for sorption/bioavailability.

4.1.6.4 Seasonality of Degradation

SMPC P3 showed more degradation than P1 (except for CAR and FEX). The two sampling campaigns P1 and P3 were performed under different meteorological conditions. Samples for P1 were taken in spring, whereas samples for P3 were taken in July. Biological degradation and photochemical transformation are influenced by seasonality. For biotransformation, this influence can be direct in the form of higher bioactivity due to higher temperature, or indirect in the form of specific microbial community changes that occur during summer (e.g., fostered by increased growth and activity of phototrophic organisms). For phototransformation, we expect a direct effect from the higher incoming radiance, which was already considered in the k_{photo} prior. Consequently, an increased $k'_{bio,field}$ for P3 suggests that for those compounds the increase of phototransformation was not enough to cause the observed surplus removal, and that biotransformation of those compounds was indeed faster in P3.

We currently cannot distinguish between biotransformation and other abiotic transformation processes based on observed data alone, because they would produce similar longitudinal flux profiles along the Rhine. That is why we needed confident priors for k_{hydr} and k_{photo}. For compounds with known tendency for hydrolysis and phototransformation we included these mechanisms to prevent $k'_{bio,field}$ from also representing abiotic transformation mechanisms. Nevertheless, the posterior values of $k'_{bio,field}$ are still conditional on the assumptions made during model calibration and it cannot be excluded that certain loss pathways are not properly represented by the model and hence introduced some bias into $k'_{bio,field}$.

4.1.6.5 The Price of Catchment-Scale Modeling

The Rhine model calculates biotransformation for an entire catchment. Obviously, this is only possible with a number of simplifying assumptions, which come at the price of certain deficiencies. The average hydraulic properties of the 18'000 reaches of the catchment are estimated from simple known properties, such as channel slope and upstream catchment area. These are then used to calculate a steady-state sediment balance, which later plays a key role in modulating the biotransformation rate of sorbing compounds. The model suggests that biotransformation – if it ever takes place – will mostly happen in small to medium streams because (i) they receive most of the emissions, (ii) have less water per unit sediment surface, which, in-line with the k'_{bio}-hypothesis, should reduce total system half-lives, and (iii) their sediment is likely to be staying settled longer due to the weaker resuspension capacity of shallower flow. None of these assumptions could be proven by data. Yet, Boeije (2000) found that field degradation was inversely proportional to the water volume: sediment surface ratio, which suggests essentially similar behaviour.

Sorption behaviour should be as diverse as the changing bed/suspended material of the stream network. Sorption experiments carried out here in combination with literature data suggest that a significant variability can be expected for most compounds.

Moreover, it seems to be impossible to make a precise calculation of emissions for such a large, international catchment without carrying out an enormous number of emission measurements. National marketing statistics will never fully represent a catchment as they do not account for regional differences. The escape factor cannot be constant either, due to the numerous processes it integrates and that can vary, e.g., in different sewer networks, as a function of wastewater treatment technology etc.

Consequently, the parameters of the Rhine model should be considered as virtual values that describe the observed behaviour at the catchment scale, and they should not be considered measurable as such at a specific location in the catchment. This illustrates the difficulty of coming up with proper prior estimates for these quantities and validating the model structure.

According to the mathematical laws of Bayesian model calibration, the model result, including the posterior distribution of $k'_{bio,field}$, is conditional on the measured data, the model assumptions (which cannot be fully validated), and the prior distributions (which we could only estimate with significant uncertainty). Therefore, it is no surprise that the calibrated $k'_{bio,field}$ values are quite uncertain. Yet, they still show significant differences among the analysed compounds and comparison with experimental values generated in laboratory experiments may detect at least qualitative similarities between persistence in the laboratory and in the Rhine catchment.

4.2 Benchmarking Removal in the Rhine Catchment

4.2.1 Methods – Deriving a Benchmarking Model for Rivers

As shown in Chapter 4.1, the estimation of field biotransformation rate constants that would allow for assessment of environmental persistence requires a complicated model that builds on various assumptions that are difficult to prove. Moreover, such models usually suffer from weak parameter identifiability, for example there is usually a strong dependence between calibrated k_{esc} and $k'_{bio,field}$ values.

To overcome the limitations imposed by the complexity of pollutant fate models, McLachlan et al. (2017) suggested to use benchmarking instead, where the relative behavior of organic micropollutants is utilized to assess degradation from field measurements (Li and McLachlan 2020; McLachlan, Zou, and Gouin 2017; Zou, MacLeod, and McLachlan 2014; Zou, Radke, Kierkegaard, and McLachlan 2015).

Zou et al. (2014) specifically developed a benchmarking procedure for lakes. In the simplest possible setup, the first-order degradation rate constant of the target compound (S) can be estimated from the ratio of steady state in- and outflowing concentrations of the conservative benchmark (B) and the degradable target compound (S) and the water residence time:

$$k_S = \frac{1-\frac{I_S O_B}{I_B O_S}}{\tau} \quad (35)$$

where I and O are the in- and outflowing concentrations [g m^{-3}] and τ is the water residence time in the lake [d]. While its simplicity is appealing, this procedure cannot be applied to rivers for two reasons: (i) it requires a closed mass balance around the system of interest, which would bring us back to the problems of estimating emissions via k_{esc}, and (ii) it assumes full mixing within the system, which renders the locations of emissions irrelevant. Therefore, a new approach had to be developed that can account for the presence of many, unknown emission sources and the dominant longitudinal transport imposed by river flow.

As a first step, we idealized the river as a plug-flow reactor, thereby assuming a direct and unambiguous link between space (location along the river) and time. Then we replaced the set of real, discrete emission sources of B and S with two unknown continuous stochastic processes (ε_B and ε_S) that cover the entire river length. Given that the emission process is unknown and degradation followed first-order kinetics, the rational estimate for the expected value of the

accumulating pollutant flux along the river is the simple integration of a uniform distributed emission process with a magnitude of $E[\varepsilon_S]$ – that is the expected value of ε_S [g d^{-1}]:

$$E[F_S(x)] = \int_{\xi=0}^{x} E[\varepsilon_S] \exp(-k'_S x)\, d\xi \quad (36)$$

which yields:

$$E[F_S(x)] = \frac{E[\varepsilon_S]}{k'_S x}(1 - \exp(-k'_S x)) \quad (37)$$

where $F_S(x)$ is the flux of pollutant [g d^{-1}] at downstream location x [km] (x=0 at the source), and k'_S is the distance-specific degradation rate constant [km^{-1}]. When B is conservative, the expected value of the ratio between fluxes or concentrations of S and B at a specific x location becomes:

$$E\left[\frac{F_S(x)}{F_B(x)}\right] = \frac{\alpha}{x}(1 - \exp(-k'_S x)) \quad (38)$$

where α is a constant that depends on the unknown statistical properties of the two unknown emission processes and is therefore subject to calibration.

The expected value given in Equation (38) would only represent the longitudinal profile of the concentration ratio if emissions of both S and B were indeed uniformly distributed along the river and concentration measurements were perfectly accurate. As we expect this not to be the case, it is necessary to account for the variance introduced by the uneven distribution of emissions and measurement errors. It can be shown, that the variance of the benchmark ratio follows this functional form:

$$\mathrm{Var}\left[\frac{F_S(x)}{F_B(x)}\right] = \frac{\beta}{x^2}\left((1 - \exp(-2k'_S x)) + \frac{\gamma}{x}(1 - \exp(-k'_S x))^2\right) + \sigma^2 \quad (39)$$

where β and γ are two unknown constants depending on the unknown statistical properties of the emission processes and σ^2 is the (constant) variance of the measurement error.

Equations (38) and (39) describe a probabilistic model that can be used to inversely estimate k'_S from observed flux or concentration ratios. The likelihood of a specific parameter combination ($\alpha, \beta, \gamma, k'_S, \sigma^2$) can be calculated at each observation point from a normal distribution with the above-defined mean and variance.

4.2.1.1 Application to SMPC data

4.2.1.1.1 Using carbamazepine as benchmark chemical

The model described by equations (22) and (23) was applied to the P1 and P3 campaigns of SMPC using the outflow of Lake Constance as the starting point of *x*. For technical reasons, values of α, β, γ, and σ were restricted to be positive. The parameter k'_S was considered to be a dissipation rate constant as it includes all kinds of net loss mechanisms from the system.

Carbamazepin was initially chosen as benchmark compound since it is widely known to be highly recalcitrant towards both biotic and abiotic degradation processes and was again confirmed to be so in the laboratory simulation studies conducted here (section 2.6.2.1). Other benchmarks are analyzed in the following subsection. Model fit was acceptable for most compounds and even excellent for a few (Figure 20). Calibrated k'_S values are summarized in

Table 36. For a handful of compounds, the parametric uncertainty interval was so wide that it intersected 0 at several locations, which indicated that it was impossible to get a constrained confidence interval for k'_S. The reason for this was that these highly scattering measurement series could be explained similarly well by a combination of slow dissipation and high measurement uncertainty, or by coupled instantaneous dissipation and highly variable emissions.

Figure 20: Fits of the river benchmark model to SMPC data

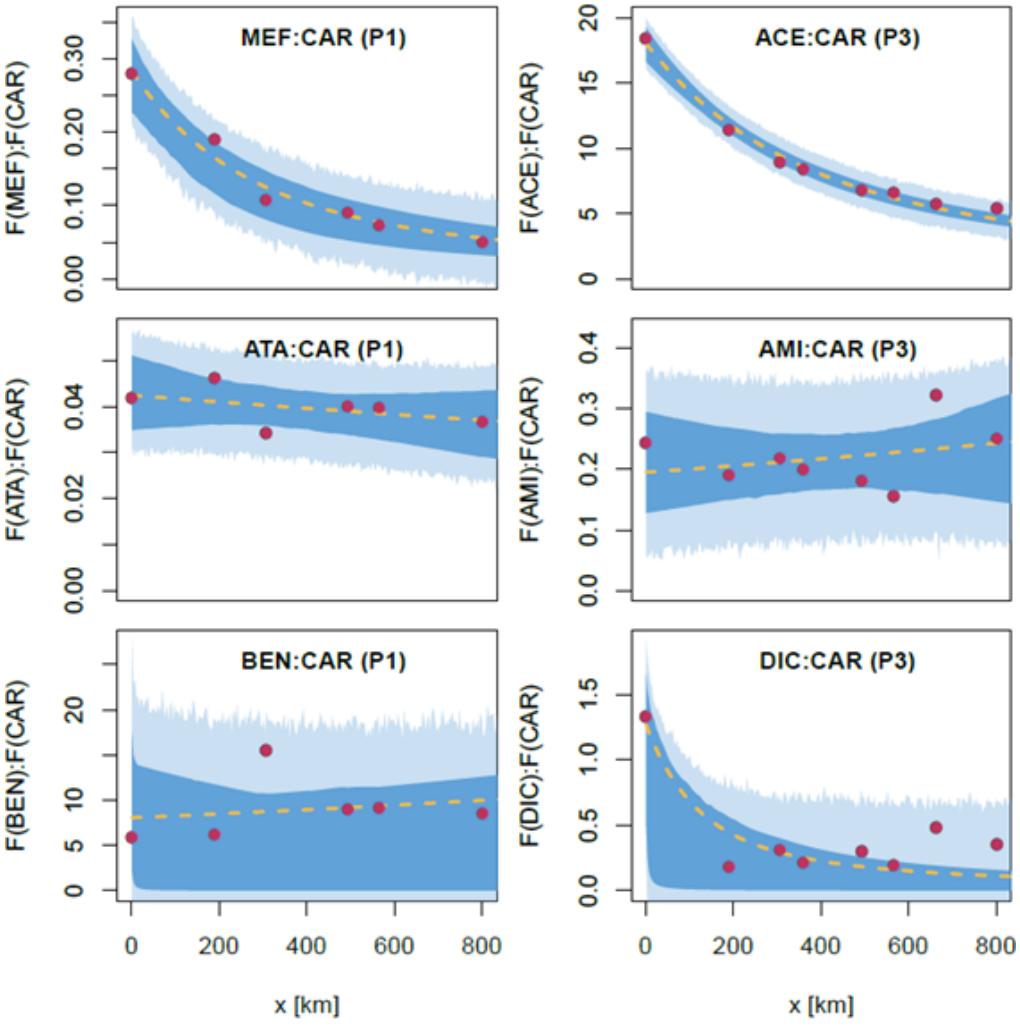

Example fits of the river benchmark model to concentration ratios from the SMPC campaign. Good fits are in the first row, highly uncertain fits in the bottom row. Dots: observed concentration ratios, dashed line: best fit, dark blue shading: parametric uncertainty, light blue shading: total uncertainty including observation error. For BEN in P1 and DIC in P3 uncertainty precluded finding a bounded range for k'_S.

Source: own figure, BME

As they account for all kinds of loss processes, the distance-specific dissipation rate constants can be used to estimate total system dissipation half-lives in the Rhine proper. The mean flow velocity in the Rhine can be estimated with the Manning equation (Manning et al. 1890). Calculated flow velocities range from 1.3 to 1.8 [m s^{-1}], represented by an average of 1.5 [m s^{-1}] or 129.6 [km d^{-1}]. Distance-specific dissipation half-lives ($DL_{50}=\ln(2)/k'_S$) multiplied with the flow velocity (Table 38) indicate that the method was capable of distinguishing between

dissipation half-lives in the range of 7 hours to about 60 days. Compounds having a longer half-life were recognised as conservative. Similarly to the mechanistic modeling attempt (Chapter 4.1), benchmarking also found faster dissipation in P3 compared to P1 (Table 38).

Table 36: Calibrated first-order distance-specific dissipation rate constants

Calibrated values of the first-order distance-specific dissipation rate constant [km^{-1}] using carbamazepine as a conservative benchmark. Negative expected values indicate conservative behavior compared to carbamazepine. Bold numbers show cases with excessive uncertainty.

	P1		P3	
Compound	**E[k's]**	**SD[k's]**	**E[k's]**	**SD[k's]**
5MB	-0.00122	0.00065	-0.00047	0.00036
ACE	0.00114	0.00021	0.00484	0.00038
ALI	0.00284	0.00326	0.00619	0.00115
AMI	-0.00051	0.00061	-0.00023	0.00094
ATA	0.00044	0.00058	0.00334	0.00225
ATE	0.00163	0.00066	0.01754	0.01717
BEN	**0.20577**	0.28071	0.00041	0.00056
BEZ	**0.31280**	0.33239	0.00834	0.00148
BIC	-0.00134	0.00070	-0.00028	0.00053
CIT	0.00061	0.00066	0.00359	0.00143
CLA	-0.00017	0.00043	0.00458	0.00103
CLO	-0.00079	0.00041	0.00032	0.00039
CYC	0.00036	0.00114	0.00450	0.00211
DIC	0.00078	0.00093	**0.33393**	0.29233
EPH	NA	NA	0.00699	0.00046
FEX	**0.38811**	0.30485	0.01147	0.05886
GAB	-0.00145	0.00058	-0.00027	0.00015
HYD	**0.09044**	0.15341	**0.05610**	0.06638
IRB	-0.00016	0.00051	0.01080	0.00184
KET	0.00248	0.00084	0.00696	0.00044
LAM	-0.00017	0.00031	0.00082	0.00022
LEV	0.00135	0.00055	**0.29630**	0.30885
LID	-0.00013	0.00030	0.00315	0.00077
MEF	0.00656	0.00133	0.01654	0.00205
MOC	-0.00065	0.00029	0.00178	0.00068
MTO	-0.00140	0.00112	-0.00041	0.00089
OLM	-0.00043	0.00029	0.00092	0.00068
OXC	**0.34637**	0.31222	**0.29712**	0.31093
OXY	-0.00142	0.00086	-0.00102	0.00065
PHE	-0.00182	0.00048	-0.00150	0.00049
PRE	0.00145	0.00092	0.00698	0.00047
PRO	0.00010	0.00022	0.00613	0.00207
RAN	0.00247	0.00081	0.00697	0.00045
SAC	**0.37355**	0.30437	**0.30500**	0.30750
SIT	-0.00119	0.00068	-0.00024	0.00034
SUL	-0.00020	0.00050	0.00088	0.00111
TRI	0.00134	0.00193	**0.33898**	0.29361
VAL	-0.00071	0.00062	**0.29707**	0.28265

	P1		P3	
Compound	E[k'_s]	SD[k'_s]	E[k'_s]	SD[k'_s]
VEN	-0.00048	0.00095	0.00232	0.00028

Table 37: Total system dissipation half-lives in the Rhine channel

Estimated mean total system dissipation half-lives (DT_{50} [d]) in the Rhine channel based on benchmarking with carbamazepine. "∞" indicates that there is no dissipation due to a zero or negative dissipation rate constant.

Compound	SMPC P1 E[DT_{50}]	SMPC P3 E[DT_{50}]
5MB	∞	∞
ACE	4.7	1.1
ALI	1.9	0.9
AMI	∞	∞
ATA	12.2	1.6
ATE	3.3	0.3
BEN	NA	12.9
BEZ	NA	0.6
BIC	∞	∞
CIT	8.8	1.5
CLA	∞	1.2
CLO	∞	17.0
CYC	15.0	1.2
DIC	6.8	NA
EPH	NA	0.8
FEX	NA	NA
GAB	∞	∞
HYD	NA	NA
IRB	∞	0.5
KET	2.2	0.8
LAM	∞	6.5
LEV	4.0	NA
LID	∞	1.7
MEF	0.8	0.3
MOC	∞	3.0
MTO	∞	∞
OLM	∞	5.8
OXC	NA	NA
OXY	∞	∞
PHE	∞	∞
PRE	3.7	0.8
PRO	55.6	0.9
RAN	2.2	0.8
SAC	NA	NA
SIT	∞	∞
SUL	∞	6.1
TRI	4.0	NA
VAL	∞	NA
VEN	∞	2.3

4.2.1.1.2 Other Benchmarks

Zou et al. (2014) highlight that the principle of benchmarking requires the benchmark compound to differ from the assessed compound only in the property of interest, in this case persistence. This implies that, e.g., sorption behavior should be the same, which is obviously not true for all compounds in relation to carbamazepine. To check the effect of the choice of benchmark compound on the outcome, we tested a set of potential benchmarks that showed conservative behavior (k'_S close to 0 or even negative) in previous calculations and have limited scattering in their field measurements: 5MB, BIC, GAB, and SIT in addition to CAR (Figure 20). For comparison, an artificial, fully conservative "flux" was also used as a benchmark in this exercise: the upstream population, which is guaranteed to accumulate along the river, representing a truly lossless quantity.

Figure 21: Calibrated k'_S values with different benchmarks

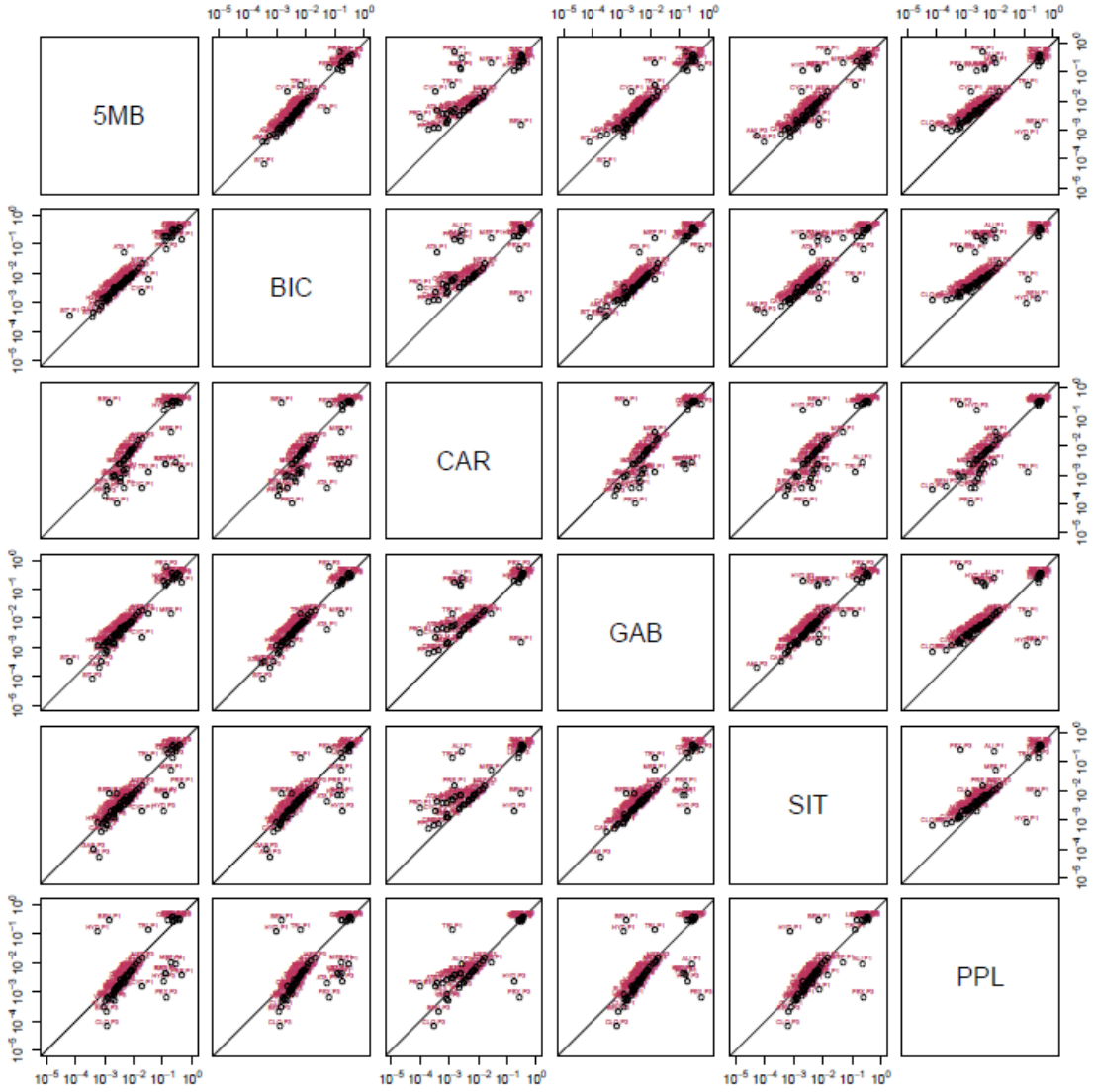

Calibrated mean values of k'_S [km^{-1}] with different benchmarks (benchmark code shown in the diagonals). PPL represents the upstream population.

Source: own figure, BME

Based on the estimates of k'_S with different benchmarks it is apparent that while the specific values indeed depend on the benchmark compound, the overall relative ranking of compounds does this to a much smaller extent. While carbamazepine (CAR) is commonly considered as conservative compound and therefore – and because of its moderate K_{oc} – promises to be a good general benchmark, the comparison shows that results obtained with it are probably in least agreement with the other benchmarks. Figure 21 and Annex A.4, Tables A10 – A11 suggest that the agreement between different benchmarks is this time not a function of similarity of sorption properties: GAB and SIT have low and high measured K_{oc} among the selected benchmark compounds (151 and 5587 L kg^{-1}), respectively, yet the k'_S values calculated by them show a close agreement. The same applies for the pair of BIC and 5MB (K_{oc}=126 and 977 L kg^{-1}, respectively).

Dissipation rate constants could again be converted to dissipation half-lives both in terms of space and time (Table 38 and Table 39). Estimated half-life quantiles ranged between about half an hour and 70 days (wherever dissipation could be assumed at all).

Table 38: Aggregated properties of distance-specific dissipation rate constants in SMPC P1 with different benchmarks

Aggregated properties of distance-specific dissipation rate constants (k'_S [km^{-1}]) in SMPC P1 with different benchmarks and the corresponding half-life quantiles. Mean values can be derived from mean k'_s as follows: $DL_{50}=\ln(2)/k'_s$, $DT_{50}=DL_{50}/129.6$.

Compound	Mean k'_S [km^{-1}]	Std. dev. k'_S [km^{-1}]	CV k'_S	DL_{50} 5% [km]	DL_{50} 95% [km]	DT_{50} 5% [d]	DT_{50} 95% [d]
5MB	-0.0002	0.0006	3.68	∞	962.0	7.42	∞
ACE	0.0040	0.0017	0.41	455.0	106.5	0.82	3.51
ALI	0.1795	0.1362	0.76	∞	1.8	0.01	∞
AMI	0.0010	0.0008	0.82	∞	322.1	2.48	∞
ATA	0.0116	0.0209	1.80	∞	16.1	0.12	∞
ATE	0.0049	0.0019	0.40	348.9	88.9	0.69	2.69
BEN	0.0986	0.1483	1.50	∞	2.2	0.02	∞
BEZ	0.0206	0.0529	2.57	∞	6.9	0.05	∞
BIC	-0.0004	0.0005	1.15	∞	2317.0	17.88	∞
CAR	0.0029	0.0008	0.29	428.2	167.4	1.29	3.30
CIT	0.0031	0.0014	0.48	790.2	132.6	1.02	6.10
CLA	0.0029	0.0026	0.92	∞	102.1	0.79	∞
CLO	0.0007	0.0007	1.09	∞	391.2	3.02	∞
CYC	0.0046	0.0073	1.58	∞	44.4	0.34	∞
DIC	0.0031	0.0012	0.40	556.7	141.7	1.09	4.30
EPH	NA	NA	NA	NA	NA	∞	∞
FEX	0.3196	0.0561	0.18	2.9	1.7	0.01	0.02
GAB	-0.0005	0.0005	1.13	∞	2065.0	15.93	∞
HYD	0.0205	0.0487	2.38	∞	7.4	0.06	∞
IRB	0.0016	0.0010	0.63	9014.9	219.5	1.69	69.56
KET	0.0645	0.0658	1.02	∞	4.2	0.03	∞
LAM	0.0018	0.0011	0.63	6649.6	202.8	1.56	51.31
LEV	0.0039	0.0015	0.37	402.3	113.0	0.87	3.10
LID	0.0020	0.0012	0.62	5397.6	180.8	1.40	41.65

Compound	Mean k'_S [km^{-1}]	Std. dev. k'_S [km^{-1}]	CV k'_S	DL_{50} 5% [km]	DL_{50} 95% [km]	DT_{50} 5% [d]	DT_{50} 95% [d]
MEF	0.0757	0.0803	1.06	∞	3.5	0.03	∞
MOC	0.0014	0.0011	0.83	∞	227.5	1.76	∞
MTO	-0.0006	0.0003	0.46	∞	∞	∞	∞
OLM	0.0018	0.0013	0.70	∞	189.7	1.46	∞
OXC	0.2127	0.0598	0.28	5.6	2.3	0.02	0.04
OXY	-0.0004	0.0006	1.61	∞	1363.3	10.52	∞
PHE	-0.0009	0.0005	0.58	∞	∞	∞	∞
PPL*	0.0006	0.0010	1.80	∞	328.5	2.53	∞
PRE	0.1305	0.1746	1.34	∞	1.8	0.01	∞
PRO	0.0022	0.0012	0.54	1708.7	172.5	1.33	13.18
RAN	0.0778	0.0814	1.05	∞	3.5	0.03	∞
SAC	0.3248	0.0600	0.18	3.0	1.7	0.01	0.02
SIT	-0.0001	0.0006	4.56	∞	833.0	6.43	∞
SUL	0.0018	0.0011	0.61	4655.8	202.8	1.56	35.92
TRI	0.0529	0.0619	1.17	∞	4.8	0.04	∞
VAL	0.0010	0.0009	0.93	∞	289.6	2.23	∞
VEN	0.0008	0.0008	0.93	∞	353.1	2.72	∞

Table 39: Aggregated properties of distance-specific dissipation rate constants in SMPC P3 with different benchmarks

Aggregated properties of distance-specific dissipation rate constants (k'_S [km^{-1}]) in SMPC P3 with different benchmarks and the corresponding half-life quantiles. Mean values can be derived from mean k'_S as follows: $DL_{50}=\ln(2)/k'_S$, $DT_{50}=DL_{50}/129.6$.

Compound	Mean k'_S [km^{-1}]	Std. dev. k'_S [km^{-1}]	CV k'_S [–]	DL_{50} 5% [km]	DL_{50} 95% [km]	DT_{50} 5% [d]	DT_{50} 95% [d]
5MB	-0.0003	0.0002	0.61	∞	∞	∞	∞
ACE	0.0052	0.0009	0.17	179.5	105.5	0.81	1.38
ALI	0.0065	0.0011	0.17	143.4	85.7	0.66	1.11
AMI	0.0001	0.0004	3.27	∞	886.7	6.84	∞
ATA	0.0037	0.0011	0.29	333.3	131.9	1.02	2.57
ATE	0.0137	0.0018	0.13	62.7	42.3	0.33	0.48
BEN	0.0007	0.0004	0.53	4633.3	519.7	4.01	35.75
BEZ	0.0088	0.0013	0.15	100.7	64.7	0.50	0.78
BIC	-0.0001	0.0002	1.42	∞	4330.9	33.42	∞
CAR	0.0004	0.0004	0.88	∞	716.3	5.53	∞
CIT	0.0039	0.0009	0.23	271.2	133.3	1.03	2.09
CLA	0.0050	0.0010	0.19	195.5	107.6	0.83	1.51
CLO	0.0007	0.0005	0.69	∞	486.2	3.75	∞
CYC	0.0049	0.0012	0.24	223.2	105.0	0.81	1.72
DIC	0.3033	0.0243	0.08	2.6	2.0	0.02	0.02
EPH	0.0073	0.0011	0.15	122.3	77.1	0.60	0.94
FEX	0.2106	0.1991	0.95	∞	1.4	0.01	∞
GAB	0.0001	0.0004	5.68	∞	1136.6	8.77	∞
HYD	0.1093	0.0878	0.80	∞	2.9	0.02	∞
IRB	0.0107	0.0014	0.13	80.9	54.1	0.42	0.62

Compound	Mean k'_S [km^{-1}]	Std. dev. k'_S [km^{-1}]	CV k'_S [–]	DL_{50} 5% [km]	DL_{50} 95% [km]	DT_{50} 5% [d]	DT_{50} 95% [d]
KET	0.0074	0.0012	0.16	123.3	75.5	0.58	0.95
LAM	0.0013	0.0005	0.41	1431.2	341.1	2.63	11.04
LEV	0.2171	0.0560	0.26	5.2	2.3	0.02	0.04
LID	0.0036	0.0008	0.23	297.8	144.2	1.11	2.30
MEF	0.0174	0.0028	0.16	52.4	32.2	0.25	0.40
MOC	0.0024	0.0007	0.29	513.8	201.6	1.56	3.96
MTO	-0.0003	0.0002	0.81	∞	11659.5	89.97	∞
OLM	0.0014	0.0007	0.47	1628.7	289.3	2.23	12.57
OXC	0.3324	0.0448	0.13	2.6	1.7	0.01	0.02
OXY	-0.0008	0.0002	0.24	∞	∞	∞	∞
PHE	-0.0013	0.0001	0.11	∞	∞	∞	∞
PPL*	0.0007	0.0004	0.54	5373.8	569.2	4.39	41.46
PRE	0.0073	0.0011	0.14	121.6	78.3	0.60	0.94
PRO	0.0062	0.0011	0.18	152.1	87.8	0.68	1.17
RAN	0.0073	0.0010	0.14	120.6	78.9	0.61	0.93
SAC	0.3486	0.0328	0.09	2.3	1.7	0.01	0.02
SIT	0.0000	0.0003	9.38	∞	1324.9	10.22	∞
SUL	0.0016	0.0009	0.55	2441.8	238.3	1.84	18.84
TRI	0.3224	0.0144	0.04	2.3	2.0	0.02	0.02
VAL	0.2589	0.0238	0.09	3.1	2.4	0.02	0.02
VEN	0.0027	0.0006	0.24	393.9	188.2	1.45	3.04

5 Comparison of Biotransformation in the Laboratory and in the Rhine River Catchment

Data from biotransformation simulation studies, in particular from modified OECD 308-type studies, and from the field study in the Rhine river catchment allowed deriving different persistence indicators, i.e., half-lives and k'_{bio} values, that each describe in a specific way a compound's recalcitrance toward transformation. Here, we investigate how those different indicators from laboratory studies relate to indicators derived for a real, large-scale system like the Rhine river catchment. In the following, we directly compare half-lives and k'_{bio} values derived from modified OECD 308-type experiments to values derived from the field study in the Rhine river catchment. It has to be noted that degradation half-lives considered in Chapter 5.1 were calculated based on the compounds' respective k'_{bio} values in laboratory studies and/or the Rhine river catchment ("field") as outlined in Chapter 2.5.1. Besides a direct comparison of values, we also quantified the strength of the correlation between laboratory and field metrics.

Generally, when comparing outcomes of the here conducted biotransformation simulation studies to modelled compound behavior in the field, it may be most meaningful to consider persistence metrics derived from data of the P3 campaign as the water temperatures in the Rhine were comparable to temperatures during biotransformation simulation studies, i.e., 22 ±2°C (see Chapter 2.1.4.1 and Annex A.3.2, Table A2). Unfortunately, the influence of temperature on the biotransformation capacity of a microbial community and, hence, on degradation half-lives cannot easily be determined based on the here presented datasets. Generally, the Arrhenius equation suggests that the biotransformation capacity of a microbial community is reduced by a factor of ~2.5 with a temperature decrease of 10°C. As shown in Figure 19, there is no systematic difference between the $k'_{bio,field}$ values derived from P1 and P3, i.e., several compounds appeared to be biotransformed more rapidly during P3, however, some compounds were transformed to the same extent during both field campaigns or even faster during P1 (i.e., FEX, BEN, CAR, and GAB). Therefore, the difference in temperature may only be one of several factors influencing the differences in biotransformation capacity of the microbial communities in the river Rhine during P1 and P3. Furthermore, besides matching the temperatures at which laboratory experiments were performed, P3 data allowed to more clearly observe a biotransformation signal for the majority of compounds as dissipation from the individual river stretches of the Rhine was increased compared to P1.

Figure A10 in Annex A.5 and Tables in Annex A.5.1 show a compilation of correlations between laboratory and field persistence indicators together with their Pearson correlation coefficient. In the following, several correlations shown in Figure A10 are discussed individually.

5.1 Comparison between Persistence Indicators derived from Laboratory and Field based on the k'_{bio}-Assumptions

5.1.1 Comparison of Half-Lives in Water

Figure 22 shows a comparison of dissipation half-lives $DT_{50,w.mod308}$ observed during modified OECD 308-type studies in inoculum sampled from the Rhine to degradation half-lives $DegT_{50,w,field}$ derived from the P3 campaign. When directly comparing values describing laboratory and field half-lives in water, several compounds have a shorter $DT_{50,w,mod308}$ than $DegT_{50,w,field}$ (see Annex A.5, Table A13). However, compounds with lower K_{oc} values appear to be closer to the 1:1 line and therewith behave rather similar in both laboratory and field studies. Since sorption is less relevant for the removal of those substances from the water phase in the

laboratory experiments, dissipation from the water column and $DegT_{50,w,field}$ do not differ as significantly as for compounds strongly sorbing to, e.g., suspended particles or bed sediment. While this is now a lab to field comparison, this pattern is very similar to what is shown in Figure 11 for just the lab data. Hence, using $DT_{50,w,mod308}$ as a persistence indicator may result in an underestimation of a compound's environmental persistence for compounds having increased K_{oc} values, i.e., $logK_{oc}$ ≥2.5.

Nevertheless, there is a statistically significant, moderate correlation between $DT_{50,w,mod308}$ and $DegT_{50,w,field}$ in case of P3 (p-value<0.001, R^2=0.51, Pearson's r= 0.71). However, it has to be noted that phase transfer processes are rather minor in both systems, i.e., the main channel of the river Rhine and in the modified OECD 308-type Rhine experiments. The correlation between dissipation half-lives from the water column of laboratory systems with degradation half-lives in a river may be compromised in systems in which sorption processes contribute more significantly to the compounds removal from the water phase (as can be seen for the Rhine already for the more strongly sorbing compounds). In case of P1, there was no statistically significant correlation between $DegT_{50,w,field}$ and $DT_{50,w,mod308}$ (Annex A.5, Figure A11).

Figure 22: Comparison of $DT_{50,w}$ derived from laboratory data and $DegT_{50,w}$ derived from P3 field data

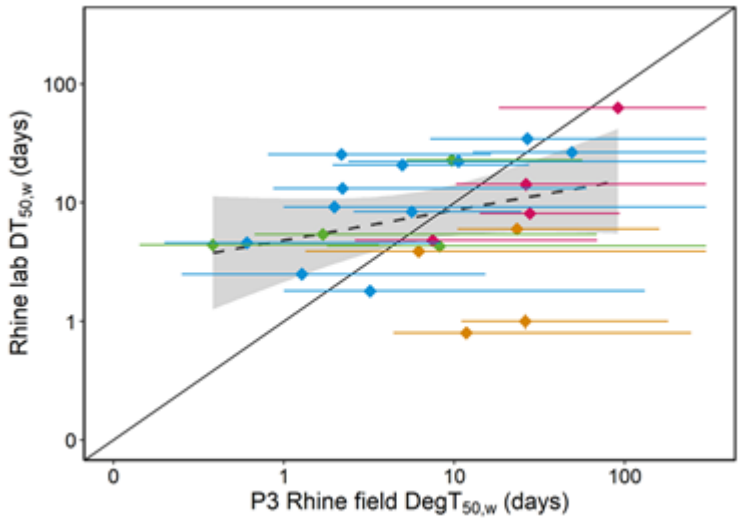

Comparison of $DT_{50,w}$ derived from modified OECD 308-type studies employing sediment and water sampled from the Rhine to $DegT_{50,w}$ calculated based on the compounds $k'_{bio,field}$ and catchment properties of the Rhine. Diamonds show mean values, the errorbars on the x-axis expand from the smallest to the largest value calculated for the respective $DegT_{50,w}$. Diamonds are colored with respect to their calibrated rounded logKoc values (green= 1, blue= 2, red= 3, yellow= 4). The 1:1 line is plotted as solid black lines. The linear regression line and its 95% confidence interval are shown as dotted line and grey area, respectively. For the linear regression line, R^2= 0.5, Pearson's r= 0.71, and p-value <0.001. Please note that 5MB was excluded from this plot since our analytical method does not allow to differentiate between 5MB and the more persistent 4MB, which might be present in the samples from the Rhine river catchment.

Source: own figure, Eawag

Figure 23 shows a comparison between degradation half-lives in the Rhine catchment $DegT_{50,w,field}$ and degradation half-lives in the modified OECD 308-type experiments $DegT_{50,w,mod308}$ employing inoculum sampled from the Rhine. In this case, both degradation half-lives – in laboratory and field – were calculated based on the compounds' respective k'_{bio} values as outlined in Chapter 2.5.1.

In agreement with the results of Honti et al. (2018), $DegT_{50,w,mod308}$ are higher than $DegT_{50,w,field}$ (see Annex A.5, Table A14). However, systematic differences between laboratory and field could result from the rather rough estimate of TOC in the field, i.e., 1% in the entire catchment of the river Rhine. Nevertheless, there is a moderate to good correlation between the compound's degradation half-lives in water in laboratory experiments and in the Rhine river catchment during the P3 campaign (i.e., p-value <0.001, R^2= 0.79, Pearson's r= 0.89). This correlation suggests that degradation half-lives derived based on the assumptions of the k'_{bio} –model may indeed support the translation of laboratory to field values. The correlation may be further increased with a more precise measure of degrader biomass in aquatic systems.

However, there was no statistically significant correlation between $DegT_{50,w,mod308}$ and $DegT_{50,w,field}$ for the P1 campaign (Annex A.5, Figure A12).

Figure 23: Comparison of $DegT_{50,w}$ derived from laboratory data and $DegT_{50,w}$ derived from P3 field data

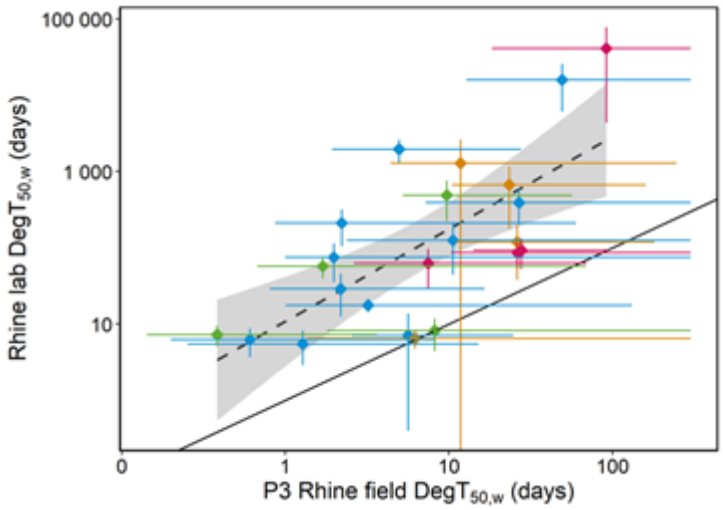

Comparison of $DegT_{50,w}$ calculated based on $k'_{bio,lab}$(joint fit) in modified OECD 308-type studies employing sediment and water sampled from the Rhine to $DegT_{50,w}$ calculated based on the compounds $k'_{bio,field}$ and catchment properties of the Rhine. Diamonds show mean values, the errorbars on the x-axis expand from the smallest to the largest value calculated for the respective $DegT_{50,w}$. Diamonds are colored with respect to their calibrated rounded logKoc values (green= 1, blue= 2, red= 3, yellow= 4). The 1:1 line is plotted as a solid black line. Linear regression and the 95% confidence interval are shown as dotted line and grey area, respectively. For the linear regression, R^2= 0.79, Pearson's r= 0.89, and p-value <0.001. Please note that 5MB was excluded from this plot since our analytical method does not allow to differentiate between 5MB and the more persistent 4MB, which might be present in the samples from the Rhine river catchment.
Source: own figure, Eawag

5.1.2 Comparison of Total System Half-Lives

Figure 24: Comparison of $DT_{50,TS}$ derived from laboratory data and $DegT_{50,TS}$ derived from P3 field data

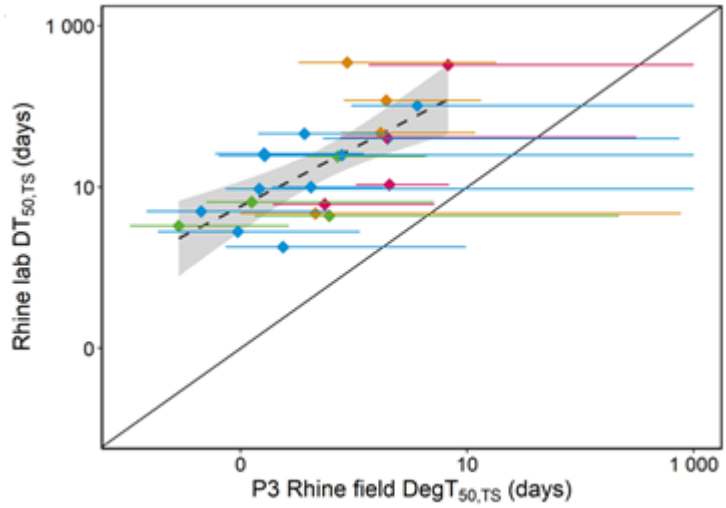

Comparison of $DT_{50,TS}$ in modified OECD 308-type studies employing sediment and water sampled from the Rhine to $DegT_{50,TS}$ calculated based on the compounds $k'_{bio,field}$ and catchment properties of the Rhine. Diamonds show mean values, the errorbars on the x-axis expand from the smallest to the largest value calculated for the respective $DegT_{50,TS}$. Diamonds are colored with respect to their calibrated rounded logKoc values (green= 1, blue= 2, red= 3, yellow= 4). The 1:1 line is plotted as a solid black line. The linear regression and its 95% confidence interval are shown as dotted line and grey area, respectively. For the linear regression, R^2= 0.41, Pearson's r= 0.64, and p-value <0.001. Please note that 5MB was excluded from this plot since our analytical method does not allow to differentiate between 5MB and the more persistent 4MB, which might be present in the samples from the Rhine river catchment.
Source: own figure, Eawag

A comparison of total system dissipation half-lives $DT_{50,TS,mod308}$ in experimental vessels of modified OECD 308-type Rhine studies to degradation half-lives in the Rhine river catchment $DegT_{50,TS,field}$ are shown in Figure 24. $DT_{50,TS,mod308R}$ values are generally higher than $DegT_{50,TS,field}$ values, indicating that the here derived $DT_{50,TS,mod308}$ may be considered a conservative estimate for the compounds' persistence in the field (see Annex A.5, Table A15).

$DegT_{50,TS,field}$ values were calculated based on the compounds' $k'_{bio,field}$ values and are therewith corrected for the compounds' bioavailability and depict transformation kinetics of the freely dissolved fraction of compound mass. In contrast, $DT_{50,TS,mod308}$ does not explicitly separate transformation and phase transfer processes and is therefore influenced by system geometry (e.g., vessel diameter, height of water and sediment layer) and sediment properties (Honti and Fenner, 2015). Therefore, compound degradation in the laboratory systems does not only depend on the compounds' susceptibility toward transformation but also on the fraction of compound mass being freely dissolved and available for transformation. Hence, by default, $DT_{50,TS,mod308}$ are equal or higher than $DegT_{50,TS,field}$.

Nevertheless, there is a statistically significant, moderate correlation between $DT_{50,TS,mod308}$ derived from modified OECD 308-type studies in Rhine inoculum and $DegT_{50,TS,field}$ describing compound transformation during P3 (i.e., p-value <0.001, R^2= 0.41, Pearson's r= 0.64). The relationship between $DT_{50,TS,mod308}$ and $DegT_{50,TS,field}$ suggests, that the experimental setup of the modified OECD 308-type studies seems to represent to some extent the geometrical/ physicochemical properties of the Rhine river channel. However, it has to be noted that it is

unclear how strongly $DT_{50,TS,mod308}$ and $DegT_{50,TS,field}$ would correlate in other test systems, i.e., in systems in which phase transfer processes can be assumed to more significantly impact the compounds' bioavailability.

5.1.3 Comparison of $k'_{bio,lab}$ and $k'_{bio,field}$

Figure 25 shows a comparison of the k'_{bio} values derived when individually and jointly fitting data from modified OECD 308-type studies in Rhine and CMP inocula ($k'_{bio,lab,CMP}$, $k'_{bio,lab,R}$, and $k'_{bio,lab,joint}$, respectively) to $k'_{bio,field}$ values derived from P3 data. In theory, unlike half-lives, k'_{bio} is supposed to be an universally valid system-independet indicator, therefore, $k'_{bio,lab}$ values from all three calibration processes are compared against $k'_{bio,field.}$ In line with the results of Honti et al. (2018), $k'_{bio,lab}$ is generally lower than $k'_{bio,field}$ (see Annex A.5, Table A15). However, the values may be more similar in case of a more precise measure of active degrader biomass in both laboratory and field. In case of $k'_{bio,field}$ values derived from P3 data, there is a statistically significant moderate correlation with $k'_{bio,lab,R}$ and $k'_{bio,lab,joint}$ (p-value <0.0001, R^2= 0.57 and p-value= 0.001, R^2= 0.37, respectively) . In this context, it has to be noted that mean $k'_{bio,lab,R}$ values are much more uncertain than mean $k'_{bio,lab,joint}$ values (Figure 6). The low correlation between $k'_{bio,field}$ values derived from P3 data and $k'_{bio,lab,CMP}$ values suggests that TOC, as expected, might not be an ideal measure for degrader biomass, i.e., that a compounds biotransformation potential does not simply scale with TOC content in a given system. Other parameters, such as pre-exposure to the test compounds (i.e., as elaborated for the artificial sweeteners in Chapter 2.3.3) may alter the microbial test communities' ability to degrade certain compounds, regardless of the presence of other easily assimilable carbon sources. Furthermore, in this context, we acknowledge that the assumption behind using Koc values to describe a compound's sorption behaviour, i.e., that compounds predominantly sorb to organic carbon, is not necessarily correct for small polar or charged compounds that might also sorb to minerals. Instead of carrying out more detailed studies to clarify these mechanisms, which would not have been possible for the large number of compounds studied here, we attempted to account for this uncertainty by defining priors based on Koc values derived from sediments/soils differing in TOC, grain size distribution, and pH conditions. In doing so, we try to describe a reasonable range of sorption behaviour a compound might exhibit when exposed to different environmental conditions and sediments in an entire river catchment.

Further, our data suggest that changes in temperature affect a microbial community's biotransformation capacity differently for different compounds. This is indicated by the weakly or non-correlating $k'_{bio,field}$ values derived from P1 data with $k'_{bio,lab}$ values (Annex A.5, Figure A14), suggesting to conduct laboratory studies at field temperatures in order to gather more representative results.

Based on the here presented datasets, it is difficult to evaluate whether $k'_{bio,lab}$ values capture a compound's environmental persistence in a better way than $DT_{50,TS,mod308}$ values. In both cases, the translation from laboratory to field works better for test systems in which compound removal from the water phase via sorption is less significant. However, it could be speculated that the correlation of $k'_{bio,lab}$ and $k'_{bio,field}$ may be increased when employing a more precise measure for the microbial communities' biotransformation potential, i.e., bacterial abundance, diversity or activity (Seller et al. 2021).

Figure 25: Comparison of $k'_{bio,lab}$ and $k'_{bio,field,P3}$

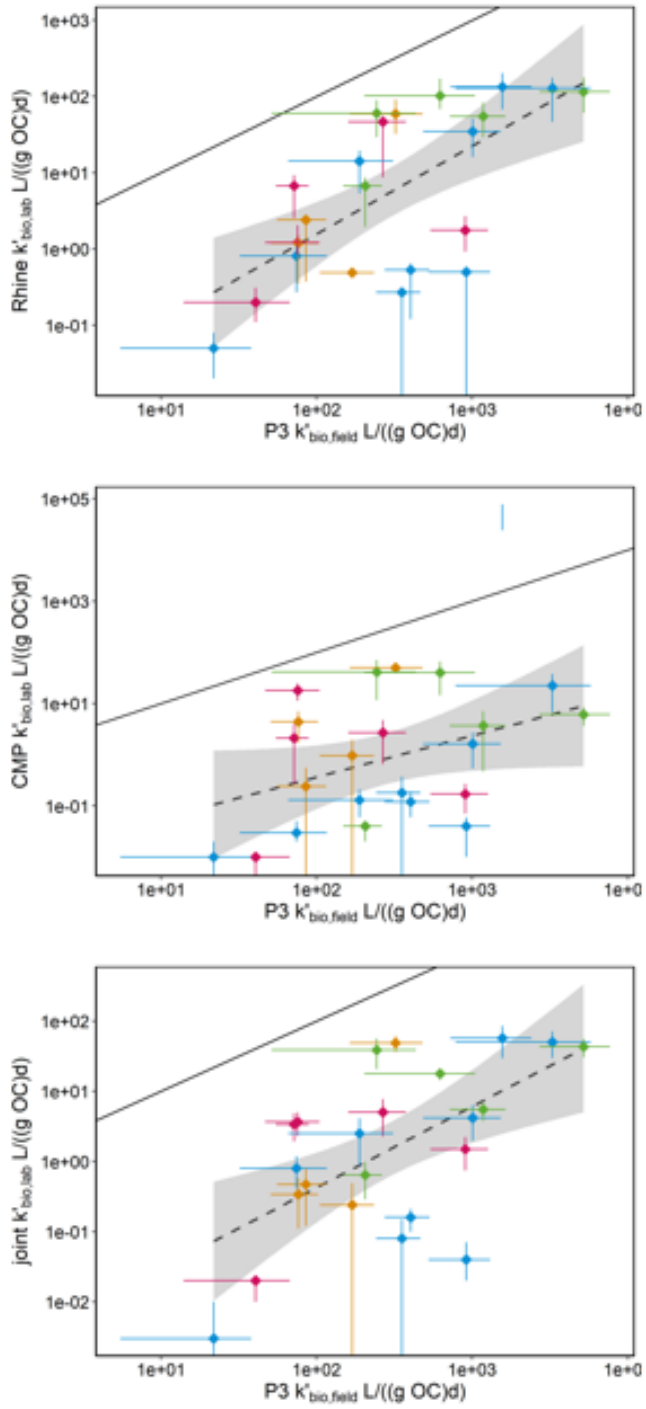

Comparison of $k'_{bio,lab}$ values derived when individually and jointly fitting the experimental data of the two modified OECD 308-type studies to $k'_{bio,field}$ calculated for the P3 sampling campaigns. Diamonds show mean values and are colored with respect to their calibrated rounded logKoc values (green= 1, blue= 2, red= 3, yellow= 4). The 1:1 lines are plotted as solid black lines. Linear regressions and their 95% confidence interval are shown as dotted line and grey area, respectively. For the linear regressions, R^2 values are 0.5, 0.004 and 0.37, Pearson's r values are 0.71, 0.06 and 0.6, and p-values <0.001, 0.77 and 0.001 when $k'_{bio,lab}$ was calibrated based on experimental data from the Rhine study exclusively, based on experimental data from the CMP study exclusively, and based on a joint model fit, respectively. Please note that 5MB was excluded from this plot since our analytical method does not allow to differentiate between 5MB and the more persistent 4MB, which might be present in the samples from the Rhine river catchment.

Source: own figure, Eawag

6 Summary and Conclusions

The aims of this research project were to

1. improve the test design for laboratory studies on transformation in surface water and water/sediment-systems to reduce variability in study outcomes and to improve their interpretability regarding biotransformation;
2. provide guidance and a tool to evaluate laboratory study results regarding biotransformation, including additional (meta)data requirements needed for the improved evaluation;
3. compare different persistence indicators derived from laboratory studies (i.e., half-lives and k'_{bio} values) to persistence indicators derived by measurements and modeling for the Rhine river catchment.

It is important to note that the outcomes always need to be considered within the limits given by the context of the experimental and modeling work. It needs to be considered that the evaluation procedures for kinetic fitting of laboratory experiments is not directly comparable to regulatory evaluation of data. Additionally, as already mentioned, the experiments conducted in this project were modified in some aspects relative to studies obtained for regulatory purposes. Thus the results might not be free of influencing factors that are not fully known or understood. Likewise, for the modeling of field data, assumptions had to be made, that may not completely reflect reality (e.g., assuming 1% TOC content for TSS uniformly along the Rhine catchment). Furthermore, not all possible loss processes might be completely reflected in the Rhine model (e.g., burial in sediment), which could lead to wrongly attributing other loss processes to biotransformation and biased half-life estimates for the Rhine system. Also, variability in different river systems is assumed to be large, and the project results are based on one river catchment, the Rhine. This is an important catchment with regard to area covered, inhabitants and importance for drinking water production by bank filtration. However, it should be kept in mind, that for other river systems, results might look different. Therefore, care should be taken to not overly generalize results. It is also worth noting that the project centered on processes in surface water (including the water phase and the sediment-water interface). It was not an objective of this project to examine processes in sediment below the sediment surface layer.

In the following, the outcomes of the project are summarized:

Evaluation of Aquatic Biotransformation in Laboratory Test Systems.

OECD 309-type suspension tests: Outcomes of OECD 309-type suspension tests were highly variable both within but also between test systems. Least intrastudy variabilities were observed in the test systems with the highest sediment content, i.e., 10 g solid L^{-1}. In the 1 g solids L^{-1} suspension tests, derived $DT_{50,TS,susp}$ differed by up to two orders of magnitude between studies and experimental replicates. Intrastudy variations, i.e., experimental replicates drifting apart over the time course of an experiment, make the interpretation of biotransformation study outcomes challenging. Interstudy variations depend on origin and sampling period of the microbial test community and may be considered an indicator of strong fluctuations in biotransformation potential for a given a compound under spatially and temporally varying conditions of natural aquatic environments (Gilbert et al. 2012; Staley et al. 2015; Sun et al. 2017). Furthermore, the here presented data show, in agreement with the results of Shrestha et al. (2016), that keeping sediment in suspension in OECD 309 studies via magnetic stirrer leads

to grinding of particles and continuously increasing sorption of chemicals, which makes differentiation between compound removal via transformation versus sorption difficult.

Standard and modified OECD 308-type studies: Generally, biotransformation in standard and modified OECD 308-type studies appeared more reproducible, yielding more robust results than in suspension tests, as indicated by short lag phases and low intrastudy variabilities. The modifications introduced in the modified OECD 308-type studies had aimed to (i) further standardize the test system by reducing variability in test setup (define vessel geometry, water and sediment thickness and ratio, and aeration to obtain more homogenous redox conditions in sediment layer), and (ii) to shift observed processes from sorption to transformation and increasing the transformation signal. Indeed, when comparing compound dissipation from standard and modified OECD 308-type studies, biotransformation appeared to be enhanced in modified systems. We further observed smaller interstudy variability in the modified system compared to the standard system for the majority of compounds.This could at least partially be due to higher bioavailability and hence less influence of different TOC contents in modified studies. However, based on our data, we cannot fully elucidate the additional influence of other factors such as compound concentration, mixture spike or system geometry on the compounds' biotransformation behavior.

Data evaluation to obtain degradation half-lives for the water phase ($DegT_{50,w}$): Disentangling sorption and transformation was achieved by an evaluation procedure that is able to derive compartment-specific DegT50 values. When comparing degradation half-lives in water ($DegT_{50,w}$) to dissipation half-lives in water in modified OECD 308-type studies ($DT_{50,w}$), it was obvious that $DT_{50,w}$ are strongly influenced by dispersion and phase transfer processes, and hence depend on the experimental system and employed sediment. Especially for compounds that tend to sorb to particles, $DT_{50,w}$ underestimates persistence considerably, and hence should not be used in persistence assessment. However, to derive proper degradation half-lives in water ($DegT_{50,w}$), measurement and recording of additional (meta)data is required (i.e., K_{oc} for the sediment(s) in the simulation test, porosity and organic carbon content of the sediment, DOC and TOC in the water phase, hydrolysis rate (if applicable), and exact height of water and sediment column), which are presently not included at all or not required to be reported in the OECD 308 test guideline. This evaluation procedure can be applied to both standard and modified OECD 308 tests, if the respective (meta)data are measured and reported. By using the software OECD Analyser (Honti et al. (2016), further developed in this project), derivation of degradation indicators from OECD 308-type studies is possible.

Comparison of degradation indicators derived from OECD 309 and 308 studies: $DT_{50,TS,mod308}$ values derived from modified OECD 308-type systems were in the same range as the more variable $DT_{50,TS,susp}$ values derived from OECD 309 suspension tests for the majority of test compounds.

Comparison of Persistence Indicators Derived from Laboratory and Field Studies

Derivation of k'_{bio} values from simulation study and field data: For modified OECD 308-type studies, it was possible to derive second-order biomass-normalized and bioavailability-corrected rate constants ($k'_{bio,lab}$) which well described compound dissipation from sediment and water phase in both studies. For the field, the model centred around $k'_{bio,field}$ could be fitted well to the SMPC observations, yet the derived biotransformation rate constants contained significant

uncertainty due to the cross-dependence with other, weakly defined quantities, such as exact emissions and abiotic transformation rates. Still, there was a clear pattern between the P1 and P3 campaigns of SMPC, suggesting that the warmer weather and the corresponding higher microbial activity contributed to elevated biotransformation rates. The second-order rates could be transformed into average field half-lives by using the physical dimensions and sediment concentrations from the characteristic cross-section of the Rhine. These average field half-lives highlighted that field data can only be used to identify transformation half-lives on the time-scale comparable to travel times between the observation points, which was equal to a few hours to a couple of days for the Rhine.

Comparison of persistence indicators from laboratory and field studies: A comparison between half-lives and k'_{bio} values derived from modified OECD 308-type studies and the field study in the Rhine river catchment revealed that persistence indicators correlated when derived from data of the P3 campaign. However, there was no perfect equivalence and different indicators explain varying fractions of observed variance. For $k'_{bio,mod308}$, $k'_{bio,field}$, $DegT_{50,w,mod308}$, $DegT_{50,w,field}$ and $DegT_{50,TS,field}$, we found a statistically significant moderate correlation between compound behavior in modified OECD 308-type studies and in the Rhine river catchment. Correlations were strongest when comparing $k'_{bio,lab}$ and $k'_{bio,field}$ values or half-lives derived thereof, i.e., $DegT_{50,w,mod308}$ and $DegT_{50,w,field}$, respectively. Also when compared to degradation in the field, it became clear that laboratory-derived dissipation half-lives in water, i.e., $DT_{50,w}$ values, underestimate persistence.
Total system half-lives are more easily derived from laboratory OECD 308-type studies than degradation indicators that require more complicated inverse modeling. Therefore, also total system half-lives $DT_{50,TS}$ and total system degradation $DegT_{50,TS,field}$ were compared. The resulting correlation was still statistically significant, yet it was the weakest amongst all comparisons of degradation indicators.
Biotransformation indicators derived from the modified OECD 308 studies were about two orders of magnitude lower on average than those derived from the field data. This difference might partially reflect true differences in biomass activity and compound bioavailability between batch laboratory systems and continuously flowing field systems, yet it might also partially be an artifact of TOC normalization. TOC used as proxy for degrader biomass is a practical but certainly not very accurate choice. It is worth acknowledging the double role that TOC plays. On the one hand side increasing TOC signifies more biomass, more biological activity and thus increased biotransformation, and on the other side increasing TOC levels (not for all but for many of the studied compounds) predicts higher sorption and therefore lower bioavailability and consequently lower biotransformation. Developments for better predictors for active biomass are underway (Seller et al. 2021) and values between laboratory and field may converge more for more accurate estimators of degrader biomass in the respective system that might become available in the future.

A number of discussion points arise from the above summarized main outcomes of the project:

Deriving robust degradation information based on biotransformation simulation studies: Both persistence and exposure assessment ultimately rely on robust degradation information, i.e., information that is ideally valid across similar environments and independent of differences in experimental setup. In this work, we contributed toward the goal of deriving robust degradation information in two ways. We showed that alternative data evaluation procedures, such as the k'bio-concept, can support the evaluation of variable outcomes of biotransformation simulation studies; it was possible to derive $k'_{bio,lab}$ values that unified observations in two different water-sediment laboratory systems. The further exploration of the k'_{bio}-concept and its potential to bridge between compound behavior in different aquatic systems may benefit from a better

description of degrader biomass present in the respective systems, as our data shows that a community's biotransformation capacity does not scale proportionally with TOC and might even dynamically change during experiments, at least in the case of OECD 309 studies. We showed that the modified OECD 308 setup (in combination with inverse modeling) further allows disentangling degradation from phase transfer processes and deriving compartment-specific half-lives that represent mostly aerobic biotransformation at the water-sediment interface. In combination with a strict anaerobic OECD 308 study, k'_{bio} and compartment-specific half-lives values thus derived should allow representing a wide range of environmental situations encountered in surface water bodies.

Estimating persistence in river catchments from laboratory simulation studies: There is no generally valid answer to the question how well persistence indicators derived from laboratory studies can predict observed degradation behavior in the field. We can think about this in terms of rough categories, relative and absolute behavior. In terms of categories, compounds consistently classified as hardly degraded in the laboratory simulation studies (i.e., carbamazepine, lamotrigine, gabapentin, venlafaxine, citalopram, etc.) were also found to be not or slowly transformed in the field. Similarly, compounds consistently degraded to large extents in the laboratory simulation studies (i.e., valsartan, levetiracetam, bezafibrate, atenolol, sulfamethoxazole, saccharin, cyclamate, etc.) also showed clearly observable degradation in the field during the P3 campaign. In terms of relative behavior, total half-lives derived from modified OECD 308 test systems as well as k'_{bio} values yield moderate, statistically significant correlations between laboratory and field data. Interestingly, however, correlations were stronger in case persistence indicators were derived based on the k'_{bio}-concept (e.g. $DegT_{50w}$). The absolute comparison between persistence indicators derived from laboratory experiments and the field study suggested that biotransformation is generally slower in modified OECD 308-type experiments than the model predicts for the Rhine river catchment. However, this absolute difference could also result from the fact that microbial degrader activity does not scale with TOC. We therefore recommend to explore further methods for improved characterization of specific degrader biomass in order to reevaluate the k'_{bio}- concept, as it has the potential to further improve the estimation of persistence in the field from laboratory-based simulation studies.

7 List of References

Achermann, Stefan, Per Falås, Adriano Joss, Cresten B. Mansfeldt, Yujie Men, Bernadette Vogler, and Kathrin Fenner. 2018. 'Trends in Micropollutant Biotransformation along a Solids Retention Time Gradient', *Environmental Science & Technology*, 52: 11601-11.

Ahtiainen, Jukka, Miia Aalto, and Piia Pessala. 2003. 'Biodegradation of chemicals in a standardized test and in environmental conditions', *Chemosphere*, 51: 529-37.

Anliker, Sabine, Martin Loos, Rahel Comte, Matthias Ruff, Kathrin Fenner, and Heinz Singer. 2020. 'Assessing Emissions from Pharmaceutical Manufacturing Based on Temporal High-Resolution Mass Spectrometry Data', *Environmental Science & Technology*, 54: 4110-20.

Appiani, Elena, Rachele Ossola, Douglas E Latch, Paul R Erickson, and Kristopher McNeill. 2017. 'Aqueous singlet oxygen reaction kinetics of furfuryl alcohol: effect of temperature, pH, and salt content', *Environmental Science: Processes & Impacts*, 19: 507-16.

Azuma, T., N. Arima, A. Tsukada, S. Hirami, R. Matsuoka, R. Moriwake, H. Ishiuchi, T. Inoyama, Y. Teranishi, M. Yamaoka, M. Ishida, K. Hisamatsu, A. Yunoki, and Y. Mino. 2017. 'Distribution of six anticancer drugs and a variety of other pharmaceuticals, and their sorption onto sediments, in an urban Japanese river', *Environ Sci Pollut Res Int*, 24: 19021-30.

Bayer, A., Asner, R., Schüssler, W., Kopf, W., Weiss, K., Segel, M., Letzel, M. 2014. Behavior of sartans (antihypertensive drugs) in wastewater treatment plants, their occurrence and risk for the aquatic environment. Environ Sci Pollut Res 21, 10830–10839 (2014). https://doi.org/10.1007/s11356-014-3060-z

Beretsou, Vasiliki G., Aikaterini K. Psoma, Pablo Gago-Ferrero, Reza Aalizadeh, Kathrin Fenner, and Nikolaos S. Thomaidis. 2016. 'Identification of biotransformation products of citalopram formed in activated sludge', *Water Research*, 103: 205-14.

Besmer, Michael D., David G. Weissbrodt, Bradley E. Kratochvil, Jürg A. Sigrist, Mathias S. Weyland, and Frederik Hammes. 2014. 'The feasibility of automated online flow cytometry for in-situ monitoring of microbial dynamics in aquatic ecosystems', *Frontiers in Microbiology*, 5.

Birch, Heidi, Rikke Hammershøj, Mike Comber, and Philipp Mayer. 2017. 'Biodegradation of hydrocarbon mixtures in surface waters at environmentally relevant levels – Effect of inoculum origin on kinetics and sequence of degradation', *Chemosphere*, 184: 400-07.

Blunt, Susanna M., Joshua D. Sackett, Michael R. Rosen, Mark J. Benotti, Rebecca A. Trenholm, Brett J. Vanderford, Brian P. Hedlund, and Duane P. Moser. 2018. 'Association between degradation of pharmaceuticals and endocrine-disrupting compounds and microbial communities along a treated wastewater effluent gradient in Lake Mead', *Science of the Total Environment*, 622-623: 1640-48.

Boeije, G. 2000. Incorporation of biofilm activity in river biodegradation modeling: a case study for linear alkylbenzene sulphonate (LAS). Water Research 34(5), 1479-1486. doi:10.1016/s0043-1354(99)00279-1.

Boethling, Robert, Kathrin Fenner, P Howard, Gary Klečka, Torben Madsen, Jason R Snape, and Mick J Whelan. 2009. 'Environmental Persistence of Organic Pollutants: Guidance for Development and Review of POP Risk Profiles', *Integrated Environmental Assessment and Management*, 5: 539-56.

Castiglioni S, Bagnati R, Fanelli R, Pomati F, Calamari D, Zuccato E (2006): Removal of pharmaceuticals in sewage treatment plants in Italy. Environ Sci Technol 40:357–363

Castronovo, S., Wick, A., Scheurer, M., Nödler, K., Schulz, M., & Ternes, T. A. (2017). Biodegradation of the artificial sweetener acesulfame in biological wastewater treatment and sandfilters. *Water Research*, 110, 342–353. doi:10.1016/j.watres.2016.11.041

CHMP, Committee for Medical Products for Human Use. 2006. 'EMEA/CHMP/SWP/4447/00 corr 2 Guideline on the Environmental Risk Assessment of Medical Products for Human Use'.

Coll, Claudia, Raven Bier, Zhe Li, Silke Langenheder, Elena Gorokhova, and Anna Sobek. 2020. 'Association between Aquatic Micropollutant Dissipation and River Sediment Bacterial Communities', *Environmental Science & Technology*, 54: 14380-92.

Comber, M, Holt, M. 2010. 'Developing a set of reference chemicals for use in biodegradability tests for assessing the persistency of chemicals'.

Cousins, Ian T., Carla A. Ng, Zhanyun Wang, and Martin Scheringer. 2019. 'Why is high persistence alone a major cause of concern?', *Environmental Science: Processes & Impacts*, 21: 781-92.

Davis, C. A., Erickson, P. R., McNeill, K., & Janssen, E. M. L. (2017): Environmental photochemistry of fenamate NSAIDs and their radical intermediates. Environ. Sci.: Processes Impacts, 2017, 19, 656. doi: 10.1039/c7em00079k.

Davis, Caroline A., and Elisabeth M. L. Janssen. 2020. 'Environmental fate processes of antimicrobial peptides daptomycin, bacitracins, and polymyxins', Environment International, 134: 105271.

Delli Compagni, Riccardo, Fabio Polesel, Kerstin J. F. von Borries, Zhen Zhang, Andrea Turolla, Manuela Antonelli, and Luca Vezzaro. 2020. 'Modelling the fate of micropollutants in integrated urban wastewater systems: Extending the applicability to pharmaceuticals', *Water Research*, 184: 116097.

Dulin, David, and Theodore Mill. 1982. 'Development and evaluation of sunlight actinometers', *Environmental Science & Technology*, 16: 815-20.

ECHA. 2017. 'Guidance on Information Requirements and Chemical Safety Assessment, Chapter R.11: PBT/vPvB assessment, Version 3.0'.

EFSA, European Food Safety Authority. 2014. 'EFSA Guidance Document for evaluating laboratory and field dissipation studies to obtain DegT50 values of active substances of plant protection products and transformation products of these active substances in soil', *EFSA Journal*, 12: 3662.

Ejarque, Elisabet, Anna Freixa, Eusebi Vazquez, Alba Guarch, Stefano Amalfitano, Stefano Fazi, Anna M. Romaní, and Andrea Butturini. 2017. 'Quality and reactivity of dissolved organic matter in a Mediterranean river across hydrological and spatial gradients', *Science of the Total Environment*, 599-600: 1802-12.

EP&C. 2006. 'Regulation (EC) No 1907/2006 of the European Parliament and of the Council of 18 December 2006 concerning the registration, evaluation, authorisation and restriction of chemicals (REACH), establishing a European chemicals agency, amending directive 1999/45/EC and repealing Council Regulation (EEC) No 793/93 and Commission Regulation (EC) No 1488/94 as well as Council Directive 76/769/EEC and Commission Directives 91/155/EEC, 93/67/EEC, 93/105/EC and 2000/21/EC. Off J Eur Commun, L 396/1', *Official Journal of the European Union*.

Fahlman, Johan, Jerker Fick, Jan Karlsson, Micael Jonsson, Tomas Brodin, and Jonatan Klaminder. 2018. 'Using laboratory incubations to predict the fate of pharmaceuticals in aquatic ecosystems', *Environmental Chemistry*, 15: 463-71.

Falås, P., Wick, A., Castronovo, S., Habermacher, J., Ternes, T. A., & Joss, A. (2016). Tracing the limits of organic micropollutant removal in biological wastewater treatment. *Water Research, 95, 240–249.* doi:10.1016/j.watres.2016.03.009

Fenner, K., Stamm, C., Bischoff, F., Honti, M., Varga, L. (2017): Suitability of laboratory simulation tests for the identification of persistence in surface waters. Umweltbundesamt, Texte 40/2017. FKZ 3715 65 415 3. URL: https://www.umweltbundesamt.de/en/publikationen/suitability-of-laboratory-simulation-tests-for-the

Fick J, Lindberg RH, Kaj L, Brorström-Lundén E (2011): Results from the Swedish National Screening Programme 2010; Subreport 3. Pharmaceuticals. Swedish Environmental Research Institute.

Fischer, Helmut, Susanne C. Wanner, and Martin Pusch. 2002. 'Bacterial abundance and production in river sediments as related to the biochemical composition of particulate organic matter (POM)', *Biogeochemistry*, 61: 37-55.

FOCUS. 2006. ' "Guidance Document on Estimating Persistence and Degradation Kinetics from Environmental Fate Studies on Pesticides in EU Registration" Report of the FOCUS Work Group on Degradation Kinetics, EC Document Reference Sanco/10058/2005 version 2.0, 434 pp'.

Gilbert, Jack A., Joshua A. Steele, J. Gregory Caporaso, Lars Steinbrück, Jens Reeder, Ben Temperton, Susan Huse, Alice C. McHardy, Rob Knight, Ian Joint, Paul Somerfield, Jed A. Fuhrman, and Dawn Field. 2012. 'Defining seasonal marine microbial community dynamics', *The ISME Journal*, 6: 298-308.

Goodhead, Andrew K., Ian M. Head, Jason R. Snape, and Russell J. Davenport. 2014. 'Standard inocula preparations reduce the bacterial diversity and reliability of regulatory biodegradation tests', *Environmental Science and Pollution Research*, 21: 9511-21.

Götz, C.; Otto, J.; Singer, H. . 2015. 'Überprüfung des Reinigungseffekts. Auswahl geeigneter organisher Spurenstoffe ', *Aqua & Gas*, 95: 34-40.

Gulkowska A, Leung H W, So M K, Taniyasu S, Yamashita N, Yeung LW Y, Richardson B J, Lei A P, Giesy J P, Lam P K S (2008): Removal of antibiotics from wastewater by sewage treatmentfacilities in Hong Kong and Shenzhen, China. Water Research, 42(1-2): 395–403

Gurke R, Rößler M, Marx C, et al. (2015): Occurrence and removal of frequently prescribed pharmaceuticals and corresponding metabolites in wastewater of a sewage treatment plant. Sci. Total. Environ. 532:762-770. doi:10.1016/j.scitotenv.2015.06.067

Hammershøj, Rikke, Heidi Birch, Aaron D. Redman, and Philipp Mayer. 2019. 'Mixture Effects on Biodegradation Kinetics of Hydrocarbons in Surface Water: Increasing Concentrations Inhibited Degradation whereas Multiple Substrates Did Not', *Environmental Science & Technology*, 53: 3087-94.

Hart, D. S., L. C. Davis, L. E. Erickson, and T. M. Callender. 2004. 'Sorption and partitioning parameters of benzotriazole compounds', *Microchemical Journal*, 77: 9-17.

Helbling, Damian E., Juliane Hollender, Hans-Peter E. Kohler, Heinz Singer, and Kathrin Fenner. 2010. 'High-Throughput Identification of Microbial Transformation Products of Organic Micropollutants', *Environmental Science & Technology*, 44: 6621-27.

Henning, Nina, Per Falås, Sandro Castronovo, Kevin S. Jewell, Kai Bester, Thomas A. Ternes, and Arne Wick. 2019. 'Biological transformation of fexofenadine and sitagliptin by carrier-attached biomass and suspended sludge from a hybrid moving bed biofilm reactor', *Water Research*, 167: 115034.

Hoch, N. (2019): Mass balance modelling in Lake Greifensee – How much evidence is there for pharmaceutical biotransformation?, Master thesis, ETH Zürich, 2019.

Honti, M., F. Bischoff, A. Moser, C. Stamm, S. Baranya, and K. Fenner. 2018. 'Relating Degradation of Pharmaceutical Active Ingredients in a Stream Network to Degradation in Water-Sediment Simulation Tests', *Water Resources Research*, 54: 9207-23.

Honti, Mark, and Kathrin Fenner. 2015. 'Deriving Persistence Indicators from Regulatory Water-Sediment Studies - Opportunities and Limitations in OECD 308 Data', *Environmental Science & Technology*, 49: 5879-86.

Honti, Mark, Stefan Hahn, Dieter Hennecke, Thomas Junker, Prasit Shrestha, and Kathrin Fenner. 2016. 'Bridging across OECD 308 and 309 Data in Search of a Robust Biotransformation Indicator', *Environmental Science & Technology*, 50: 6865-72.

Jaeger, A., M. Posselt, A. Betterle, J. Schaper, J. Mechelke, C. Coll, and J. Lewandowski. 2019. 'Spatial and Temporal Variability in Attenuation of Polar Organic Micropollutants in an Urban Lowland Stream', *Environmental Science & Technology*, 53: 2383-95.

Jaeger, Anna, Claudia Coll, Malte Posselt, Jonas Mechelke, Cyrus Rutere, Andrea Betterle, Muhammad Raza, Anne Mehrtens, Karin Meinikmann, Andrea Portmann, Tanu Singh, Phillip J. Blaen, Stefan Krause, Marcus A. Horn, Juliane Hollender, Jonathan P. Benskin, Anna Sobek, and Joerg Lewandowski. 2019. 'Using recirculating flumes and a response surface model to investigate the role of hyporheic exchange and bacterial diversity on micropollutant half-lives', *Environmental Science: Processes & Impacts*, 21: 2093-108.

Johnson, D. R., D. E. Helbling, T. K. Lee, J. Park, K. Fenner, H. P. E. Kohler, and M. Ackermann. 2015. 'Association of Biodiversity with the Rates of Micropollutant Biotransformations among Full-Scale Wastewater Treatment Plant Communities', *Applied and Environmental Microbiology*, 81: 666-75.

Kahl, Stefanie, Sabine Kleinsteuber, Jaime Nivala, Manfred van Afferden, and Thorsten Reemtsma. 2018. 'Emerging Biodegradation of the Previously Persistent Artificial Sweetener Acesulfame in Biological Wastewater Treatment', *Environmental Science & Technology*, 52: 2717-25.

Kasprzyk-Hordern, Barbara, Richard M. Dinsdale, and Alan J. Guwy. 2009. 'The removal of pharmaceuticals, personal care products, endocrine disruptors and illicit drugs during wastewater treatment and its impact on the quality of receiving waters', *Water Research*, 43: 363-80.

Kern, Susanne, Rebekka Baumgartner, Damian Helbling, Juliane Hollender, Heinz Singer, Martin Loos, René Schwarzenbach, and Kathrin Fenner. 2010. 'A tiered procedure for assessing the formation of biotransformation products of pharmaceuticals and biocides during activated sludge treatment', *Journal of environmental monitoring : JEM*, 12: 2100-11.

Kleinsteuber, Sabine, Thore Rohwerder, Ute Lohse, Bettina Seiwert, and Thorsten Reemtsma. 2019. 'Sated by a Zero-Calorie Sweetener: Wastewater Bacteria Can Feed on Acesulfame', *Frontiers in Microbiology*, 10.

Lara-Martín, P. A.; Gómez-Parra, A.; Köchling, T.; Sanz, J. L.; Amils, R.; González-Mazo, E., Anaerobic Degradation of Linear Alkylbenzene Sulfonates in Coastal Marine Sediments. Environ. Sci. Technol. 2007, 41 (10), 3573-3579.

Laszakovits, Juliana, Stephanie Berg, Brady Anderson, Jessie O'Brien, Kristine Wammer, and Charles Sharpless. 2016. 'The p-Nitroanisole/Pyridine and p-Nitroacetophenone/Pyridine Actinometers Revisited: Quantum Yield in Comparison to Ferrioxalate', *Environmental Science & Technology Letters*, 4.

Launay, Marie A., Ulrich Dittmer, and Heidrun Steinmetz. 2016. 'Organic micropollutants discharged by combined sewer overflows – Characterisation of pollutant sources and stormwater-related processes', *Water Research*, 104: 82-92.

Li, S., Geng, J., Wu, G. et al. (2018): Removal of artificial sweeteners and their effects on microbial communities in sequencing batch reactors. Sci Rep 8, 3399 (2018). https://doi.org/10.1038/s41598-018-21564-x

Li, Zhe, Sarit L. Kaserzon, Merle M. Plassmann, Anna Sobek, Maria Jose Gomez Ramos, and Michael Radke. 2017. 'A strategic screening approach to identify transformation products of organic micropollutants formed in natural waters', *Environmental Science-Processes & Impacts*, 19: 488-98.

Li, Zhe, and Michael S. McLachlan. 2019. 'Biodegradation of Chemicals in Unspiked Surface Waters Downstream of Wastewater Treatment Plants', *Environmental Science & Technology*, 53: 1884-92.

Li, Zhe, and Michael S. McLachlan. 2020. 'Comparing non-targeted chemical persistence assessed using an unspiked OECD 309 test to field measurements', *Environmental Science: Processes & Impacts*, 22: 1233-42.

Loeffler, Dirk, Annika Hatz, Dinah Albrecht, Marvin Fligg, Jens Hogeback, and Thomas A. Ternes. 2020. 'Determination of non-extractable residues in soils: Towards a standardised approach', *Environmental Pollution*, 259: 113826.

Manning, Robert, John Purser Griffith, TF Pigot, and Leveson Francis Vernon-Harcourt. 1890. *On the flow of water in open channels and pipes*.

Martin, Timothy J., Jason R. Snape, Abigail Bartram, Aidan Robson, Kishor Acharya, and Russell J. Davenport. 2017. 'Environmentally Relevant Inoculum Concentrations Improve the Reliability of Persistent Assessments in Biodegradation Screening Tests', *Environmental Science & Technology*, 51: 3065-73.

Mbah, Chika. 2005. 'Kinetics of decomposition of irbesartan in aqueous solutions determined by high performance liquid chromatography', *Die Pharmazie*, 59: 920-2.

McLachlan, Michael S., Hongyan Zou, and Todd Gouin. 2017. 'Using Benchmarking To Strengthen the Assessment of Persistence', *Environmental Science & Technology*, 51: 4-11.

Neumann M, Schliebner I 2019. 'Protecting the sources of our drinking water: The criteria for identifying Persistent, Mobile, and Toxic (PMT) substances and very Persistent, and very Mobile (vPvM) substances under the EU chemical legislation REACH', *UBA Texte 127/2019. ISSN: 1862-4804*.

Oberoi, Akashdeep Singh, Yanyan Jia, Huiqun Zhang, Samir Kumar Khanal, and Hui Lu. 2019. 'Insights into the Fate and Removal of Antibiotics in Engineered Biological Treatment Systems: A Critical Review', *Environmental Science & Technology*, 53: 7234-64.

OECD. 2002. *Test No. 308: Aerobic and Anaerobic Transformation in Aquatic Sediment Systems*.

OECD. 2004. *Test No. 309: Aerobic Mineralisation in Surface Water – Simulation Biodegradation Test*.

Oelkers, Kim, and Carolin Floeter. 2019. 'The accessibility of data on environmental risk assessment of pharmaceuticals: Is the marketing authorisation procedure in conflict with the international right of access to environmental information?', *Environmental sciences Europe*, 31: 58.

Ort, Christoph, Michael G. Lawrence, Julien Reungoat, and Jochen F. Mueller. 2010. 'Sampling for PPCPs in Wastewater Systems: Comparison of Different Sampling Modes and Optimization Strategies', *Environmental Science & Technology*, 44: 6289-96.

Ort, Christoph, Michael G. Lawrence, Jörg Rieckermann, and Adriano Joss. 2010. 'Sampling for Pharmaceuticals and Personal Care Products (PPCPs) and Illicit Drugs in Wastewater Systems: Are Your Conclusions Valid? A Critical Review', *Environmental Science & Technology*, 44: 6024-35.

Ott, Amelie, Timothy J. Martin, Jason R. Snape, and Russell J. Davenport. 2020. 'Increased cell numbers improve marine biodegradation tests for persistence assessment', *Science of the Total Environment*, 706: 135621.

Otto, J., Singer, H. und Götz, C. (2014): Substanzen zur Überprüfung des Reinigungseffekts weitergehender Abwasserbehandlungsverfahren, Fachbericht im Auftrag des Bundesamts für Umwelt BAFU, Eawag, Dübendorf.

Patrolecco, Luisa, Silvio Capri, and Nicoletta Ademollo. 2014. 'Occurrence of selected pharmaceuticals in the principal sewage treatment plants in Rome (Italy) and in the receiving surface waters', *Environmental Science and Pollution Research*, 22.

Paxeus N (2004): Removal of selected non-steroidal anti-inflammatory drugs (NSAIDs), gemfibrozil, carbamazepine, beta-blockers, trimethoprim and triclosan in conventional wastewater treatment plants in five EU countries and their discharge to the aquatic environment. Water Sci Technol 50:253–260

Poursat, Baptiste AJ, Rob JM van Spanning, Pim de Voogt, and John R Parsons. 2019. 'Implications of microbial adaptation for the assessment of environmental persistence of chemicals', *Critical Reviews in Environmental Science and Technology*, 49: 2220-55.

R Core Team (2013): R: A language and environment for statistical computing. R Foundation for Statistical Computing, Vienna, Austria. url: https://www.R-project.org/.

Radke, Michael, and Michael P. Maier. 2014. 'Lessons learned from water/sediment-testing of pharmaceuticals', *Water Research*, 55: 63-73.

Rúa-Gómez PC, Püttmann W (2012): Occurrence and removal of lidocaine, tramadol, venlafaxine, and their metabolites in German wastewater treatment plants. Environ Sci Pollut Res 19:689–699

Ruff, Matthias, Miriam S. Mueller, Martin Loos, and Heinz P. Singer. 2015. 'Quantitative target and systematic non-target analysis of polar organic micro-pollutants along the river Rhine using high-resolution mass-spectrometry – Identification of unknown sources and compounds', *Water Research*, 87: 145-54.

Scheurer, M., Brauch, H.-J., Lange, F.T., (2009): Analysis and occurrence of seven artificial sweeteners in German waste water and surface water and in soil aquifertreatment (SAT). Anal. Bioanal. Chem. 394, 1585–1594, http://dx.doi.org/10.1007/s00216-009-2881-y.

Schmidt, K.-H., & Unbenannt, M. (2003): Schwebstofftransport–die Fliessgewässer als

Transportbänder. In S. Tzschaschel (Ed.), Nationalatlas Bundesrepublik Deutschland—Band 2, Natur und Umwelt I: Relief, Boden und Wasser (pp. 136–137). Leipzig, Germany: Institut für Länderkunde".

Schymanski, Emma L., Heinz P. Singer, Philipp Longrée, Martin Loos, Matthias Ruff, Michael A. Stravs, Cristina Ripollés Vidal, and Juliane Hollender. 2014. 'Strategies to Characterize Polar Organic Contamination in Wastewater: Exploring the Capability of High Resolution Mass Spectrometry', *Environmental Science & Technology*, 48: 1811-18.

Seller, Carolin, Mark Honti, Heinz Singer, and Kathrin Fenner. 2020. 'Biotransformation of Chemicals in Water–Sediment Suspensions: Influencing Factors and Implications for Persistence Assessment', *Environmental Science & Technology Letters*, 7: 854-60.

Seller, C.; Özel Duygan, B. D.; Honti, M.; Fenner, K., Biotransformation of Chemicals at the Water–Sediment Interface—Toward a Robust Simulation Study Setup. *ACS Environmental Au* 2021.

Shrestha, P., T. Junker, K. Fenner, S. Hahn, M. Honti, R. Bakkour, C. Diaz, and D. Hennecke. 2016. 'Simulation Studies to Explore Biodegradation in Water-Sediment Systems: From OECD 308 to OECD 309', *Environmental Science & Technology*, 50: 6856-64.

Singer, Heinz, Sylvia Jaus, Irene Hanke, Alfred Lück, Juliane Hollender, and Alfredo C. Alder. 2010. 'Determination of biocides and pesticides by on-line solid phase extraction coupled with mass spectrometry and their behaviour in wastewater and surface water', *Environmental Pollution*, 158: 3054-64.

Singer, Heinz P., Annika E. Wössner, Christa S. McArdell, and Kathrin Fenner. 2016. 'Rapid Screening for Exposure to "Non-Target" Pharmaceuticals from Wastewater Effluents by Combining HRMS-Based Suspect Screening and Exposure Modeling', *Environmental Science & Technology*, 50: 6698-707.

Sipma, J., Osuna, B., Collado, N., Monclus, H., Ferrero, G., Comas, J. and Rodriguez-Roda, I. (2010): Comparison of removal of pharmaceuticals in MBR and activated sludge systems. Desalination, 250 (2010), pp. 653-659

Staley, Christopher, Trevor J. Gould, Ping Wang, Jane Phillips, James B. Cotner, and Michael J. Sadowsky. 2015. 'Species sorting and seasonal dynamics primarily shape bacterial communities in the Upper Mississippi River', *Science of the Total Environment*, 505: 435-45.

Sun, Wei, Chunyu Xia, Meiying Xu, Jun Guo, and Guoping Sun. 2017. 'Seasonality Affects the Diversity and Composition of Bacterioplankton Communities in Dongjiang River, a Drinking Water Source of Hong Kong', *Frontiers in Microbiology*, 8.

Ternes T. (1998): Occurrence of drugs in German sewage treatment plants and rivers.Wat.Res.,32(11), 3245-3260.

TK Consult AG (2013): Überflutung Beznau – Ermittlung der maximalen Überflutungshöhe der Beznau-Insel unter Berücksichtigung von Feststofftransport (Tech. Rep.) Zürich, Switzerland: Eidgenössisches Nuklearsicherheitsinspektorat ENSI.

Vieno NM, Tuhkanen T, Kronberg L (2005): Seasonal variation in the occurrence of pharmaceuticals in effluents from a sewage treatment plant and in the recipient water. Environ Sci Technol 39:8220–8226

Wang, Y., Fenner, K., Helbling, D.E. (2020): Clustering micropollutants based on initial biotransformations for improved prediction of micropollutant removal during conventional activated sludge treatment. Environmental Science: Water Research & Technology, 6(3), 554-565. doi:10.1039/C9EW00838A

Whitman, William, David Coleman, and W. J. Wiebe. 1998. 'Prokaryotes: the unseen majority', *Proceedings of the National Academy of Sciences of the United States of America*, 95: 6578-83.

Xu, Yibo, Xiaoqin Yu, Baile Xu, Dan Peng, and Xuetao Guo. 2021. 'Sorption of pharmaceuticals and personal care products on soil and soil components: Influencing factors and mechanisms', *Science of the Total Environment*, 753: 141891.

Zou, Hongyan, Matthew MacLeod, and Michael S. McLachlan. 2014. 'Evaluation of the potential of benchmarking to facilitate the measurement of chemical persistence in lakes', *Chemosphere*, 95: 301-09.

Zou, Hongyan, Michael Radke, Amelie Kierkegaard, Matthew MacLeod, and Michael S. McLachlan. 2015. 'Using Chemical Benchmarking to Determine the Persistence of Chemicals in a Swedish Lake', *Environmental Science & Technology*, 49: 1646-53.

Zou, Hongyan, Michael Radke, Amelie Kierkegaard, and Michael S. McLachlan. 2015. 'Temporal Variation of Chemical Persistence in a Swedish Lake Assessed by Benchmarking', *Environmental Science & Technology*, 49: 9881-88.

A Appendix

Table of Content

List of Tables

List of Figures

A.1 Supplementary Methods for Evaluation of Biotransformation Simulation Studies

Figure A 1: Sampling of sediment from the Rhine for OECD 309-type suspension tests

Sampling site at Mumpf, Switzerland. Sediment for OECD 309-type suspension tests was being sampled by carefully sucking the surface layer of the bottom 1 cm bulk sediment through a tube (Ø= 2 cm) connected to a drill pump.
Source: own figure, Eawag

Figure A 2: Experimental setup of OECD 309-type suspension tests

Source: own figure, Eawag

Figure A 3: Experimental setup of OECD 308-type studies

Source: own figure, Eawag

Table A 1: Data requirements necessary to derive k'_{bio}, $DegT_{50,w}$ and $DegT_{50,sed}$ from modified OECD 308-type studies

Parameter	Meaning	Unit
K_{oc}	Sediment adsorption coefficient (ideally determined for the same sediment as in the simulation study).	L kg^{-1}
$f_{oc,sed}$	Organic carbon content of sediment.	%
TOC_w	Total organic carbon concentration in the water phase	mg L^{-1}
k_{hydr}	First-order hydrolysis rate.	d^{-1}
$m_{sed,dry}$	Dry sediment mass added to the test system. Bulk density and porosity can be calculated based on sediment dry mass and volume of the bulk sediment layer.	g
Z_w	Height of the water column in modified OECD 308-tpye studies.	cm
Z_s	Height of the sediment column in modified OECD 308-type studies.	cm
Ø	Diameter of test vessel. Needed to calculate volume of bulk sediment laver.	cm

A.2 Complementary Results of Biotransformation Simulation Studies

Figure A 4: Compound concentration in the water phase during OECD 309-type suspension tests

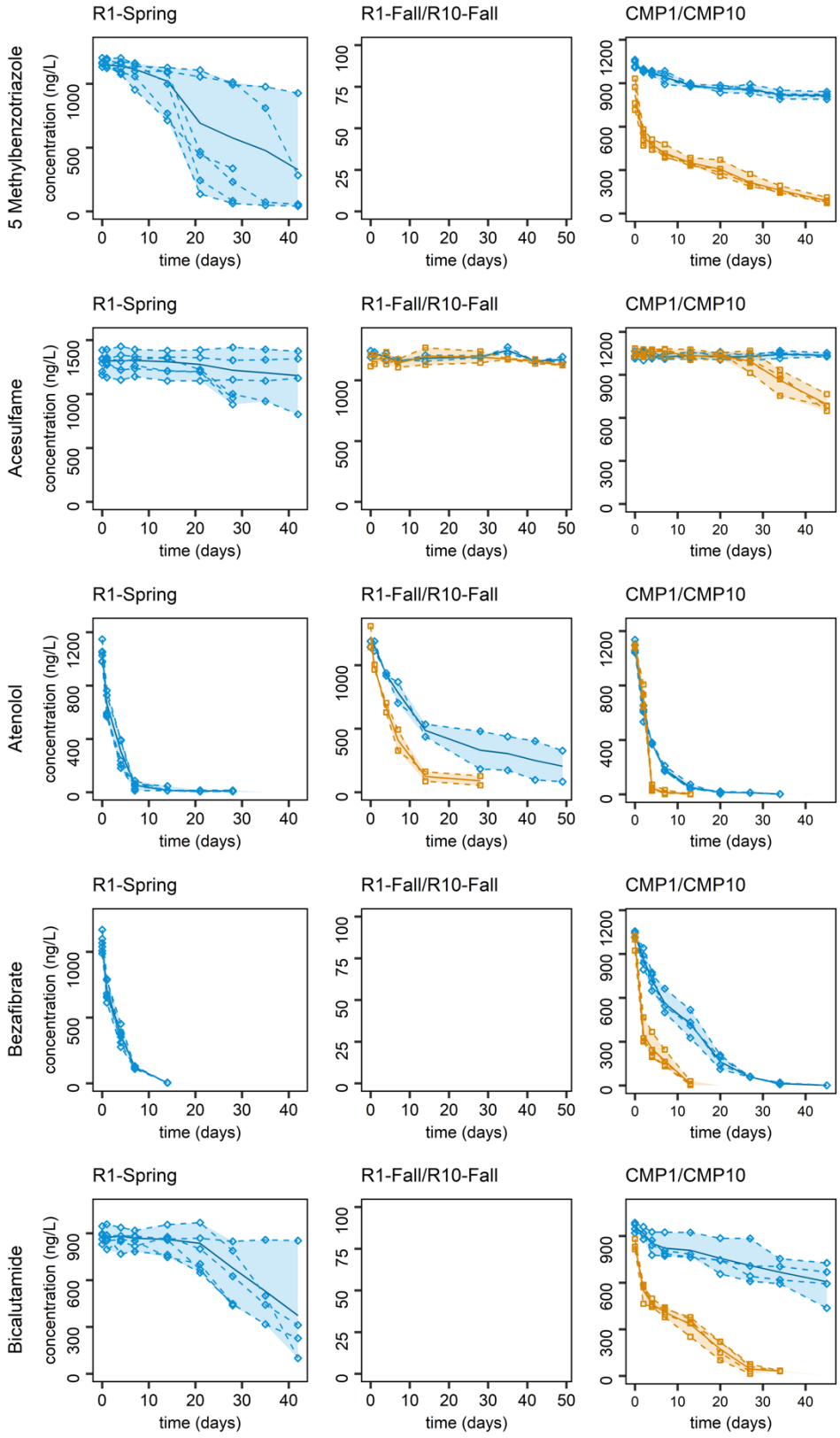

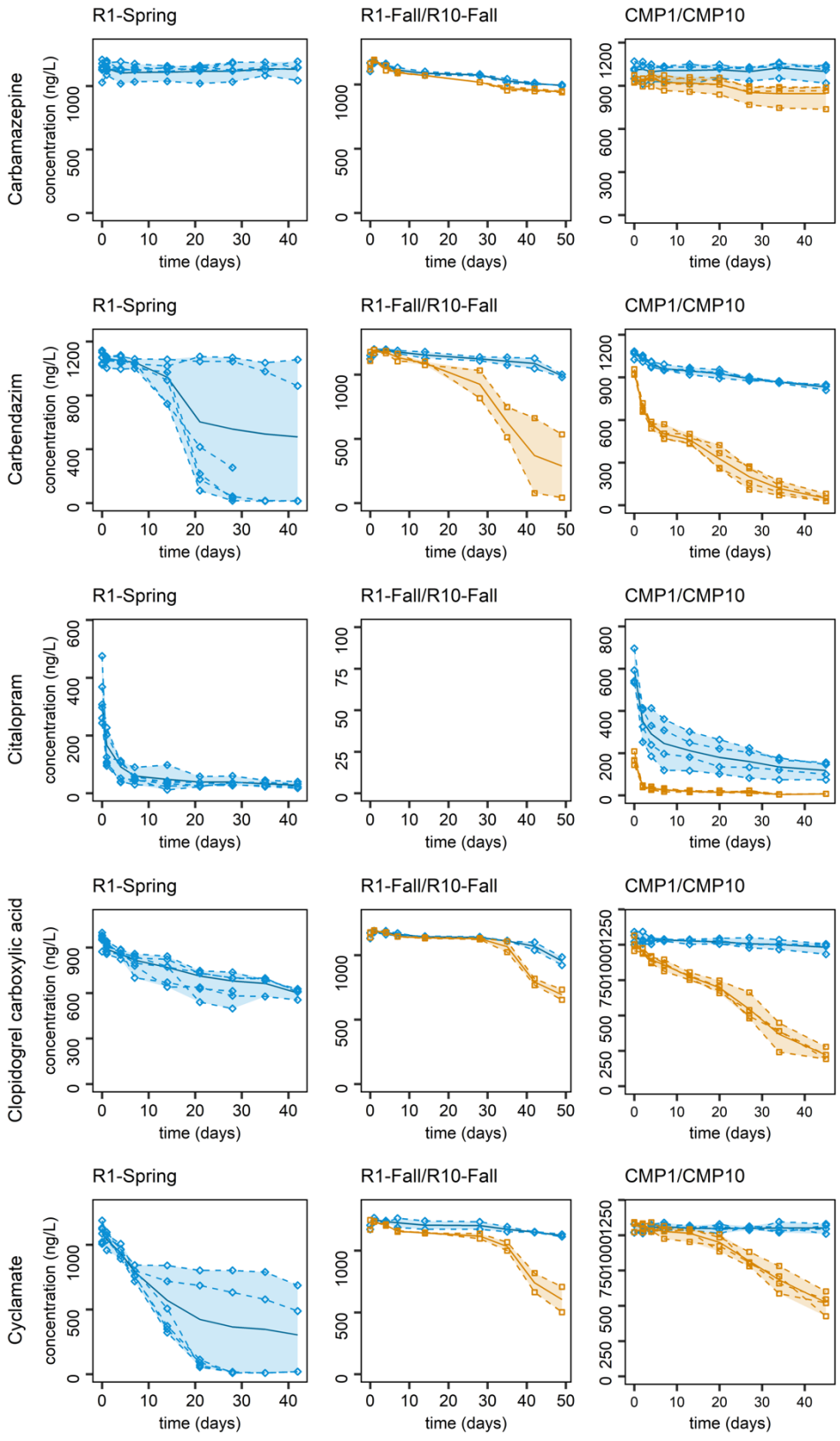
R1-Spring
R1-Fall/R10-Fall
CMP1/CMP10
Carbamazepine
Carbendazim
Citalopram
Clopidogrel carboxylic acid
Cyclamate
concentration (ng/L)
time (days)

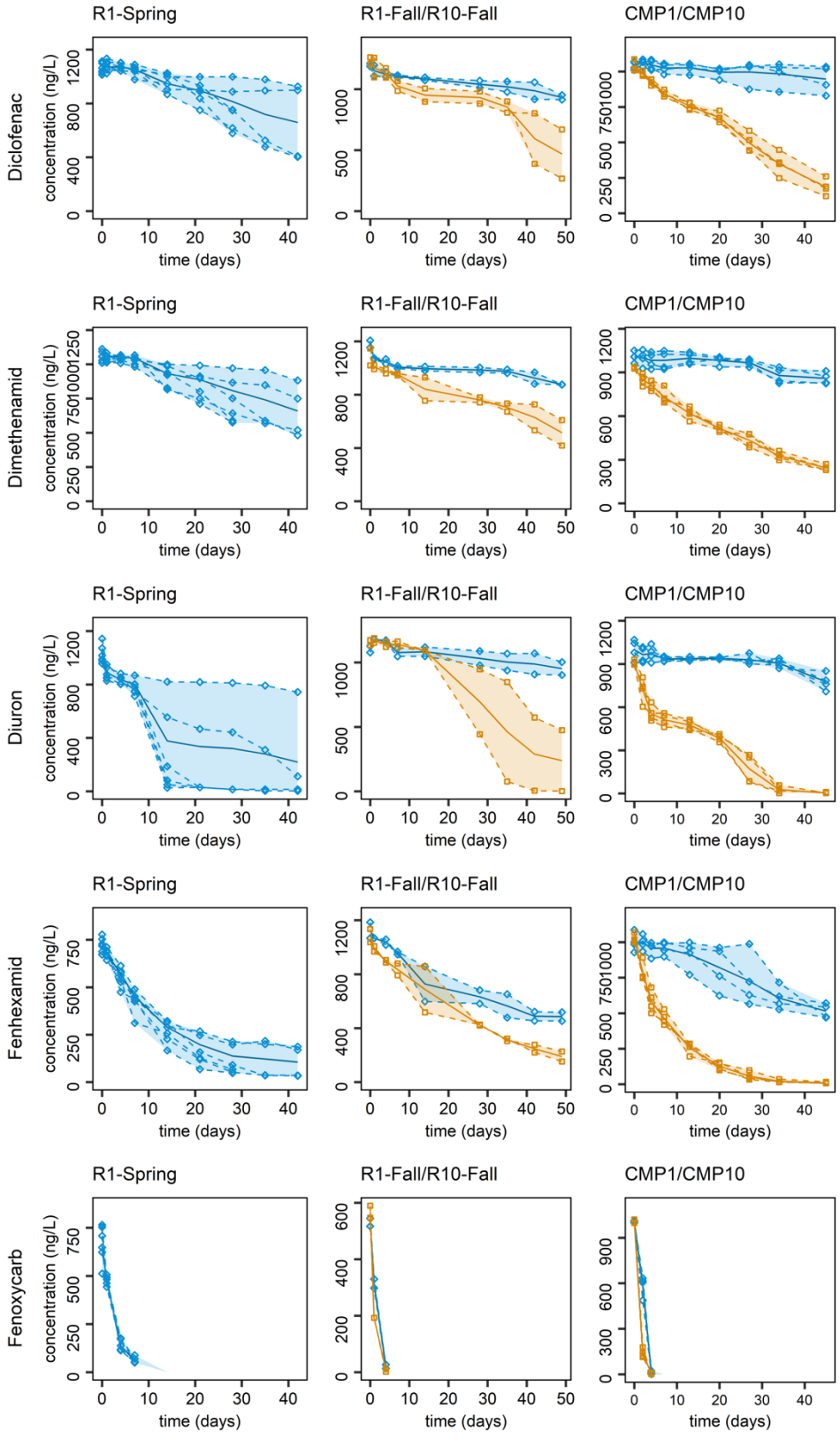
R1-Spring
R1-Fall/R10-Fall
CMP1/CMP10
Diclofenac
Dimethenamid
Diuron
Fenhexamid
Fenoxycarb
concentration (ng/L)
time (days)

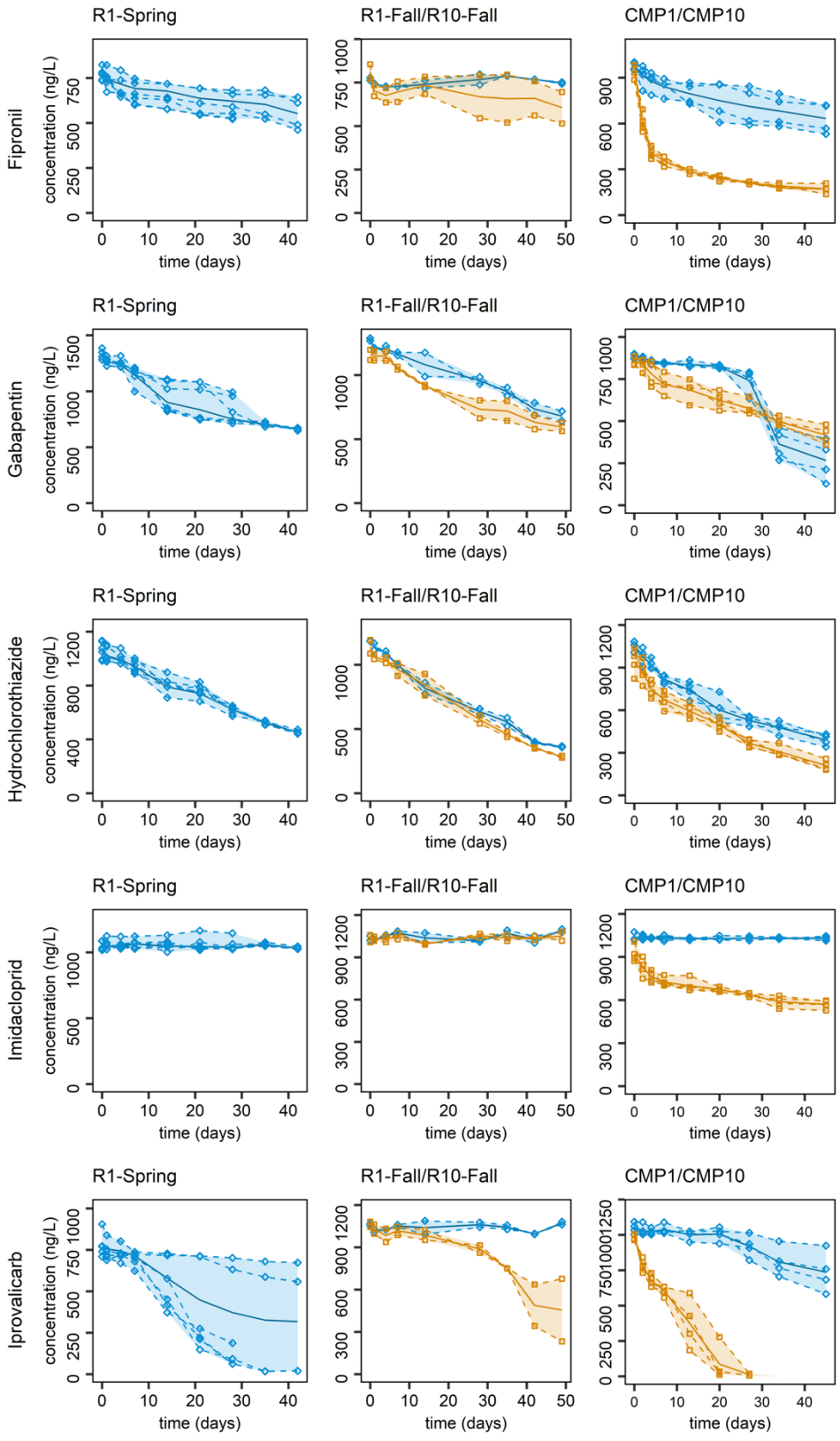
R1-Spring
R1-Fall/R10-Fall
CMP1/CMP10
Fipronil
Gabapentin
Hydrochlorothiazide
Imidacloprid
Iprovalicarb
concentration (ng/L)
time (days)

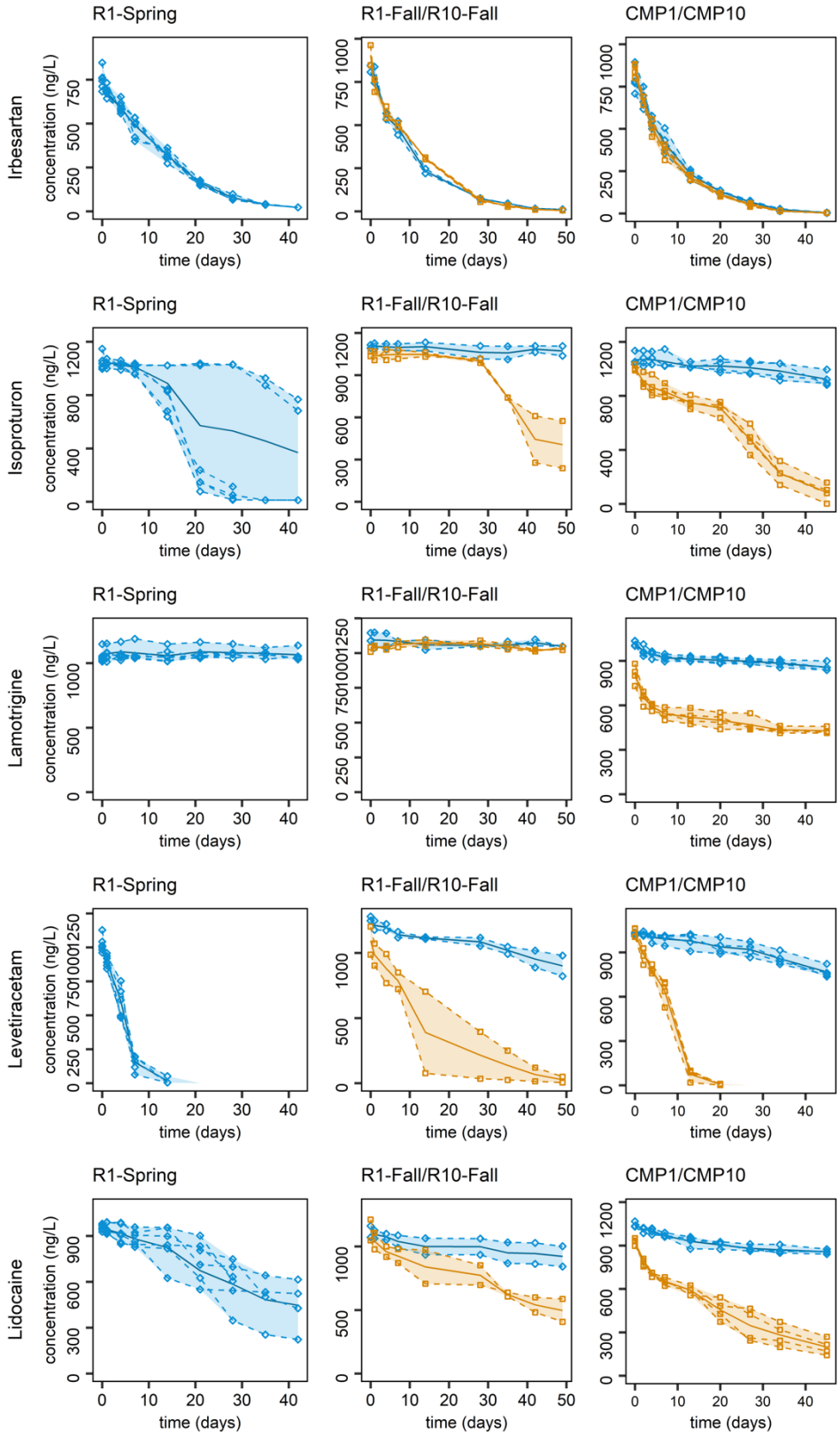
R1-Spring
R1-Fall/R10-Fall
CMP1/CMP10
Irbesartan
Isoproturon
Lamotrigine
Levetiracetam
Lidocaine
concentration (ng/L)
time (days)

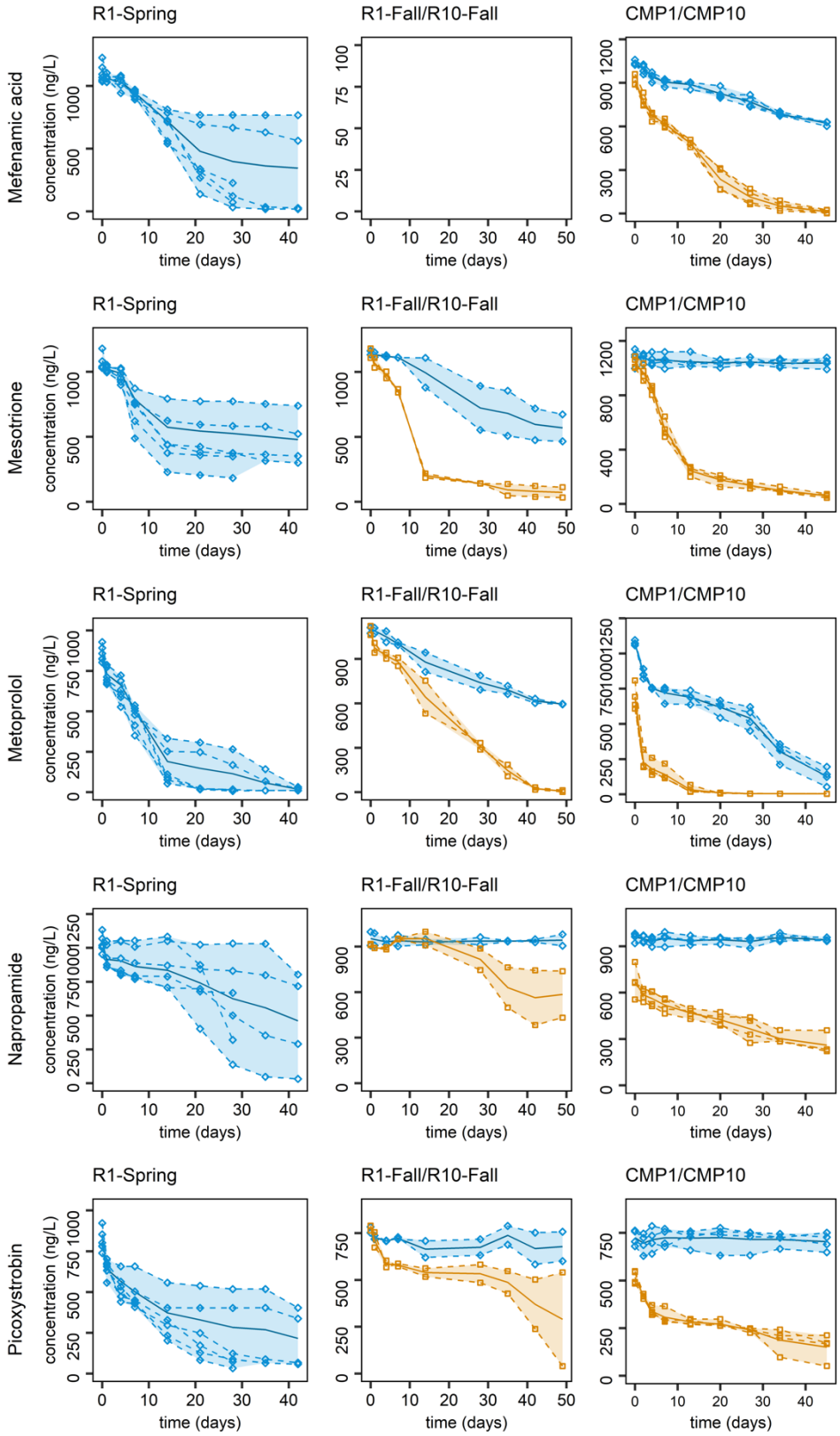
R1-Spring
R1-Fall/R10-Fall
CMP1/CMP10
Mefenamic acid
Mesotrione
Metoprolol
Napropamide
Picoxystrobin
concentration (ng/L)
time (days)

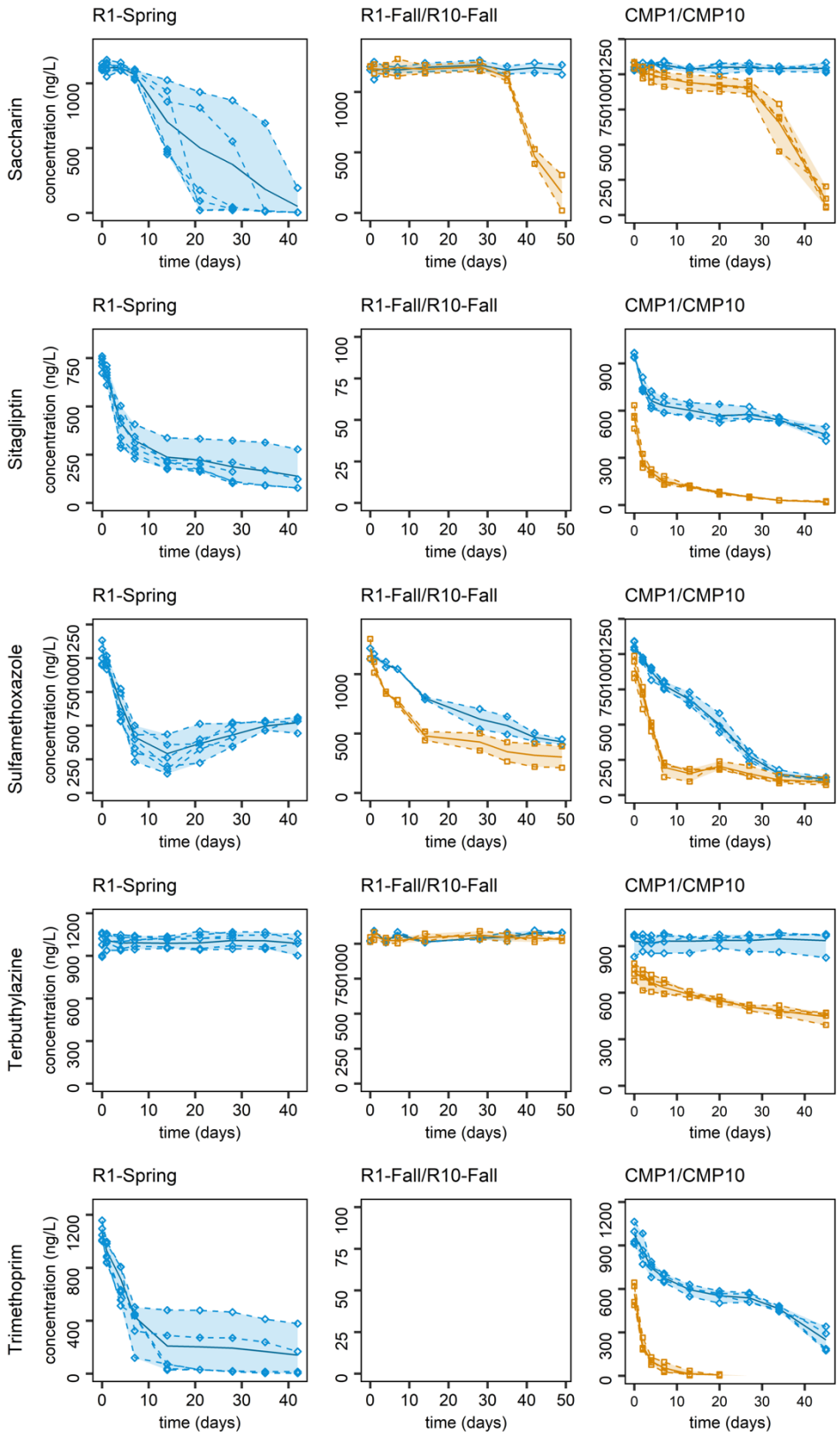
R1-Spring
R1-Fall/R10-Fall
CMP1/CMP10
Saccharin
Sitagliptin
Sulfamethoxazole
Terbuthylazine
Trimethoprim
concentration (ng/L)
time (days)

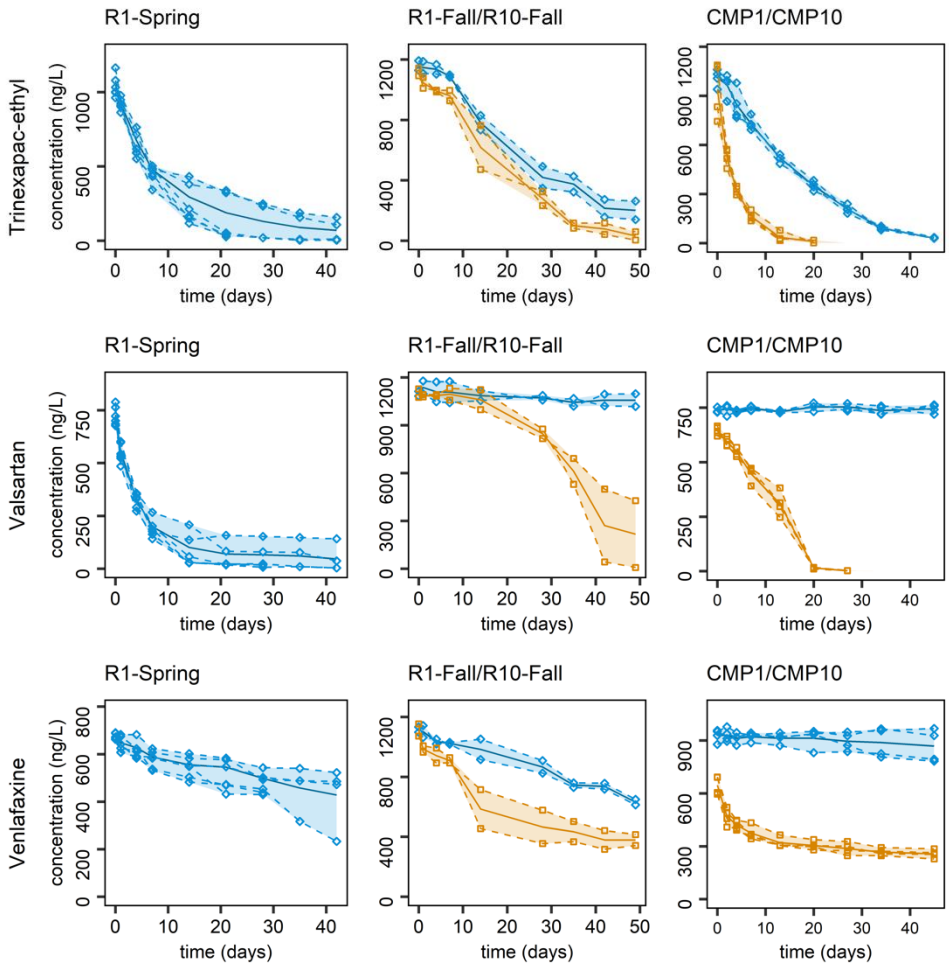

Suspensions containing 1 g solids L^{-1} are colored in blue with measured data represented as diamonds, and suspensions containing 10 g solids L^{-1} are shown in yellow with measured data represented as squares. Measurement points belonging to the same experimental replicate are connected with dashed lines. The solid line shows the average concentration calculated from the plotted experimental replicates, shaded areas indicate the spread of the concentrations measured at the same time point. Based on compound selection for R1-Fall/R10-Fall were not conducted, additional substances were added to perform R1-Spring, CMP1 and CMP10 (see Chapter 4.1.2.1).

Source: Seller et al. 2020 (Figure SI1)

Figure A 5: Compound residues in modified OECD 308-type studies

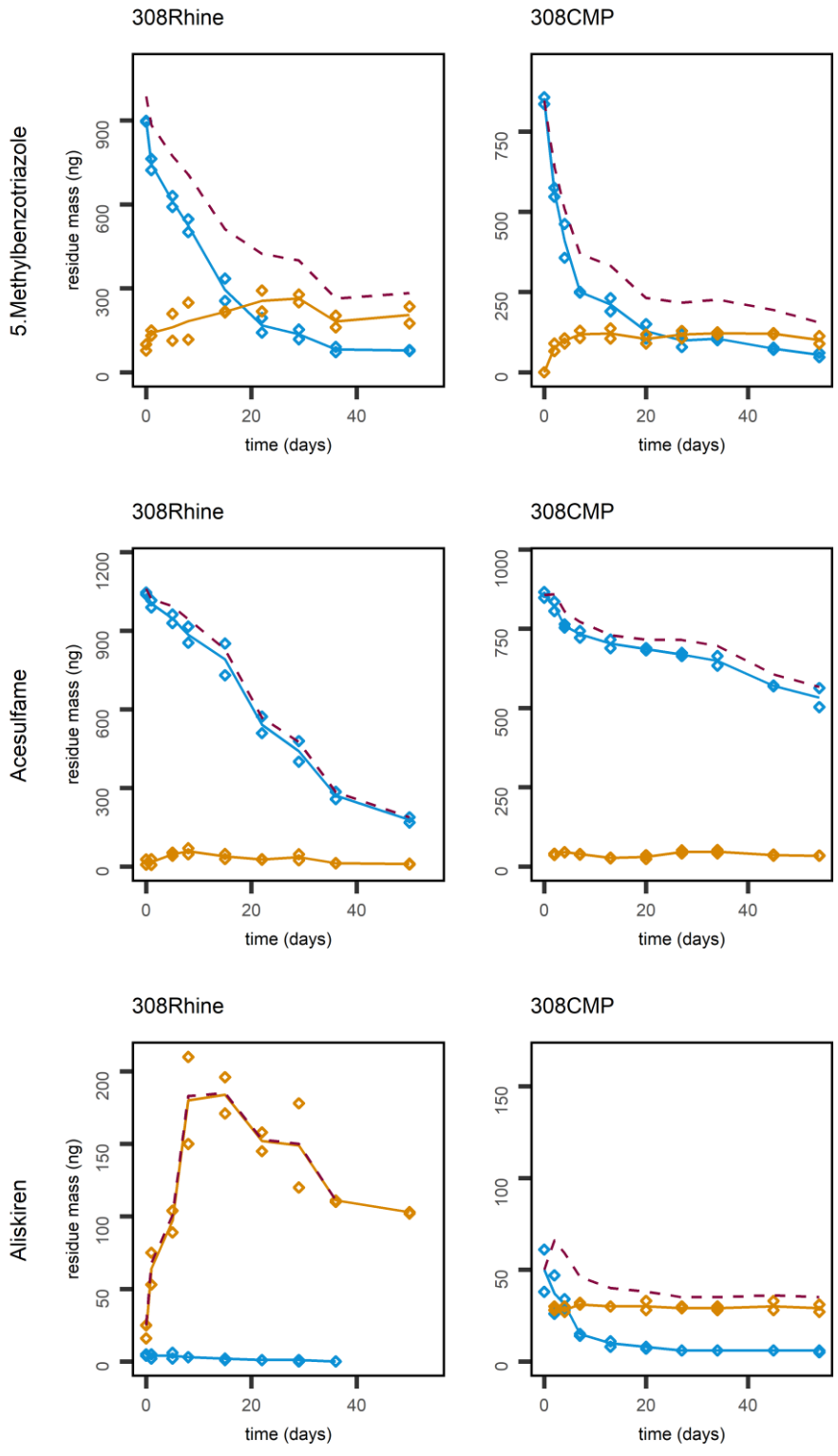

The graph shows compound mass residues of aliskiren measured in the sediment and water phase, as well as total compound mass residues in modified OECD 308-type studies conducted in river and pond inoculum. Compound mass in the water phase deceased over time while it inceased in the sediment layer, still, total compound concentration decraseed during both studies.

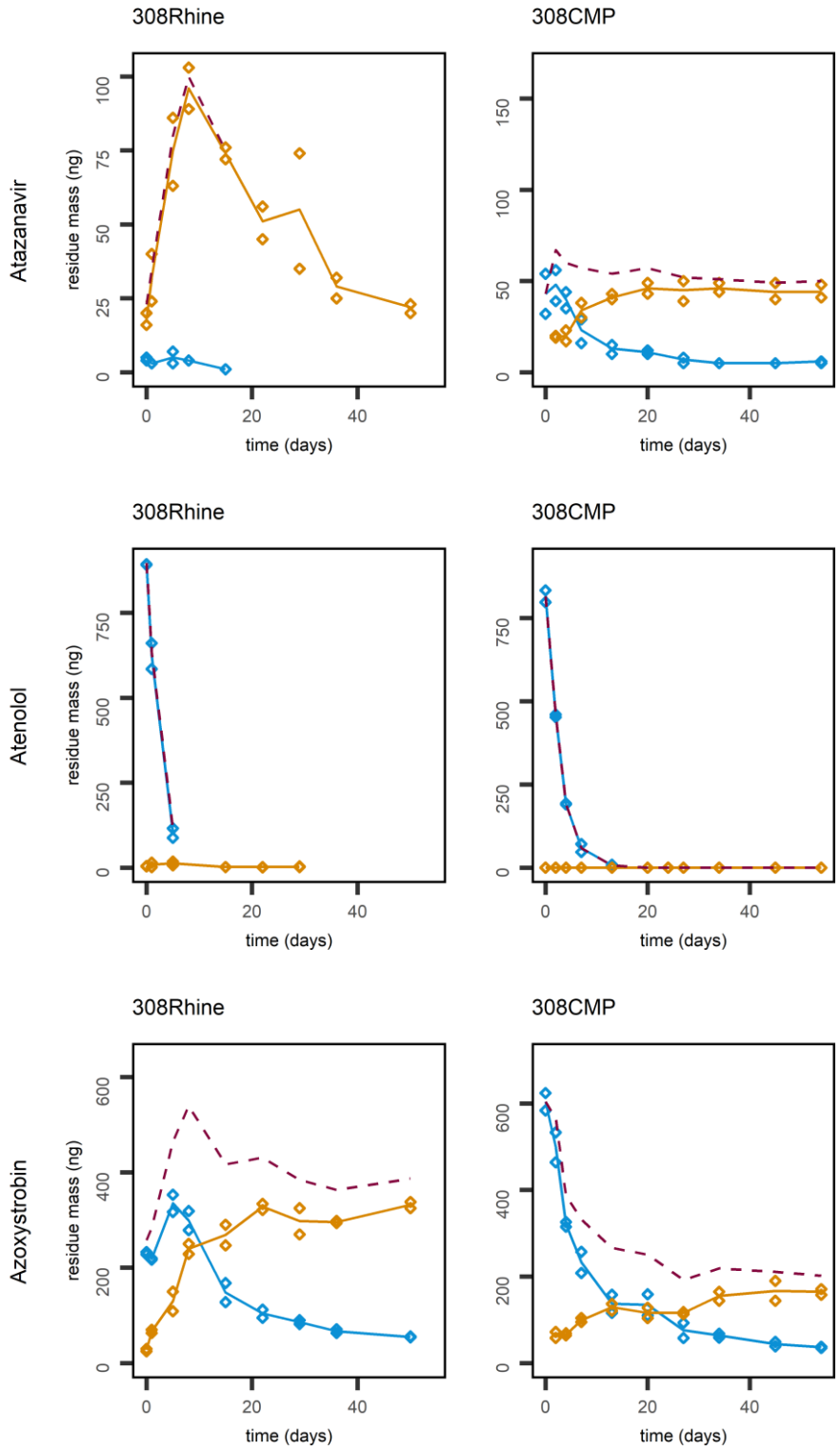
Atazanavir
308Rhine
308CMP
residue mass (ng)
time (days)
Atenolol
308Rhine
308CMP
residue mass (ng)
time (days)
Azoxystrobin
308Rhine
308CMP
residue mass (ng)
time (days)

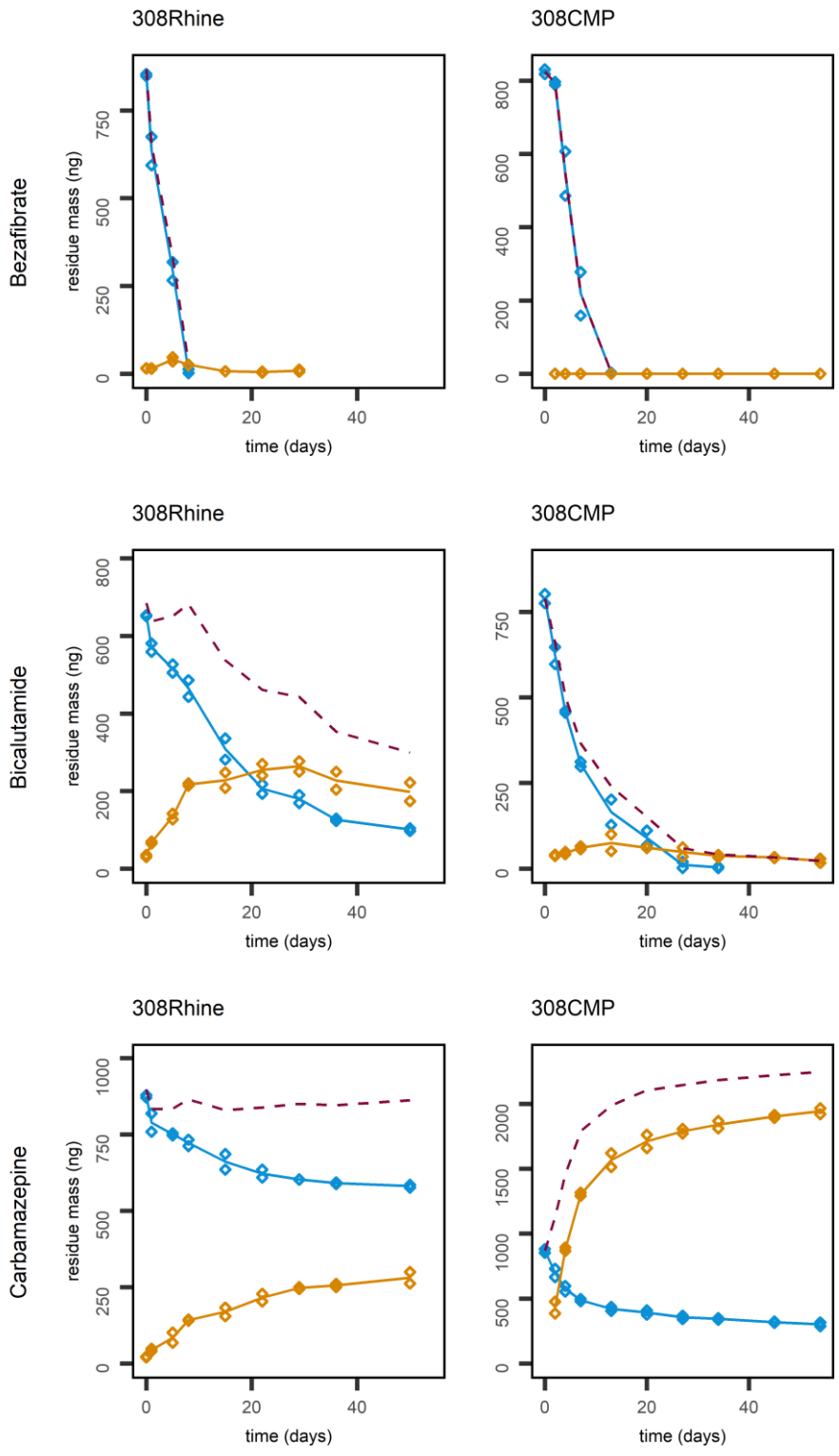
Bezafibrate
308Rhine
308CMP
residue mass (ng)
time (days)
Bicalutamide
308Rhine
308CMP
residue mass (ng)
time (days)
Carbamazepine
308Rhine
308CMP
residue mass (ng)
time (days)

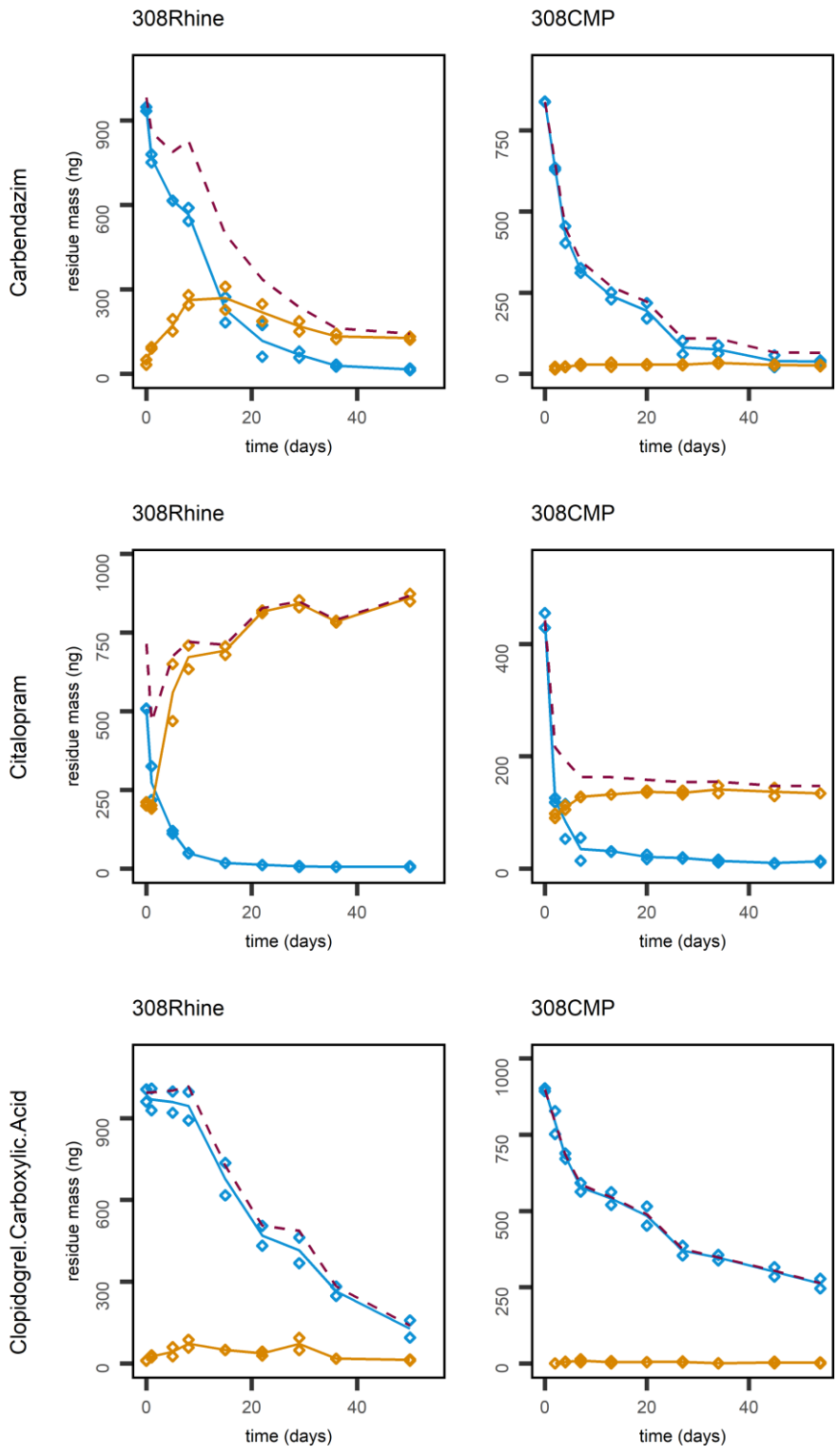
Carbendazim
308Rhine
308CMP
residue mass (ng)
time (days)
Citalopram
308Rhine
308CMP
residue mass (ng)
time (days)
Clopidogrel.Carboxylic.Acid
308Rhine
308CMP
residue mass (ng)
time (days)

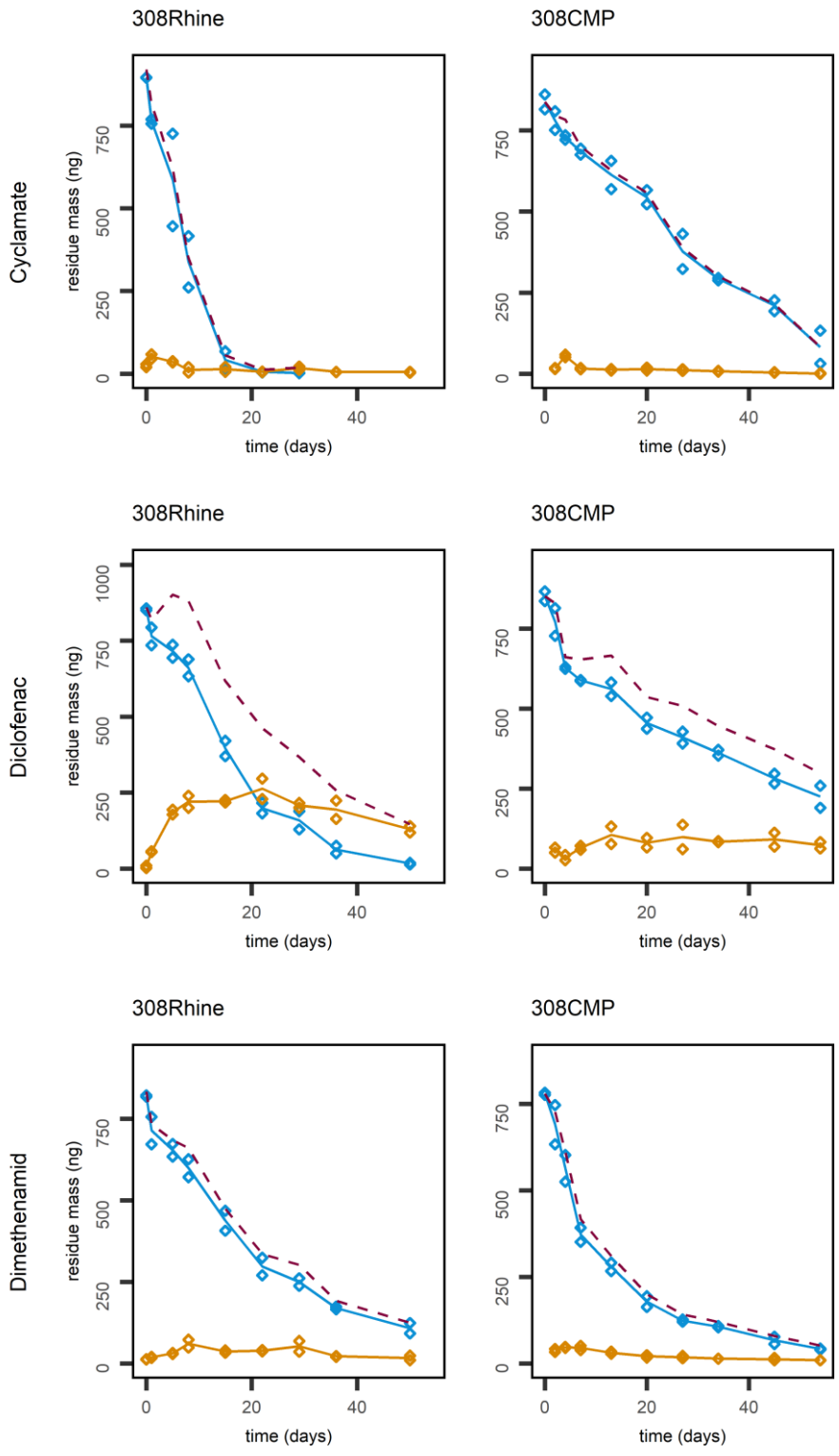
Cyclamate
Diclofenac
Dimethenamid
308Rhine
308CMP
residue mass (ng)
time (days)
0
250
500
750
1000
20
40

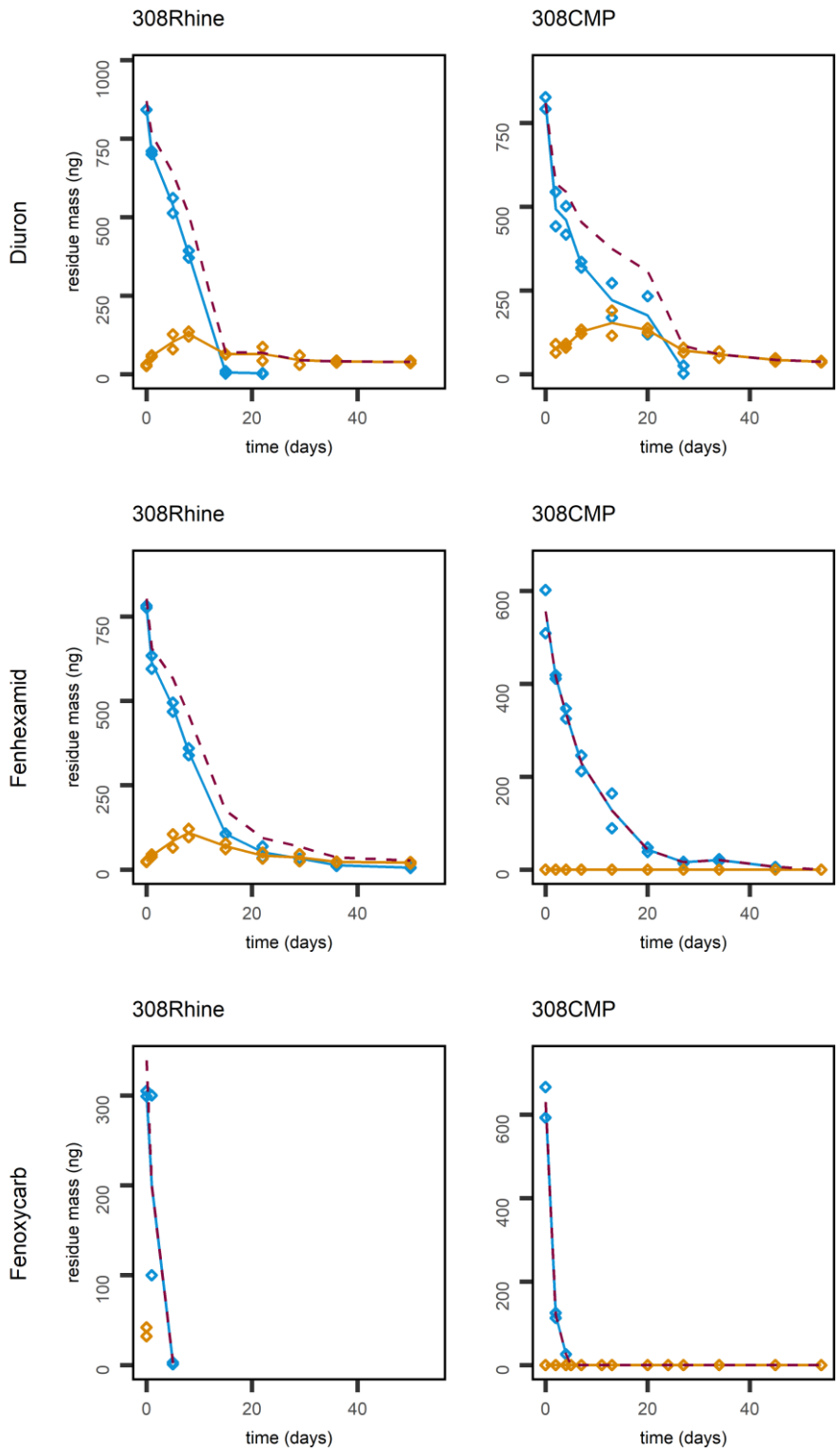
Diuron
308Rhine
308CMP
residue mass (ng)
time (days)
Fenhexamid
308Rhine
308CMP
residue mass (ng)
time (days)
Fenoxycarb
308Rhine
308CMP
residue mass (ng)
time (days)

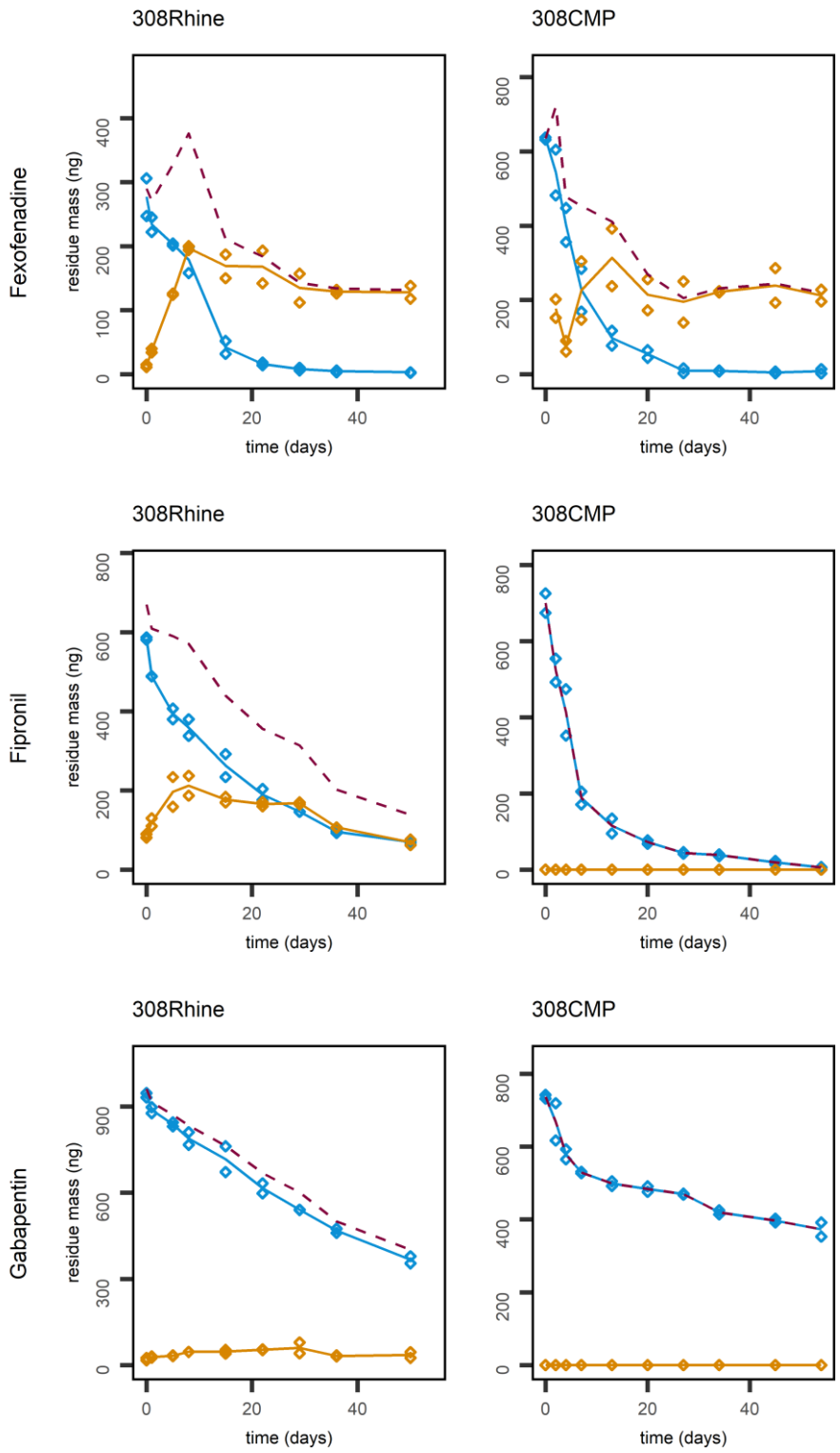
Fexofenadine
308Rhine
308CMP
residue mass (ng)
time (days)
Fipronil
308Rhine
308CMP
residue mass (ng)
time (days)
Gabapentin
308Rhine
308CMP
residue mass (ng)
time (days)

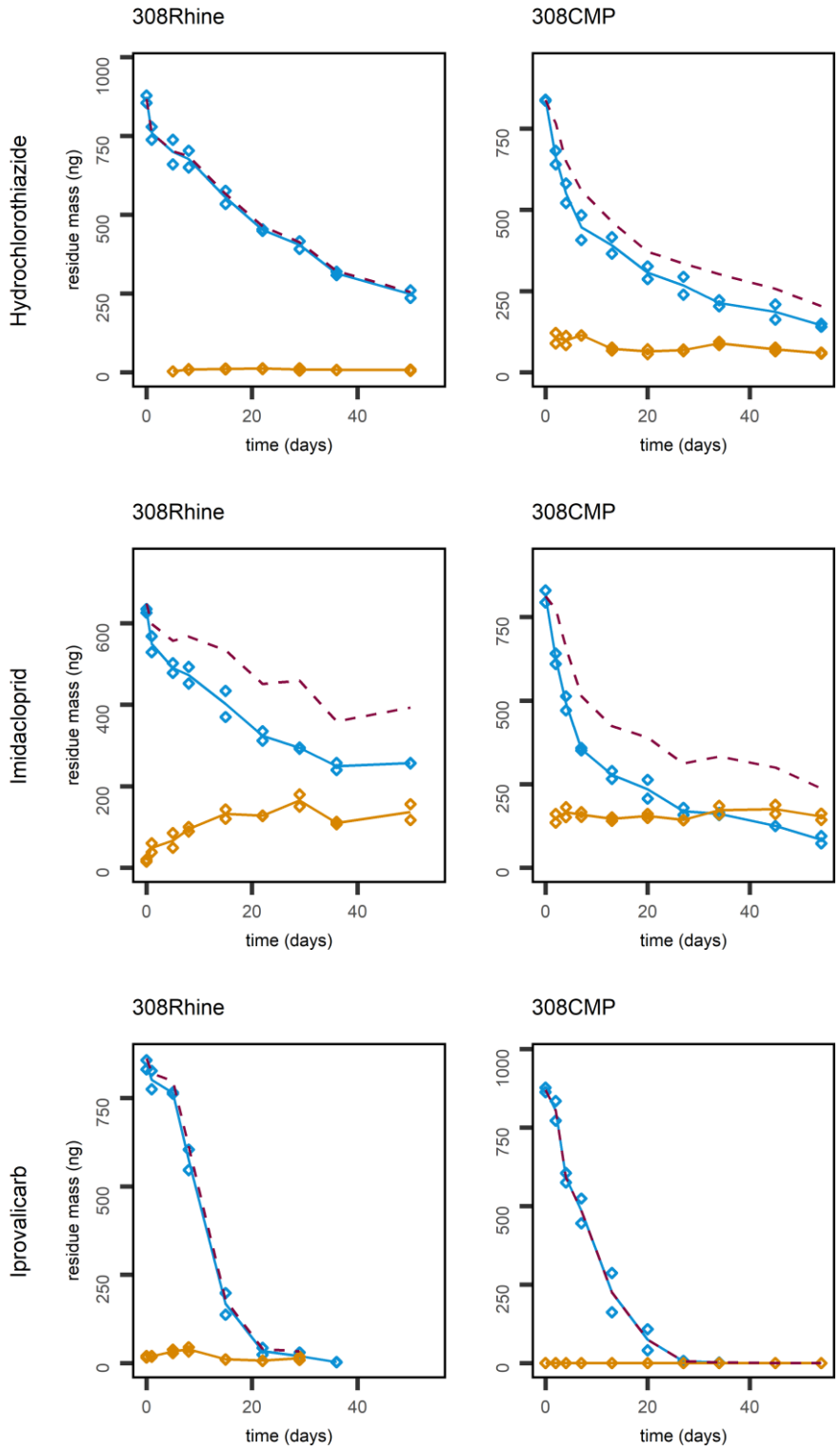
Hydrochlorothiazide
308Rhine
308CMP
residue mass (ng)
time (days)
Imidacloprid
308Rhine
308CMP
residue mass (ng)
time (days)
Iprovalicarb
308Rhine
308CMP
residue mass (ng)
time (days)

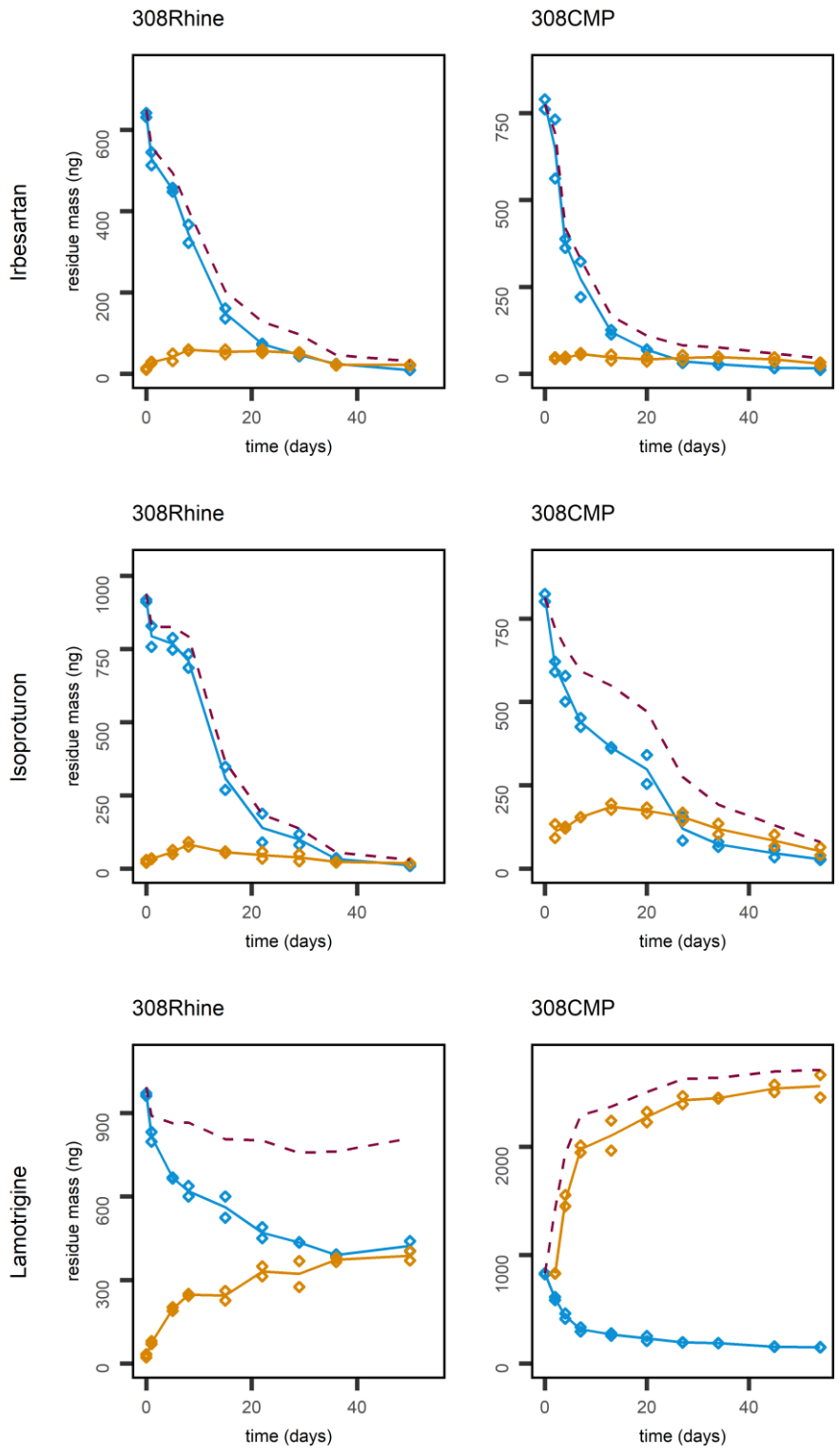
Irbesartan
Isoproturon
Lamotrigine
308Rhine
308CMP
residue mass (ng)
time (days)

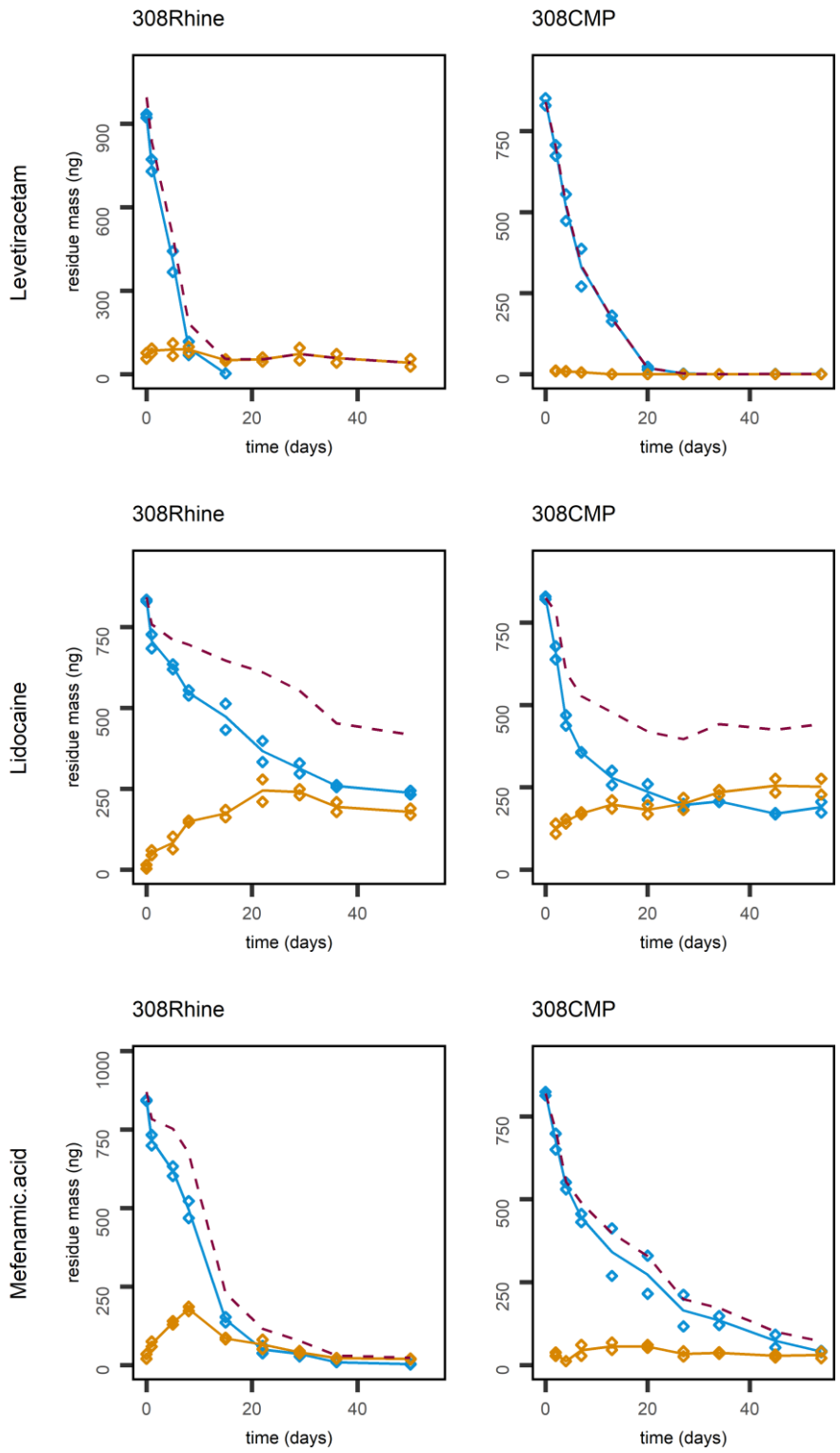
Levetiracetam
Lidocaine
Mefenamic.acid
308Rhine
308CMP
residue mass (ng)
time (days)

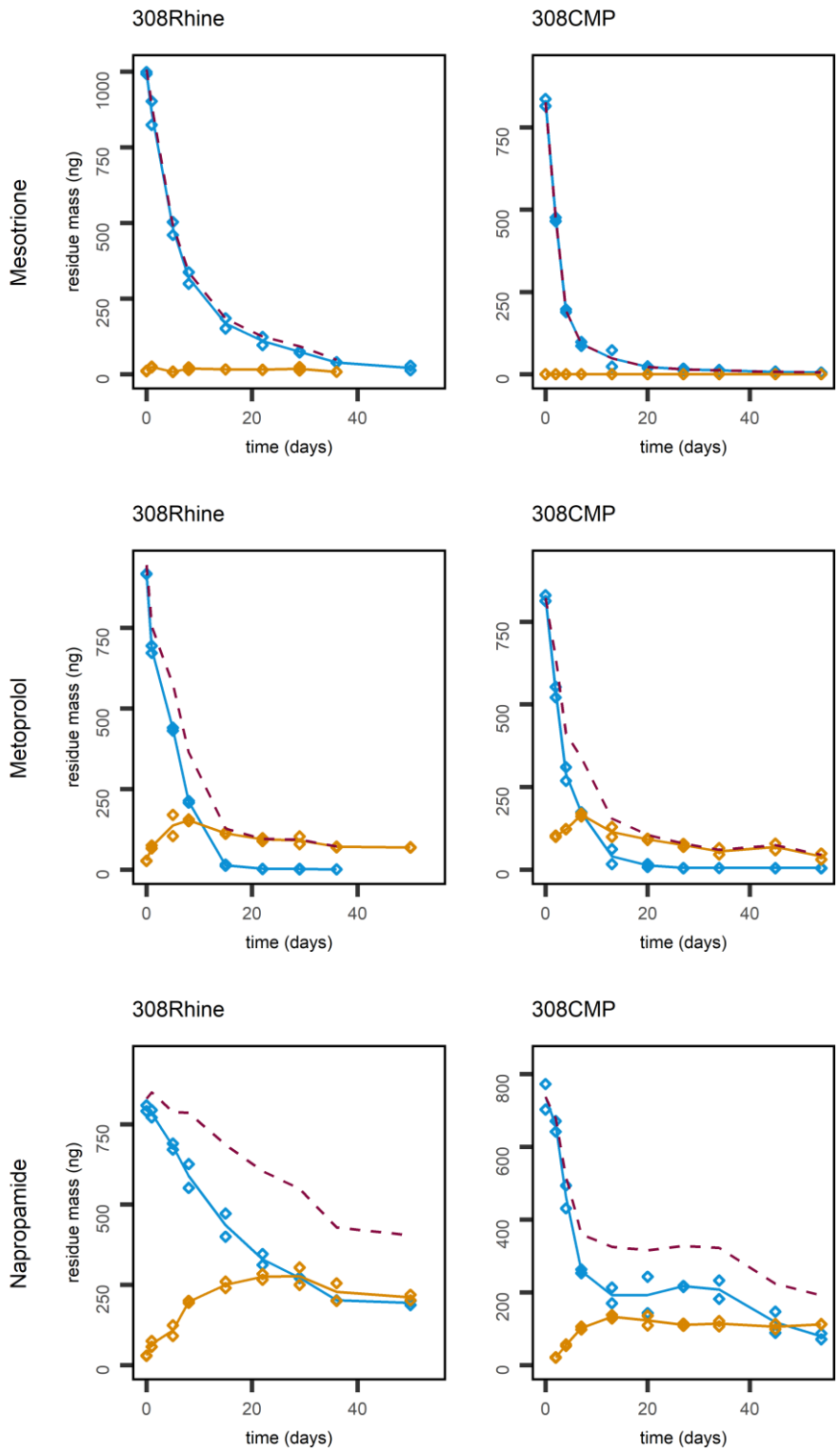
Mesotrione
308Rhine
308CMP
residue mass (ng)
time (days)
Metoprolol
308Rhine
308CMP
residue mass (ng)
time (days)
Napropamide
308Rhine
308CMP
residue mass (ng)
time (days)

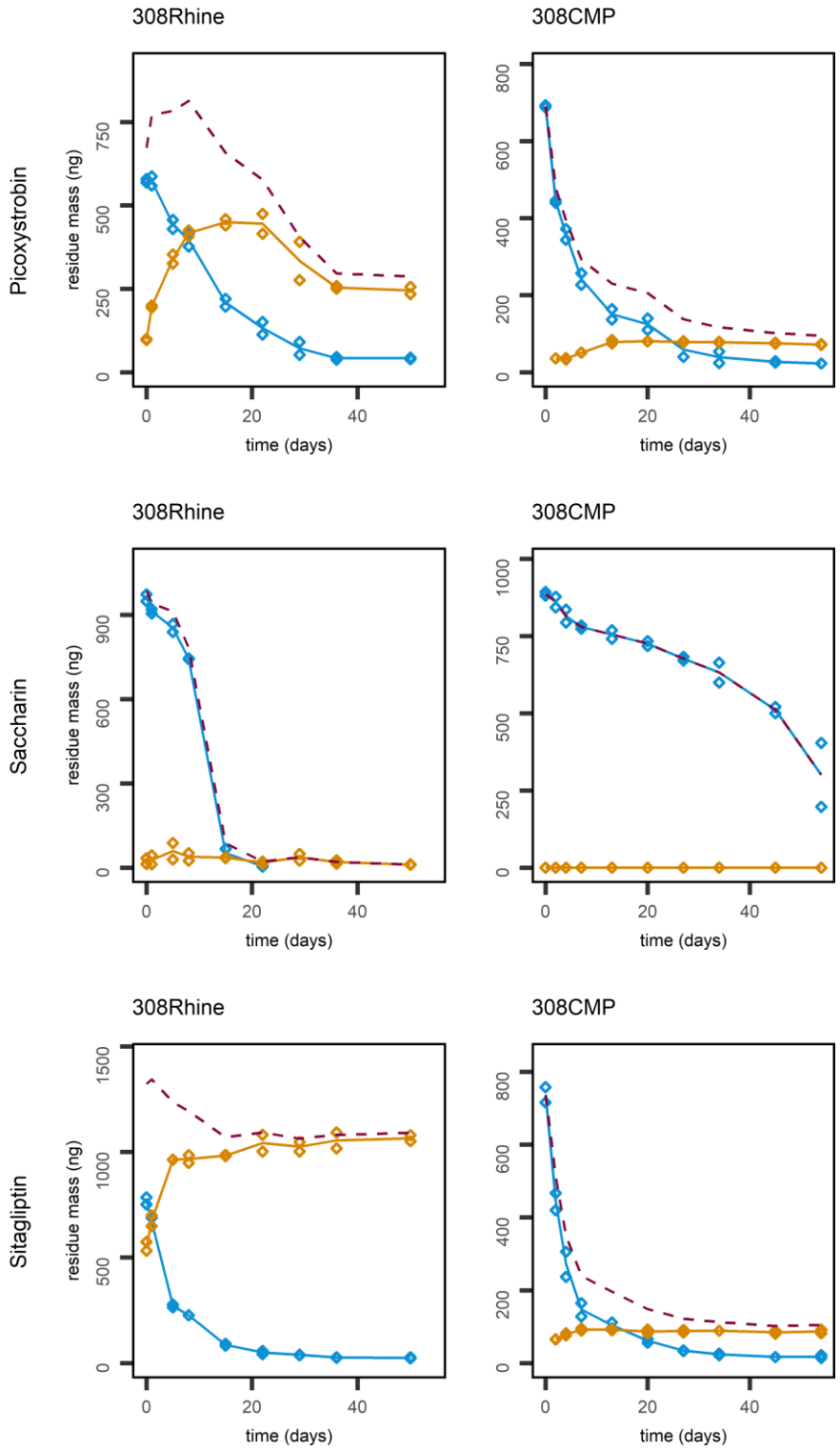
Picoxystrobin
308Rhine
308CMP
residue mass (ng)
time (days)
Saccharin
308Rhine
308CMP
residue mass (ng)
time (days)
Sitagliptin
308Rhine
308CMP
residue mass (ng)
time (days)

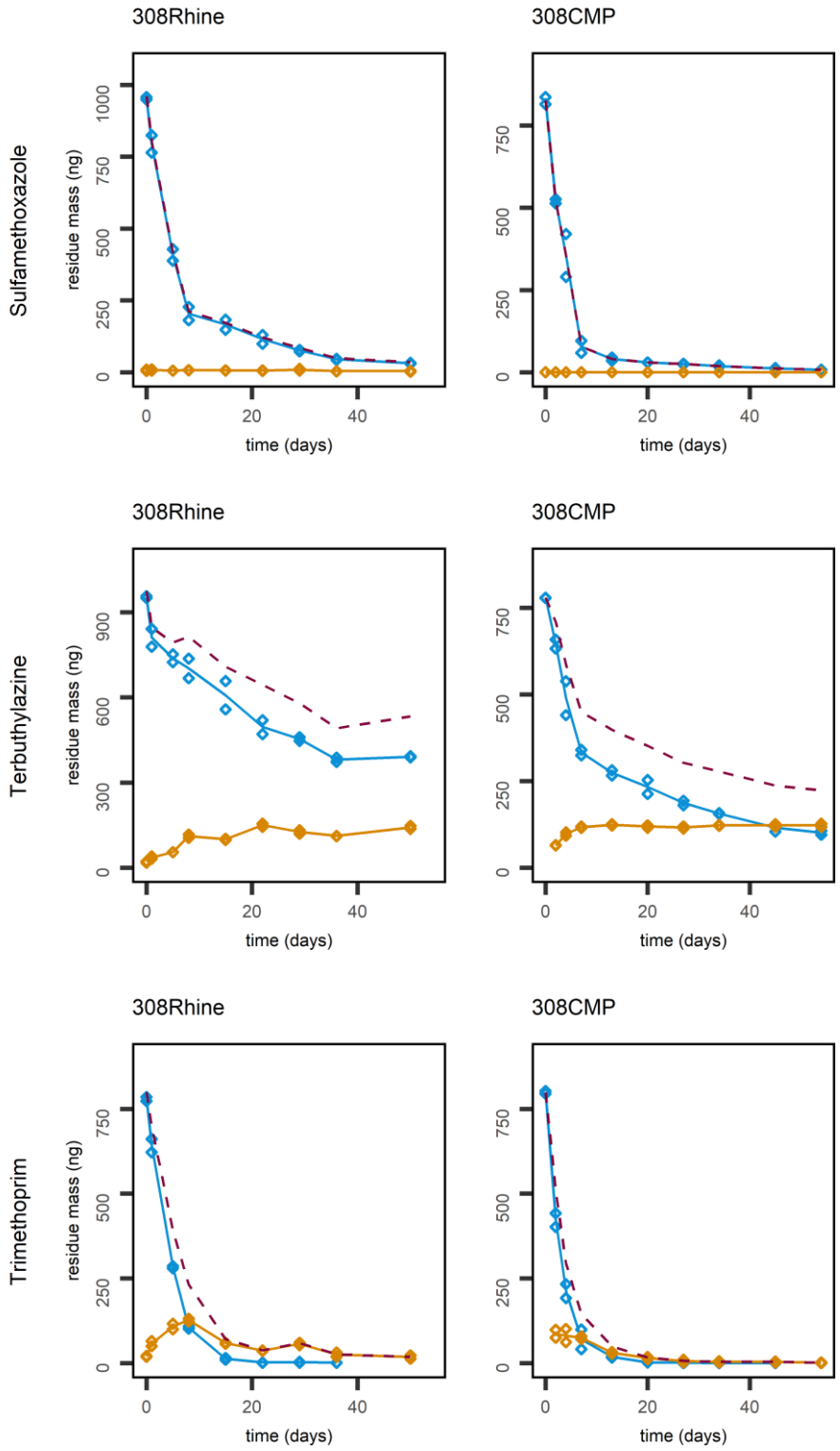
Sulfamethoxazole
308Rhine
308CMP
residue mass (ng)
time (days)
Terbuthylazine
308Rhine
308CMP
residue mass (ng)
time (days)
Trimethoprim
308Rhine
308CMP
residue mass (ng)
time (days)

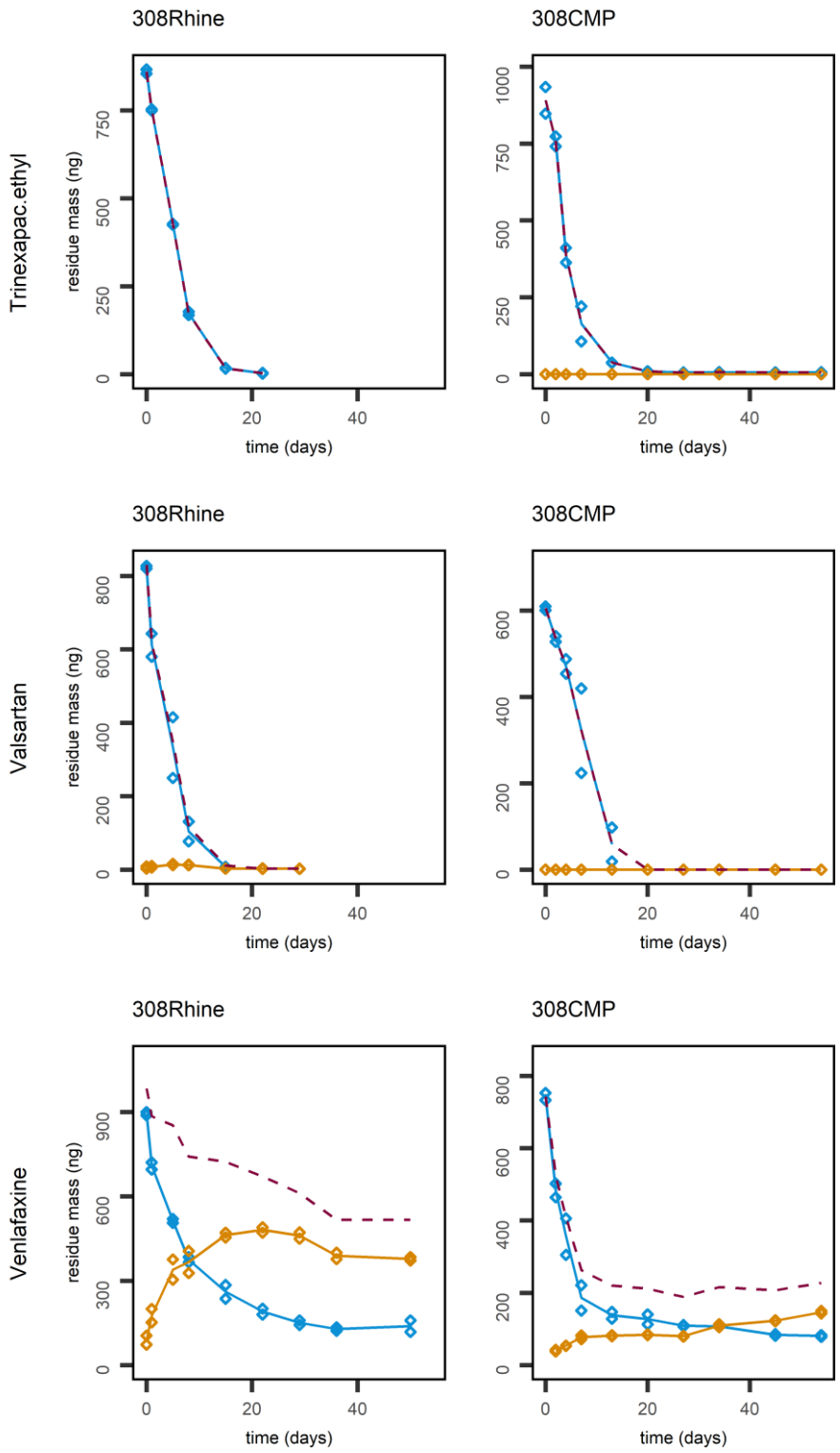

Parent compound measured in the water phase (blue diamonds) and sediment (yellow diamonds) over the time course of modified OECD 308-type studies. Solid lines show the average between residues measured in the sampled duplicates at each time point in the water phase and sediment, respectively. Dotted line shows the average total compound residues as a sum of residues in the water phase and sediment.

Source: own figure, Eawag

Figure A 6: $k'_{bio,lab,joint}$ model fits to modified OECD 308-type data

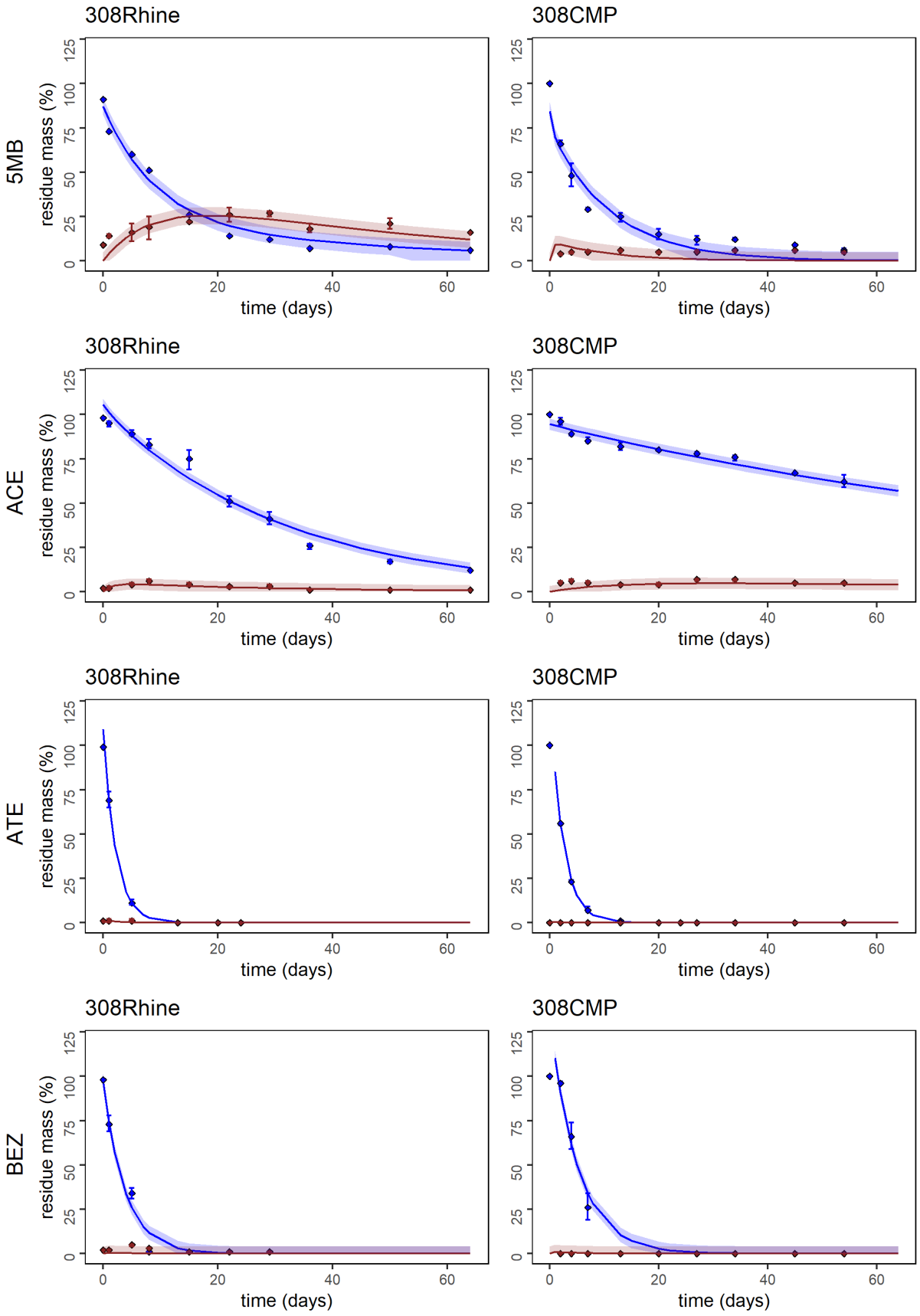

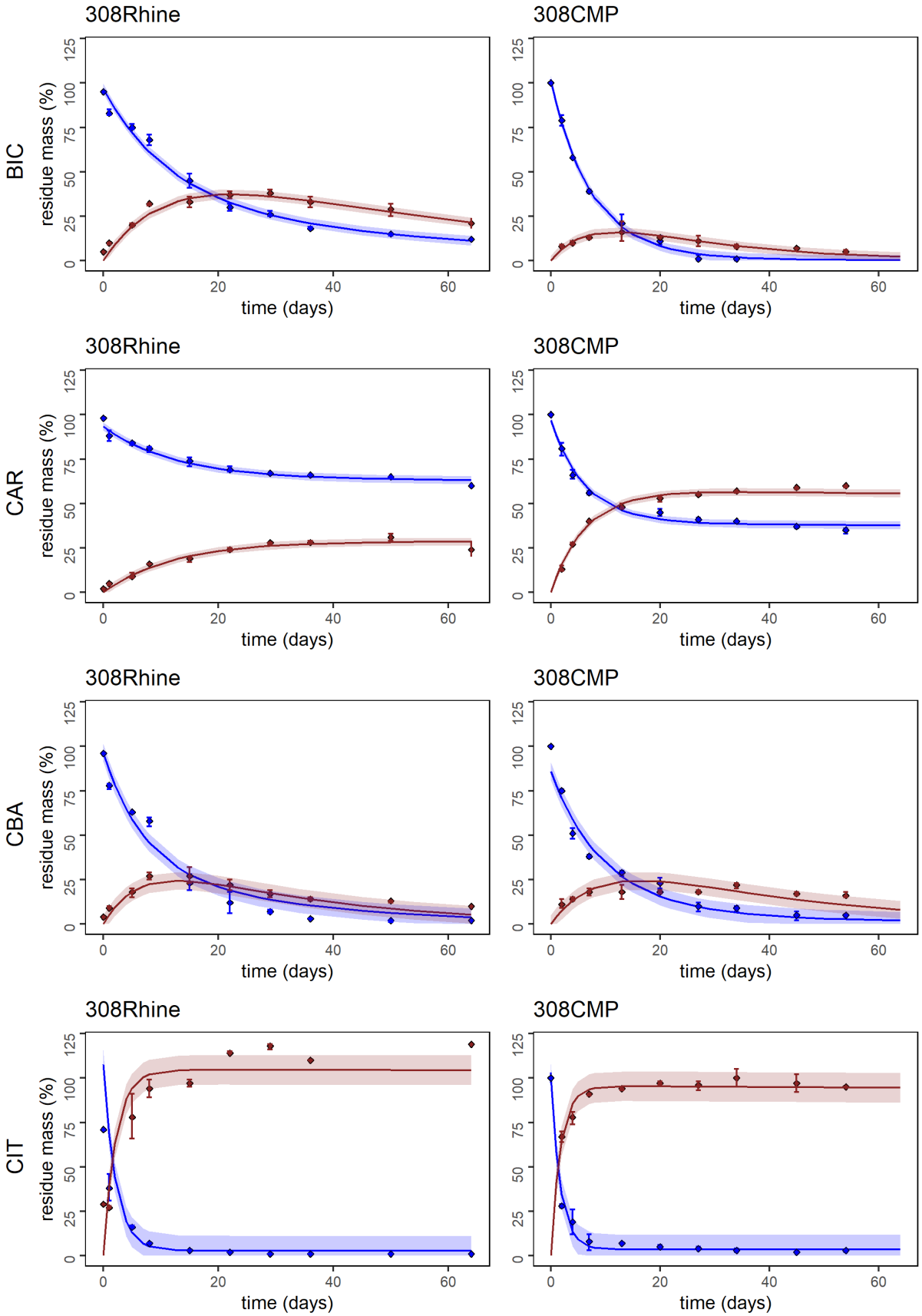
308Rhine
308CMP
BIC
CAR
CBA
CIT
residue mass (%)
time (days)
0
25
50
75
100
125
0
20
40
60

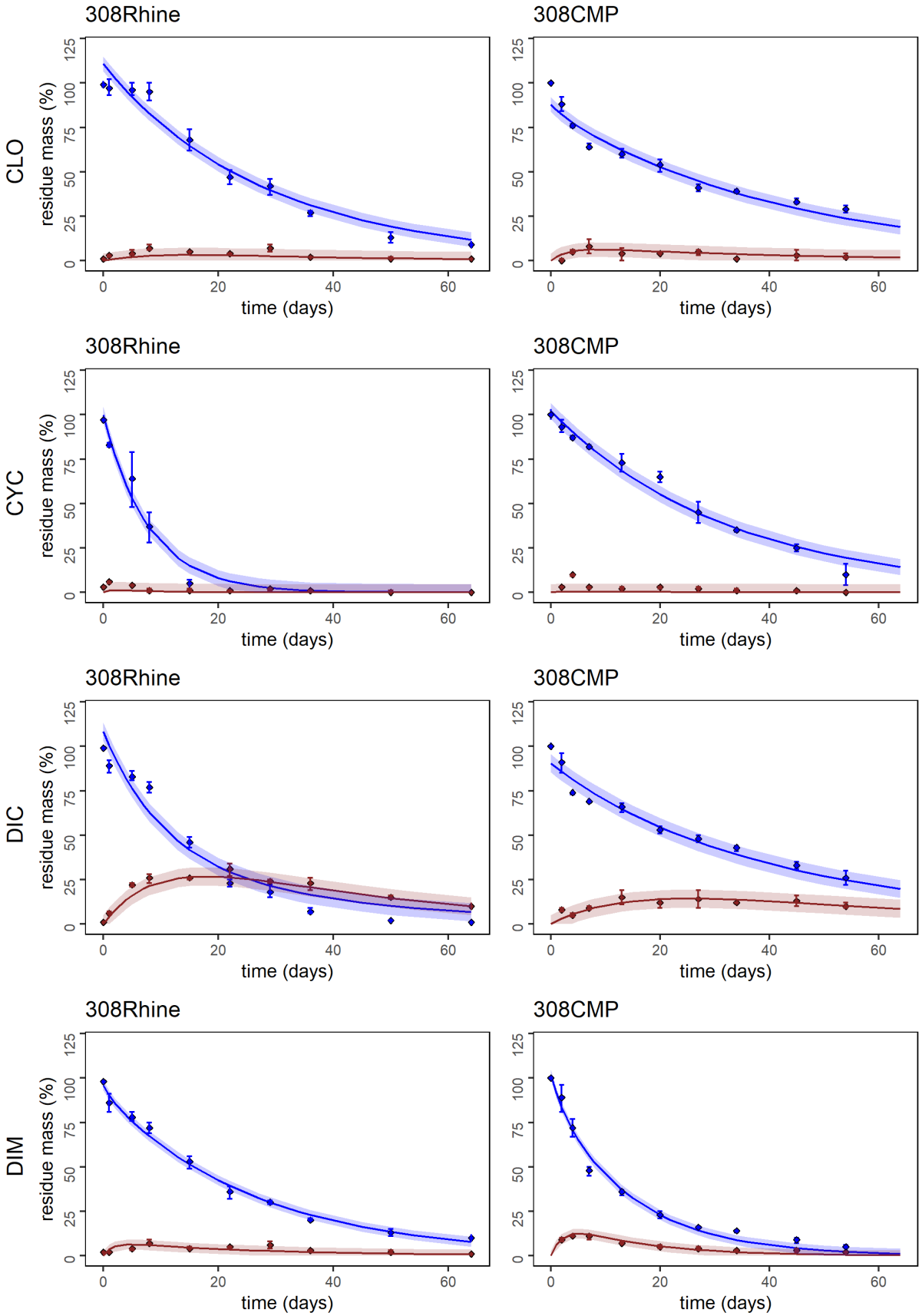
308Rhine
308CMP
CLO
CYC
DIC
DIM
residue mass (%)
time (days)
0
25
50
75
100
125
0
20
40
60

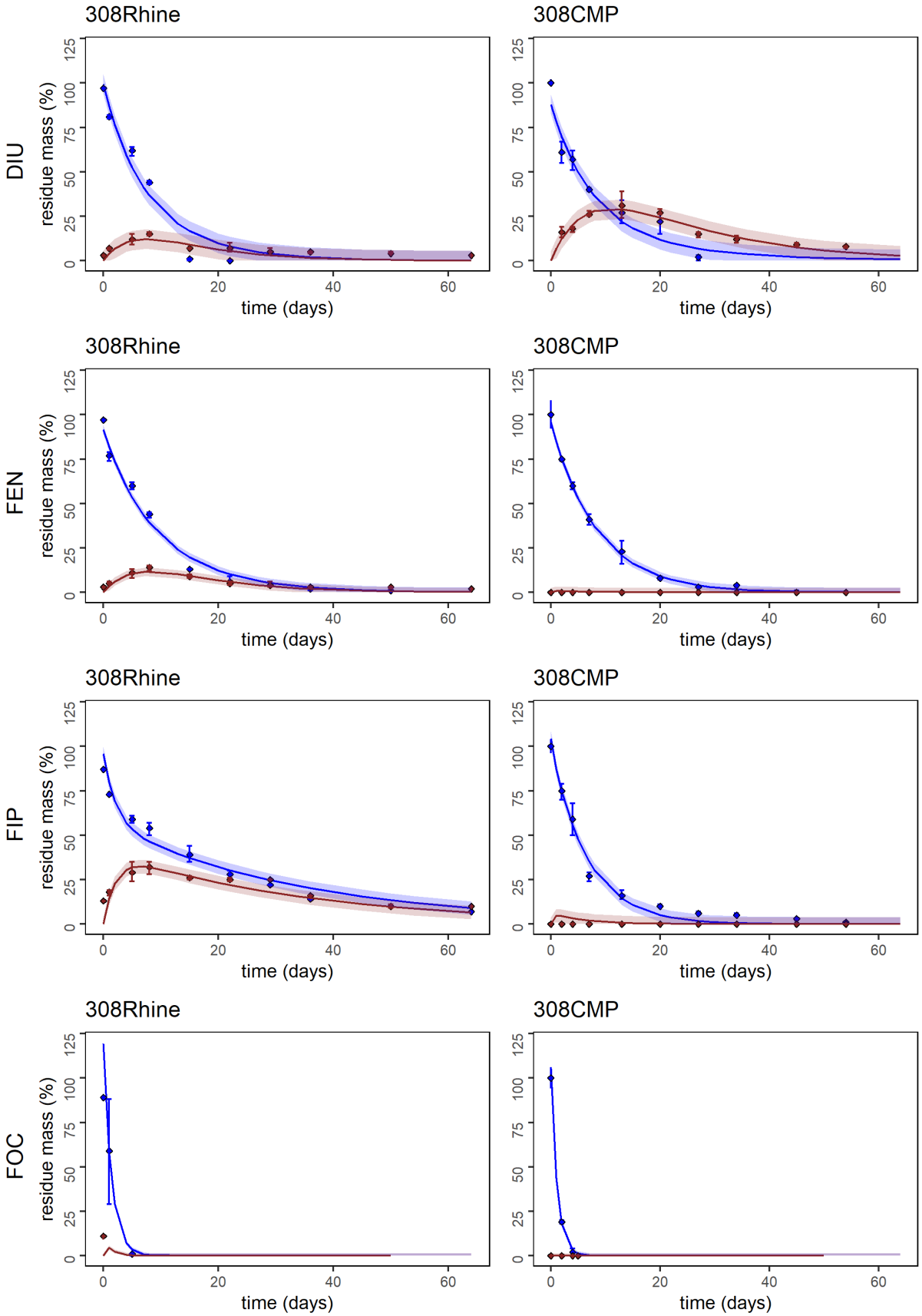
308Rhine
308CMP
DIU
FEN
FIP
FOC
residue mass (%)
time (days)
0
25
50
75
100
125
0
20
40
60

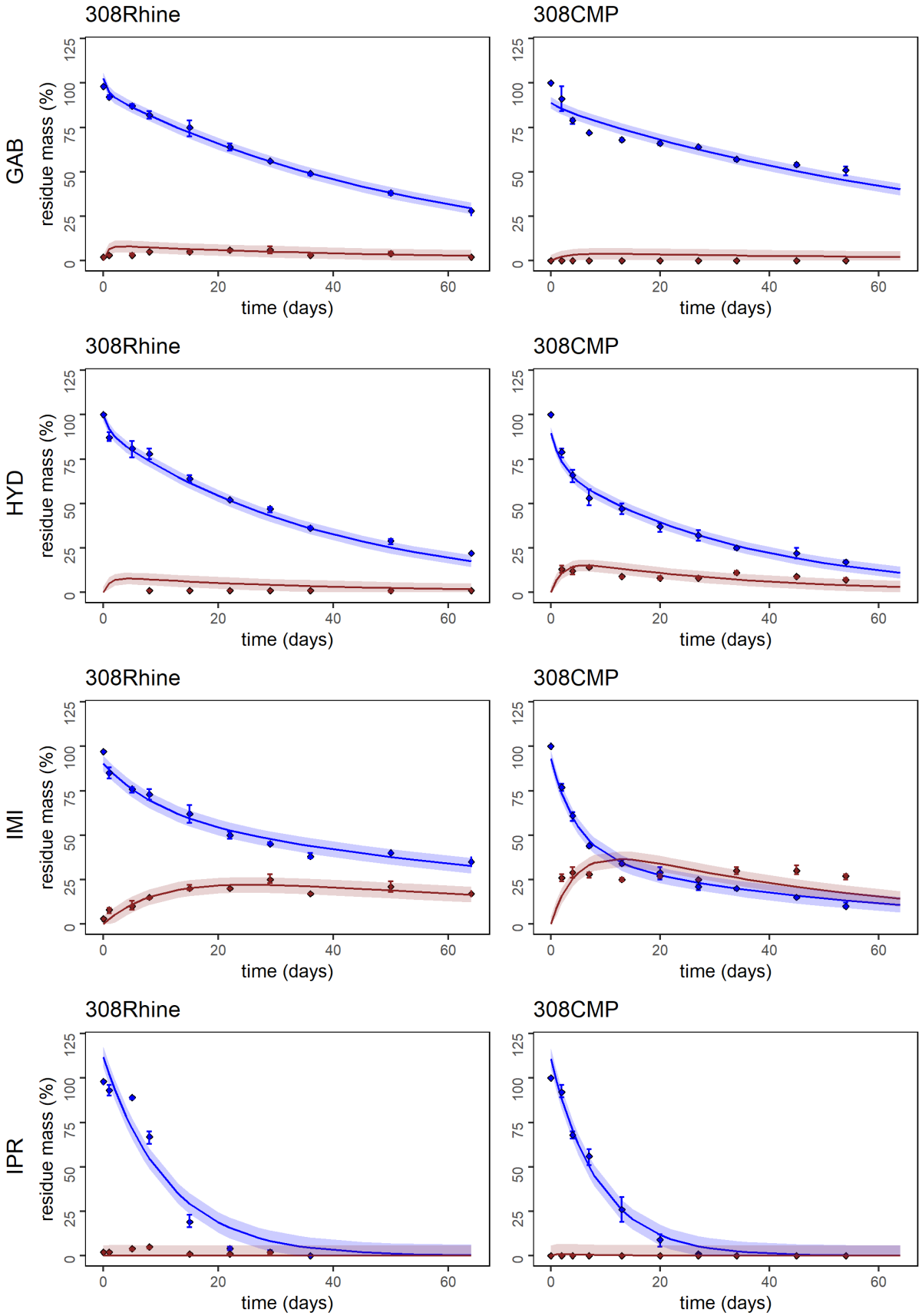
308Rhine
308CMP
GAB
HYD
IMI
IPR
residue mass (%)
time (days)
0
25
50
75
100
125
0
20
40
60

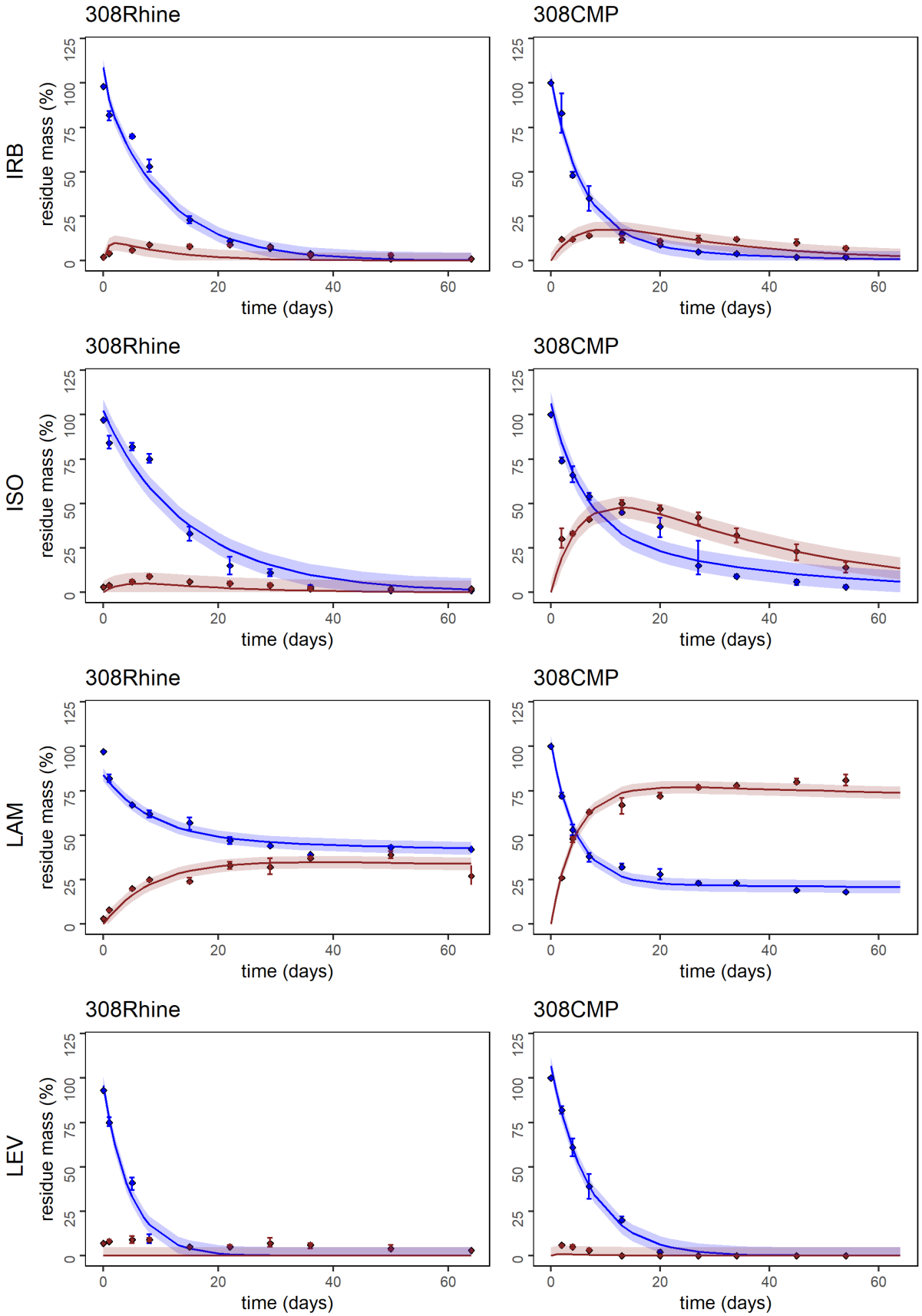
308Rhine
308CMP
IRB
ISO
LAM
LEV
residue mass (%)
time (days)
0
25
50
75
100
125
0
20
40
60

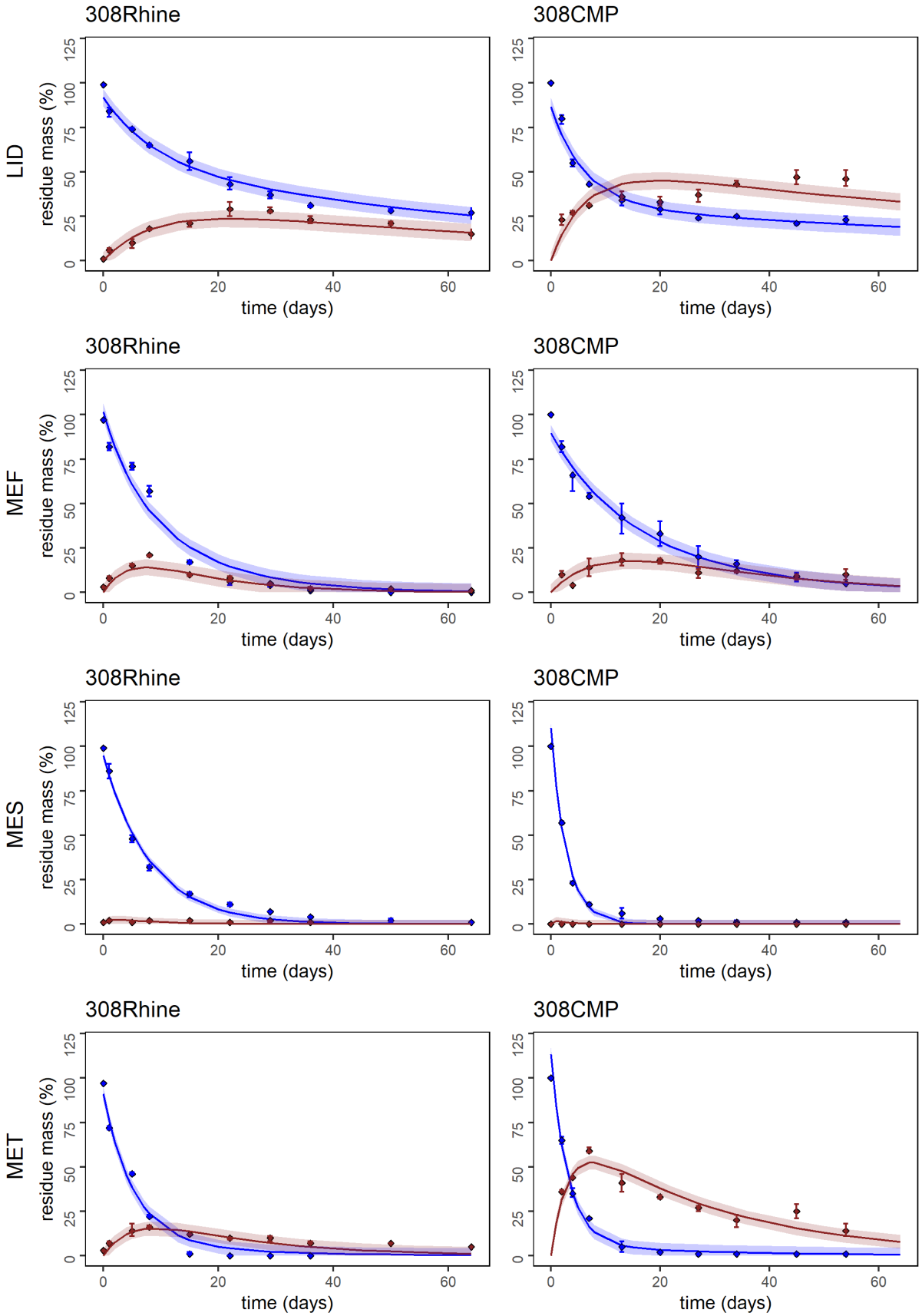
LID
MEF
MES
MET
308Rhine
308CMP
residue mass (%)
time (days)
0
25
50
75
100
125
0
20
40
60

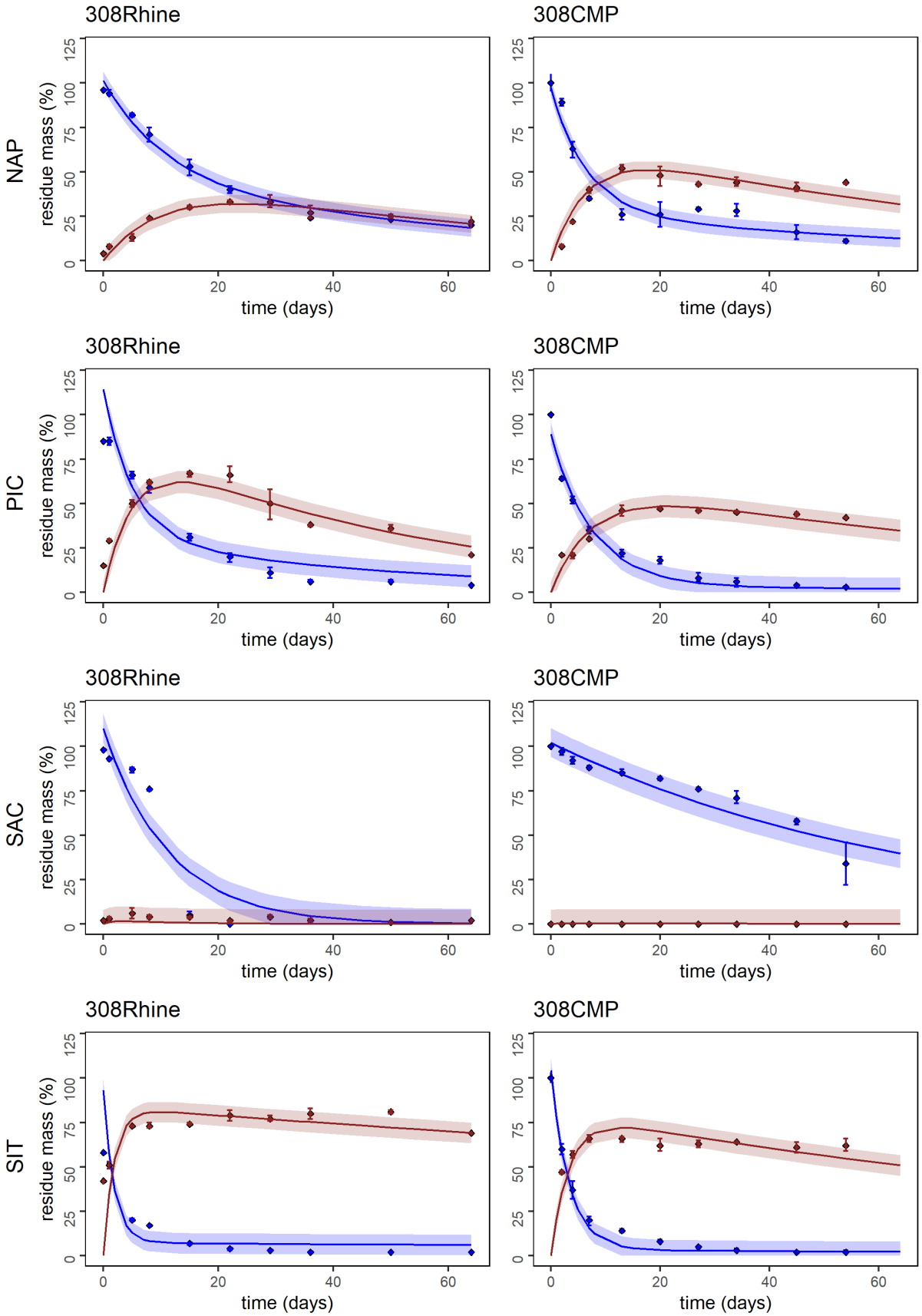
308Rhine
308CMP
NAP
PIC
SAC
SIT
residue mass (%)
time (days)
0
25
50
75
100
125
0
20
40
60

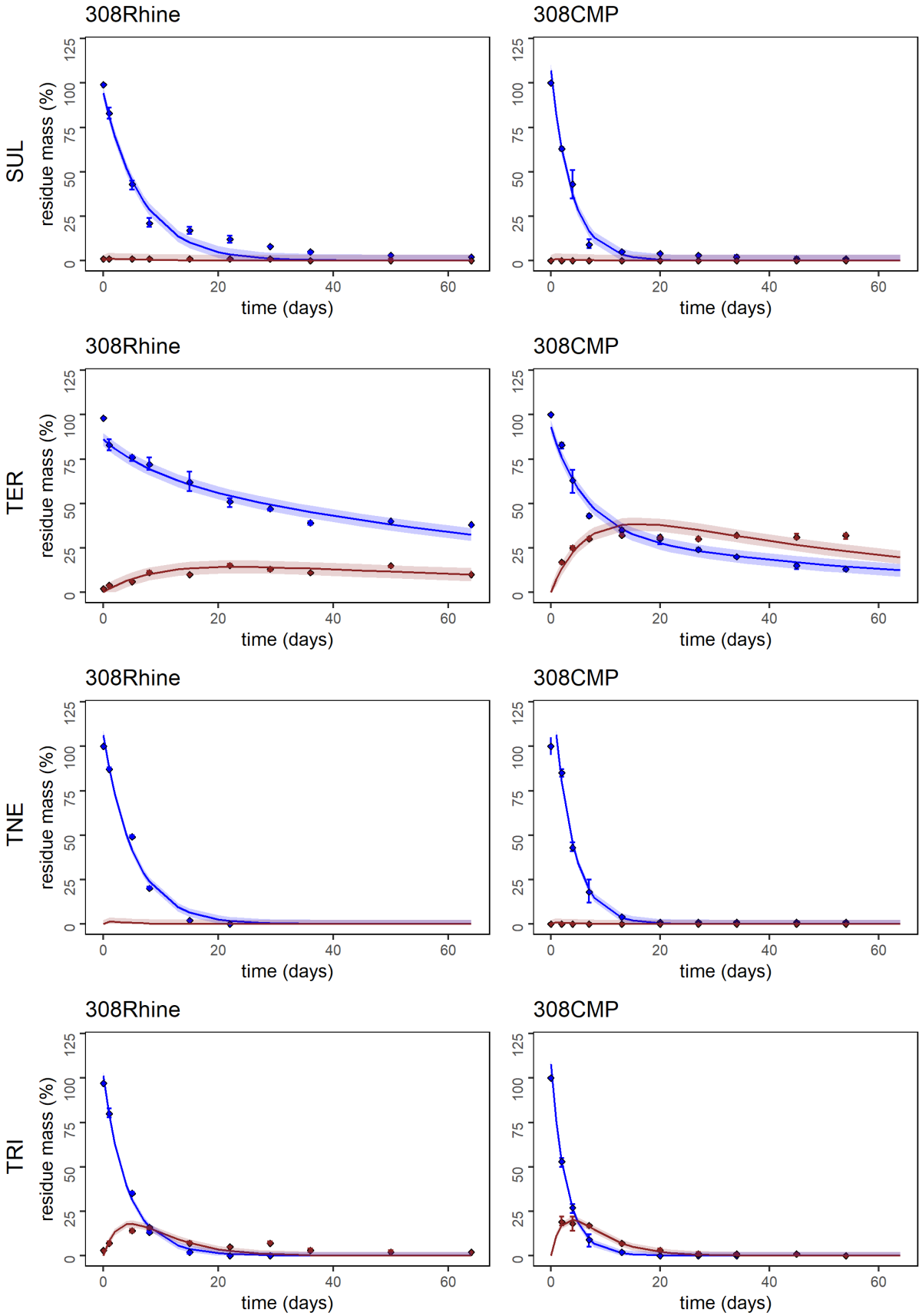
308Rhine
308CMP
SUL
TER
TNE
TRI
residue mass (%)
time (days)
0
25
50
75
100
125
0
20
40
60

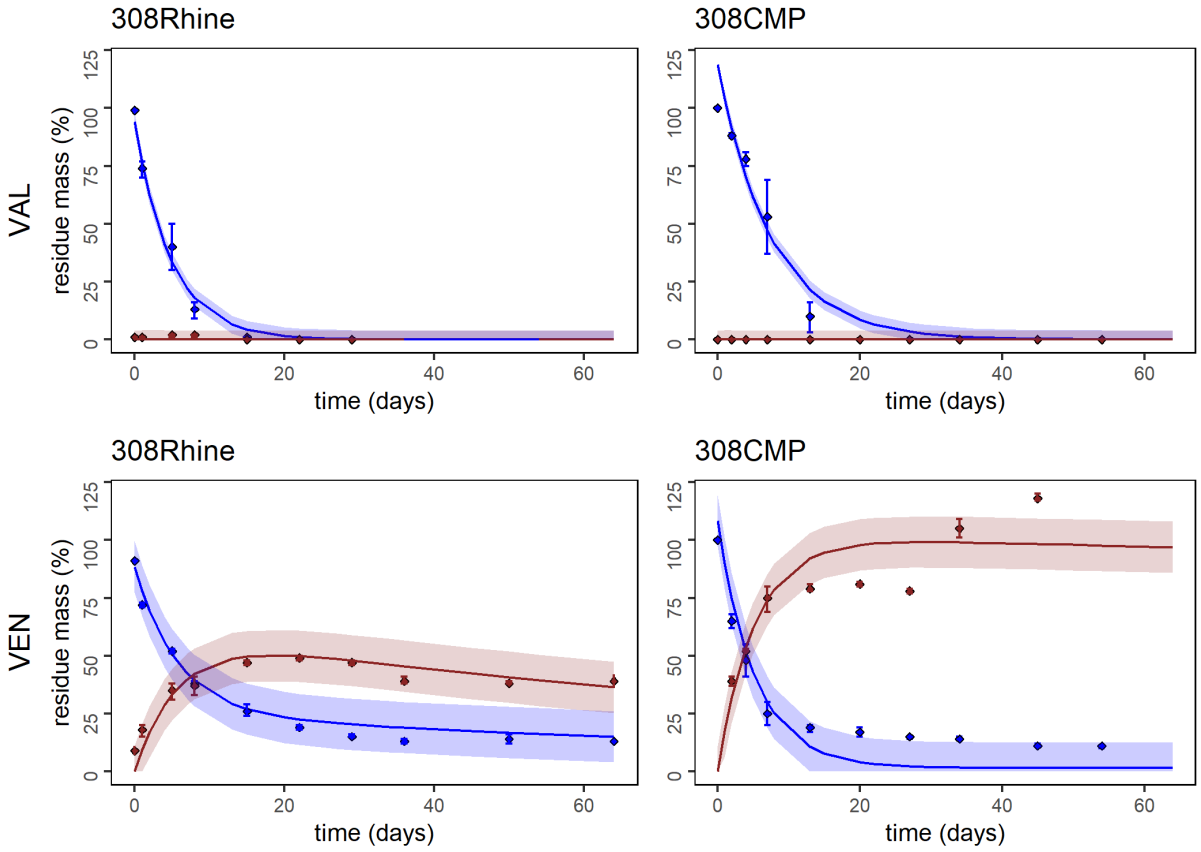

Model fits to experimental data when using $k'_{bio,lab,joint}$ to predict residue-time series. Average residues measured in the water phase and sediment of experimental duplicates are shown as blue and brown diamonds, respectively. Solid lines show the model fit to the data.

Source: own figure, Eawag

A.3 Supporting Information on the Rhine Field Study

A.3.1 Stream geometry, flow velocity, sediment grainsize distribution, and total suspended solids concentrations

The calculation of API degradation requires the knowledge of Z_w, Z_a, SSC, S, and τ_w in each stream reach. These values are not available on the stream network scale, observations are concentrated in a few points. Therefore, reach-specific values have to be estimated based on the few properties, which are known, namely the drainage area, and the channel slope. Obviously, such estimation is very crude, it just serves finding the approximate order of magnitude for the estimated values.

In a specific catchment discharge of a certain probability is commonly estimated as a power function of drainage area, and depth is estimated with another power function of discharge [Simons and Albertson, 1960; Wharton et al., 1989; Mosley and McKerchar, 1993; Andreadis et al., 2013]. Nested power functions form a power function again, so stream depth at mean flow (Z_w [m]) can be estimated a power function of drainage area (A [km^2]):

$$Z_w = a\,A^b$$

The parameters a (0.15) and b (0.3) are set to yield a minimal depth of 0.15 m at the drainage area of 1 km^2, and provide the known 5-6 m along the lower half of the Rhine (A > 100'000 km^2). Since most natural and channelized streams have high width:depth ratios, the hydraulic radius (R [m]) is approximately equal to Z_w.

We assume that flow extremes determine the long-term grain size distribution of streambed. Relative flow variability is calculated based on statistics of discharge and drainage area in multiple streams (Figure A7):

$$\frac{MHQ}{MQ} = 40.928\,A^{-0.217}$$

where MHQ, and MQ are mean high flow and mean flow, respectively. Similarly,

$$\frac{MHQ}{MLQ} = 298.77\,A^{-0.336}$$

where MLQ is mean low flow. Mapping from discharge to stage is usually performed by a common power-type rating curve:

$$Q \propto Z_w^k$$

From this

$$Z_w \propto Q^{\frac{1}{k}}$$

For natural channels where flow depth is small compared to width and bank slopes are gentle, k can be approximated with 2 based on the Manning-Chézy equation. Thus,

$$\frac{MHZ}{MZ} \approx \sqrt{\frac{MHQ}{MQ}} \text{ and } \frac{MHZ}{MLZ} \approx \sqrt{\frac{MHQ}{MLQ}}$$

where MHZ, MLZ, and MZ are the mean high, low, and mean flow depths, respectively.

Figure A 7: Mean high flow (MHQ) relative to mean flow (MHQ) and mean low flow (MLQ) in 100 selected gauges of Bayern and Baden-Württemberg (Rheingebiet I and II)

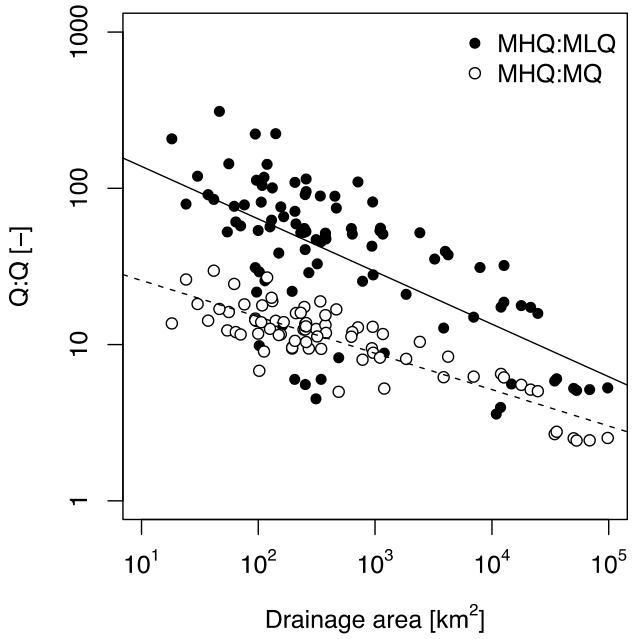

Source: own figure, BME

The shear velocity [m s^{-1}] for a given flow depth is

$$u^* = \sqrt{g\, Z_w I}$$

where I is the channel slope [–]. For the extreme flows

$$u_H^* = \sqrt{g\, Z_w \frac{MHZ}{MZ} I} \text{ and } u_L^* = \sqrt{g\, Z_w \frac{MLZ}{MZ} I}$$

because Zw = MZ, as we generally assume mean flow.

These shear velocities allow calculating the extreme values of the grainsize-distribution based on the Rouse numbers ($P = \frac{v_s}{\kappa u^*}$, where vs is settling velocity [m s-1] and κ = 0.4 is the von Kármán constant) belonging to full suspension (0.8) and instability (2.5). As the first step, the settling velocity for a particle with D diameter [m] is calculated [Ferguson and Church, 2004]:

$$v_s = \frac{1.65\, g\, D^2}{18 \cdot 10^{-6} + \sqrt{0.75 \cdot 1.65\, g\, D^3}}$$

It is assumed that the largest grainsize is at the limit of stability during high flow, while the smallest is that can be resuspended at low flows. Accordingly, for D90 the target settling velocity 2.5 $\kappa\, u_H^*$, while for D10 it is 0.8 $\kappa\, u_L^*$.

From D90 the base Manning roughness of the channel is calculated according to a polynomial fit to the USGS channel roughness data for different grainsizes [Arcement and Schneider, 1989]:

$$n = 0.00017\, d^3 - 0.00147\, d^2 + 0.00547\, d + 0.02598$$

where d = log D90 and D90 has the units of [mm].

Mean flow velocity (U [m s-1]) is calculated by using the Manning and Chézy equations:

$$U = \frac{1}{n} R^{\frac{2}{3}} \sqrt{I}$$

Knowing D10 and D90 lets us estimate the entire grainsize-distribution (unimodal, log-normal, with D50 = pD10D90) and from that the fraction of suspendible material (sand and finer, below 2 mm grainsize):

$$q_{\text{sand}} = \frac{1}{2}\left(1 + \text{erf}\left(\frac{\log 0.002 - \log D_{50}}{2.56\, (\log D_{90} - \log D_{10})\, \sqrt{2}}\right)\right)$$

A.3.1.1 Capacity-limited SSC

A significant number of semi-empirical formulas can be found in the literature to quantify suspended sediment loads. The formulas are generally based on hydrological/hydraulic parameters, such as flow depth, flow velocity, bed shear stress, critical bed shear and sediment parameters, e.g. characteristic grain diameter. In this study we use the model of van Rijn [1984], which is one of the most tested formulas for the sediment carrying capacity of flow and has been successfully used in a wide variety of riverine applications. Hereby we assume that the suspended sediment is represented by an average sand particle with D = 0.5 [mm].

The critical depth-averaged velocity for initiation of motion [m s^{-1}] is:

$$U_{cr} = 8.5\, D_{50}^{0.6} \log\left(12\, \frac{Z_w}{Z_a}\right)$$

where Z_a is the thickness of the active sediment layer ([m] $Z_a = 3\ D_{50}$). The mobility parameter [–]:

$$M_e = \frac{U - U_{cr}}{\sqrt{1.65\, g\, D}}$$

where U is the mean flow velocity [m s^{-1}]. The dimensionless particle size [–]:

$$D^* = D\, \left(\frac{1.65\, g}{\nu^2}\right)^{\frac{1}{3}}$$

where ν is the kinematic viscosity of water [10^{-6} m^2 s^{-1}].

Specific suspended sediment discharge or sediment transport rate [kg m^{-1} s^{-1}]:

$$q_{s,cap} = 0.012\, \rho\, U\, D\, M_e^{2.4} D^{*-0.6}$$

where ρ = 2650 [kg m^{-3}] is the sediment density (for quartz).

SSC assuming capacity limitation [kg m^{-3}]:

$$SSC_{cap} = \frac{q_{s,cap}}{q_w} = \frac{q_{s,cap}}{U\, Z_w}$$

where $q_w = U \cdot Z_w$ is the specific flow discharge [$m^2\ s^{-1}$].

A.3.1.2 Supply-limited SSC

Assume that SSC is determined by sediment supply, and source of the suspended material is the streambed (by mean flow land supply should be negligible due to the lack of current surface runoff). For the supply-limited transport it is again assumed that the resuspended particle is an average sand with D = 0.5 [mm].

The settled (suspendible) sediment stock calculates from the active sediment depth ($Z_a = 3\ D$), the sediment porosity (θ), and the sand content:

$$S = Z_a(1-\theta)\ \rho\ q_{sand}$$

The resuspension rate constant [m s□□$^{-1}$] is expressed as function of the excess shear velocity:

$$k_s = \alpha \left(\frac{u^*}{v_s} - 1\right) \exp\left(-\frac{D_{50}}{D}\right)$$

where $\alpha = 0.52$ [$m\ s^{-1}$] is a calibrated constant, D_{50}/D is a grain-diameter ratio between the 'average' sand particle and D_{50}, because high grain diversity hinders resuspension of finer particles due to streambed armouring.

The suspended sediment transport rate under supply-limitation [$kg\ m^{-1}\ s^{-1}$]:

$$q_{s,\mathrm{sup}} = k_s S$$

SSC assuming supply limitation [$kg\ m^{-3}$]:

$$SSC_{sup} = \frac{q_{s,\mathrm{sup}}}{q_w} = \frac{q_{s,\mathrm{sup}}}{U\ Z_w}$$

A.3.1.3 Actual SSC

The actual SSC is the smaller value from the capacity- and supply-limited pair:

$$SSC = \min\left(SSC_{sup}, SSC_{cap}\right)$$

In the Rhine basin SSC_{sup} was almost exclusively determining SSC, so most channels are possibly supply-limited. Modelled SSCs were typically between 30 and 100 [mg L^{-1}] (Fig. S5) in major rivers. For the Rhine channel mean annual SSCs are reported to be 27 [mg L^{-1}] at Maxau [Maniak, 2010], and 20-50 [mg L^{-1}] along the entire German section [Schmidt and Unbenannt, 2003]. The modelled values fell into the same range. Smaller tributaries had typically higher SSCs, with channel slope as a secondary selection factor. Among the major inflows, the Main had the lowest and the Aare had the highest modelled SSCs. Mean measured SSC in the lower Aare varies between 80-200 [mg L^{-1}] [TK Consult AG, 2013].

Figure A 8: Modelled SSCs in major rivers

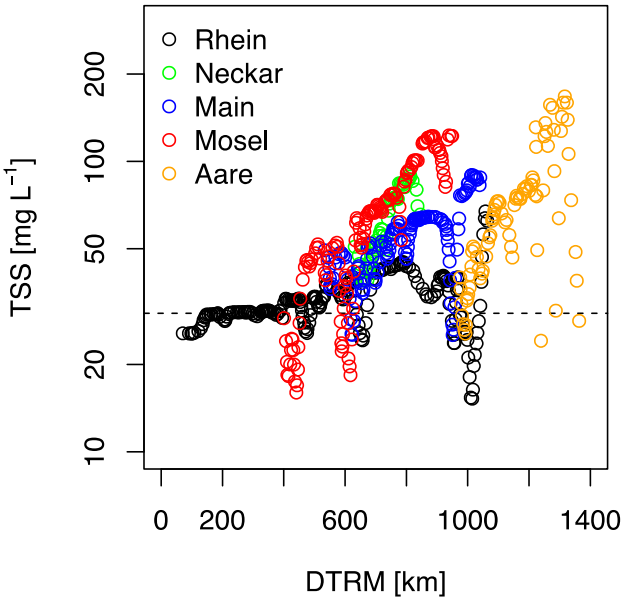

DTRM: distance to Rhine mouth. Dashed line: mean measured concentrations for the Rhine channel. High amplitude fluctuations in SSC are due to the coarse resolution of channel slope data and the lack of longitudinal coherence in the presented simple SSC approximation.

Source: own figure, BME

A.3.2 Water temperature during the SMPC campaigns

Table A 2: Water temperatures in the Rhine during P1 and P3

Data is available at http://iksr.bafg.de/iksr/daten.asp?S=0&JA=2017&PH=W&KG=WT

Date	Location	Temperature water (°C)
20.03.2017 (P1)	Rekingen	8.39
	Weil am Rhein	9.5
	Karlsruhe	10.6
	Koblenz	11.5
	Koblenz (Mosel)	10.4
	Bimmen	10.9
	Lobith	11.1
	Kampen (Ijssel)	-
	Maassluis (Waal)	-
03.04.2017 (P1)	Rekingen	10.8

Date	Location	Temperature water (°C)
	Weil am Rhein	12
	Karlsruhe	13.2
	Koblenz	14.1
	Koblenz (Mosel)	13
	Bimmen	13.1
	Lobith	13.4
	Kampen (Ijssel)	13
	Maassluis (Waal)	12.5
10.07.2017 (P3)	Rekingen	22.1
	Weil am Rhein	22.4
	Karlsruhe	23.5
	Koblenz	24.5
	Koblenz (Mosel)	24.5
	Bimmen	23.2
	Lobith	23.6
	Kampen (Ijssel)	-
	Maassluis (Waal)	-
24.07.2017	Rekingen	20.6
	Weil am Rhein	21.4
	Karlsruhe	22.1
	Koblenz	22.9
	Koblenz (Mosel)	23.2
	Bimmen	22
	Lobith	22.3
	Kampen (Ijssel)	21.9
	Maassluis (Waal)	21.7

A.4 Complementary Results of the Rhine Field Study

Table A 3: Discharge and concentrations for the SMPC P1 campaign (Part 1)

The measurements at locations (coloured with red) where only grab samples were taken or where there was no measured discharge were discarded from flux calculations. Concentration values in square brackets are above the calibration curve, in round brackets are between LOD (limit of detection) and LOQ (limit of quantification).

		Concentration [ng/L]																	
Compound	**Q (m^3/s)**	**5MB**	**ACE**	**ALI**	**AMI**	**ATA**	**ATE**	**BEN**	**BEZ**	**BIC**	**CAR**	**CIT**	**CLA**	**CLO**	**CYC**	**DIC**	**FEX**	**GAB**	**HYD**
LOQ		**10**	**10**	**3**	**1**	**0.5**	**1**	**50**	**4**	**0.5**	**1**	**2**	**3**	**2**	**5**	**1**	**0.5**	**10**	**5**
Reckingen/ Rhein	350	54	310	4.2	3.6	0.7	1.1	110		0.6	12	2.3	5	2.8	16	12	4.3	56	10
Brugg	293	68	440	6.7	4.1	0.9	5.2	130	-2.1	0.5	10	3.7	6.4	4.3	33	29	8.7	49	15
Weil am Rhein	1010	62	400	14	4.9	1	4.3	140	-1.1	0.6	24	3.4	6.8	3.7	24	27	9.3	52	16
Karlsruhe	1180	72	380	20	6.1	1.2	3.9	160	-1.5	0.7	26	3.3	8.9	5	32	22	8.6	66	13
Mean of Worms right and left side	1311	180	520	13	12	1.3	5.2	590	6.4	1.9	38	4.8	11	9.2	69	51	12	160	51
Schwarzbach	NA	900	[3500]	[160]	[260]	24	29	[3400]	68	20	510	45	100	150	75	810	160	[1300]	[1300]
Bischofsheim	191	300	990	16	36	2.9	7.3	840	26	5.2	81	10	22	25	150	170	560	500	200
Mainz	NA	200	460	17	9.2	1.3	3.8	350	-3.9	1.5	33	4	9.7	7.5	50	32	11	120	28

Concentration [ng/L]																		
Compound	**Q (m^3/s)**	**5MB**	**ACE**	**ALI**	**AMI**	**ATA**	**ATE**	**BEN**	**BEZ**	**BIC**	**CAR**	**CIT**	**CLA**	**CLO**	**CYC**	**DIC**	**FEX**	**GAB**	**HYD**
Koblenz/Rhein	1530	200	500	19	13	1.6	4.5	360	5.9	2	40	6.4	13	9.7	50	38	57	170	43
Koblenz/Mosel	211	350	480	12	9.5	1.2	10	210	6.3	1.9	31	3.6	12	15	89	29	8.5	260	34
Bad Honnef	1825	200	500	22	11	1.7	4.6	390	8.4	2.3	43	5.2	16	10	66	40	55	190	39
Düsseldorf Rechts	NA	260	540	16	18	1.7	5.8	560	9.3	2.2	44	5.9	14	12	59	52	57	230	60
Dinslaken	13	[5900]	[10000]	[170]	[400]	24	170	[5200]	430	20	450	85	150	140	33	[1300]	250	[5100]	[1800]
Lobith	1847	320	680	10	24	1.6	8.2	520	15	2.7	54	6.2	14	14	67	60	54	310	74
Bimmen	1857	250	560	13	14	1.8	5.8	420	8.4	2.6	49	5	15	12	48	42	53	240	55
Kampen	289	310	710	12	20	2.1	8.4	520	11	3.8	62	6.3	14	19	40	34	75	340	47
Maassluis	1194	300	590	13	13	1.5	8.3	470	8.9	2.3	47	4.4	12	15	54	28	47	270	44

Table A 4: Discharge and concentrations for the SMPC P1 campaign (Part 2)

The measurements at locations (coloured with red) where only grab samples were taken or where there was no measured discharge were discarded from flux calculations. Concentration values in square brackets are above the calibration curve, in round brackets are between LOD (limit of detection) and LOQ (limit of quantification).

		Concentration [ng/L]																	
Compound	**Q (m^3/s)**	**IRB**	**LAM**	**LEV**	**LID**	**MEF**	**MOC**	**MTO**	**OXC**	**PHE**	**PRE**	**PRO**	**RAN**	**SAC**	**SIT**	**SUL**	**TRI**	**VAL**	**VEN**
LOQ		**0.5**	**2**	**13**	**1**	**0.5**	**2**	**2**	**1**	**3**	**35**	**1**	**5**	**20**	**1**	**4**	**1**	**3**	**5**
Reckingen/ Rhein	350	3.8	14	6.5	2.4	3	-0.3	5.6		-1.1		-0.5			13	4.8	-0.6	8.1	-4.8
Brugg	293	15	16	25	4.6	7.6	-0.5	15		-1.6		-0.8		52	18	6	3.5	53	7.6
Weil am Rhein	1010	11	17	-11	4.6	6.7	-0.4	11		-1.7		-0.9		28	18	5.2	2.4	46	7.3
Karlsruhe	1180	17	22	-9.7	4.9	4.9	-0.4	11		-2.3		1		-12	24	5	1.3	43	8.4
Mean of Worms right and left side	1311	23	32	17	7.8	4.1	-0.7	43	1.4	5.3		1.6		110	51	9.3	3.7	92	15
Schwarzbach	NA	390	570	29	110	6.1	5.2	430	9.9	54	93	15	10	810	940	67	53	180	190
Bischofsheim	191	63	75	22	17	0.8	-1.9	170	3	21	61	2.7	5.6	220	180	20	8.7	350	47
Mainz	NA	21	32	-11	6.3	4	-0.6	27	1.1	4.4		1.4		38	37	8.4	2.6	84	12

Concentration [ng/L]																		
Compound	**Q (m^3/s)**	**IRB**	**LAM**	**LEV**	**LID**	**MEF**	**MOC**	**MTO**	**OXC**	**PHE**	**PRE**	**PRO**	**RAN**	**SAC**	**SIT**	**SUL**	**TRI**	**VAL**	**VEN**
Koblenz/Rhein	1530	26	36	14	9.2	3.6	-0.8	44		6.2		1.6		73	59	11	2.7	89	22
Koblenz/Mosel	211	41	29	18	6.8	(0.2)	-0.6	28		-2.8	-34	3.7		74	63	6	2.5	120	13
Bad Honnef	1825	27	35	13	8.4	3.1	-0.9	45		7.1	-22	1.6		66	63	9.4	3.6	120	19
Düsseldorf Rechts	NA	29	45	13	9.5	2.9	-0.9	56	1	8.9	-30	2		70	72	13	4.2	140	19
Dinslaken	13	280	460	57	97	3.4	17	[1700]	14	140	580	22	76	690	[1400]	120	130	1000	240
Lobith	1847	29	41	14	11	2.6	-1.4	70		11	-34	2		140	92	11	5.2	160	21
Bimmen	1857	27	39	14	9.7	2.4	-1	58		9.5	-26	1.8		57	73	11	3.1	120	19
Kampen	289	43	55	-10	12	1.8	-1.4	96		12	36	2.2		49	84	17	4.7	180	25
Maassluis	1194	32	48	13	9.4	2.2	-1	67		8	-32	2.3		70	67	21	4.5	160	19

Table A 5: Discharge and concentrations for the SMPC P3 campaign (Part 1)

The measurements at locations (coloured with red) where only grab samples were taken or where there was no measured discharge were discarded from flux calculations. Concentration values in square brackets are above the calibration curve, in round brackets are between LOD (limit of detection) and LOQ (limit of quantification)

		Concentration [ng/L]																	
Compound	**Q (m^3/s)**	**5MB**	**ACE**	**ALI**	**AMI**	**ATA**	**ATE**	**BEN**	**BEZ**	**BIC**	**CAR**	**CIT**	**CLA**	**CLO**	**CYC**	**DIC**	**FEX**	**GAB**	**HYD**
LOQ		**10**	**10**	**3**	**1**	**0.5**	**1**	**50**	**4**	**0.5**	**1**	**2**	**3**	**2**	**5**	**1**	**0.5**	**10**	**5**
Reckingen/ Rhein	412	61	220	-2.9	1.7	0.8	-0.8	150		0.8	11	-1.4	-2.9	-1.9	40	5.4	6	40	6.1
Brugg	300	63	220	5.5	2.3	0.8	5.2	150	-1.3	-0.4	10	2.5	3.9	3.2	65	14	16	40	13
Weil am Rhein	900	66	220	8.8	2.9	0.9	2.9	170		0.6	12	2.8	4	2.8	46	16	13	40	8.5
Karlsruhe	895	100	240	7.7	4	0.8	1.5	230		0.8	21	2.3	3.9	4	33	3.8	8	74	6.4
Mannheim	58	790	580	15	29	2.8	2.9	[1800]	5	7	130	13	12	24	84	26	32	580	45
Mean of Worms right and left side	963	220	290	10.5	7.05	1.2	2.2	445	0.5	2.1	32.5	4	4.9	6.2	61.5	9.9	14.5	121.5	15
Schwarzbach	NA	[1300]	[1100]	[93]	[250]	18	9.3	[5100]	9.9	17	520	34	18	130	2.5	330	130	1000	580
Kornsand	NA	180	240	7.8	4.9	1	1.6	340		1.9	28	3.7	4.7	4.9	43	3.3	11	93	7

	Concentration [ng/L]																		
Compound	**Q (m^3/s)**	**5MB**	**ACE**	**ALI**	**AMI**	**ATA**	**ATE**	**BEN**	**BEZ**	**BIC**	**CAR**	**CIT**	**CLA**	**CLO**	**CYC**	**DIC**	**FEX**	**GAB**	**HYD**
Bischofsheim	133	500	460	13	32	3	2.7	[1300]	16	6	120	7.5	8	26	220	250	710	470	110
Mainz	1112	220	260	8	6.2	1.1	1.9	380		2.1	31	4.3	4.6	5.6	52	6.6	19	110	9.5
Koblenz/Rhein	1087	280	290	11	7.8	1.5	1.5	500		2.5	43	4.6	5.4	7.6	61	13	71	150	11
Koblenz/Mosel	48	990	550	9.3	6	2	2	650		5.7	94	3.8	7.6	16	73	2.8	23	420	5.5
Bad Honnef	1169	280	310	11	7.3	1.5	-0.9	470	-1.2	2.7	47	4.5	5.9	8.4	81	9.1	77	180	17
Düsseldorf Rechts	1210	380	320	9.5	18	2	2.6	850	-1.7	3.1	56	6	6.8	12	77	27	79	220	40
Duisburg Links	1290	410	320	9	16	1.8	2.2	650	-1.4	4	61	5.2	6.9	13	80	22	58	240	38
Dinslaken	19	[3300]	[2500]	[110]	[290]	15	110	[4300]	150	15	350	64	90	98	150	550	150	[1200]	940
Lobith	1210	490	410	8.3	21	2	4.2	730	4.6	3.5	70	5.4	7.1	14	150	32	65	280	54
Bimmen	1272	400	320	13	15	2.5	2.5	640	-1.9	3.4	60	5.1	7.5	12	100	21	63	220	29
Kampen	326	460	420	12	16	2.2	4.3	840	-2.5	4.7	77	6	7.7	19	160	20	27	330	29
Maassluis	1107	380	290	8.5	10	1.4	3.5	610	-2.8	3	50	3.9	5.5	12	96	12	29	200	25

Table A 6: Discharge and concentrations for the SMPC P3 campaign (Part 2)

The measurements at locations (coloured with red) where only grab samples were taken or where there was no measured discharge were discarded from flux calculations. Concentration values in square brackets are above the calibration curve, in round brackets are between LOD (limit of detection) and LOQ (limit of quantification).

		Concentration [ng/L]																
Compound	**Q (m^3/s)**	**IRB**	**LAM**	**LEV**	**LID**	**MEF**	**MOC**	**MTO**	**OXC**	**PHE**	**PRE**	**PRO**	**RAN**	**SAC**	**SIT**	**SUL**	**TRI**	**VAL**	**VEN**
LOQ		**0.5**	**2**	**13**	**1**	**0.5**	**2**	**2**	**1**	**3**	**35**	**1**	**5**	**20**	**1**	**4**	**1**	**3**	**5**
Reckingen/ Rhein	412	3.5	14	-2.6	3.6	1.5	-0.3	4.5		1				10	8.5	4.1	1	9.5	-2.9
Brugg	300	16	15	13	4.5	4.6	-0.4	12		-1.5		-0.6		53	14	4.6	2.7	27	20
Weil am Rhein	900	11	18	-5.6	5.1	4.2	-0.4	6.9		-1.5		-0.6		-14	14	4.9	1.9	24	10
Karlsruhe	895	7	30	-5	5.5	2.6	-0.5	6.1	1.5	-1.9				45	18	10	-0.1	3.9	13
Mannheim	58	14	170	15	23	0.6	2.2	120	4.2	20	39	1.1		91	170	51	3.4	47	51
Mean of Worms right and left side	963	8.45	42	19.5	7.6	2.45	-0.6	24		4.75	17.5	-0.8	2.5	21	38	11.5	2.2	10.4	18
Schwarzbach	NA	160	670	20	86	5.1	6.3	270	35	42	71	6.2		490	650	110	9.8	28	150
Kornsand	NA	5.9	36	-5.4	6.5	1.6	-0.5	14		3.7		-0.5		10	28	7.3	1.2	16	14

Concentration [ng/L]																		
Compound	**Q (m^3/s)**	**IRB**	**LAM**	**LEV**	**LID**	**MEF**	**MOC**	**MTO**	**OXC**	**PHE**	**PRE**	**PRO**	**RAN**	**SAC**	**SIT**	**SUL**	**TRI**	**VAL**	**VEN**
Bischofsheim	133	15	130	-8.3	21	0.7	2.3	70	1.7	48	-30	1.9		90	150	38	2.5	11	40
Mainz	1112	7.2	39	-5.3	7.2	1.7	-0.7	17		4.4				-17	36	9.9	1.3	6.6	18
Koblenz/Rhein	1087	9.2	53	-6	8.6	1.6	-0.8	21		8.9		-0.7		25	47	13	1.1	18	20
Koblenz/Mosel	48	9.4	120	-2.8	11	-0.1	-1.3	26	2.1	10	-24	-0.6		24	97	27	-0.7	13	23
Bad Honnef	1169	8.1	50	-5.3	8.9	1.1	-0.9	23		9.4		-0.7		10	51	9.8	1.1	7.5	22
Düsseldorf Rechts	1210	11	67	-7.7	11	1.5	-1.2	38	1	12		1		-14	67	24	1.5	12	24
Duisburg Links	1290	11	70	-6.8	11	1	-1.1	33	0.5	12		1.1		-13	72	14	1.8	38	23
Dinslaken	19	150	360	24	110	1.6	16	460	10	110	370	12	30	140	940	170	22	60	190
Lobith	1210	9.4	76	13	13	1	-1.7	66		16		1		41	90	16	3.2	27	29
Bimmen	1272	7.9	70	-9.2	11	1.2	-1.1	39	1	12		-0.9		10	71	24	1.5	22	23
Kampen	326	20	83	-12	14	0.8	-1.4	73	1.2	13		1.8		36	87	27	2.7	20	31
Maassluis	1107	11	64	13	9.5	1	-0.9	48		7.9		0.9		22	53	29	1.2	57	21

Table A 7: **k_{hydr} [d^{-1}] and k_{photo} [d^{-1}] priors and posteriors statistics (arithmetic mean and standard deviation (SD)) from the P1 campaign.**

	Prior				Posterior			
	k_{hydr}		k_{photo}		k_{hydr}		k_{photo}	
Compound	Mean	SD	Mean	SD	Mean	SD	Mean	SD
5MB	0.0008	0.0001	0	0	0.0008	0.0001	0	0
ALI	0	0	0.0980	0.0098	0	0	0.0985	0.0099
ATA	0	0	0.0910	0.0091	0	0	0.0920	0.0095
DIC	0	0	0.7000	0.0700	0	0	0.7083	0.0685
HYD	0.0310	0.0031	0.3700	0.0370	0.0316	0.0032	0.3765	0.0368
IRB	0.1110	0.0111	0	0	0.1107	0.0111	0	0
SIT	0.0050	0.0005	0	0	0.0051	0.0005	0	0
SUL	0	0	0.0560	0.0056	0	0	0.0563	0.0054

Table A 8: **k_{hydr} [d^{-1}] and k_{photo} [d^{-1}] priors and posteriors statistics (arithmetic mean and standard deviation (SD)) from the P3 campaign.**

	Prior				Posterior			
	k_{hydr}		k_{photo}		k_{hydr}		k_{photo}	
Compound	Mean	SD	Mean	SD	Mean	SD	Mean	SD
5MB	0.0008	0.0001	0	0	0.0008	0.0001	0	0
ALI	0	0	0.3100	0.0310	0	0	0.3092	0.0310
ATA	0	0	0.2800	0.0280	0	0	0.2781	0.0229
DIC	0	0	2.2000	0.2200	0	0	2.1953	0.2095
HYD	0.0310	0.0031	1.1600	0.1160	0.0312	0.0032	1.1603	0.1058
IRB	0.1110	0.0111	0	0	0.1117	0.0109	0	0
SIT	0.0050	0.0005	0	0	0.0050	0.0005	0	0
SUL	0	0	0.1700	0.0170	0	0	0.1741	0.0186

Figure A 9: Removal rates (k_{rem}) in the Rhine vs. k'bio values in SMPC P1 (orange dots) and P3 (blue dots).

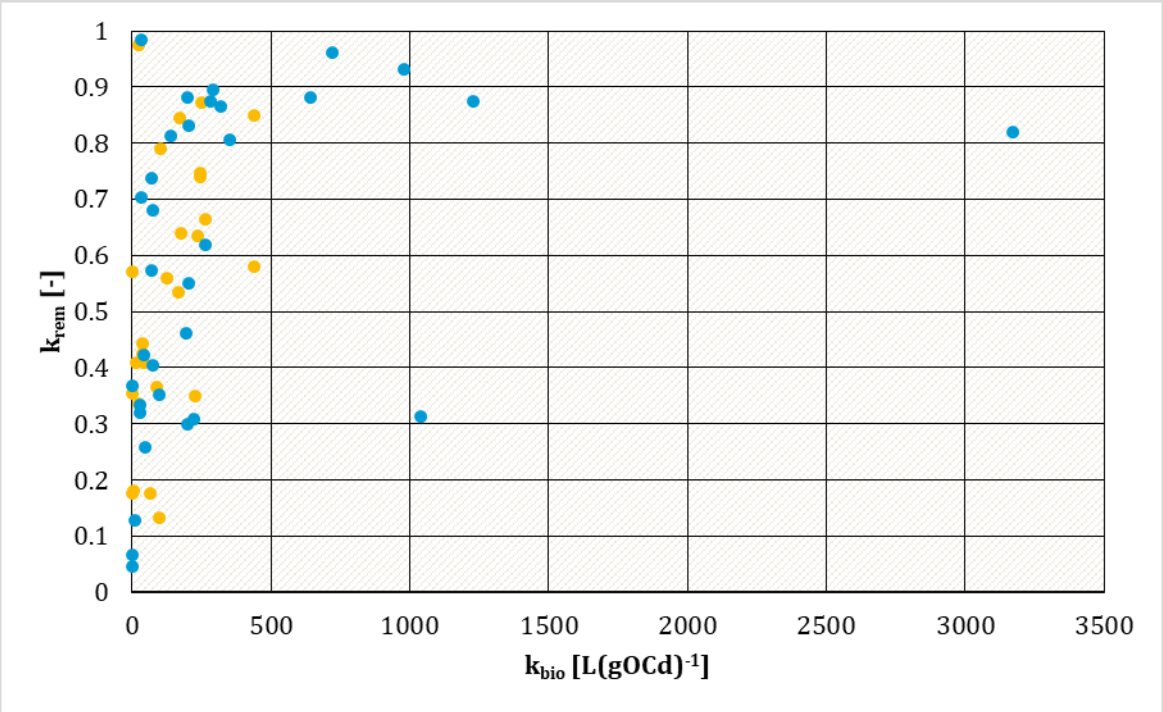

Source: own figure, BME

Table A 9: Removal rates (k_{rem}) in the Rhine vs. k'_{bio} values in SMPC P1 and P3

When removal rate was negative, it was replaced by 'NA'.

	P1		P3	
Compound	**k'_{bio}**	**k_{rem}**	**k'_{bio}**	**k_{rem}**
5MB	0.06	NA	0.01	NA
ACE	67.4	0.18	193.6	0.46
ALI	0.35	0.57	75.2	0.68
AMI	437	0.58	223	0.31
ATA	16.8	0.41	30.3	0.33
ATE	237.68	0.64	263	0.62
BEN	265.0	0.66	75.6	0.40
BEZ	0.40	NA	1229	0.88
BIC	35.7	0.43	70.7	0.57
CAR	40.0	0.44	0.10	0.07

	P_1		P_3	
Compound	**k'_{bio}**	**k_{rem}**	**k'_{bio}**	**k_{rem}**
CIT	104	0.79	141	0.81
CLA	0.00	0.18	40.8	0.42
CLO	168	0.54	97.2	0.35
CYC	229	0.35	1041	0.31
DIC	173	0.84	723	0.96
FEX	0.01	NA	0.03	0.05
GAB	87.0	0.37	47.8	0.26
HYD	244	0.74	642	0.88
IRB	0.01	0.35	321	0.86
LAM	22.7	0.34	10.75	0.13
LEV	438	0.85	978	0.93
LID	244	0.75	350	0.81
MEF	3.51	0.18	71.4	0.74
MOC	98.7	0.13	199	0.30
MTO	127	0.56	205	0.55
OXC	24.2	0.98	31.8	0.98
PHE	0.01	NA	0.28	NA
PRE	175	0.64	280	0.88
PRO	40.3	0.41	206	0.83
RAN	251	0.87	294	0.90
SAC	258	NA	32.1	0.70
SIT	33.9	0.45	26.9	0.32
SUL	219.6	0.46	0.24	0.37
TRI	11.6	0.39	200	0.88
VAL	0.32	NA	3173	0.82
VEN	0.00	0.31	79.0	0.68

Table A 10: Distance-specific dissipation rate constants in SMPC P1 with different benchmarks

Mean distance-specific dissipation rate constants (k'_S [km^{-1}]) in SMPC P1 with different benchmarks. PPL represents the upstream population. As calibration is a stochastic algorithm, these values for CAR as a benchmark may slightly deviate from values in Table 36.

Benchmark Compound	5MB	BIC	CAR	GAB	SIT	PPL*
5MB	NA	0.00030	-0.00114	0.00027	-0.00001	-0.00022
ACE	0.00470	0.00553	0.00113	0.00509	0.00469	0.00296
ALI	0.27739	0.29652	0.00277	0.26162	0.22938	0.00933
AMI	0.00124	0.00165	-0.00048	0.00153	0.00121	0.00065
ATA	0.00459	0.05417	0.00038	0.00420	0.00439	0.00209
ATE	0.00553	0.00683	0.00159	0.00602	0.00577	0.00360
BEN	0.00144	0.00146	0.29669	0.00146	0.00729	0.28315
BEZ	-0.00094	-0.00100	-0.00137	-0.00083	-0.00096	0.12861
BIC	-0.00024	NA	-0.00123	0.00002	-0.00025	-0.00038
CAR	0.00301	0.00374	NA	0.00333	0.00280	0.00151
CIT	0.00344	0.00441	0.00061	0.00425	0.00350	0.00210
CLA	0.00262	0.00321	-0.00018	0.00276	0.00756	0.00119
CLO	0.00094	0.00138	-0.00063	0.00120	0.00083	0.00031
CYC	0.01952	0.00225	0.00034	0.00225	0.00189	0.00151
DIC	0.00341	0.00392	0.00080	0.00389	0.00380	0.00260
EPH	NA	NA	NA	NA	NA	NA
FEX	0.22798	0.33871	0.33808	0.27605	0.36785	0.36867
GAB	-0.00025	0.00001	-0.00142	NA	-0.00030	-0.00046
HYD	0.00057	0.00097	-0.00055	0.00120	0.00077	0.11997
IRB	0.00209	0.00259	-0.00017	0.00231	0.00186	0.00101
KET	0.12391	0.12301	0.00247	0.12681	0.00658	0.00451
LAM	0.00216	0.00283	-0.00016	0.00250	0.00213	0.00111
LEV	0.00435	0.00536	0.00135	0.00484	0.00458	0.00310
LID	0.00236	0.00333	-0.00012	0.00276	0.00230	0.00125
MEF	0.19141	0.16313	0.02752	0.01375	0.04807	0.01040
MOC	0.00165	0.00230	-0.00065	0.00218	0.00192	0.00072
MTO	-0.00067	-0.00045	-0.00120	-0.00040	-0.00062	-0.00050
OLM	0.00229	0.00279	-0.00043	0.00268	0.00230	0.00103
OXC	0.15457	0.16877	0.25571	0.17666	0.21056	0.30980
OXY	-0.00030	-0.00005	-0.00146	-0.00016	-0.00040	0.00021
PHE	-0.00070	-0.00048	-0.00182	-0.00047	-0.00079	-0.00092
PPL*	0.00083	0.00130	-0.00122	0.00118	0.00075	NA
PRE	0.45452	0.14431	0.00153	0.16424	0.01456	0.00374
PRO	0.00267	0.00333	0.00010	0.00305	0.00262	0.00151
RAN	0.12788	0.17248	0.00243	0.15244	0.00698	0.00452
SAC	0.21238	0.31417	0.36740	0.35515	0.32483	0.37498
SIT	0.00006	0.00036	-0.00123	0.00031	NA	-0.00023
SUL	0.00216	0.00269	-0.00017	0.00258	0.00223	0.00121
TRI	0.03252	0.00644	0.00130	0.01378	0.12939	0.13387
VAL	0.00132	0.00174	-0.00071	0.00169	0.00136	0.00058
VEN	0.00107	0.00150	-0.00056	0.00138	0.00103	0.00050

Table A 11: Distance-specific dissipation rate constants in SMPC P3 with different benchmarks

Mean distance-specific dissipation rate constants (k'S [km-1]) in SMPC P3 with different benchmarks. PPL represents the upstream population. As calibration is a stochastic algorithm, these values for CAR as a benchmark may slightly deviate from values in Table 36.

Benchmark Compound	5MB	BIC	CAR	GAB	SIT	PPL*
5MB	NA	-0.00008	-0.00045	-0.00023	-0.00025	-0.00056
ACE	0.00606	0.00621	0.00485	0.00560	0.00468	0.00388
ALI	0.00751	0.00739	0.00628	0.00715	0.00563	0.00481
AMI	0.00064	0.00059	-0.00026	0.00019	0.00005	-0.00042
ATA	0.00478	0.00468	0.00325	0.00418	0.00303	0.00209
ATE	0.01474	0.01416	0.01463	0.01569	0.01183	0.01124
BEN	0.00118	0.00119	0.00043	0.00077	0.00068	0.00020
BEZ	0.00973	0.01043	0.00834	0.00934	0.00795	0.00697
BIC	0.00012	NA	-0.00027	-0.00003	-0.00012	-0.00040
CAR	0.00075	0.00077	NA	0.00031	0.00037	-0.00012
CIT	0.00477	0.00471	0.00351	0.00438	0.00330	0.00259
CLA	0.00590	0.00595	0.00466	0.00551	0.00444	0.00350
CLO	0.00121	0.00128	0.00030	0.00070	0.00065	0.00007
CYC	0.00606	0.00584	0.00449	0.00559	0.00399	0.00314
DIC	0.28110	0.27886	0.34037	0.32125	0.29082	0.30767
EPH	0.00820	0.00867	0.00697	0.00781	0.00660	0.00570
FEX	0.13416	0.06435	0.25946	0.56201	0.24295	0.00066
GAB	0.00040	0.00043	-0.00027	NA	0.00010	-0.00035
HYD	0.10808	0.17798	0.17306	0.19205	0.00205	0.00236
IRB	0.01185	0.01159	0.01078	0.01198	0.00929	0.00864
KET	0.00825	0.00900	0.00696	0.00780	0.00665	0.00572
LAM	0.00180	0.00190	0.00082	0.00122	0.00121	0.00060
LEV	0.21948	0.18326	0.24312	0.20556	0.14303	0.30798
LID	0.00448	0.00439	0.00311	0.00389	0.00316	0.00237
MEF	0.02016	0.02083	0.01655	0.01780	0.01479	0.01408
MOC	0.00308	0.00320	0.00223	0.00245	0.00210	0.00130
MTO	0.00006	-0.00011	-0.00039	-0.00026	-0.00042	-0.00056
OLM	0.00215	0.00215	0.00094	0.00152	0.00118	0.00053
OXC	0.37229	0.37031	0.29394	0.27798	0.37506	0.30492
OXY	-0.00065	-0.00064	-0.00103	-0.00087	-0.00060	-0.00098
PHE	-0.00114	-0.00129	-0.00149	-0.00137	-0.00126	-0.00152
PPL*	0.00102	0.00106	0.00020	0.00058	0.00052	NA
PRE	0.00828	0.00834	0.00696	0.00783	0.00655	0.00571
PRO	0.00734	0.00717	0.00597	0.00694	0.00540	0.00455
RAN	0.00819	0.00827	0.00698	0.00784	0.00658	0.00572
SAC	0.37684	0.36837	0.31266	0.30473	0.37976	0.34899
SIT	0.00037	0.00032	-0.00024	0.00008	NA	-0.00036
SUL	0.00206	0.00313	0.00084	0.00123	0.00145	0.00086
TRI	0.31744	0.29672	0.32843	0.33849	0.32331	0.33004
VAL	0.23090	0.24344	0.29692	0.25881	0.24846	0.27509
VEN	0.00338	0.00349	0.00230	0.00284	0.00249	0.00183

A.5 Complementary Results on the Comparison of Persistence Indicators derived from Laboratory and Field

Figure A 10: Correlations between persistence indicators derived from modified OECD 308-type studies and from the field study in the Rhine river catchment

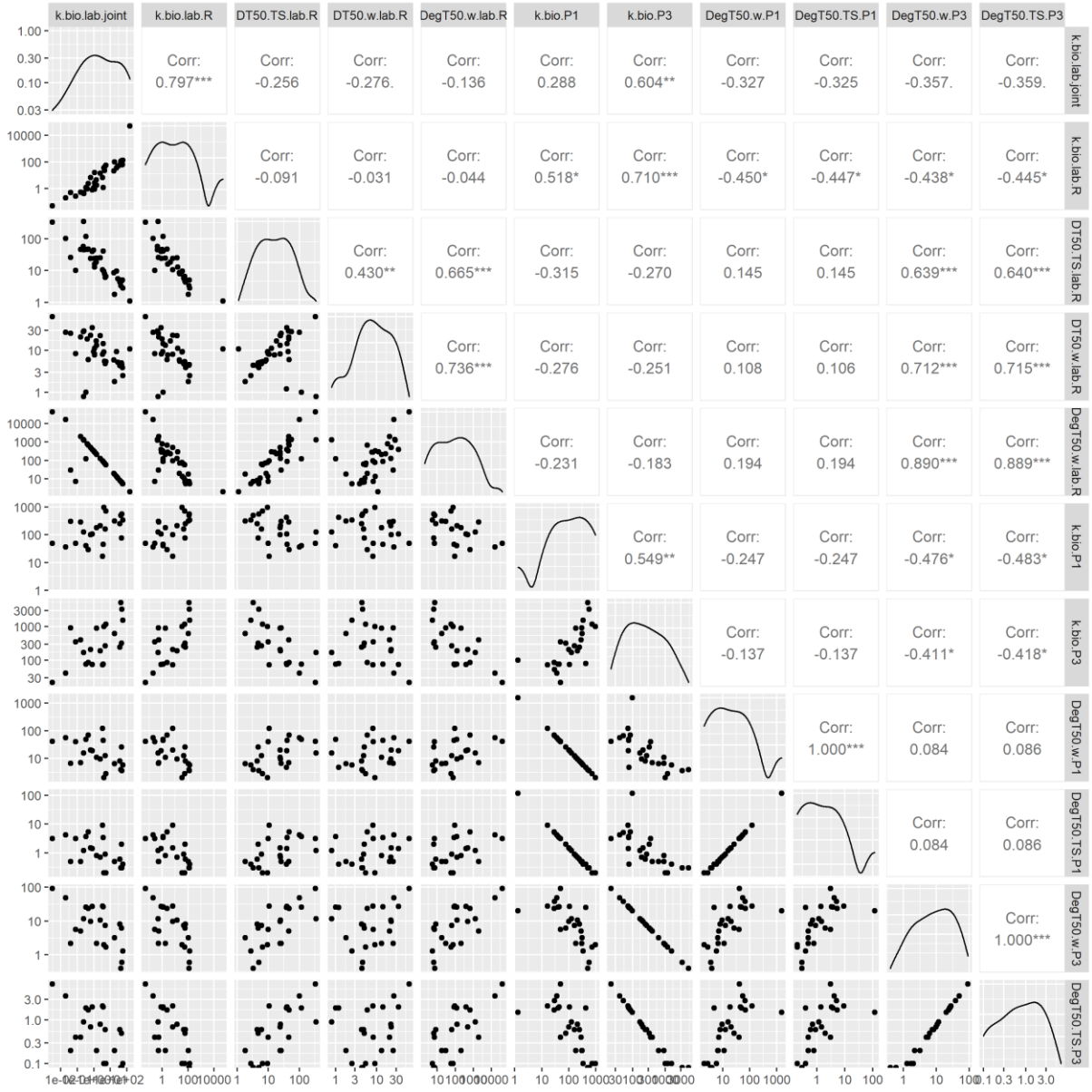

Corr. shows the respective Pearson correlation coefficients, asterisks indicate the statistical significance of the correlation with ***p<0.01, **p<0.05, *p<0.1. Note that all degradation half-lives ($DegT_{50}$) were calculated based on the compounds respective k'_{bio} values.

Source: own figure, Eawag

A.5.1 Correlations between parameters derived from laboratory studies and from the Rhine model

Correlations of k'_{bio}

Comparison	r	R^2
$k'_{bio,lab,R}$ versus $k'_{bio,lab,joined}$	0.797	0.64
$k'_{bio,lab,R}$ versus $k'_{bio,field,P1}$	0.518	0.27
$k'_{bio,lab,R}$ versus $k'_{bio,field,P3}$	0.710	0.50
$k'_{bio,lab,joined}$ versus $k'_{bio,field,P3}$	0.604	0.37
$k'_{bio,field,P1}$ versus $k'_{bio,field,P3}$	0.549	0.30

Correlations of $DT_{50,TS,lab,OECD\ 308,R}$

Comparison	r	R^2
$DT_{50,TS,lab,R}$ versus $DT_{50w,lab,R}$	0.430	0.18
$DT_{50,TS,lab,R}$ versus $DegT_{50,w,lab,R}$	0.67	0.45
$DT_{50,TS,lab,R}$ versus $DegT_{50,w,P3}$	0.639	0.41
$DT_{50,TS,lab,R}$ versus $DegT_{50,TS,field\ P3}$	0.640	0.41

Correlations of $DT_{50,w,lab,OECD\ 308,R}$

Comparison	r	R^2
$DT_{50,w.lab\ R}$ versus $DegT_{50TS,lab,R}$	0.665	0.44
$DT_{50,w.R}$ versus $DegT_{50,w,CMP}$	0.736	0.54
$DT_{50,w,lab,R}$ versus $DegT_{50,w,,field\ P3}$	0.712	0.51
$DT_{50,w.R}$ versus $DegT_{50\ TS,P3}$	0.715	0.51

Correlations of $DegT_{50,w,lab,OECD\ 308,R}$

Comparison	r	R^2
$DegT_{50,w,lab,R}$ versus $DT_{50TS,lab,R}$	0.665	0.44
$DegT_{50,w,lab,R}$ versus $DT_{50\ w,lab,R}$	0.736	0.54
$DegT_{50,w,lab,R}$ versus $DegT_{50w\ field\ P3}$	0.889	0.79
$DegT_{50,w,lab,R}$ versus $DegT_{50,w,P3}$	0.890	0.79

Table A 12: Ratio of $DegT_{50,w,field}$ to $DT_{50,w,mod308}$

$DegT_{50,w,field}$ were calculated based on the compounds respective $k'_{bio,field}$ values. $DT_{50,w,mod308}$ were derived from modified OECD 308-type studies conducted in inoculum sampled from the Rhine.

Compound	Ratio $DegT_{50,w,field,P1}/DT_{50,w,mod308}$	Ratio $DegT_{50,w,field,P3}/DT_{50,w,mod308}$
ACE	0.88	0.43
ALI	n.d.	n.d.
ATA	n.d.	n.d.
ATE	3.56	1.72
BEZ	2.32	0.52
BIC	3.13	1.84
CAR	0.65	1.45
CIT	19.63	14.75
CLO	0.43	0.48
CYC	0.52	0.31
DIC	0.83	0.17
FEX	0.57	3.09
GAB	0.54	0.78
HYD	0.26	0.09
IRB	4.83	0.67
LAM	2.09	1.85
LEV	0.78	0.13
LID	0.34	0.24
MEF	14.94	3.43
MTO	2.58	1.56
SAC	0.22	0.22
SIT	49	26.1
SUL	1.86	1.91
TRI	6.62	1.59
VAL	0.89	0.09
VEN	11.6	3.90
Average	**5.38**	**2.80**

Table A 13: Ration of $DegT_{50,w,field}$ to $DegT_{50,w,mod308}$

$DegT_{50,w,field}$ and $DegT_{50,w,mod308}$ were calculated based on the compounds respective $k'_{bio,field}$ and $k'_{bio,lab,joint}$ values. $DegT_{50,w,mod308}$ were derived from modified OECD 308-type studies conducted in inoculum sampled from the Rhine.

Compound	Ratio $DegT_{50,w,field,P1}/DegT_{50,w,mod308}$	Ratio $DegT_{50,w,field,P3}/ DegT_{50,w,mod308}$
ACE	0.04	0.02
ALI	n.d.	n.d.
ATA	n.d.	n.d.
ATE	0.36	0.18
BEZ	1.05	0.24
BIC	0.52	0.31
CAR	0.001	0.002
CIT	0.01	0.009
CLO	0.08	0.08
CYC	0.05	0.03
DIC	0.05	0.01
FEX	n.d.	n.d.
GAB	0.05	0.068
HYD	0.23	0.08
IRB	5.72	0.79
LAM	0.003	0.0031
LEV	0.57	0.1
LID	0.004	0.0025
MEF	1.30	0.3
MET	0.20	0.12
SAC	0.03	0.027
SIT	0.41	0.22
SUL	0.98	1
TRI	3.97	0.95
VAL	0.53	0.05
VEN	0.10	0.03
Average	**0.71**	**0.2**

Table A 14: Ratio of $DegT_{50,TS,field}$ to $DT_{50,TS,mod308}$

$DegT_{50,TS,field}$ were calculated based on the compounds respective $k'_{bio,field}$ values. $DT_{50,TS,mod308}$ were derived from modified OECD 308-type studies conducted in inoculum sampled from the Rhine.

Compound	Ratio $DegT_{50,TS,field,P1}/DT_{50,TS,mod308}$	Ratio $DegT_{50,TS,field,P3}/DT_{50,TS,mod308}$
ACE	0.06	0.03
ALI	n.d.	n.d.
ATA	n.d.	n.d.
ATE	0.28	0.11
BEZ	0.14	0.04
BIC	0.08	0.05
CAR	0.01	0.02
CIT	0.003	0.003
CLO	0.03	0.03
CYC	0.03	0.02
DIC	0.03	0.01
FEX	0.01	0.05
GAB	0.04	0.05
HYD	0.02	0.01
IRB	0.31	0.04
LAM	0.04	0.04
LEV	0.06	0
LID	0.01	0.01
MEF	0.86	0.2
MET	0.15	0.1
SAC	0.02	0.01
SIT	0.03	0.02
SUL	0.14	0.14
TRI	0.43	0.11
VAL	0.09	0
VEN	0.11	0.04
Average	**0.12**	**0.05**

Table A 15: Ratio of $k'_{bio,field}$ to $k'_{bio,lab}$

Compound	Ratio $k'_{bio,field,P1}$/ $k'_{bio,lab,CMP}$	Ratio $k'_{bio,field,P1}$/ $k'_{bio,lab,R}$	Ratio $k'_{bio,field,P1}$/ $k'_{bio,lab,joint}$	Ratio $k'_{bio,field,P3}$/ $k'_{bio,lab,CMP}$	Ratio $k'_{bio,field,P3}$/ $k'_{bio,lab,R}$	Ratio $k'_{bio,field,P3}$/ $k'_{bio,lab,joint}$
ACE	2488	15	155	5150	31	322
ALI	19	n.d.	n.d.	n.d.	n.d.	n.d.
ATA	14	n.d.	n.d.	n.d.	n.d.	n.d.
ATE	8	3	17	16	6	35
BEZ	0	3	6	0	12	27
BIC	2	37	12	4	63	21
CAR	4900	980	16333	2180	436	7267
CIT	132	259	529	176	345	704
CLO	1615	15	84	1454	13	75
CYC	195	13	132	317	21	214
DIC	1065	103	121	5306	513	605
FEX	26	n.d.	n.d.	5	n.d.	n.d.
GAB	3567	132	134	2477	92	93
HYD	7600	608	7600	22900	1832	22900
IRB	273	182	614	1967	1311	4425
LAM	3590	180	1795	4060	203	2030
LEV	25	4	11	148	26	65
LID	2383	540	1788	3358	760	2519
MEF	8	2	5	34	11	21
MTO	60	3	32	100	6	53
SAC	605	28	234	622	29	241
SIT	9	34	120	17	64	224
SUL	6	4	6	6	4	6
TRI	2	1	2	6	5	7
VAL	83	4	12	857	45	121
VEN	120	12	61	356	36	182
Average	**1107**	**138**	**1296**	**2146**	**255**	**1833**

Figure A 11: Comparison of $DT_{50,w}$ derived from laboratory data and $DegT_{50,w}$ derived from P1 field data

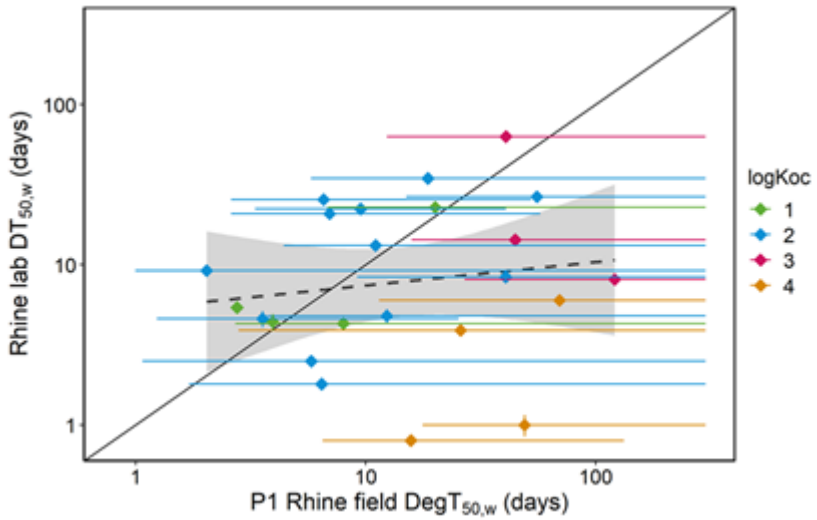

Comparison of $DT_{50,w}$ derived from modified OECD 308-type studies employing sediment and water sampled from the Rhine to $DegT_{50,w}$ calculated based on the compounds $k'_{bio,field}$ and catchment properties of the Rhine. Diamonds show mean values, the errorbars on the x-axis expand from the smallest to the largest value calculated for the respective $DegT_{50,w}$. Diamonds are colored with respect to their calibrated rounded logKoc values. The 1:1 line is plotted as solid black lines. The linear regression line and its 95% confidence interval are shown as dotted line and grey area, respectively. The linear regression line has a R^2 of 0.007 and a p-value of 0.7. Please note that 5MB was excluded from this plot since our analytical method does not allow to differentiate between 5MB and the more persistent 4MB, which might be present in the samples from the Rhine river catchment.

Source: own figure, Eawag

Figure A 12: Comparison of $DegT_{50,w}$ derived from laboratory data and $DegT_{50,w}$ derived from P1 field data

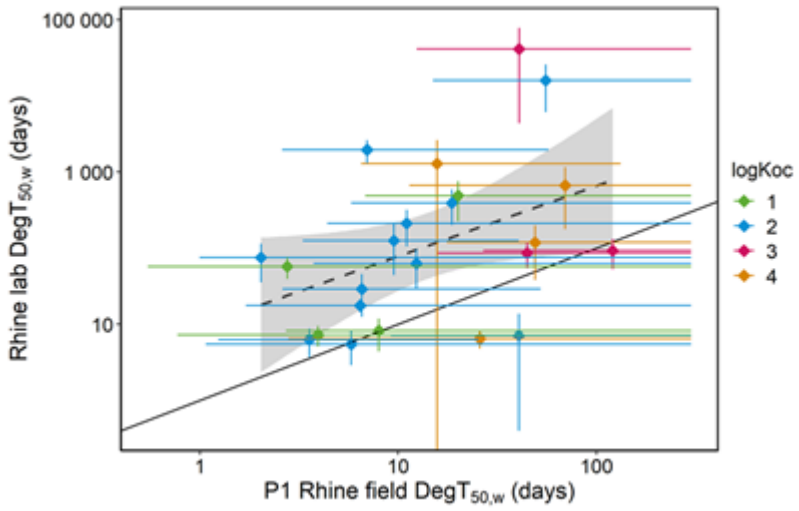

Comparison of $DegT_{50,w}$ calculated based on $k'_{bio,lab}$(joint fit) in modified OECD 308-type studies employing sediment and water sampled from the Rhine to $DegT_{50,w}$ calculated based on the compounds $k'_{bio,field}$ and catchment properties of the Rhine. Diamonds show mean values, the errorbars on the x-axis expand from the smallest to the largest value calculated for the respective $DegT_{50,w}$. Diamonds are colored with respect to their calibrated rounded logKoc values. The 1:1 line is plotted as a solid black line. Linear regression and the 95% confidence interval are shown as dotted line and grey area, respectively. The linear regression line has a R^2 of 0.038 and a p-value of 0.37. Please note that 5MB was excluded from this plot since our analytical method does not allow to differentiate between 5MB and the more persistent 4MB, which might be present in the samples from the Rhine river catchment.
Source: own figure, Eawag

Figure A 13: Comparison of $DT_{50,TS}$ derived from laboratory data and $DegT_{50,TS}$ derived from P1 field data

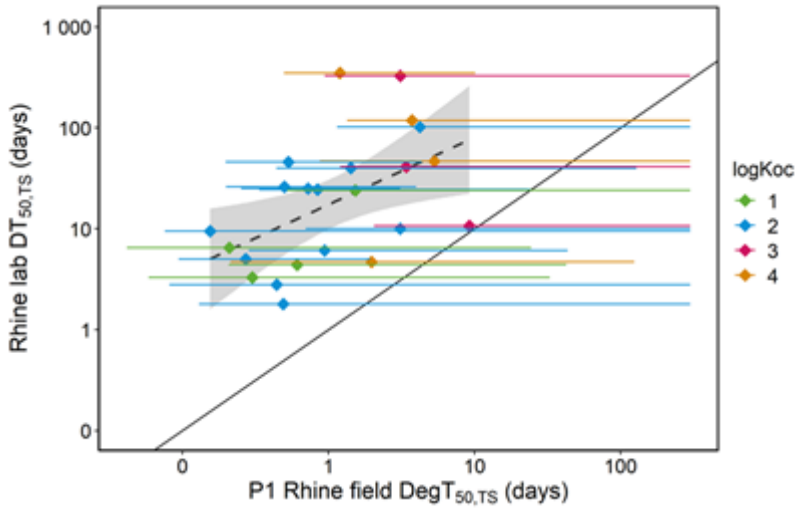

Comparison of $DT_{50,TS}$ in modified OECD 308-type studies employing sediment and water sampled from the Rhine to $DegT_{50,TS}$ calculated based on the compounds $k'_{bio,field}$ and catchment properties of the Rhine. Diamonds show mean values, the errorbars on the x-axis expand from the smallest to the largest value calculated for the respective $DegT_{50,TS}$. Diamonds are colored with respect to their calibrated rounded logKoc values. The 1:1 line is plotted as a solid black line. The linear regression and its 95% confidence interval are shown as dotted line and grey area, respectively. The linear regression has a R^2 of 0.02 and a p-value of 0.52. Please note that 5MB was excluded from this plot since our analytical method does not allow to differentiate between 5MB and the more persistent 4MB, which might be present in the samples from the Rhine river catchment.

Source: own figure, Eawag

Figure A 14: Comparison of $k'_{bio,lab}$ and $k'_{bio,field,P1}$

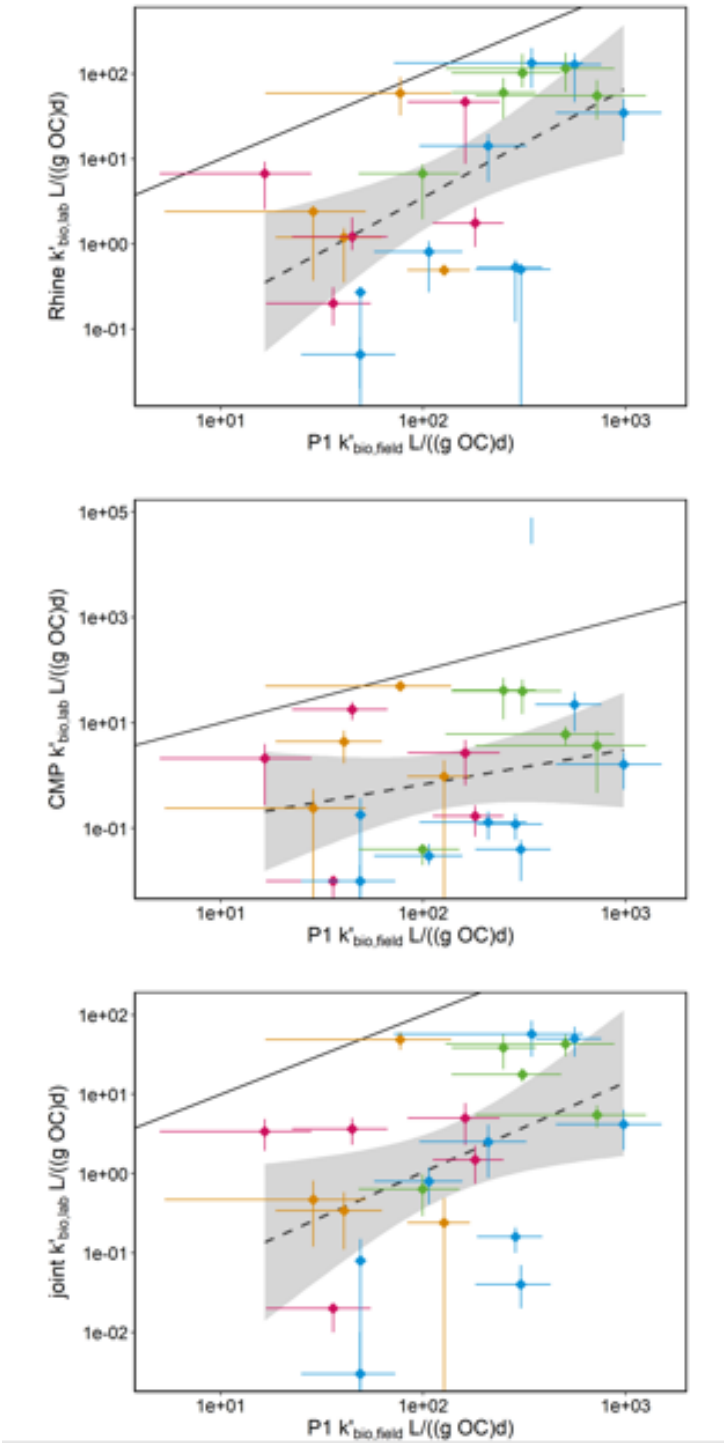

Comparison of $k'_{bio,lab}$ values derived when individually and jointly fitting the experimental data of the two modified OECD 308-type studies to $k'_{bio,field}$ calculated for the P1 sampling campaigns. Diamonds show mean values and are colored with respect to their calibrated rounded logKoc values. The 1:1 lines are plotted as solid black lines. Linear regressions and their 95% confidence interval are shown as dotted line and grey area, respectively. Linear regressions have a R^2 of 0.27, 0.001 and 0.087 and p-values of 0.009, 0.88 and 0.16 when $k'_{bio,lab}$ was calibrated based on experimental data from the Rhine study exclusively, based on experimental data from the CMP study exclusively, and based on a joint model fit, respectively. Please note that 5MB was excluded from this plot since our analytical method does not allow to differentiate between 5MB and the more persistent 4MB, which might be present in the samples from the Rhine river catchment.
Source: own figure, Eawag

List of References

Andreadis, K. M., G. J.-P. Schumann, and T. Pavelsky (2013), A simple global river bankfull width and depth database, Water Resources Research, 49(10), 7164–7168, doi:10.1002/wrcr.20440.

Arcement, G. J., and V. R. Schneider (1989), Guide for selecting Manning's roughness coefficients for natural channels and flood plains, Tech. rep., U. S. Geological Survey.

Ferguson, R., and M. Church (2004), A simple universal equation for grain settling velocity, Journal of Sedimentary Research, 74(6), 933–937, doi:10.1306/051204740933.

Honti, M., S. Hahn, D. Hennecke, T. Junker, P. Shrestha, and K. Fenner (2016), Bridging across OECD 308 and 309 data in search of a robust biotransformation indicator, Environmental Science & Technology, 50(13), 6865–6872, doi:10.1021/acs.est.6b01097.

Maniak, U. (2010), Hydrologie und Wasserwirtschaft - Eine Einführung für Ingenieure, Springer Berlin Heidelberg, doi:10.1007/978-3-642-05396-2.

Mosley, M. P., and A. I. McKerchar (1993), Chapter 8: Streamflow, in Handbook of Hydrology, edited by D. R. Maidment, chap. 8, pp. 8.1 – 8.39, McGraw-Hill Education,New York.

Schmidt, K.-H., and M. Unbenannt (2003), Schwebstofftransport – die Fliessgewässer als Transportbänder, in Nationalatlas Bundesrepublik Deutschland – Band 2, Natur und Umwelt I: Relief, Boden und Wasser, edited by S. Tzschaschel, pp. 136 – 137, Institut für Länderkunde, Leipzig, Germany.

Simons, D. B., and M. L. Albertson (1960), Uniform water conveyance channels in alluvial materials, ASCE Journal of the Hydraulics Division, 86(5), 33–71.

TK Consult AG (2013), Überflutung Beznau – Ermittlung der maximalen Überflutungshöhe der Beznau-Insel unter Berücksichtigung von Feststofftransport, Tech. rep., Eidgenössisches Nuklearsicherheitsinspektorat ENSI, Zürich, Switzerland.

van Rijn, L. C. (1984), Sediment transport, part II: Suspended load transport, Journal of Hydraulic Engineering, 110(11), 1613–1641, doi:10.1061/(asce)0733-9429(1984)110:11(1613).

Wharton, G., N. Arnell, K. Gregory, and A. Gurnell (1989), River discharge estimated from channel dimensions, Journal of Hydrology, 106(3-4), 365–376, doi:10.1016/0022-1694(89)90080-2.